

**Photosensitizer-free visible light-mediated gold-catalysed
cis-difunctionalization of silyl-substituted alkynes**

Jie-Ren Deng, Wing-Cheung Chan, Nathanael Chun-Him Lai, Bin Yang, Chui-Shan Tsang,
Ben Chi-Bun Ko, Sharon Lai-Fung Chan, and Man-Kin Wong*

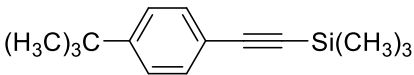
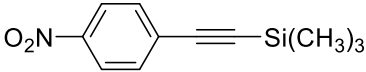
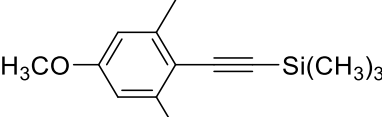
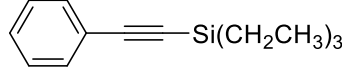
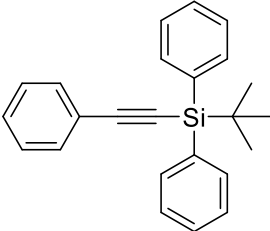
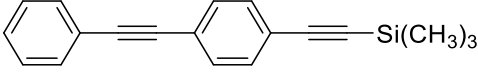
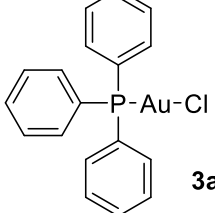
The Hong Kong Polytechnic University Shenzhen Research Institute, Shenzhen, People's
Republic of China

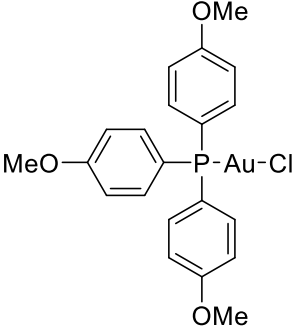
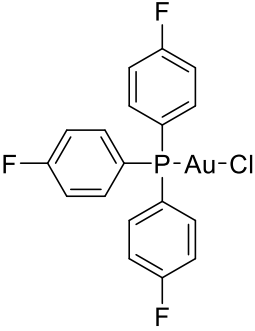
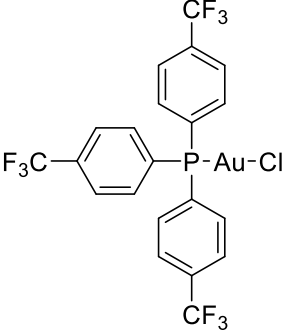
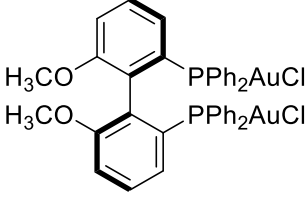
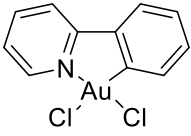
State Key Laboratory of Chirosciences and Department of Applied Biology and Chemical
Technology, The Hong Kong Polytechnic University, Hung Hum, Hong Kong

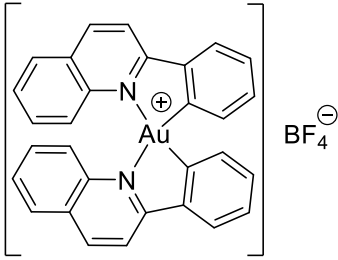
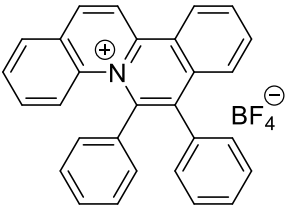
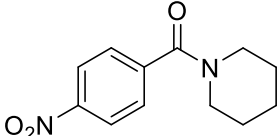
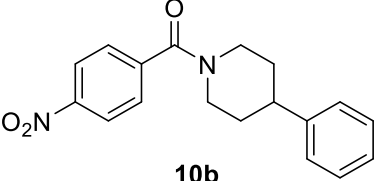
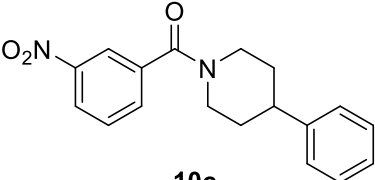
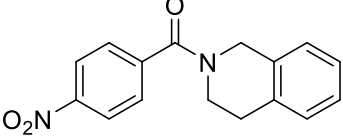
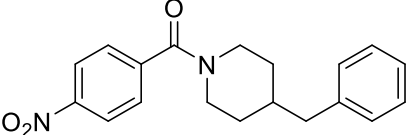
E-mail: mankin.wong@polyu.edu.hk

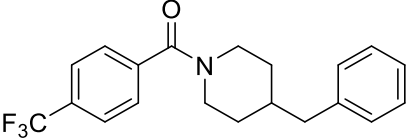
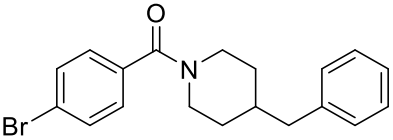
Supporting Information

Literature references

 <p style="text-align: center;">2c</p>	<p>I. Kownacki, B. Marciniak, B. Dudziec and M. Kubicki, <i>Organometallics</i>, 2011, 30, 2539.</p>
 <p style="text-align: center;">2l</p>	<p>N. Sakai, K. Annaka and T. Konakahara, <i>Org. Lett.</i>, 2004, 6, 1527.</p>
 <p style="text-align: center;">2r</p>	<p>E. R. Neil, M. A. Fox, R. Pal, L.-O. Pålsson, B. A. O'Sullivan and D. Parker, <i>Dalton Trans.</i>, 2015, 44, 14937.</p>
 <p style="text-align: center;">2s</p>	<p>M. Carril, A. Correa and C. Bolm, <i>Angew. Chem. Int. Ed.</i>, 2008, 47, 4862.</p>
 <p style="text-align: center;">2t</p>	<p>S. Kim, J. Rojas-Martina and F. D. Toste, <i>Chem. Sci.</i>, 2016, 7, 85.</p>
 <p style="text-align: center;">2z</p>	<p>K. Li and Q. Wang, <i>Chem. Commun.</i>, 2005, 4786.</p>
 <p style="text-align: center;">3a</p>	<p>P. Braunstein, H. Lehner and D. Matt, <i>Inorg. Synth.</i>, 1990, 27, 218.</p>

 <p style="text-align: right;">3b</p>	<p>R. J. Cross and M. F. Davidson, <i>J. Chem. Soc., Dalton Trans.</i>, 1986, 0, 411.</p>
 <p style="text-align: right;">3c</p>	<p>J. Cordón, J. M. L.-d.-Luzuriaga and M. Monge, <i>Organometallics</i>, 2016, 35, 732.</p>
 <p style="text-align: right;">3d</p>	<p>K. Nunokawa, S. Onaka, T. Tatematsu, M. Ito and J. Sakai, <i>Inorg. Chim. Acta</i>, 2001, 322, 56.</p>
 <p style="text-align: right;">3f</p>	<p>E. S. Andreiadis, M. R. Vitale, N. Mézailles, X. L. Goff, P. L. Floch, P. Y. Toullec and V. Michelet, <i>Dalton Trans.</i>, 2010, 39, 10608.</p>
 <p style="text-align: right;">3i</p>	<p>E. C. Constable and T. A. Leese, <i>J. Organomet. Chem.</i>, 1989, 363, 419.</p>

 <p style="text-align: center;">3j</p>	<p>H.-M. Ko, K. K.-Y. Kung, J.-F. Cui and M.-K. Wong, <i>Chem. Commun.</i>, 2013, 49, 8869.</p>
 <p style="text-align: center;">7c</p>	<p>G. Zhang, L. Yang, Y. Wang, Y. Xie and H. Huang, <i>J. Am. Chem. Soc.</i>, 2013, 135, 8850.</p>
 <p style="text-align: center;">10a</p>	<p>F. K.-C. Leung, J.-F. Cui, T.-W. Hui, K. K.-Y. Kung and M.-K. Wong, <i>Asian J. Org. Chem.</i>, 2015, 4, 533.</p>
 <p style="text-align: center;">10b</p>	<p>F. K.-C. Leung, J.-F. Cui, T.-W. Hui, K. K.-Y. Kung and M.-K. Wong, <i>Asian J. Org. Chem.</i>, 2015, 4, 533.</p>
 <p style="text-align: center;">10c</p>	<p>F. K.-C. Leung, J.-F. Cui, T.-W. Hui, K. K.-Y. Kung and M.-K. Wong, <i>Asian J. Org. Chem.</i>, 2015, 4, 533.</p>
 <p style="text-align: center;">10d</p>	<p>F. K.-C. Leung, J.-F. Cui, T.-W. Hui, K. K.-Y. Kung and M.-K. Wong, <i>Asian J. Org. Chem.</i>, 2015, 4, 533.</p>
 <p style="text-align: center;">10e</p>	<p>F. K.-C. Leung, J.-F. Cui, T.-W. Hui, K. K.-Y. Kung and M.-K. Wong, <i>Asian J. Org. Chem.</i>, 2015, 4, 533.</p>

 <p style="text-align: center;">10f</p>	<p>F. K.-C. Leung, J.-F. Cui, T.-W. Hui, K. K.-Y. Kung and M.-K. Wong, <i>Asian J. Org. Chem.</i>, 2015, 4, 533.</p>
 <p style="text-align: center;">10g</p>	<p>F. K.-C. Leung, J.-F. Cui, T.-W. Hui, K. K.-Y. Kung and M.-K. Wong, <i>Asian J. Org. Chem.</i>, 2015, 4, 533.</p>
<p style="text-align: center;">$[\text{Cp}^*\text{RhCl}_2]_2$</p>	<p>J. W. Kang, K. Moseley and P. M. Maitlis, <i>J. Am. Chem. Soc.</i>, 1969, 91, 5970.</p>

General procedure

All reagents were commercially available and used without further purification. Flash column chromatography was performed using silica gel 60 (230-400 mesh ASTM) with ethyl acetate/*n*-hexane or methanol/dichloromethane as eluent. ^1H , ^{13}C and ^{19}F NMR spectra were recorded on a Bruker DPX-400 or DPX-600 spectrometer. All chemical shifts are quoted on the scale in ppm using TMS or residual solvent as the internal standard. Coupling constants (J) are reported in Hertz (Hz) with the following splitting abbreviations: s = singlet, br s = broad singlet, d = doublet, dd = double doublet, t = triplet and m = multiplet. High resolution mass spectra were obtained on an Agilent 6540 UHD Accurate-Mass Q-TOF LC/MS system equipped with an ion spray source in the positive ion mode. For ESI-MS/MS analysis, collision energy was set at 10, 15 or 20 eV. X-ray crystal structures were obtained by Bruker D8 Venture single crystal X-Ray diffractometer.

All of the photochemical experiments were performed in a custom made “light box” with 4 reaction vessels surrounded by 16 blue LEDs. The temperature was maintained by a fan attached to the “light box”. A voltage transformer was connected with the blue LEDs and employed to monitor the power of the light source ($P = U \times I = 14.3 \text{ V} \times 2.3 \text{ A} = 32.9 \text{ W}$). 4 reactions were performed in the “light box” every time for measurement of the reaction yields. The emission spectra of the blue LEDs revealed a maximum emission wavelength of the light source at $\lambda_{\text{max}} = 468 \text{ nm}$. The emission spectra of the light source was shown below.

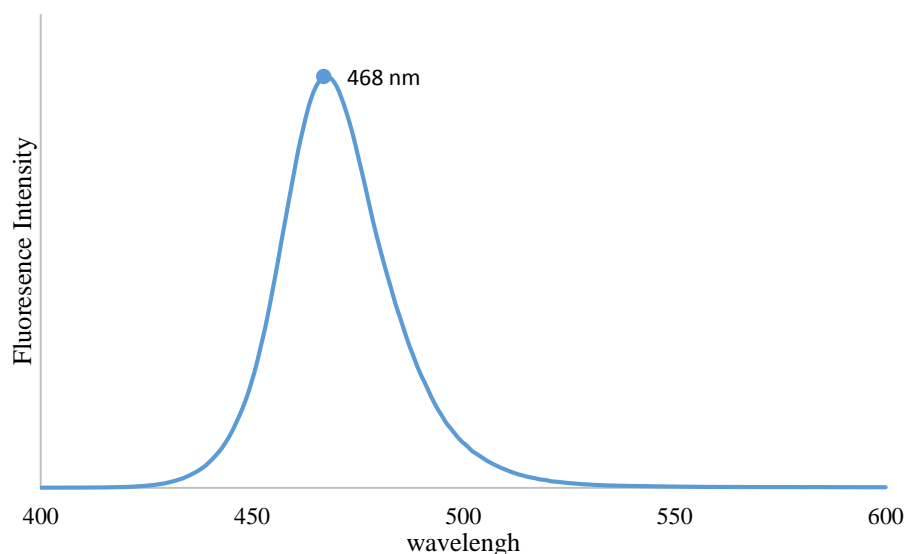
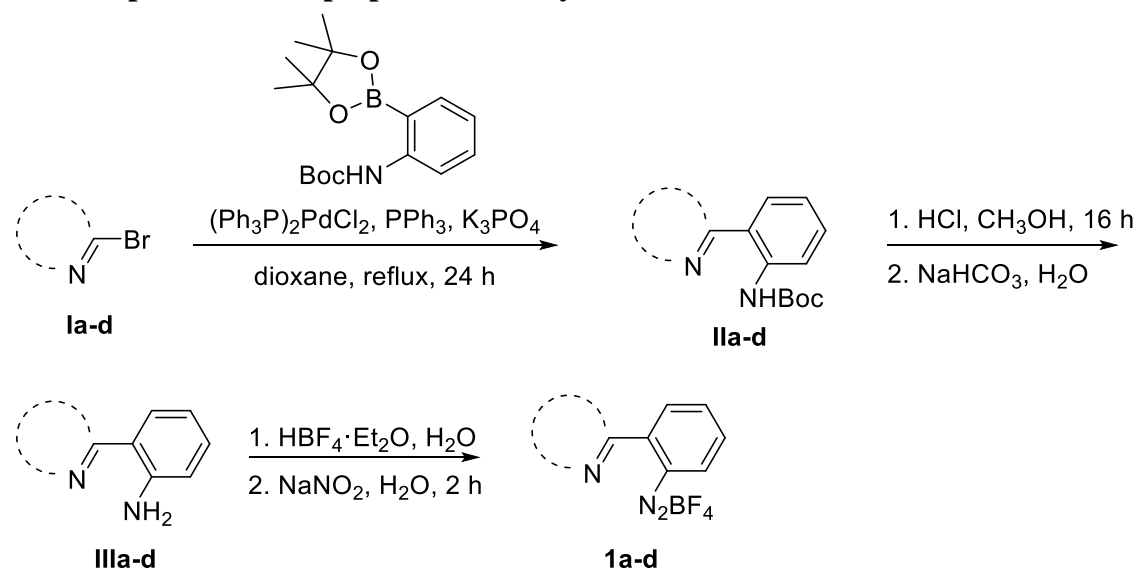
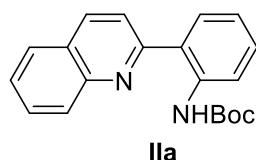


Figure S1 Emission spectrum of the Blue LEDs light source.

General procedure for preparation of aryl diazoniums 1a-d



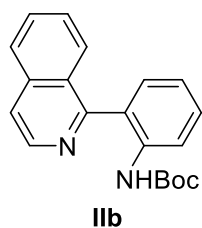
A mixture of aryl bromides **Ia-d** (10 mmol, 1 equiv.), 2-(N-Boc-amino)-phenylboronic acid pinacol ester (3.35 g, 1.05 equiv.), $(\text{PPh}_3)_2\text{PdCl}_2$ (0.14 g, 2 mol%), triphenylphosphine (0.10 g, 4 mol%) and K_3PO_4 (6.37 g, 3 equiv.) in 40 mL of 1,4-dioxane/ H_2O (3:1) was heated in a 100 mL round bottom flask at 100 °C under N_2 for 3-16 h. The reaction was monitored by TLC analysis until all starting materials consumed. After the reaction, the reaction mixture was extracted by ethyl acetate for three times. The organic layer collected was dried by anhydrous MgSO_4 and purified by flash column chromatography using EtOAc/hexane as eluent to give the desired products **IIa-d**.



White solid, 95% yield.

$^1\text{H NMR}$ (400 MHz, CDCl_3) δ 12.26 (s, 1H), 8.42 (d, $J = 8.3$ Hz, 1H), 8.26 (d, $J = 8.8$ Hz, 1H), 8.09 (d, $J = 8.4$ Hz, 1H), 7.92 – 7.70 (m, 4H), 7.58 (t, $J = 7.5$ Hz, 1H), 7.46 – 7.36 (m, 1H), 7.13 (dd, $J = 11.1, 4.0$ Hz, 1H), 1.55 (s, 9H).

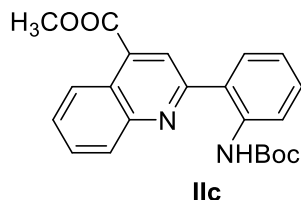
$^{13}\text{C NMR}$ (100 MHz, CDCl_3) δ 158.24, 153.58, 146.39, 139.45, 137.42, 130.59, 130.27, 129.42, 128.83, 127.59, 126.90, 126.56, 124.37, 122.05, 120.67, 120.20, 79.78, 28.57.



White solid, 92% yield.

$^1\text{H NMR}$ (400 MHz, CDCl_3) δ 8.63 (d, $J = 5.7$ Hz, 1H), 8.33 – 8.21 (m, 2H), 8.02 (d, $J = 8.5$ Hz, 1H), 7.90 (d, $J = 8.2$ Hz, 1H), 7.76 – 7.65 (m, 2H), 7.55 (ddd, $J = 8.2, 6.9, 1.1$ Hz, 1H),

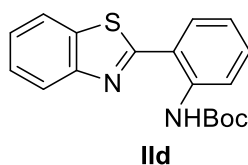
7.50 – 7.43 (m, 1H), 7.39 (dd, $J = 7.7, 1.5$ Hz, 1H), 7.15 (td, $J = 7.6, 1.1$ Hz, 1H), 1.42 (s, 9H).
 $^{13}\text{C NMR}$ (100 MHz, CDCl_3) δ 158.91, 153.10, 141.69, 137.61, 137.03, 131.66, 130.59, 129.73, 127.88, 127.57, 127.31, 127.17, 122.21, 121.28, 120.47, 80.31, 28.42.



White solid, 90% yield.

$^1\text{H NMR}$ (400 MHz, CDCl_3) δ 12.07 (s, 1H), 8.76 (d, $J = 8.5$ Hz, 1H), 8.43 (d, $J = 7.7$ Hz, 2H), 8.13 (d, $J = 8.3$ Hz, 1H), 7.87 (dd, $J = 7.9, 1.2$ Hz, 1H), 7.85 – 7.79 (m, 1H), 7.70 – 7.64 (m, 1H), 7.50 – 7.41 (m, 1H), 7.16 (m, 1H), 4.08 (s, 3H), 1.55 (s, 9H).

$^{13}\text{C NMR}$ (100 MHz, CDCl_3) δ 166.62, 157.67, 153.48, 147.35, 139.54, 136.30, 131.03, 130.54, 129.41, 129.30, 128.32, 125.66, 123.62, 123.43, 122.18, 120.32, 79.95, 52.99, 28.54.

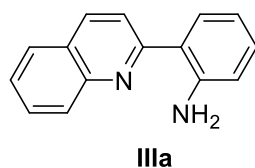


White solid, 98% yield.

$^1\text{H NMR}$ (400 MHz, CDCl_3) δ 11.69 (s, 1H), 8.53 (d, $J = 8.4$ Hz, 1H), 8.03 (d, $J = 8.1$ Hz, 1H), 7.90 (d, $J = 7.9$ Hz, 1H), 7.81 (dd, $J = 7.9, 1.3$ Hz, 1H), 7.56 – 7.36 (m, 3H), 7.13 – 6.98 (m, 1H), 1.59 (s, 9H).

$^{13}\text{C NMR}$ (100 MHz, CDCl_3) δ 168.70, 153.49, 153.18, 138.90, 133.55, 131.94, 130.07, 126.55, 125.70, 122.97, 121.90, 121.43, 119.42, 118.72, 80.32, 28.53.

For deprotection, **IIa-d** was treated with $\text{CH}_3\text{OH}/37\%$ hydrochloric acid (3:1) and stirred at room temperature overnight. After that, CH_3OH in the reaction mixture was removed by rotatory evaporation. Then, in an ice bath, NaOH solution (2 M in H_2O) was dropwise added into the crude mixture until the $\text{pH} = 10$. The resulting mixture was extracted by CH_2Cl_2 for three times. The organic layers were combined and dried by anhydrous MgSO_4 . Then, the resulting mixture was purified by flash column chromatography using $\text{EtOAc}/\text{hexane}$ as eluent to give the desired products **IIIa-d**.

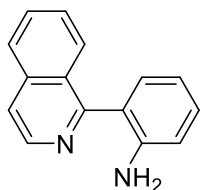


Yellow solid, 97% yield.

$^1\text{H NMR}$ (400 MHz, CDCl_3) δ 8.20 (d, $J = 8.8$ Hz, 1H), 8.05 (d, $J = 8.4$ Hz, 1H), 7.83 (m, 2H),

7.76 – 7.65 (m, 2H), 7.52 (t, J = 7.5 Hz, 1H), 7.25 – 7.15 (m, 1H), 6.82 (t, J = 7.7 Hz, 2H), 6.20 (s, 2H).

$^{13}\text{C NMR}$ (100 MHz, CDCl_3) δ 159.38, 147.57, 146.99, 136.74, 130.42, 129.96, 129.71, 128.96, 127.54, 126.40, 126.24, 121.68, 120.59, 117.56, 117.46.

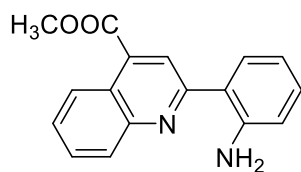


IIIb

Yellow solid, 85% yield.

$^1\text{H NMR}$ (400 MHz, CDCl_3) δ 8.59 (d, J = 5.7 Hz, 1H), 8.03 (d, J = 8.5 Hz, 1H), 7.85 (d, J = 8.2 Hz, 1H), 7.71 – 7.60 (m, 2H), 7.51 (t, J = 7.6 Hz, 1H), 7.27 (m, 2H), 6.87 (m, 2H), 4.26 (s, 2H).

$^{13}\text{C NMR}$ (100 MHz, CDCl_3) δ 159.83, 145.39, 142.00, 137.32, 131.65, 130.30, 129.73, 127.88, 127.44, 127.25, 127.01, 123.92, 120.02, 117.93, 116.83.

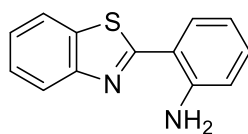


IIIc

White solid, 95% yield.

$^1\text{H NMR}$ (400 MHz, CDCl_3) δ 8.75 (d, J = 8.5 Hz, 1H), 8.42 (s, 1H), 8.11 (d, J = 8.4 Hz, 1H), 7.77 (m, 2H), 7.63 (t, J = 7.6 Hz, 1H), 7.26 (m, 1H), 6.85 (m, 2H), 6.27 (s, 2H), 4.09 (s, 3H).

$^{13}\text{C NMR}$ (100 MHz, CDCl_3) δ 166.91, 158.75, 147.89, 147.75, 135.56, 130.85, 129.97, 129.84, 129.41, 127.61, 125.54, 123.13, 122.04, 120.58, 117.56, 117.55, 52.82.



III d

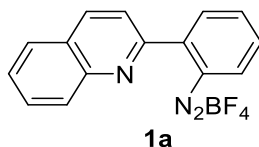
Pale yellow solid, 99% yield.

$^1\text{H NMR}$ (400 MHz, CDCl_3) δ 7.98 (d, J = 8.1 Hz, 1H), 7.88 (d, J = 7.9 Hz, 1H), 7.72 (d, J = 7.9 Hz, 1H), 7.46 (t, J = 7.7 Hz, 1H), 7.36 (t, J = 7.6 Hz, 1H), 7.23 (t, J = 7.7 Hz, 1H), 6.83 – 6.70 (m, 2H), 6.40 (s, 2H).

$^{13}\text{C NMR}$ (100 MHz, CDCl_3) δ 169.39, 153.91, 146.91, 133.44, 131.71, 130.49, 126.16, 125.00, 122.60, 121.32, 117.05, 116.94, 115.47.

A mixture of anilines **IIIa-d** (5 mmol, 1 equiv.) in 5 mL of H_2O in a 20 mL glass bottle in an ice bath was treated with tetrafluoroboric acid $\text{HBF}_4 \cdot \text{Et}_2\text{O}$ (0.82 mL, 1.2 equiv.) by

dropwise addition. After that, NaNO₂ (0.52 g, 1.5 equiv.) was dissolved in 3.5 mL of H₂O and dropwise added into the reaction mixture. The resulting mixture was stirred at room temperature for 3 h. Then, the mixture was filtered and the solid was stepwise washed by ethanol and followed by diethyl ether and further collected as products **1a-d**.



Pale yellow solid, 92% yield.

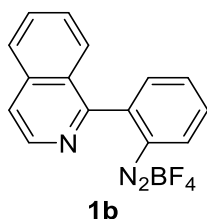
¹H NMR (400 MHz, *d*₆-DMSO) δ 8.98 (dd, *J* = 8.2, 0.8 Hz, 1H), 8.85 (m, 2H), 8.57 (d, *J* = 8.7 Hz, 1H), 8.47 – 8.40 (m, 1H), 8.36 (d, *J* = 8.5 Hz, 1H), 8.23 (d, *J* = 8.0 Hz, 1H), 8.17 (t, *J* = 7.8 Hz, 1H), 8.05 – 7.97 (m, 1H), 7.90 – 7.81 (m, 1H).

¹³C NMR (100 MHz, *d*₆-DMSO) δ 148.13, 144.94, 140.42, 140.10, 135.74, 132.61, 131.97, 130.16, 129.11, 128.55, 128.12, 126.94, 118.83.

DEPT 135 (100 MHz, *d*₆-DMSO) δ 140.42, 140.12, 135.73, 132.63, 131.99, 130.15, 129.13, 128.56, 126.93, 118.83.

¹⁹F NMR (376 MHz, *d*₆-DMSO) δ -148.26.

HRMS (ESI) calcd for C₁₅H₁₀N (M – N₂BF₄)⁺ 204.0808, found 204.0823.



Yellow solid, 86% yield.

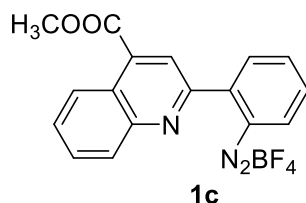
¹H NMR (400 MHz, *d*₆-DMSO) δ 9.01 (d, *J* = 8.2 Hz, 1H), 8.79 (d, *J* = 5.7 Hz, 1H), 8.43 (m, 2H), 8.22 (m, 4H), 7.98 (t, *J* = 7.5 Hz, 1H), 7.86 (t, *J* = 7.7 Hz, 1H).

¹³C NMR (100 MHz, *d*₆-DMSO) δ 150.81, 141.28, 140.08, 137.05, 135.56, 133.26, 131.65, 131.47, 129.42, 127.81, 126.07, 125.57, 123.42.

DEPT 135 (100 MHz, *d*₆-DMSO) δ 141.76, 140.55, 136.04, 133.74, 132.14, 131.94, 129.90, 128.29, 126.56, 123.90.

¹⁹F NMR (376 MHz, *d*₆-DMSO) δ -148.26.

HRMS (ESI) calcd for C₁₅H₁₀N (M – N₂BF₄)⁺ 204.0808, found 204.0818.



Pale yellow solid, 63% yield.

¹H NMR (400 MHz, CD₃CN) δ 8.76 (d, *J* = 8.6 Hz, 1H), 8.68 (d, *J* = 8.3 Hz, 1H), 8.63 – 8.53

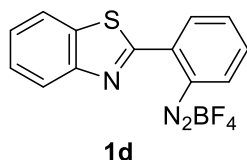
(m, 2H), 8.39 (t, $J = 7.8$ Hz, 1H), 8.28 (d, $J = 8.4$ Hz, 1H), 8.01 (m, 2H), 7.88 (m, 1H), 4.08 (s, 3H).

^{13}C NMR (100 MHz, CD_3CN) δ 166.95, 150.07, 148.85, 142.89, 140.97, 139.82, 137.29, 133.53, 132.83, 132.49, 131.59, 130.20, 127.06, 126.26, 120.92, 113.56, 54.04.

DEPT 135 (100 MHz, CD_3CN) δ 142.59, 136.99, 133.23, 132.53, 132.19, 131.30, 129.90, 126.76, 120.63, 53.75.

^{19}F NMR (376 MHz, CD_3CN) δ -151.88.

HRMS (ESI) calcd for $\text{C}_{17}\text{H}_{12}\text{NO}_2$ ($\text{M} - \text{N}_2\text{BF}_4$) $^+$ 262.0863, found 262.0874.



Yellow solid, 87% yield.

^1H NMR (400 MHz, d_6 -DMSO) δ 8.99 (d, $J = 8.2$ Hz, 1H), 8.56 (d, $J = 7.9$ Hz, 1H), 8.45 – 8.33 (m, 2H), 8.26 (d, $J = 7.9$ Hz, 1H), 8.15 (t, $J = 7.9$ Hz, 1H), 7.69 (m, 2H).

^{13}C NMR (100 MHz, d_6 -DMSO) δ 160.04, 152.45, 141.48, 135.84, 135.16, 132.87, 132.34, 131.63, 127.89, 127.72, 123.94, 123.09, 112.47.

DEPT 135 (100 MHz, d_6 -DMSO) δ 141.95, 136.31, 133.35, 132.10, 128.36, 128.19, 124.41, 123.56.

^{19}F NMR (376 MHz, d_6 -DMSO) δ -148.25.

HRMS (ESI) calcd for $\text{C}_{13}\text{H}_8\text{NS}$ ($\text{M} - \text{N}_2\text{BF}_4$) $^+$ 210.0372, found 210.0392.

General procedure for visible light-mediated gold-catalysed synthesis of quinolizinium compounds

A mixture of aryl diazonium salts (1.2 equiv.), silyl substituted alkynes (1 equiv.), Ph_3PAuCl (10 mol%) and 5 mL of CH_3CN was added into a 20 mL test tube. The test tube capped with a rubber septum was evacuated and refilled with nitrogen three times. After that, the tube containing the reaction mixture was irradiated with Blue LEDs for 16 h. After the reaction completed, the mixture was concentrated under reduced pressure.

For determination of NMR yield, an internal standard fluorobenzene (9.3 μL , 0.1 mmol, 1 equiv.) and 2 mL of CD_3OD were mixed with the resulting residue for ^{19}F NMR analysis.

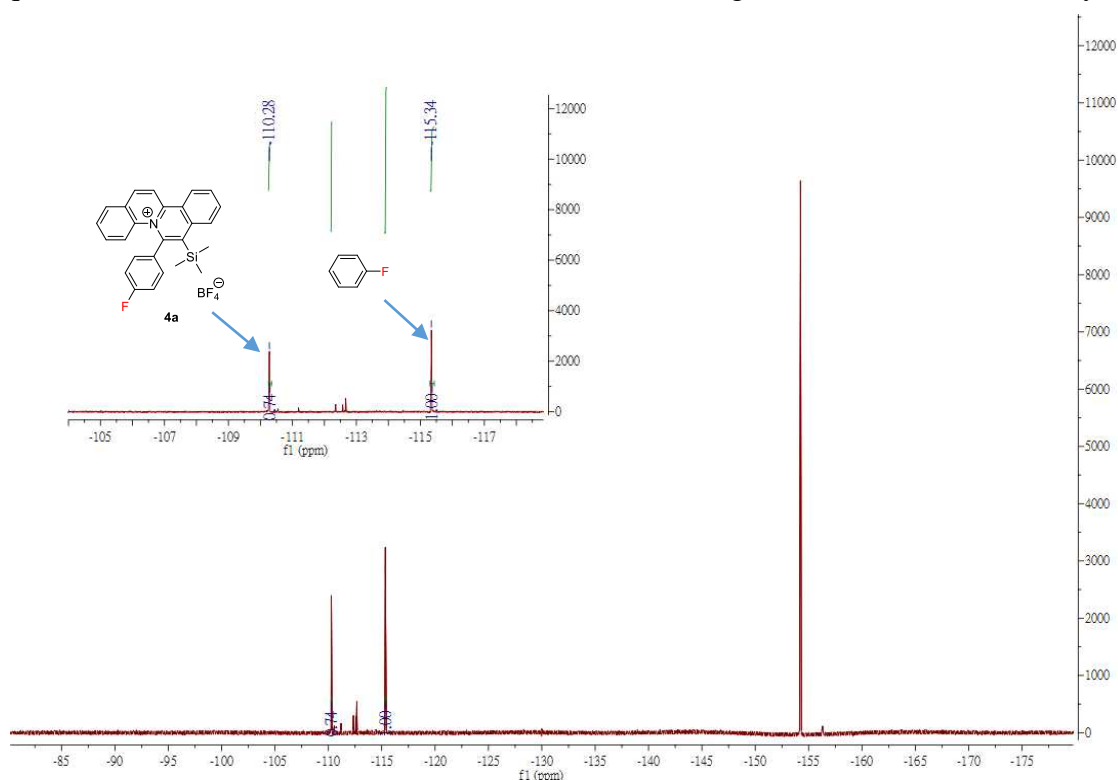
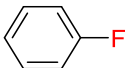
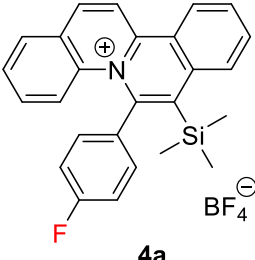
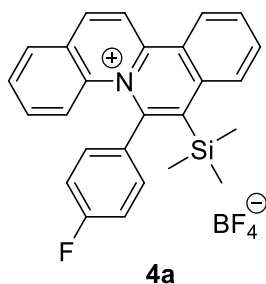


Figure S2 Determination of the NMR yield of **4a** (74%) employing fluorobenzene as internal standard.

Table S1 Chemical shifts of compounds in CD_3OD

Compound	Chemical shift (σ) of the F in ^{19}F NMR
	-115.45
	-110.24

For product isolation, the resulting residue was purified by flash chromatography on silica gel using CH₂Cl₂/CH₃OH (19:1) as eluent to give the desired product.



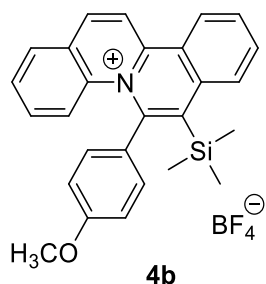
Yellow solid, 65% yield.

¹H NMR (400 MHz, CD₃OD) δ 9.16 (d, J = 9.0 Hz, 1H), 9.05 (d, J = 8.4 Hz, 1H), 8.95 (d, J = 9.0 Hz, 1H), 8.46 (d, J = 8.3 Hz, 1H), 8.27 (d, J = 7.9 Hz, 1H), 8.19 (t, J = 7.7 Hz, 1H), 8.07 (t, J = 7.7 Hz, 1H), 7.79 – 7.63 (m, 1H), 7.58 (m, 1H), 7.42 (t, J = 8.0 Hz, 1H), 7.29 (t, J = 8.6 Hz, 1H), 0.15 (s, 1H).

¹³C NMR (100 MHz, CD₃OD) δ 150.63, 146.69, 142.77, 138.07, 137.62, 136.24, 135.36, 135.27, 135.19, 135.02, 131.16, 130.51, 130.14, 129.89, 127.80, 126.29, 126.18, 119.37, 117.53, 117.31, 1.78.

¹⁹F NMR (376 MHz, CD₃OD) δ -110.24, -154.92.

HRMS (ESI) calcd for C₂₆H₂₃NFSi (M – BF₄)⁺ 396.1578, found 396.1574.

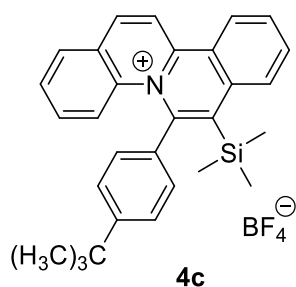


Orange solid, 69% yield.

¹H NMR (400 MHz, CD₃OD) δ 9.12 (d, J = 9.0 Hz, 1H), 9.02 (d, J = 8.5 Hz, 1H), 8.92 (d, J = 8.9 Hz, 1H), 8.43 (d, J = 8.2 Hz, 1H), 8.24 (d, J = 7.2 Hz, 1H), 8.17 (t, J = 7.6 Hz, 1H), 8.04 (t, J = 7.6 Hz, 1H), 7.72 (m, 1H), 7.49 – 7.32 (m, 1H), 7.06 (d, J = 8.7 Hz, 1H), 3.90 (s, 1H), 0.14 (s, 1H).

¹³C NMR (100 MHz, CD₃OD) δ 163.38, 150.82, 148.23, 142.86, 138.66, 138.27, 135.40, 134.89, 134.73, 132.62, 131.24, 130.62, 130.41, 130.38, 130.11, 128.06, 126.50, 119.68, 116.01, 56.16, 2.20.

HRMS (ESI) calcd for C₂₇H₂₆ONSi (M – BF₄)⁺ 408.1778, found 408.1793.

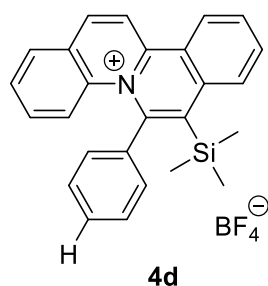


Yellow solid, 66% yield.

¹H NMR (400 MHz, CD₃OD) δ 9.15 (d, J = 9.0 Hz, 1H), 9.03 (d, J = 8.4 Hz, 1H), 8.93 (d, J = 8.9 Hz, 1H), 8.45 (d, J = 8.2 Hz, 1H), 8.24 (d, J = 7.7 Hz, 1H), 8.18 (t, J = 7.6 Hz, 1H), 8.05 (t, J = 7.7 Hz, 1H), 7.70 (m, 2H), 7.58 (d, J = 8.3 Hz, 2H), 7.45 (d, J = 8.2 Hz, 2H), 7.32 (t, J = 7.9 Hz, 1H), 1.39 (s, 9H), 0.12 (s, 9H).

¹³C NMR (100 MHz, CD₃OD) δ 156.35, 150.75, 148.22, 142.91, 138.55, 138.13, 137.40, 135.42, 135.01, 133.00, 131.32, 130.51, 130.41, 130.14, 130.08, 128.10, 127.61, 126.55, 126.47, 119.68, 35.95, 31.58, 2.11.

HRMS (ESI) calcd for C₃₀H₃₂NSi (M – BF₄)⁺ 434.2299, found 434.2308.

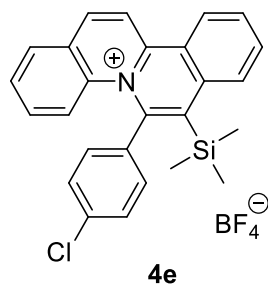


Yellow solid, 68% yield.

¹H NMR (400 MHz, CD₃OD) δ 9.16 (d, J = 9.0 Hz, 1H), 9.04 (d, J = 8.4 Hz, 1H), 8.94 (d, J = 8.9 Hz, 1H), 8.46 (d, J = 8.3 Hz, 1H), 8.25 (d, J = 7.1 Hz, 1H), 8.18 (t, J = 7.3 Hz, 1H), 8.06 (t, J = 7.7 Hz, 1H), 7.75 – 7.66 (m, 2H), 7.65 – 7.58 (m, 1H), 7.52 (m, 4H), 7.39 – 7.27 (m, 1H), 0.12 (s, 10H).

¹³C NMR (100 MHz, CD₃OD) δ 151.04, 148.30, 143.23, 140.40, 138.69, 138.28, 135.67, 135.37, 133.54, 132.31, 131.63, 130.93, 130.69, 130.62, 130.35, 128.33, 126.82, 126.71, 119.88, 2.31.

HRMS (ESI) calcd for C₂₆H₂₄NSi (M – BF₄)⁺ 378.1673, found 378.1691.



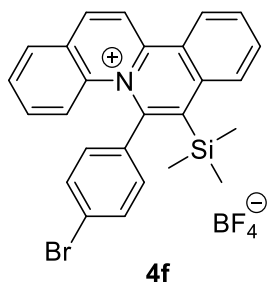
Yellow solid, 66% yield.

¹H NMR (400 MHz, CD₃OD) δ 9.16 (d, J = 9.0 Hz, 1H), 9.05 (d, J = 8.3 Hz, 1H), 8.96 (d, J = 8.9 Hz, 1H), 8.46 (d, J = 8.2 Hz, 1H), 8.27 (d, J = 7.7 Hz, 1H), 8.19 (t, J = 7.5 Hz, 1H), 8.07 (t,

$J = 7.5$ Hz, 1H), 7.79 – 7.66 (m, 2H), 7.56 (d, $J = 9.2$ Hz, 4H), 7.56 (m, 4H), 7.48 – 7.38 (m, 1H), 0.15 (s, 9H).

$^{13}\text{C NMR}$ (100 MHz, CD_3OD) δ 150.97, 146.81, 143.18, 138.78, 138.36, 138.33, 137.87, 135.54, 135.49, 134.90, 131.57, 130.95, 130.88, 130.52, 130.47, 130.29, 130.26, 128.15, 126.70, 126.53, 119.71, 2.17.

HRMS (ESI) calcd for $\text{C}_{26}\text{H}_{23}\text{NClSi}$ ($\text{M} - \text{BF}_4$) $^+$ 412.1283, found 412.1281.

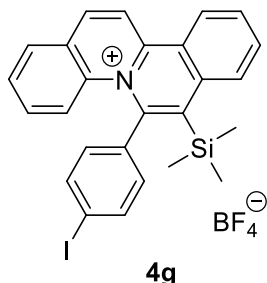


Yellow solid, 58% yield.

$^1\text{H NMR}$ (400 MHz, CD_3OD) δ 9.16 (d, $J = 9.0$ Hz, 1H), 9.05 (d, $J = 8.4$ Hz, 1H), 8.96 (d, $J = 8.9$ Hz, 1H), 8.46 (d, $J = 8.2$ Hz, 1H), 8.27 (d, $J = 7.9$ Hz, 1H), 8.19 (t, $J = 7.6$ Hz, 1H), 8.07 (t, $J = 7.7$ Hz, 1H), 7.73 (dd, $J = 18.7, 7.8$ Hz, 4H), 7.45 (dd, $J = 16.6, 8.3$ Hz, 3H), 0.15 (s, 9H).

$^{13}\text{C NMR}$ (100 MHz, CD_3OD) δ 150.97, 146.86, 143.18, 139.18, 138.36, 137.86, 135.55, 135.47, 135.05, 133.92, 131.57, 130.97, 130.52, 130.47, 130.31, 130.26, 128.15, 126.71, 126.52, 126.43, 119.70, 2.16.

HRMS (ESI) calcd for $\text{C}_{26}\text{H}_{23}\text{NBrSi}$ ($\text{M} - \text{BF}_4$) $^+$ 456.0788, found 456.0788.

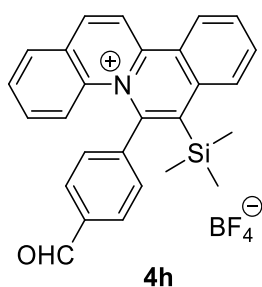


Yellow solid, 31% yield.

$^1\text{H NMR}$ (400 MHz, CD_3OD) δ 9.16 (d, $J = 8.9$ Hz, 1H), 9.04 (d, $J = 8.3$ Hz, 1H), 8.95 (d, $J = 8.9$ Hz, 1H), 8.46 (d, $J = 8.3$ Hz, 1H), 8.27 (d, $J = 8.0$ Hz, 1H), 8.19 (t, $J = 7.6$ Hz, 1H), 8.07 (t, $J = 7.6$ Hz, 1H), 7.91 (d, $J = 8.3$ Hz, 2H), 7.74 (m, 2H), 7.44 (t, $J = 8.0$ Hz, 1H), 7.31 (d, $J = 8.3$ Hz, 2H), 0.15 (s, 9H).

$^{13}\text{C NMR}$ (100 MHz, CD_3OD) δ 150.94, 147.05, 143.17, 140.02, 139.60, 138.37, 137.87, 135.54, 135.43, 134.91, 131.56, 130.98, 130.52, 130.46, 130.32, 130.25, 128.15, 126.71, 126.51, 119.69, 98.05, 2.17.

HRMS (ESI) calcd for $\text{C}_{26}\text{H}_{23}\text{NISi}$ ($\text{M} - \text{BF}_4$) $^+$ 504.0639, found 504.0659.

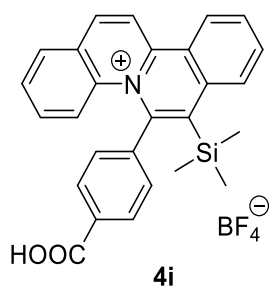


Yellow solid, 53% yield.

¹H NMR (400 MHz, *d*₆-DMSO) δ 10.12 (s, 1H), 9.37 (d, *J* = 8.9 Hz, 1H), 9.15 (m, 2H), 8.45 (d, *J* = 8.2 Hz, 1H), 8.34 (d, *J* = 7.9 Hz, 1H), 8.22 (t, *J* = 7.6 Hz, 1H), 8.11 (t, *J* = 7.7 Hz, 1H), 8.03 (d, *J* = 7.8 Hz, 2H), 7.82 (d, *J* = 7.7 Hz, 2H), 7.72 (t, *J* = 7.5 Hz, 1H), 7.58 (d, *J* = 8.9 Hz, 1H), 7.39 (t, *J* = 8.0 Hz, 1H), 0.06 (s, 9H).

¹³C NMR (100 MHz, *d*₆-DMSO) δ 192.80, 149.08, 145.19, 143.69, 142.05, 136.84, 136.14, 135.82, 134.36, 133.14, 132.77, 130.36, 130.00, 129.56, 129.15, 128.98, 128.92, 128.70, 127.15, 125.38, 124.95, 119.04, 1.86.

HRMS (ESI) calcd for C₂₇H₂₄ONSi (M – BF₄)⁺ 406.1627, found 406.1629.

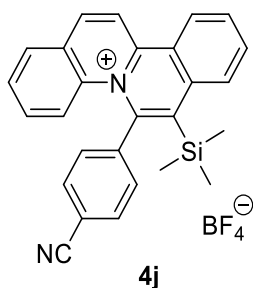


Yellow solid, 56% yield.

¹H NMR (400 MHz, CD₃OD) δ 9.17 (d, *J* = 9.0 Hz, 1H), 9.06 (d, *J* = 8.4 Hz, 1H), 8.96 (d, *J* = 8.9 Hz, 1H), 8.47 (d, *J* = 8.2 Hz, 1H), 8.26 (d, *J* = 7.8 Hz, 1H), 8.19 (t, *J* = 7.6 Hz, 1H), 8.15 – 8.02 (m, 3H), 7.76 – 7.66 (m, 2H), 7.63 (d, *J* = 8.1 Hz, 2H), 7.37 (t, *J* = 7.5 Hz, 1H), 0.13 (s, 9H).

¹³C NMR (100 MHz, CD₃OD) δ 150.91, 147.21, 143.21, 138.35, 137.90, 135.53, 133.33, 131.62, 131.00, 130.57, 130.42, 130.31, 130.22, 128.15, 126.68, 126.53, 119.67, 2.17.

HRMS (ESI) calcd for C₂₇H₂₄O₂NSi (M – BF₄)⁺ 422.1571, found 422.1571.



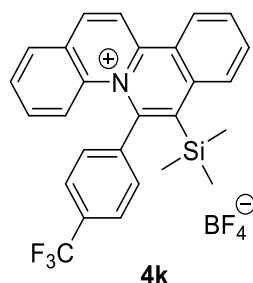
Yellow solid, 65% yield.

¹H NMR (400 MHz, CD₃OD) δ 9.19 (d, *J* = 9.0 Hz, 1H), 9.07 (d, *J* = 8.4 Hz, 1H), 8.99 (d, *J* = 8.9 Hz, 1H), 8.49 (d, *J* = 8.2 Hz, 1H), 8.29 (d, *J* = 8.1 Hz, 1H), 8.21 (t, *J* = 7.5 Hz, 1H), 8.09 (t, *J* = 7.7 Hz, 1H), 7.90 (d, *J* = 8.4 Hz, 2H), 7.75 (t, *J* = 7.8 Hz, 3H), 7.63 (d, *J* = 8.9 Hz, 1H), 7.43

(m, 1H), 0.15 (s, 9H).

¹³C NMR (100 MHz, CD₃OD) δ 151.08, 145.97, 144.25, 143.45, 138.17, 137.62, 135.98, 135.65, 134.38, 134.32, 131.82, 131.22, 130.66, 130.51, 130.42, 130.38, 128.22, 126.75, 126.58, 119.75, 118.70, 115.57, 2.17.

HRMS (ESI) calcd for C₂₇H₂₃N₂Si (M – BF₄)⁺ 403.1625, found 403.1634.



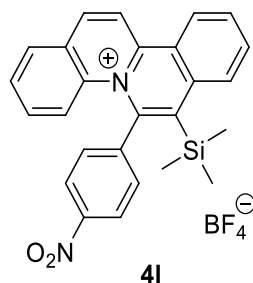
Yellow solid, 45% yield.

¹H NMR (400 MHz, CD₃OD) δ 9.19 (d, J = 8.9 Hz, 1H), 9.08 (d, J = 8.4 Hz, 1H), 8.99 (d, J = 8.9 Hz, 1H), 8.49 (d, J = 8.2 Hz, 1H), 8.28 (d, J = 7.6 Hz, 1H), 8.21 (t, J = 7.5 Hz, 1H), 8.09 (t, J = 7.8 Hz, 1H), 7.85 (d, J = 8.2 Hz, 2H), 7.75 (m, 3H), 7.65 (d, J = 9.0 Hz, 1H), 7.40 (t, J = 7.5 Hz, 1H), 0.13 (s, 9H).

¹³C NMR (100 MHz, CD₃OD) δ 151.05, 146.32, 143.35, 138.24, 137.71, 135.64, 134.15, 131.75, 131.05, 130.63, 130.51, 130.39, 130.33, 128.21, 127.54, 126.74, 126.57, 119.74, 2.10.

¹⁹F NMR (376 MHz, CD₃OD) δ -154.93.

HRMS (ESI) calcd for C₂₇H₂₃NF₃Si (M – BF₄)⁺ 446.1546, found 446.1568.

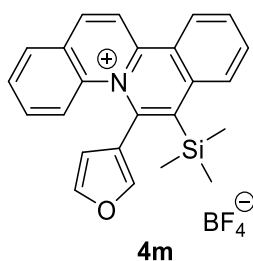


Yellow solid, 58% yield.

¹H NMR (400 MHz, CD₃OD) δ 9.21 (d, J = 9.0 Hz, 1H), 9.09 (d, J = 8.4 Hz, 1H), 9.01 (d, J = 8.9 Hz, 1H), 8.51 (d, J = 8.2 Hz, 1H), 8.38 (d, J = 8.8 Hz, 2H), 8.30 (d, J = 7.5 Hz, 1H), 8.22 (t, J = 7.4 Hz, 1H), 8.11 (t, J = 7.5 Hz, 1H), 7.84 (d, J = 8.5 Hz, 2H), 7.74 (t, J = 7.5 Hz, 1H), 7.64 (d, J = 9.0 Hz, 1H), 7.44 (d, J = 7.4 Hz, 1H), 0.16 (s, 9H).

¹³C NMR (100 MHz, CD₃OD) δ 151.13, 150.34, 145.83, 143.51, 138.15, 137.63, 136.17, 135.71, 134.74, 131.90, 131.34, 130.71, 130.48, 130.42, 128.25, 126.77, 126.61, 125.58, 119.76, 2.21.

HRMS (ESI) calcd for C₂₆H₂₃O₂N₂Si (M – BF₄)⁺ 423.1525, found 423.1537.

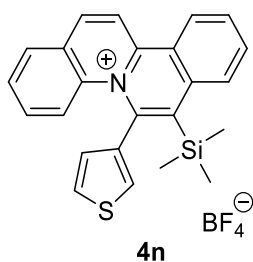


Yellow solid, 68% yield.

$^1\text{H NMR}$ (400 MHz, CD_3OD) δ 9.13 (d, $J = 9.0$ Hz, 1H), 9.02 (d, $J = 8.4$ Hz, 1H), 8.95 (d, $J = 8.9$ Hz, 1H), 8.43 (d, $J = 8.2$ Hz, 1H), 8.29 (d, $J = 8.0$ Hz, 1H), 8.18 (m, 3H), 8.05 (t, $J = 7.7$ Hz, 1H), 7.82 (t, $J = 7.5$ Hz, 1H), 7.68 (s, 1H), 7.60 (d, $J = 8.5$ Hz, 1H), 6.24 (s, 1H), 0.28 (s, 9H).

$^{13}\text{C NMR}$ (100 MHz, CD_3OD) δ 150.81, 147.12, 145.75, 143.10, 139.78, 138.37, 137.89, 136.07, 135.43, 131.46, 131.15, 130.52, 130.42, 130.36, 130.07, 128.14, 126.52, 126.20, 126.15, 119.69, 113.66, 2.35.

HRMS (ESI) calcd for $\text{C}_{24}\text{H}_{22}\text{ONSi}$ ($\text{M} - \text{BF}_4$)⁺ 368.1465, found 368.1455.

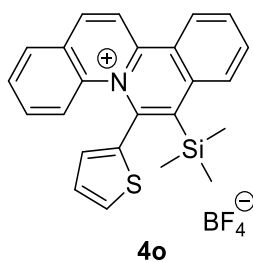


Yellow solid, 65% yield.

$^1\text{H NMR}$ (400 MHz, CD_3OD) δ 9.13 (d, $J = 9.0$ Hz, 1H), 9.03 (d, $J = 8.4$ Hz, 1H), 8.93 (d, $J = 8.9$ Hz, 1H), 8.44 (d, $J = 8.2$ Hz, 1H), 8.26 (d, $J = 7.0$ Hz, 1H), 8.17 (t, $J = 7.3$ Hz, 1H), 8.05 (t, $J = 7.6$ Hz, 1H), 7.94 (dd, $J = 2.8, 1.0$ Hz, 1H), 7.81 (d, $J = 9.0$ Hz, 1H), 7.75 (t, $J = 7.5$ Hz, 1H), 7.59 (dd, $J = 5.0, 3.0$ Hz, 1H), 7.52 – 7.40 (m, 1H), 7.00 (dd, $J = 4.9, 0.8$ Hz, 1H), 0.20 (s, 9H).

$^{13}\text{C NMR}$ (100 MHz, CD_3OD) δ 150.70, 143.06, 143.00, 140.44, 138.44, 138.20, 135.39, 135.35, 132.58, 131.40, 131.21, 130.99, 130.42, 130.35, 130.23, 130.09, 129.38, 128.11, 126.50, 125.36, 119.68, 1.94.

HRMS (ESI) calcd for $\text{C}_{24}\text{H}_{22}\text{NSSi}$ ($\text{M} - \text{BF}_4$)⁺ 384.1237, found 384.1244.



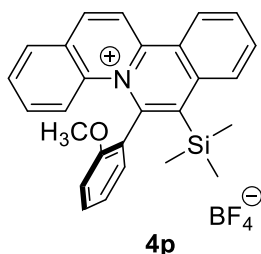
Yellow solid, 62% yield.

$^1\text{H NMR}$ (400 MHz, CD_3OD) δ 9.12 (d, $J = 9.0$ Hz, 1H), 9.02 (d, $J = 8.4$ Hz, 1H), 8.94 (d, $J =$

8.9 Hz, 1H), 8.44 (d, $J = 8.2$ Hz, 1H), 8.27 (d, $J = 7.4$ Hz, 1H), 8.18 (t, $J = 7.5$ Hz, 1H), 8.06 (t, $J = 7.6$ Hz, 1H), 7.99 (d, $J = 9.0$ Hz, 1H), 7.78 (m, 2H), 7.62 (d, $J = 3.1$ Hz, 1H), 7.47 (t, $J = 7.5$ Hz, 1H), 7.28 (dd, $J = 5.0, 3.7$ Hz, 1H), 0.23 (s, 9H).

^{13}C NMR (100 MHz, CD_3OD) δ 143.30, 141.30, 138.45, 138.25, 136.24, 135.51, 132.49, 131.68, 131.18, 130.57, 130.34, 130.20, 129.21, 128.21, 126.78, 124.73, 119.67, 1.83.

HRMS (ESI) calcd for $\text{C}_{24}\text{H}_{22}\text{NSSi}$ ($\text{M} - \text{BF}_4$) $^+$ 384.1237, found 384.1237.

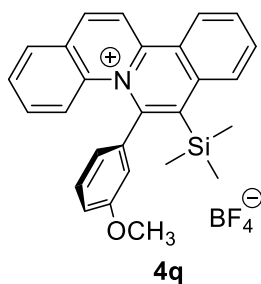


Yellow solid, 63% yield.

^1H NMR (400 MHz, CD_3OD) δ 9.16 (d, $J = 8.9$ Hz, 1H), 9.04 (d, $J = 8.4$ Hz, 1H), 8.97 (d, $J = 8.9$ Hz, 1H), 8.45 (d, $J = 8.2$ Hz, 1H), 8.30 (d, $J = 7.9$ Hz, 1H), 8.19 (t, $J = 7.2$ Hz, 1H), 8.07 (t, $J = 7.8$ Hz, 1H), 7.96 (dd, $J = 7.5, 1.6$ Hz, 1H), 7.81 (d, $J = 9.0$ Hz, 1H), 7.76 (t, $J = 7.5$ Hz, 1H), 7.71 – 7.61 (m, 1H), 7.45 – 7.23 (m, 2H), 6.92 (d, $J = 8.4$ Hz, 1H), 3.17 (s, 3H), 0.13 (s, 9H).

^{13}C NMR (100 MHz, CD_3OD) δ 158.35, 149.84, 142.74, 137.91, 135.86, 135.41, 135.15, 134.70, 131.45, 130.67, 130.46, 130.32, 130.08, 129.90, 128.17, 126.21, 124.44, 122.97, 119.86, 113.09, 102.21, 55.89, 1.87.

HRMS (ESI) calcd for $\text{C}_{27}\text{H}_{26}\text{ONSi}$ ($\text{M} - \text{BF}_4$) $^+$ 408.1788, found 408.1795.

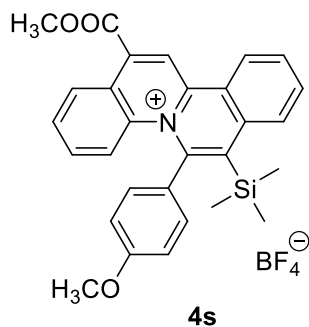


Yellow solid, 61% yield.

^1H NMR (400 MHz, CD_3OD) δ 9.15 (d, $J = 9.0$ Hz, 1H), 9.04 (d, $J = 8.4$ Hz, 1H), 8.94 (d, $J = 8.9$ Hz, 1H), 8.45 (d, $J = 8.2$ Hz, 1H), 8.26 (d, $J = 7.6$ Hz, 1H), 8.18 (t, $J = 7.6$ Hz, 1H), 8.06 (t, $J = 7.7$ Hz, 1H), 7.81 (d, $J = 9.0$ Hz, 1H), 7.73 (t, $J = 7.5$ Hz, 1H), 7.42 (m, 2H), 7.22 – 7.12 (m, 2H), 7.09 (s, 1H), 3.74 (s, 3H), 0.15 (s, 9H).

^{13}C NMR (100 MHz, CD_3OD) δ 162.09, 150.75, 147.85, 143.01, 141.14, 138.43, 138.15, 135.41, 135.02, 131.93, 131.40, 130.80, 130.46, 130.27, 130.18, 130.11, 128.11, 126.49, 126.33, 125.65, 119.67, 118.83, 117.71, 56.11, 2.11.

HRMS (ESI) calcd for $\text{C}_{27}\text{H}_{26}\text{ONSi}$ ($\text{M} - \text{BF}_4$) $^+$ 408.1788, found 408.1794.

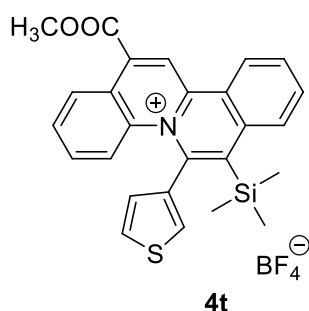


Orange solid, 63% yield.

¹H NMR (400 MHz, CD₃OD) δ 9.48 (s, 1H), 9.10 (d, J = 8.3 Hz, 1H), 8.81 (d, J = 8.1 Hz, 1H), 8.50 (d, J = 8.3 Hz, 1H), 8.23 (t, J = 7.6 Hz, 1H), 8.11 (t, J = 7.5 Hz, 1H), 7.81 (d, J = 9.0 Hz, 1H), 7.74 (t, J = 7.7 Hz, 1H), 7.46 (d, J = 8.3 Hz, 2H), 7.39 (t, J = 7.8 Hz, 1H), 7.07 (d, J = 8.8 Hz, 2H), 4.22 (s, 3H), 3.90 (s, 3H), 0.16 (s, 9H).

¹³C NMR (100 MHz, CD₃OD) δ 165.54, 163.43, 148.87, 139.41, 138.58, 137.39, 136.01, 134.80, 132.36, 131.69, 130.51, 130.45, 130.22, 128.01, 127.75, 127.04, 126.63, 122.05, 116.02, 56.17, 54.30, 2.15.

HRMS (ESI) calcd for C₂₉H₂₈O₃NSi (M – BF₄)⁺ 466.1833, found 466.1815.

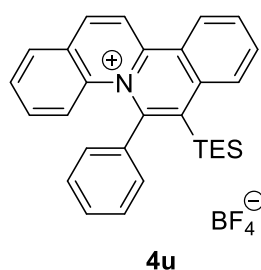


Orange solid, 65% yield.

¹H NMR (400 MHz, CD₃OD) δ 9.49 (s, 1H), 9.10 (d, J = 8.4 Hz, 1H), 8.83 (d, J = 8.1 Hz, 1H), 8.50 (d, J = 8.3 Hz, 1H), 8.24 (t, J = 7.5 Hz, 1H), 8.12 (t, J = 7.7 Hz, 1H), 7.95 (d, J = 1.8 Hz, 1H), 7.90 (d, J = 8.9 Hz, 1H), 7.78 (t, J = 7.6 Hz, 1H), 7.60 (dd, J = 5.0, 3.0 Hz, 1H), 7.45 (t, J = 7.7 Hz, 1H), 7.04 (d, J = 4.6 Hz, 1H), 4.22 (s, 3H), 0.21 (s, 9H).

¹³C NMR (100 MHz, CD₃OD) δ 165.54, 149.78, 143.72, 140.15, 139.18, 138.53, 137.77, 136.02, 132.85, 131.86, 131.20, 130.68, 130.58, 130.50, 129.43, 128.08, 127.71, 127.09, 126.65, 125.91, 122.01, 54.32, 1.88.

HRMS (ESI) calcd for C₂₆H₂₄O₂NSSi (M – BF₄)⁺ 442.1292, found 442.1307.

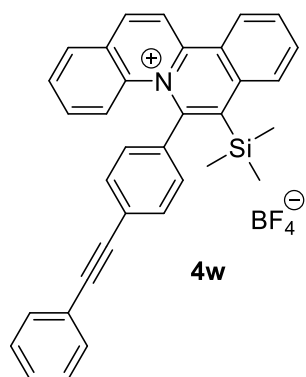


Yellow solid, 45% yield.

¹H NMR (400 MHz, CD₃OD) δ 9.17 (d, J = 8.9 Hz, 1H), 9.05 (d, J = 8.4 Hz, 1H), 8.96 (d, J = 8.9 Hz, 1H), 8.50 (d, J = 8.2 Hz, 1H), 8.30 – 8.14 (m, 2H), 8.07 (t, J = 7.5 Hz, 1H), 7.79 – 7.43 (m, 7H), 7.34 (t, J = 7.4 Hz, 1H), 0.77 (t, J = 7.6 Hz, 9H), 0.63 (q, J = 7.4 Hz, 6H).

¹³C NMR (100 MHz, CD₃OD) δ 150.82, 148.69, 143.36, 140.00, 138.76, 138.18, 135.65, 133.51, 132.26, 131.50, 130.83, 130.51, 130.44, 130.13, 130.07, 128.09, 126.59, 126.24, 119.52, 8.12, 6.59.

HRMS (ESI) calcd for C₂₉H₃₀NSi (M – BF₄)⁺ 420.2148, found 420.2156.

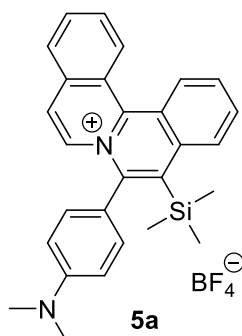


Yellow solid, 46% yield.

¹H NMR (400 MHz, CD₃OD) δ 9.17 (d, J = 9.0 Hz, 1H), 9.06 (d, J = 8.4 Hz, 1H), 8.96 (d, J = 8.9 Hz, 1H), 8.48 (d, J = 8.2 Hz, 1H), 8.28 (d, J = 8.2 Hz, 1H), 8.20 (t, J = 7.7 Hz, 1H), 8.07 (t, J = 7.8 Hz, 1H), 7.74 (m, 2H), 7.66 (d, J = 8.3 Hz, 2H), 7.57 (m, 4H), 7.51 – 7.36 (m, 4H), 0.17 (s, 9H).

¹³C NMR (100 MHz, CD₃OD) δ 150.92, 143.14, 139.80, 137.97, 135.53, 133.74, 133.51, 133.48, 132.73, 131.54, 130.96, 130.55, 130.44, 130.31, 130.23, 130.12, 129.70, 128.88, 128.15, 127.42, 126.69, 123.86, 119.70, 93.14, 88.84, 2.24.

HRMS (ESI) calcd for C₃₄H₂₈NSi (M – BF₄)⁺ 478.1986, found 478.1986.



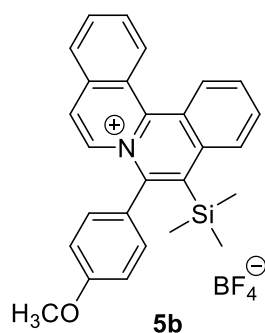
Red solid, 66% yield.

¹H NMR (400 MHz, CD₃OD) δ 9.11 (d, J = 8.5 Hz, 1H), 9.02 (d, J = 8.4 Hz, 1H), 8.55 (m, 2H), 8.30 (d, J = 7.8 Hz, 1H), 8.26 – 8.07 (m, 4H), 8.03 (t, J = 7.8 Hz, 1H), 7.40 (d, J = 8.8 Hz, 2H), C7.01 (d, J = 8.8 Hz, 2H), 3.14 (s, 6H), 0.24 (s, 9H).

¹³C NMR (100 MHz, CD₃OD) δ 153.94, 150.25, 147.51, 139.84, 136.37, 136.05, 134.75, 134.63, 134.50, 133.59, 133.34, 131.81, 130.71, 129.46, 129.40, 128.48, 126.19, 126.00,

122.31, 121.44, 113.42, 40.28, 1.76.

HRMS (ESI) calcd for $C_{28}H_{29}N_2Si$ ($M - BF_4$)⁺ 421.2095, found 421.2082.

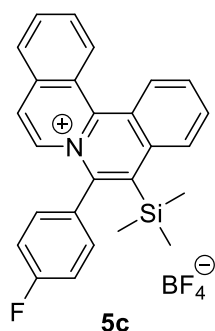


Yellow solid, 50% yield.

1H NMR (400 MHz, CD_3OD) δ 9.12 (d, $J = 8.5$ Hz, 1H), 9.05 (d, $J = 8.5$ Hz, 1H), 8.60 (d, $J = 8.4$ Hz, 1H), 8.40 (d, $J = 7.4$ Hz, 1H), 8.31 (d, $J = 8.0$ Hz, 1H), 8.28 – 7.99 (m, 5H), 7.56 (d, $J = 8.6$ Hz, 2H), 7.28 (d, $J = 8.6$ Hz, 2H), 3.98 (s, 3H), 0.22 (s, 9H).

^{13}C NMR (100 MHz, CD_3OD) δ 163.89, 150.32, 146.30, 139.47, 136.30, 136.19, 135.12, 134.91, 133.75, 133.41, 131.92, 130.95, 129.45, 129.41, 128.53, 127.08, 126.17, 126.09, 122.55, 116.46, 56.24, 1.67.

HRMS (ESI) calcd for $C_{27}H_{26}ONSi$ ($M - BF_4$)⁺ 408.1778, found 408.1801.



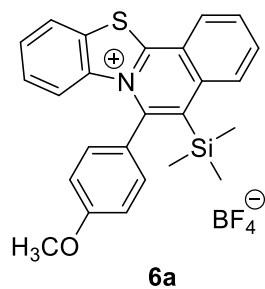
Green solid, 37% yield.

1H NMR (400 MHz, CD_3OD) δ 9.14 (d, $J = 8.5$ Hz, 1H), 9.07 (d, $J = 8.5$ Hz, 1H), 8.62 (d, $J = 8.3$ Hz, 1H), 8.33 (d, $J = 7.4$ Hz, 2H), 8.29 – 8.03 (m, 5H), 7.71 (dd, $J = 8.5, 5.3$ Hz, 2H), 7.51 (t, $J = 8.6$ Hz, 2H), 0.22 (s, 9H).

^{13}C NMR (100 MHz, CD_3OD) δ 167.42, 150.42, 145.13, 139.24, 136.32, 136.12, 136.03, 135.05, 133.87, 133.46, 132.02, 131.48, 131.16, 129.51, 129.43, 128.57, 126.16, 122.76, 118.40, 118.18, 1.62.

^{19}F NMR (376 MHz, CD_3OD) δ -109.61, -154.96.

HRMS (ESI) calcd for $C_{26}H_{23}NFSi$ ($M - BF_4$)⁺ 396.1578, found 396.1594.



White solid, 60% yield.

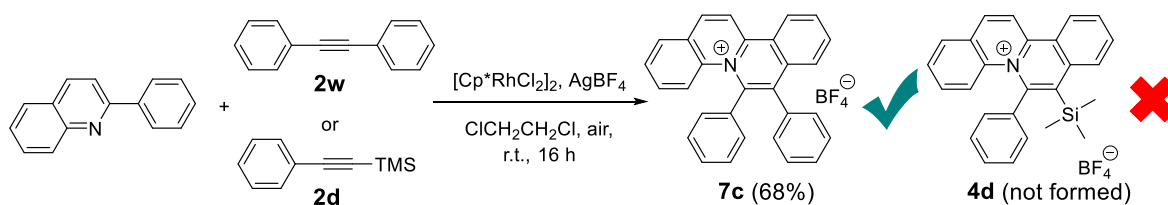
¹H NMR (400 MHz, CD₃OD) δ 8.78 (d, J = 8.1 Hz, 1H), 8.61 (d, J = 8.5 Hz, 1H), 8.46 – 8.30 (m, 1H), 8.29 – 8.15 (m, 1H), 8.08 (t, J = 7.6 Hz, 1H), 7.80 – 7.53 (m, 3H), 7.40 (m, 1H), 7.30 (m, 2H), 6.28 (d, J = 9.1 Hz, 1H), 4.02 (s, 3H), 0.25 (s, 9H).

¹³C NMR (100 MHz, CD₃OD) δ 164.09, 163.24, 147.42, 141.68, 137.60, 136.55, 134.53, 133.76, 131.85, 130.67, 130.29, 129.69, 129.14, 129.00, 128.30, 125.33, 125.14, 122.27, 116.43, 56.33, 2.32.

HRMS (ESI) calcd for C₂₅H₂₄ONSSi (M – BF₄)⁺ 414.1342, found 414.1339.

Rhodium-catalysed synthesis of quinolizinium compounds¹⁻²

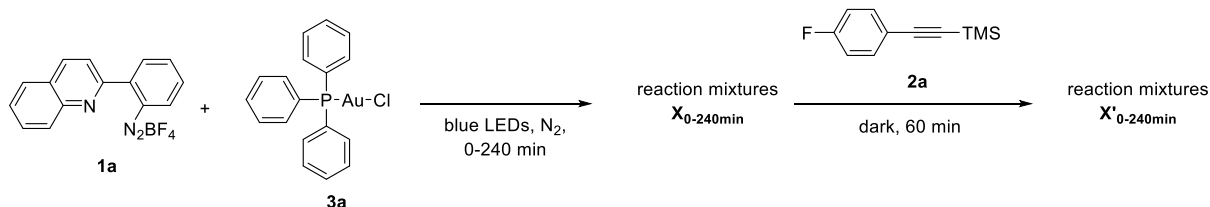
A mixture of 2-phenylquinoline (0.1 mmol, 1 equiv.), alkyne **2w** or **2d** (0.1 mmol, 1 equiv.), [Cp*RhCl₂]₂ (5 mol%), AgBF₄ (0.1 mmol, 1 equiv.) and 5 mL of 1,2-dichloroethane was added into a 20 mL glass bottle. The reaction mixture in the bottle was stirred at room temperature in open air for 16 h. After the reaction completed, the mixture was concentrated under reduced pressure. The resulting residue was purified by flash chromatography on silica gel using CH₂Cl₂/CH₃OH (19:1) as eluent to give the desired product.



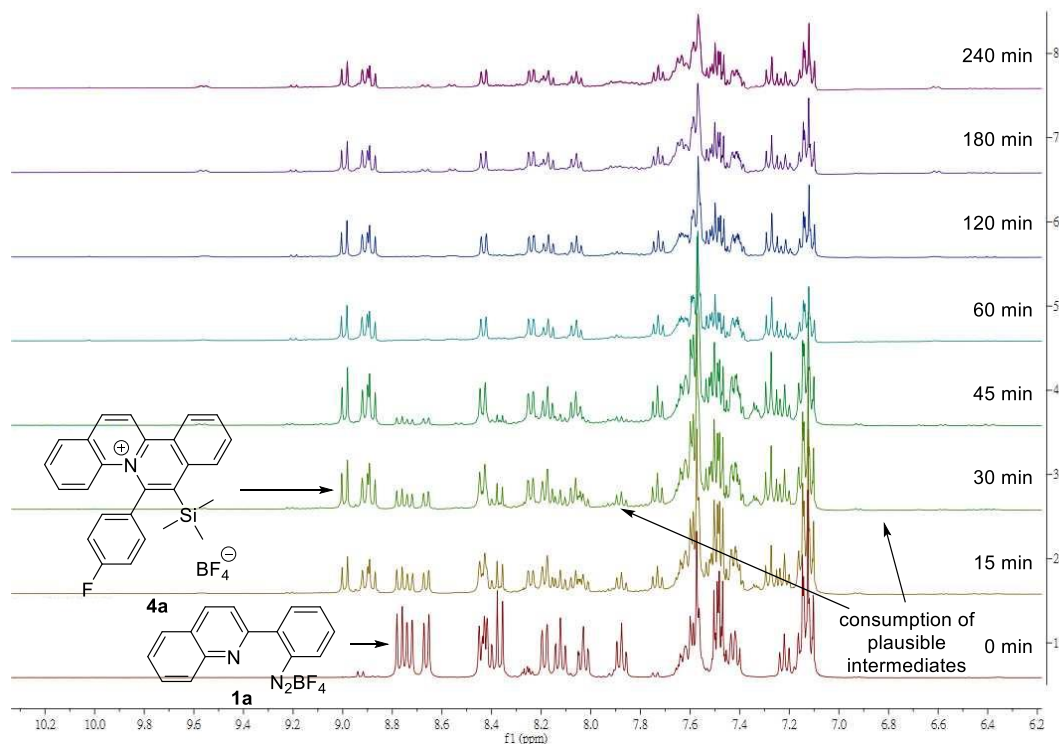
NMR monitoring of plausible intermediates

To monitor the plausible intermediates formed in the reaction, aryl diazonium salt **1a** (0.1 mmol, 1.0 equiv.) was treated with a stoichiometric amount of Au(I) catalyst Ph₃PAuCl **3a** (0.1 mmol, 1.0 equiv.) in 5 mL of CD₃CN in a 20 mL test tube. The test tube capped with a rubber septum was evacuated and refilled with nitrogen three times. After that, the tube with the reaction mixture was irradiated with Blue LEDs for 0 to 240 min. The afforded reaction mixtures **X**_{0-240min} were monitored by ¹H-NMR and ³¹P-NMR analysis.

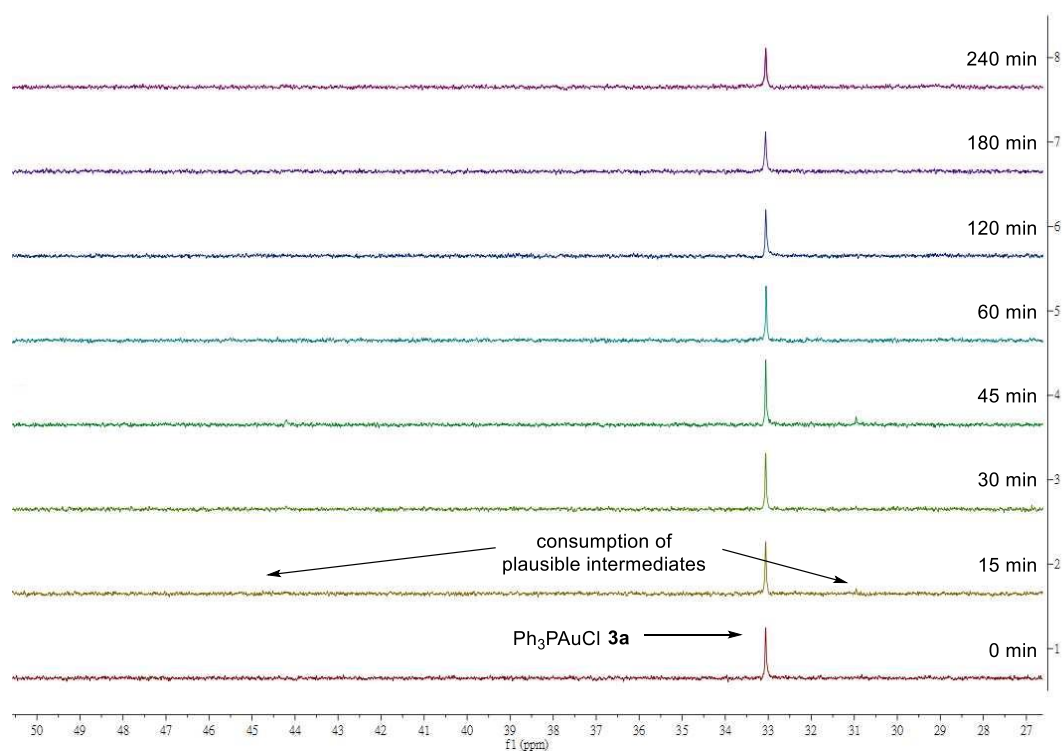
After that, (4-fluorophenylethynyl)trimethylsilane **2a** (0.15 mmol, 1.5 equiv.) was added into the mixtures **X**_{0-240min} respectively and the reaction mixtures were stirred in dark for 60 min. The afforded reaction mixtures **X'**_{0-240min} were monitored by ¹H-NMR and ³¹P-NMR. Yield of the product formation was measured by ¹⁹F-NMR analysis by addition of fluorobenzene (0.1 mmol, 1 equiv.) as internal standard. Filtration of reaction mixture **X'**_{60min} and washing the residue with diethyl ether resulted in recovery of Ph₃PAuCl **3a** in 78% yield as confirmed by NMR analysis.



(a)



(b)



(c)

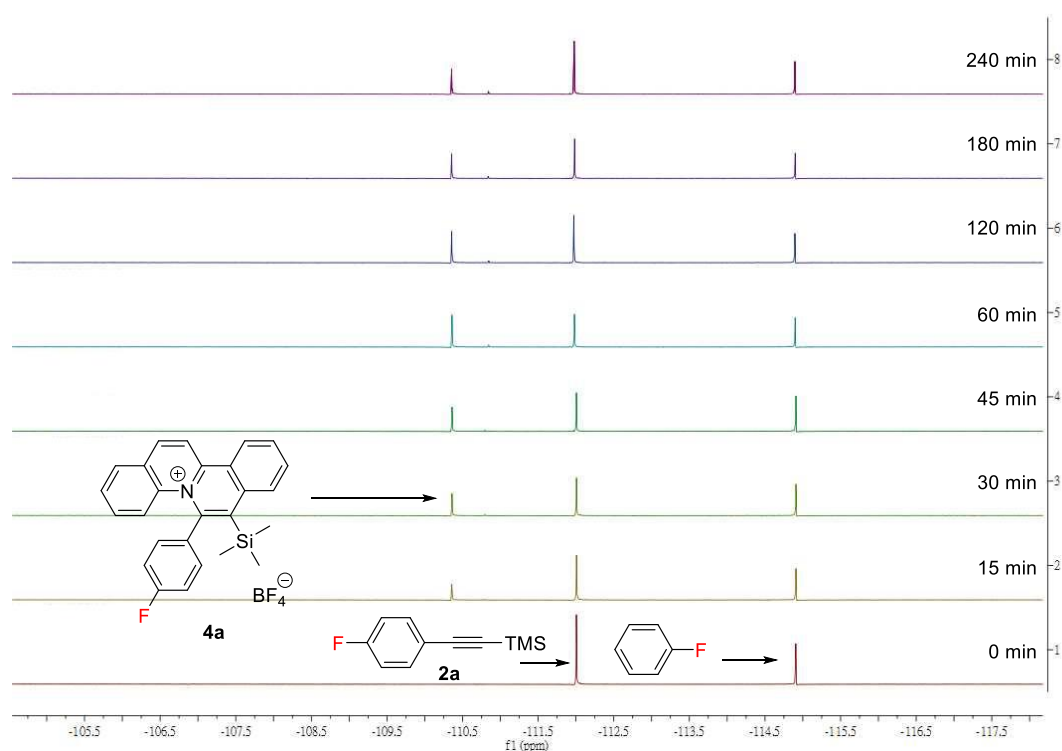


Figure S3 (a) ^1H -NMR studies on reaction mixture $X'_{0-240\text{min}}$ in CD_3CN ; (b) ^{31}P -NMR studies on reaction mixture $X'_{0-240\text{min}}$ in CD_3CN ; (c) ^{19}F -NMR studies on reaction mixture $X'_{0-240\text{min}}$ in CD_3CN .

Table S2 Yield of quinolizinium compound **4a** in reaction mixtures **X'**_{0-240min}.

Reaction mixture	X' _{0min}	X' _{15min}	X' _{30min}	X' _{45min}	X' _{60min}	X' _{120min}	X' _{180min}	X' _{240min}
Yield [%]	0	41	55	66	73	66	59	56

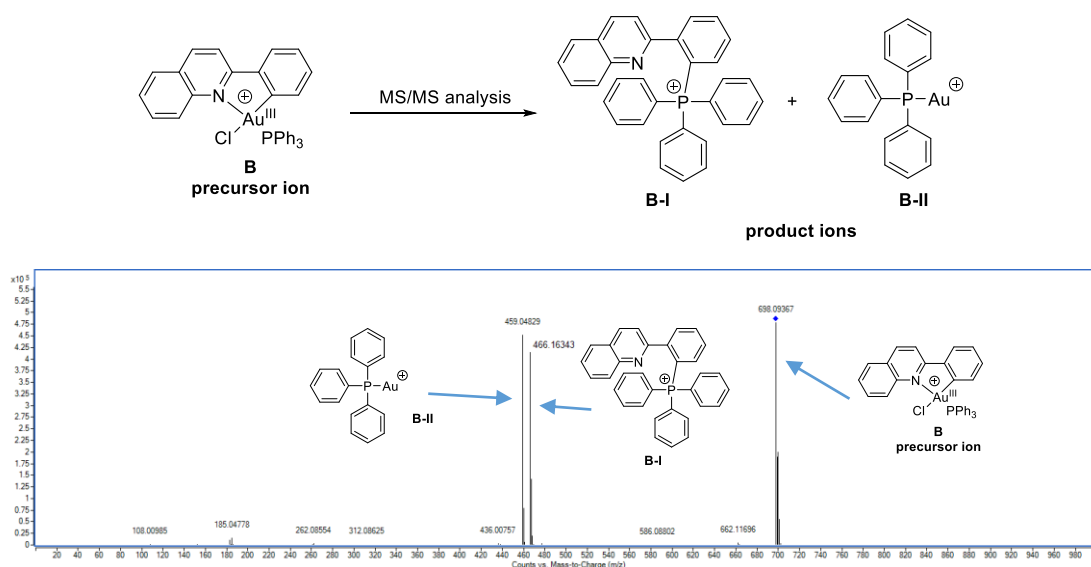
ESI-MS analysis of plausible intermediates

To investigate the plausible reaction intermediates, aryl diazonium salt **1a** (0.1 mmol, 1.0 equiv.) was treated with a stoichiometric amount of Au(I) catalyst Ph₃PAuCl **3a** (0.1 mmol, 1.0 equiv.) in 5 mL of CH₃CN in a 20 mL test tube. The test tube capped with a rubber septum was evacuated and refilled with nitrogen three times. After that, the tube with the reaction mixture was irradiated with Blue LEDs for 1 h. Then, 10 μL of the reaction mixture **Y** was diluted with 1.0 mL of CH₃CN for ESI-MS analysis.

For further investigation, (4-fluorophenylethynyl)trimethylsilane **2a** (0.1 mmol, 1 equiv.) was added into the mixture **Y** and the reaction mixture was kept in dark for 1 h. Then, 10 μL of the afforded mixture **Y'** was diluted with 1.0 mL of CH₃CN for ESI-MS analysis.

For detailed understanding of the plausible Au(III) intermediates **B** and **B'**, ESI-MS/MS analysis of species **B** (precursor ion m/z = 698) and **B'** (precursor ion m/z = 910) was conducted.

(a)



(b)

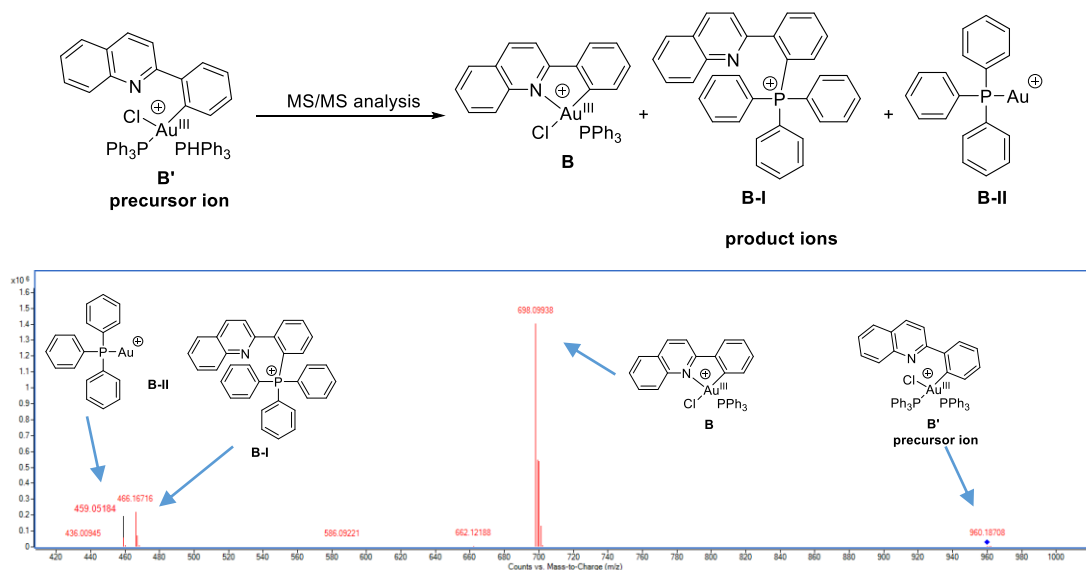
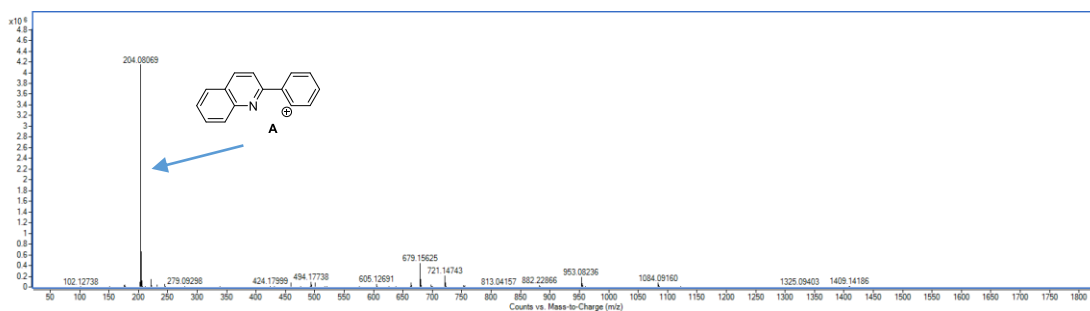
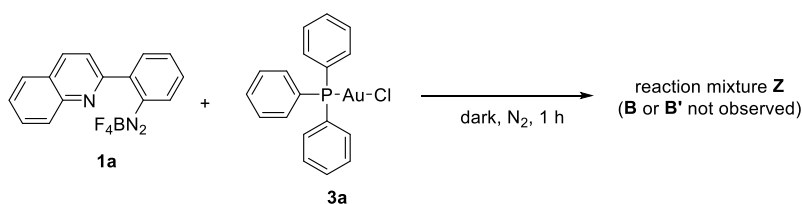


Figure S4 (a) ESI-MS/MS analysis of species **B** (precursor ion m/z = 698.10); (b) ESI-MS/MS analysis of species **B'** (precursor ion m/z = 960.20).

As a control experiment, aryl diazonium salt **1a** (0.1 mmol, 1.0 equiv.) was treated with a stoichiometric amount of Au(I) catalyst Ph₃PAuCl **3a** (0.1 mmol, 1.0 equiv.) in 5 mL of CH₃CN as the aforementioned experimental procedures except that the control experiment was conducted in dark for 1 h. Then, 10 μL of the reaction mixture **Z** was diluted with 1.0 mL of CH₃CN for ESI-MS analysis.

After that, (4-fluorophenylethynyl)trimethylsilane **2a** (0.1 mmol, 1 equiv.) was added into the reaction mixture **Z** and the reaction was conducted in dark for 1 h affording reaction mixture **Z'**. ESI-MS analysis of the reaction mixture **Z'** revealed that no expected quinolizinium product **4a** was observed, indicating that the Au(III) species **B** and **B'** would be the intermediates of this reaction.

(a)



(b)

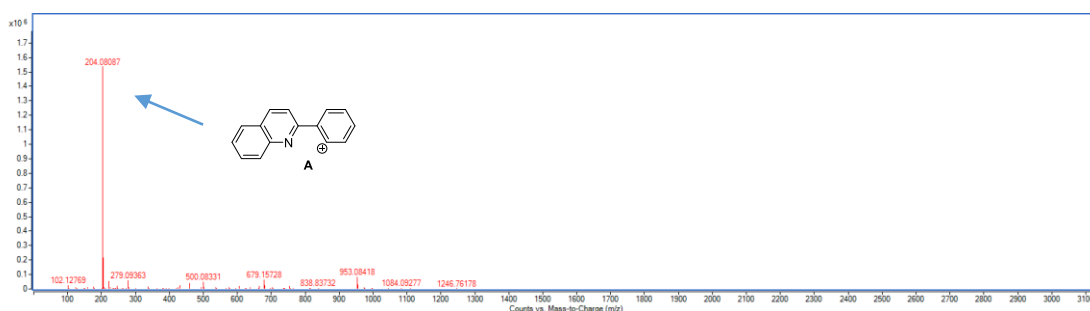
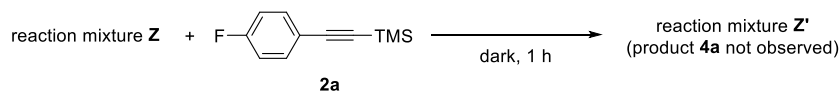
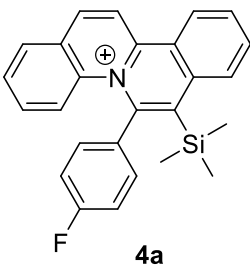
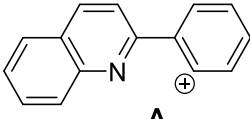
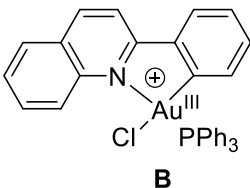
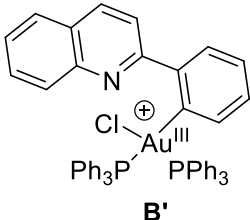
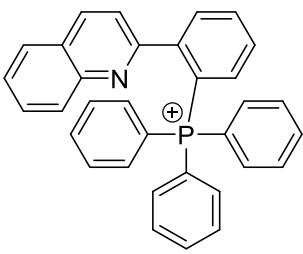
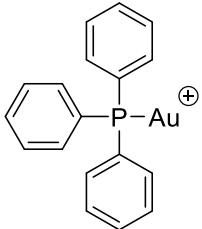


Figure S5 a) ESI-MS analysis of the reaction mixture **Z**; b) ESI-MS analysis of the reaction mixture **Z'**.

Compound	Formula	Calculated m/z
 <p>4a</p>	$C_{26}H_{23}FNSi$	396.1578
 <p>A</p>	$C_{15}H_{10}N$	204.0808
 <p>B</p>	$C_{33}H_{25}AuClNP$	698.1073
 <p>B'</p>	$C_{51}H_{40}AuClNP_2$	960.1985
 <p>B-I</p>	$C_{33}H_{25}NP$	466.1719
 <p>B-II</p>	$C_{18}H_{15}AuP$	459.0571

UV/Vis absorption measurements of Ph₃PAuCl **3a** and aryl diazonium **1a**

The absorption and emission spectra were measured by Cary 8454 UV-Vis Diode Array System and Cary Eclipse Fluorescence Spectrophotometer, respectively, and a final concentration of Ph₃PAuCl **3a**, aryl diazonium **1a** or mixture of aryl diazonium **1a** and Ph₃PAuCl **3a** (1:1) in CH₃CN was diluted to 1×10^{-4} M.

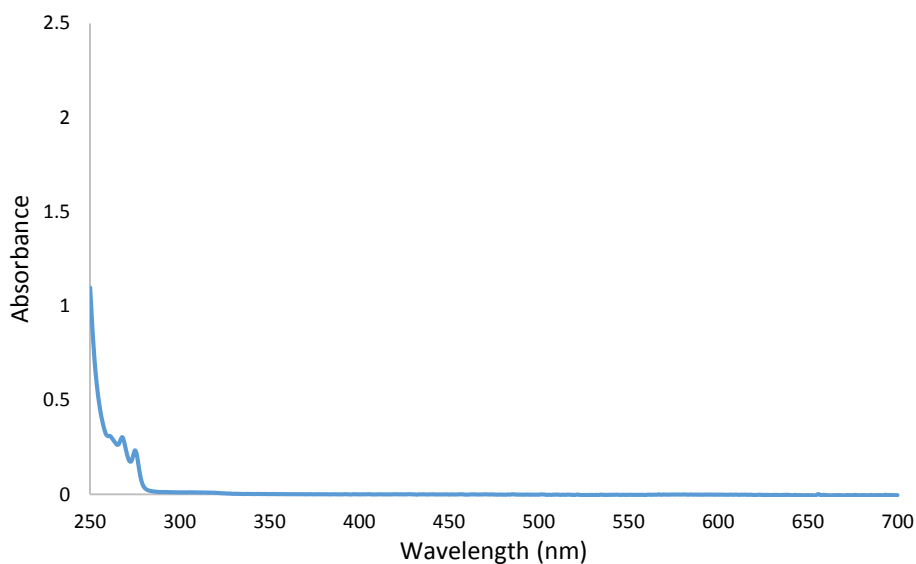


Figure S6 Absorption spectrum of PPh₃AuCl **3a**.

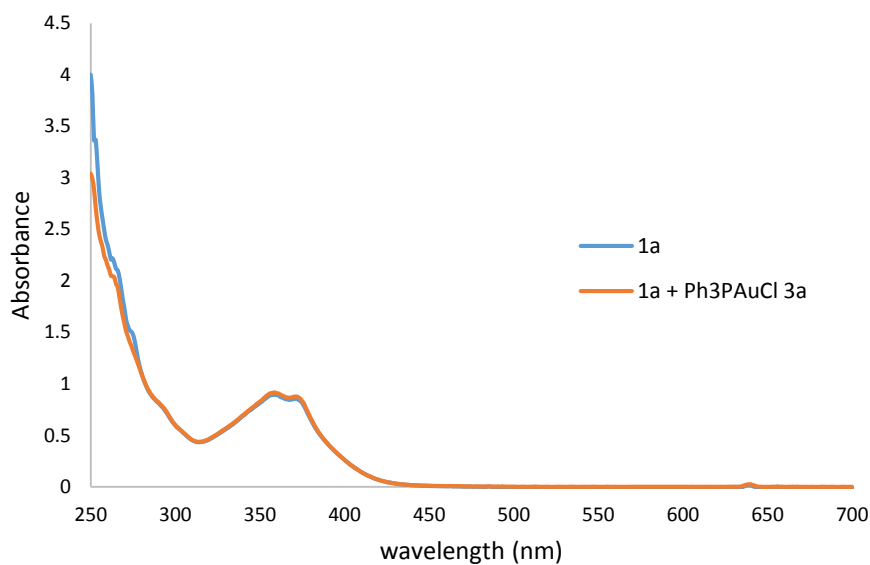


Figure S7 Overlapped spectra of absorption spectrum of aryl diazonium **1a** and a mixture of aryl diazonium **1a** and PPh₃AuCl **3a**.

Photophysical measurements of quinolizinium compounds

The absorption and emission spectra were measured by Cary 8454 UV-Vis Diode Array System and Cary Eclipse Fluorescence Spectrophotometer, respectively, and a final concentration of each quinolizinium compound in CH₂Cl₂ (except for **4i** in H₂O) was diluted to 1 × 10⁻⁵ M. The excitation slit and emission slit for emission measurement were set at 5 nm with scan rate at 120 nm/min and medium PMT voltage. Fluorescent quantum yield of each compound was determined by a comparative method employing fluorescein (Φ = 0.95 in 0.1 N NaOH solution) as standard and calculated with the following equation.³

$$\Phi_{sample} = \Phi_{standard} \times \frac{F_{sample}}{F_{standard}} \times \left(\frac{n_{sample}}{n_{standard}} \right)^2 \times \frac{Abs_{sample}}{Abs_{standard}}$$

Table S3 Photophysical properties of compounds **4a-q, s-u, w, 5a-c** and **6a**.

Compound	UV/Vis absorption	Emission	Stokes shift (cm ⁻¹)	Quantum yield
	λ _{abs} (nm) (ε (10 ⁴ dm ³ mol ⁻¹ cm ⁻¹))	mamximum λ _{em} (nm)		
4a	291 (5.11), 374 (1.51), 430 (1.14)	569	5681	0.17
4b	290 (3.55), 364 (0.89), 428 (1.10)	507	3640	0.44
4c	289 (4.00), 358 (0.90), 423 (1.45)	491	3275	0.44
4d	289 (4.13), 360 (0.87), 423 (1.39)	495	3439	0.49
4e	290 (5.16), 361 (1.21), 424 (1.62)	494	3342	0.37
4f	290 (3.21), 363 (0.67), 422 (0.95)	493	3413	0.16
4g	292 (3.49), 388 (0.82), 424 (1.00)	493	3301	0.03
4h	291 (2.98), 360 (0.62), 423 (1.06)	480	2807	0.28
4i	286 (2.51), 350 (0.49), 417 (0.75)	484	3320	0.44
4j	294 (3.46), 420 (1.30)	479	2933	0.28
4k	289 (2.73), 361 (0.69), 420 (1.17)	479	2933	0.34
4l	294 (2.66), 304 (2.75), 354 (0.71), 419 (1.23)	476	2858	0.24
4m	287 (5.89), 363 (1.22), 423 (1.45)	506	3878	0.18
4n	286 (6.76), 363 (1.43), 424 (1.68)	508	3900	0.16
4o	281 (6.77), 368 (1.56), 428 (1.43)	547	5363	0.02

4p	285 (6.85), 372 (1.38), 421 (1.50)	511	4183	0.11
4q	285 (7.33), 364 (1.46), 423 (1.80)	511	4071	0.16
4s	290 (3.44), 395 (1.19), 446 (0.79)	640	6797	0.01
4t	296 (2.90), 388 (0.86), 446 (1.05)	557	4468	0.08
4u	290 (3.56), 360 (1.11), 424 (1.42)	494	3342	0.41
4w	293 (5.03), 320 (4.28), 427 (1.05)	555	5401	0.07
5a	289 (7.13), 378 (2.72), 397 (1.74)	495	4987	0.02
5b	292 (4.68), 388 (1.09), 405 (1.23)	504	4850	0.30
5c	292 (3.38), 383 (0.99), 401 (1.09)	450	2840	0.59
6a	275 (2.23), 337 (1.28), 364 (0.87), 380 (1.10)	487	5782	0.02

Investigation of the solvent effect on the UV/Vis absorption and emission properties of compound **4b**

Solvent effect of the photophysical properties of **4b** was interpreted in terms of the Lippert-Mataga plot which correlates Stokes shift $\Delta\nu$ and orientation polarizability Δf of the compound and indicates the dipole moment change ($\Delta\mu$) between ground state (μ_g) and excited state (μ_e).⁴ Orientation polarizability Δf was calculated following the equation below, where ϵ is dielectric constant and n is refractive index of the solvent.

$$\Delta\nu = \nu_{abs} - \nu_{em} = \frac{2}{hc} \Delta f \frac{(\mu_e - \mu_g)}{a^3} = \frac{2}{hc} \left(\frac{\epsilon - 1}{2\epsilon + 1} - \frac{n^2 - 1}{2n^2 + 1} \right) \frac{(\mu_e - \mu_g)}{a^3}$$

For spectroscopic measurement, **4b** was directly diluted to 1×10^{-5} M in different solvents and the experimental details followed the aforementioned procedures. Results were summarized in the following figure.

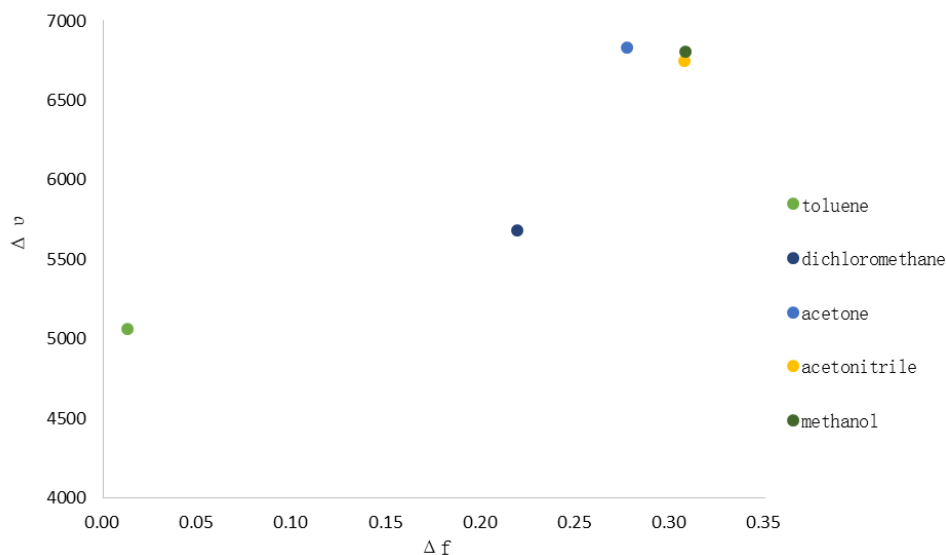


Figure S8 Plot of Stokes shift ($\Delta\nu$) versus orientation polarizability (Δf) for **4b**.

Investigation of the effect of pH on the emission properties of compound **5a**

To investigate the effect of pH on the emission properties of compound **5a**, 2 M HCl/NaOH buffer with different pH values were prepared by mixing 2 M HCl_(aq) solution and 2 M NaOH_(aq) solution monitored by a pH meter. Compound **5a** was firstly weighted and diluted to 2×10^{-4} M in CH₃CN. After that, it was further diluted with 2 M HCl/NaOH buffer with different pH values to 1×10^{-5} M in 2 M HCl/NaOH buffer/CH₃CN (19:1) for measurement. The experimental details followed the aforementioned procedures. Results were summarized in the following figure.

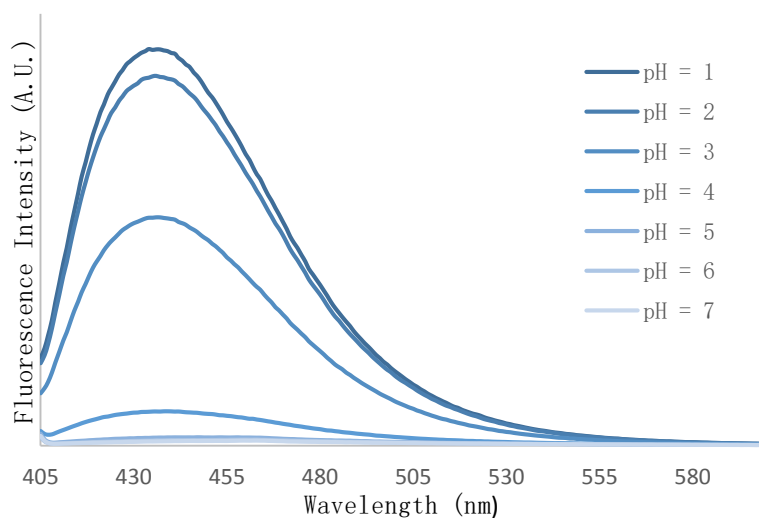


Figure S9 Plot of fluorescent intensity of **5a** versus change of pH values.

Electrochemical measurements of quinolizinium compounds

All CV experiments were recorded on a Bioanalytical Systems (BAS) at room temperature with the use of a conventional two-compartment cell separated with a sintered glass disc. All the experiments were performed using 0.1 M tetrabutylammonium hexafluorophosphate (TBHP) in HPLC graded acetonitrile (Labscan) as supporting electrolyte, and the solvent was used without further purification. The electrodes used in the experiments were as follows: a glassy carbon electrode of area 0.07 cm² (BAS M2070) was used as working electrode and was polished sequentially with 0.1 and 0.05 mm alumina (Buehler) on a micro-cloth, and rinsed with deionized water before use; a Pt wire was used as counter electrode; a Ag/AgNO₃ (0.1 M AgNO₃ in acetonitrile) was used as reference electrode without regard of the liquid-junction potential. The sample solutions in the experiments were deoxygenated by purging Ar for at least 10 minutes. The sweep rate in the experiments was 100 mV/s, and ferrocene was used as internal standard unless otherwise stated.

Table S4 Electrochemical data of **4a, b, e, f, j, p, 5a, c** and **1a**

Compound	E _{red} (V) vs FeCp ₂	E _{red} (V) vs SCE ^a	E _{ox} (V) vs FeCp ₂	E _{ox} (V) vs SCE ^a
4a	-1.04 ^b	-0.64	-	-
4b	-1.05 ^b	-0.65	-	-
4e	-1.01 ^b	-0.61	-	-
4f	-1.02 ^b	-0.62	-	-
4j	-1.01 ^b	-0.61	-	-
4p	-1.09 ^b	-0.69	-	-
5a	-1.30 ^c	-0.90	0.68 ^c	1.08
5c	-1.30 ^c	-0.90	-	-
1a	-0.21	0.19	-	-

^a E_{red} (vs SCE) = E_{red} (vs FeCp₂) + 0.40 V.

^b E_{red} refers to the anodic peak potential for the irreversible reduction wave.

^c E_{red} or E_{ox} refers to E_{1/2} = (E_{pa} + E_{pc})/2; E_{pa} or E_{pc} refers to the anodic or cathodic peak potential for the reversible or quasireversible reduction or oxidation wave.

Table S5 Excited state electrochemical properties of **4a, b, e, f, j, p** and **1a**

compound	E _{red} (V) vs SCE	E ₀₋₀ (V) ^a	E* _{red} (V) vs SCE ^b
4a	-0.64	2.83	1.99
4b	-0.65	2.62	1.97
4e	-0.61	2.82	2.21
4f	-0.62	2.84	2.22
4j	-0.61	2.85	2.24
4p	-0.69	2.76	2.07
1a	0.19	3.09	3.28

^a E₀₋₀ is estimated from λ of the intersection point between normalized absorbance and emission spectra.

^b E*_{red} = E_{red} + E₀₋₀.

Photooxidative amidation of aldehydes with secondary amines

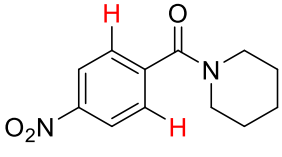
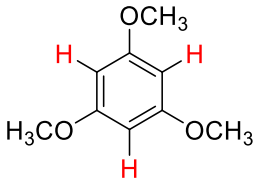
A mixture of aldehydes **8a-d** (0.1 mmol, 1.0 equiv.), secondary amines **9a-d** (0.2 mmol, 2.0 equiv.), anhydrous Na₂CO₃ (0.2 mmol, 2.0 equiv.), photocatalysts (5 mol%) and 5 mL of CH₃CN was added into a 20 mL test tube in open air. The reaction was conducted under irradiation with Blue LEDs for 16-48 h. After the reaction, the reaction mixture was concentrated under reduced pressure.

To scale up the reaction, A mixture of aldehydes **8a** (1 mmol, 1.0 equiv.), secondary amines **9a** (2 mmol, 2.0 equiv.), anhydrous Na₂CO₃ (2 mmol, 2.0 equiv.), photocatalysts (5 mol%) and 5 mL of CH₃CN was conducted under the same reaction conditions for 48 h. After that, the reaction mixture was concentrated under reduced pressure.

For determination of the NMR yield, 1.0 mL of internal standard 1,3,5-trimethoxybenzene in CDCl₃ (0.03 M) was mixed with the resulting residue for ¹H NMR analysis.

For product isolation, the resulting residue was purified by flash chromatography on silica gel using EtOAc/hexane as eluent to give the desired product.

Table S6 Chemical shifts of compounds in CDCl₃

Compound	Chemical shift (σ) of the H in ¹ H NMR
 10a	7.56
	6.09

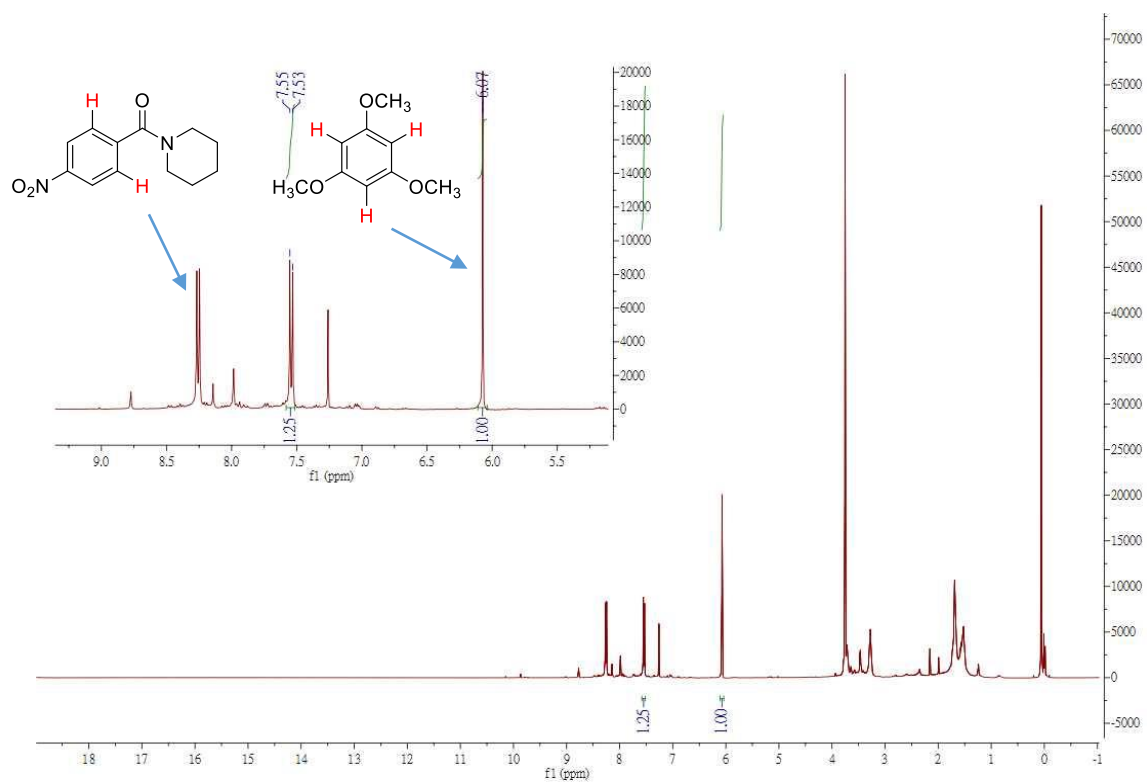


Figure S10 Determination of the NMR yield of **9a** (61%) when **2e** was employed as photocatalyst and 1,3,5-trimethoxybenzene was used as internal standard.

Determination of the reaction quantum yield

The reaction quantum yield (Φ_R) of visible light-mediated gold-catalysed difunctionalization was measured by chemical actinometry following a modified procedure reported by Melchiorre^{5a} and Glorius^{5b}. The number of moles of photons absorbed (n_p) was related to the number of moles of $\text{Fe}(\text{phen})_3^{2+}$ complexes formed (n_{Fe}) from photodecomposition of ferric oxalate anions and further coordination with 1,10-phenanthroline. n_{Fe} was determined *via* measurement of the absorbance of $\text{Fe}(\text{phen})_3^{2+}$ complexes containing solution at $\lambda_{\text{abs}} = 510$ nm and calculation based on Beer's law. Detailed procedures were listed below:

1. Preparation of the solutions:

- (1) Actinometer solution: a mixture of potassium ferrioxalate trihydrate (295 mg) and concentrated (95-98%) H_2SO_4 (140 μL) was diluted with Milli-Q[®] H_2O to the mark of a 50 mL volumetric flask. Then, for each measurement, 5 mL of the actinometer solution was transferred into a 20 mL test tube for irradiation. The preparation was conducted in dark environment.
- (2) Buffer solution: a mixture of NaOAc (2.45 g) and concentrated (95-98%) H_2SO_4 (0.5 mL) was diluted with Milli-Q[®] H_2O to the mark of a 50 mL volumetric flask.
- (3) Reaction solution: for each measurement, a mixture of aryl diazonium **1a** (3 equiv.), silyl substituted alkynes (1 equiv.), Ph_3PAuCl (15 mol%) and 5 mL of CH_3CN was added into a 20 mL test tube. The test tube capped with a rubber septum was evacuated and refilled with nitrogen three times.

2. Irradiation of the actinometer solution and reaction solution.

For each measurement, one test tube of actinometer solution and one test tube of reaction solution were placed into the reaction vessels in the "light box". The tubes with solutions were irradiated under blue LEDs for 150 s. The same process was repeated for different time intervals: 300 s and 450 s.

3. Determination of the number of moles of photons absorbed (n_p).

After irradiation, 1 mL of the irradiated actinometer solution was transferred from the test tube (with 5 mL of solution) to a 10 mL volumetric flask containing 2 mg of 1,10-phenanthroline in 2 mL of buffer solution. Then, the mixture was further diluted with Milli-Q[®] H_2O to the mark. For preparation of a blank solution, 1 mL of the actinometer solution (in dark) was transferred to a 10 mL volumetric flask containing 2 mg of 1,10-phenanthroline in 2 mL of buffer solution and further filled to the mark with Milli-Q[®] H_2O . After that, the absorbance of these solutions at $\lambda_{\text{abs}} = 510$ nm were measured by Cary 8454 UV-Vis Diode Array System using the blank solution as "blank" during the measurement. The number of moles of photons absorbed (n_p) was determined based on the number of moles of $\text{Fe}(\text{phen})_3^{2+}$ complexes formed (n_{Fe}) following the Beer's law,

$$n_p = n_{\text{Fe}} = \frac{V_1 V_3 A}{10^3 \cdot V_2 l \epsilon}$$

where V_1 is the irradiated volume (5 mL), V_2 is the aliquot of the irradiated solution taken for the determination of the ferrous ions (1 mL), V_3 is the final volume after complexation with 1,10-phenanthroline (10 mL), l is the optical path-length of the irradiation cell (1 cm), A (510 nm) is the absorbance measured at $\lambda_{\text{abs}} = 510$ nm, ϵ (510 nm) is that of the complex $\text{Fe}(\text{phen})_3^{2+}$ (11100 $\text{Lmol}^{-1}\text{cm}^{-1}$).

4. Determination of the number of moles of quinolizinium **4a** formed (n_q).

The number of moles of quinolizinium **4a** formed (n_q) was determined by ^{19}F -NMR using fluorobenzene as internal standard following the procedure mentioned before.

5. Calculation of the reaction quantum yield (Φ_R).

The number of moles of quinolizinium **4a** formed (n_q) was plotted against the number of moles of photons absorbed (n_p) as below. **The reaction quantum yield calculated was $\Phi_R = 0.91$.**

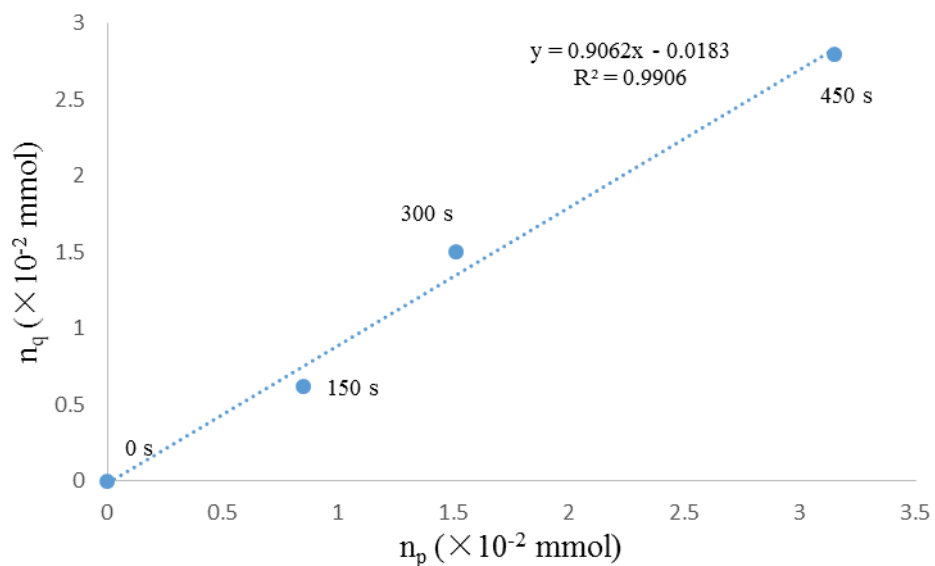


Figure S11 Moles of product **4a** formed per photon absorbed.

TD-DFT calculation of quinolizinium compound **4d**

All calculations were performed using ORCA software package (version 3.03).⁶ DFT geometry optimization on -H was performed using B3LYP functional.⁷⁻⁸ Def2-SVP basis sets were used for the all atoms.⁹ Auxiliary basis sets, used to expand the electron density in the calculation, were chosen to match the orbital basis sets.¹⁰ The combination of the resolution of the identity and the “chain of spheres exchange” algorithms (RIJCOSX) was used to accelerate all calculations.¹¹ Frequency calculations were performed for the optimized structures. No imaginary vibrational frequency was encountered confirming the optimized stationary point to be local minimum. Tight SCF convergence criteria (1×10^{-8} E_h in energy, 1×10^{-7} E_h in the density charge and 1×10^{-7} in the maximum element of the DIIS error vector) was used throughout. TD-DFT calculation was performed with the same functional and same basis sets used that for geometry optimization and with the Tamm-Dancoff approximation. The conductor-like screening model (COSMO) was used to model solvation in CH₂Cl₂.¹²

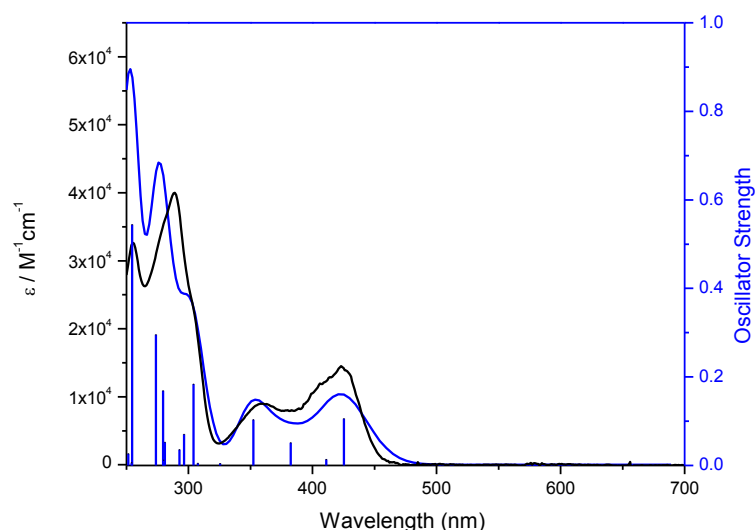


Figure S12 UV-visible absorption spectrum (black line) and TD-DFT calculated absorption spectrum (blue line) for compound **4d** in CH₂Cl₂. Excitation energies are shown by the blue vertical line; the spectrum is convoluted with a Gaussian function having a full width at half-maximum of 2500 cm⁻¹.

According to TD-DFT calculation, the low energy absorption band of **4d** at 435 nm is originated from HOMO→LUMO. HOMO is composed of π orbital of quinolizinium and phenyl ring whereas LUMO is composed of π^* of quinolizinium ring. Hence, the low energy absorption band can be assigned as admixture of $\pi \rightarrow \pi^*$ transition within the quinolizinium ring and $\pi \rightarrow \pi^*$ transition from phenyl to quinolizinium ring.

The absorption band of **4d** at 352 nm is originated from HOMO-2→LUMO in which HOMO-2 is composed of π orbital of quinolizinium ring. This transition is assigned as $\pi \rightarrow \pi^*$ transition within the quinolizinium ring. The corresponding molecular orbitals and electronic difference density plots are shown in **Figure S13-S17**.

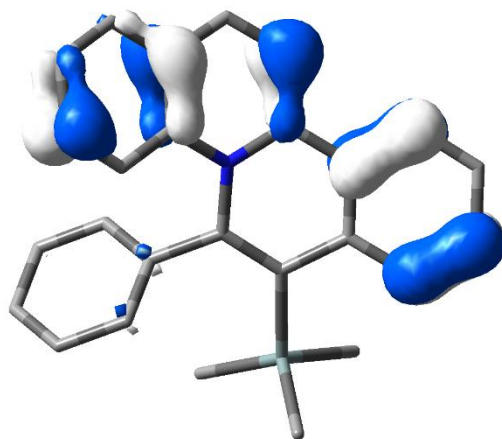


Figure S13 Molecular orbital of HOMO-2 of compound **4d** (isovalue = 0.05).

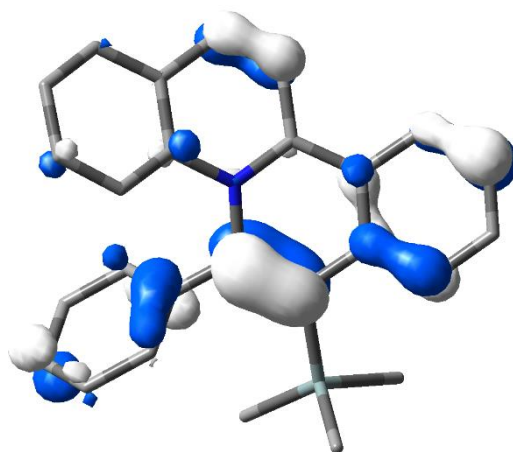


Figure S14 Molecular orbital of HOMO of compound **4d** (isovalue = 0.05).

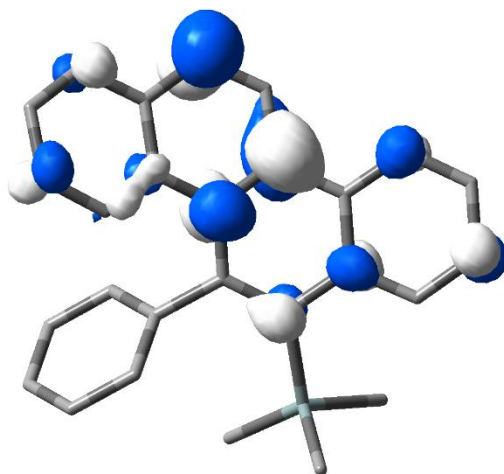


Figure S15 Molecular orbital of HOMO-2 of compound **4d** (isovalue = 0.05).

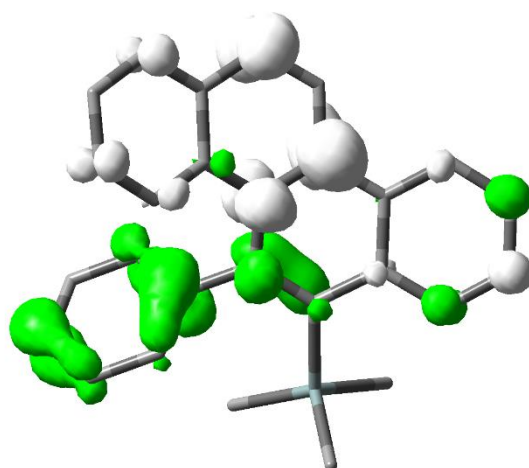


Figure S16 Electronic difference density plots responsible for low energy absorption of compound **4d** at 425 nm (isodensity value = 0.003 au; charge accumulation and depletion are represented in white and green respectively).

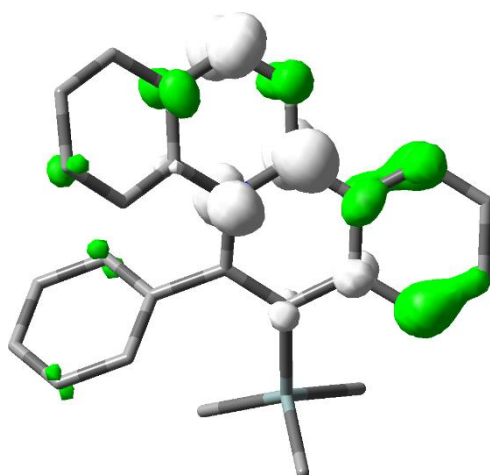


Figure S17 Electronic difference density plots responsible for low energy absorption of compound **4d** at 352 nm (isodensity value = 0.003 au; charge accumulation and depletion are represented in white and green respectively).

Optimized geometry of compound 4d

C	2.28433	0.95279	0.05103
C	0.28525	2.22388	0.50604
C	1.08877	3.37981	0.71833
C	2.45203	3.30665	0.71637
C	0.13970	-0.19756	0.64647
C	-1.14505	2.29670	0.37664
C	-1.88575	1.08336	0.26104
C	-1.23993	-0.16920	0.62249
C	-3.24377	1.17105	-0.13056

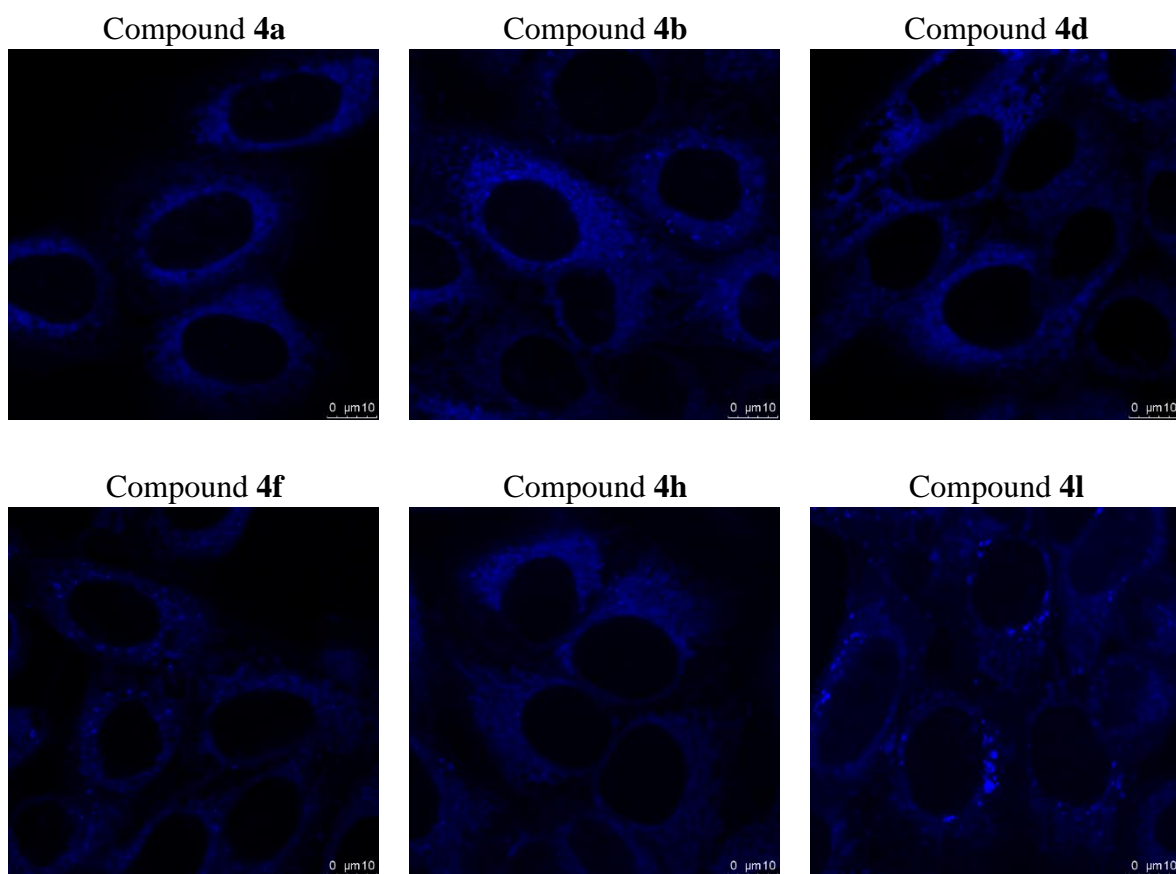
H	-3.80838	0.25940	-0.31409
C	-3.86416	2.39610	-0.30361
C	-3.15415	3.59319	-0.08003
C	-1.81323	3.54470	0.24734
H	0.59143	4.32547	0.91736
H	-4.90906	2.43537	-0.62007
H	-3.65455	4.55676	-0.19832
H	-1.26884	4.48113	0.36163
N	0.89729	0.99403	0.38476
C	3.08944	2.09783	0.31720
C	4.48420	2.04883	0.07152
C	5.05997	0.93007	-0.49904
H	6.13188	0.90121	-0.70607
C	2.87668	-0.15037	-0.59513
H	2.27608	-0.99588	-0.91319
C	4.23902	-0.15392	-0.86556
H	5.08403	2.93092	0.30878
H	4.67392	-1.01226	-1.38315
H	3.05776	4.18650	0.94612
Si	-2.41313	-1.60164	1.30413
C	-3.80189	-0.78316	2.30314
H	-4.58544	-0.27898	1.70770
H	-4.29653	-1.58504	2.88451
H	-3.40283	-0.04821	3.03354
C	-1.58290	-2.76475	2.53626
H	-0.89812	-3.49705	2.08050
H	-1.02953	-2.21568	3.32102
H	-2.39312	-3.32632	3.03452
C	-3.11532	-2.57473	-0.15810
H	-3.82633	-3.33041	0.21827
H	-3.65885	-1.94202	-0.88007
H	-2.32720	-3.11237	-0.71302
C	0.92034	-1.39903	1.06797
C	1.75127	-1.33654	2.20155
C	0.82875	-2.60804	0.35781
C	2.46332	-2.46146	2.62187
H	1.83806	-0.40409	2.76591
C	1.55016	-3.73073	0.77336
H	0.19924	-2.66514	-0.53357
C	2.36761	-3.66073	1.90677
H	3.09137	-2.40171	3.51417
H	1.46771	-4.66432	0.21127
H	2.92717	-4.53928	2.23729

Cell culture

HeLa cells were cultured in Dulbecco's modified essential medium (DMEM) supplemented with 10% fetal bovine serum (FBS), 100 U/mL penicillin and 100 g/mL streptomycin. Cells were maintained in a humidified 37 °C incubator with 5% CO₂.

Cellular localization study

The cellular localization of fluorescent dyes was determined by the colocalization of organelle specific dyes including ER-Tracker™ Red (Endoplasmic reticulum specific dye, Invitrogen), MitoTracker® Red (Mitochondria specific dye, Invitrogen), LysoTracker® Deep Red (Lysosome specific dye, Invitrogen) and BODIPY® TR ceramide (Golgi specific dye, Invitrogen). Alternatively, Rab5-RFP and Rab7-RFP cDNA were expressed in HeLa cells, which specifically labelled early endosomes and late endosome formation. For the organelle specific dye, fluorescent dyes (2 μM) and organelle specific dyes (concentration follows the protocols from the supplier) were added to the culture dish. The cells were incubated for 2 h prior to analysis by confocal microscope (Leica TCS SP8). For cDNA expression, cells were transfected with cDNA *via* ViaFect™ Transfection Reagent and incubated for 24 h. Fluorescent dyes (2 μM) were added to the culture dish and incubated for 2 h. The cells were analyzed as before.



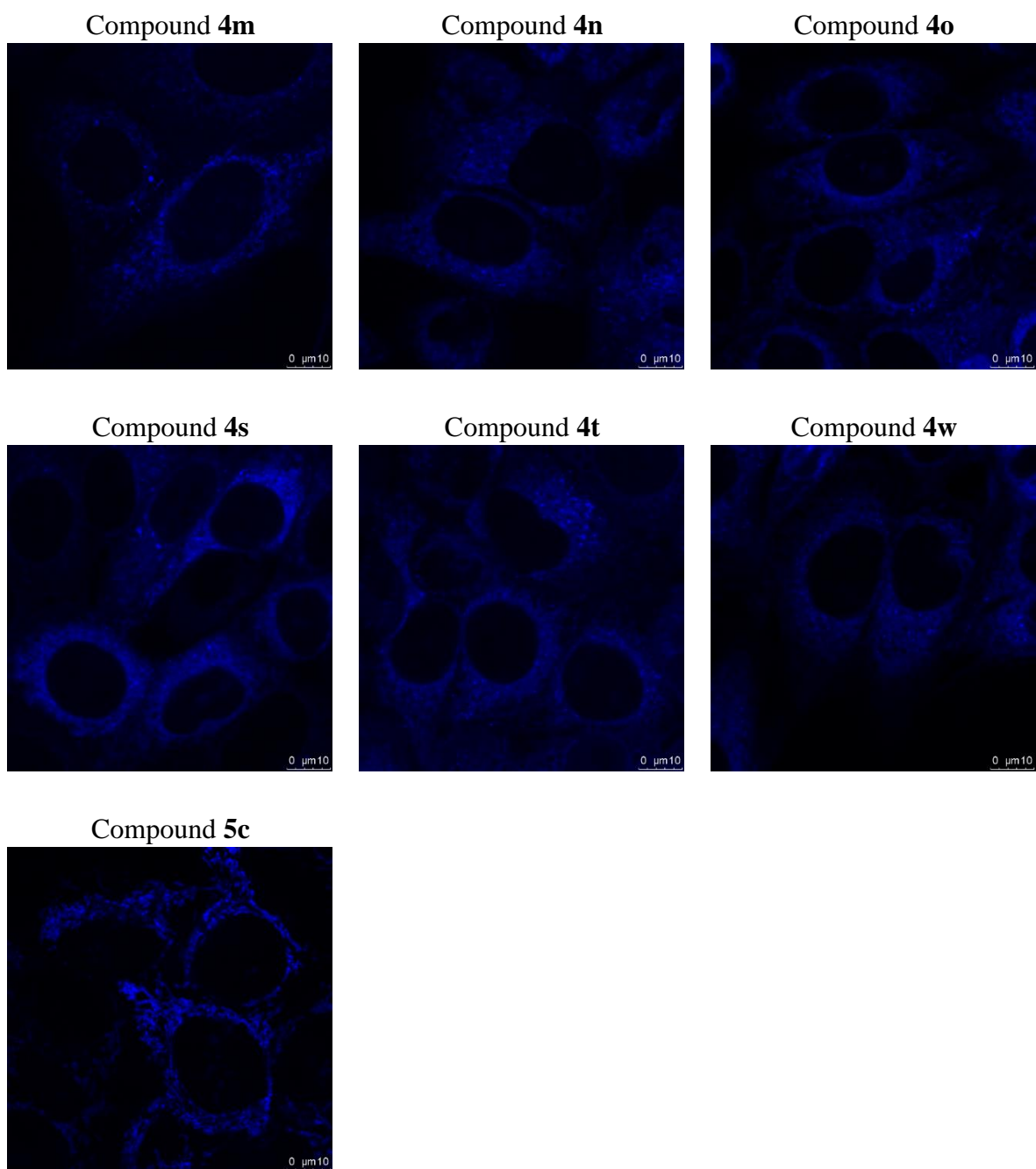
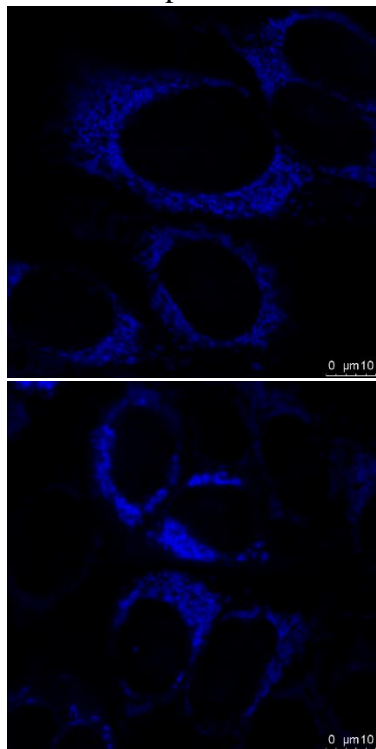
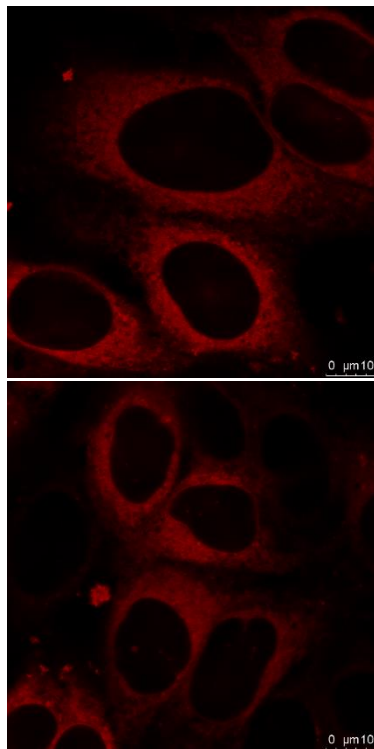


Figure S18 Confocal fluorescence microscopic images of HeLa cells with quinolizinium compounds **4a-b**, **d-f**, **h**, **l-o**, **s-t**, **y** and **5c**.

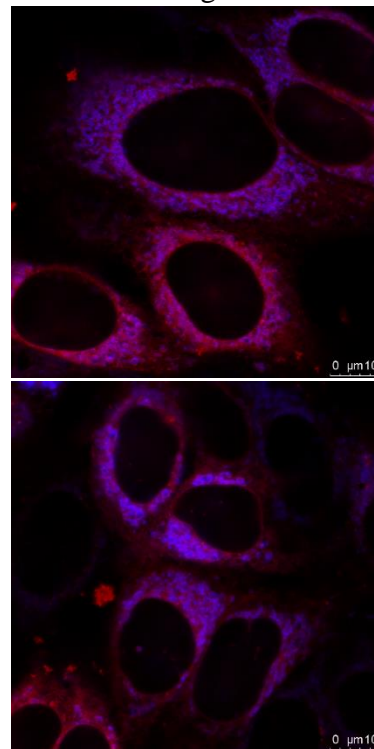
Compound 5c



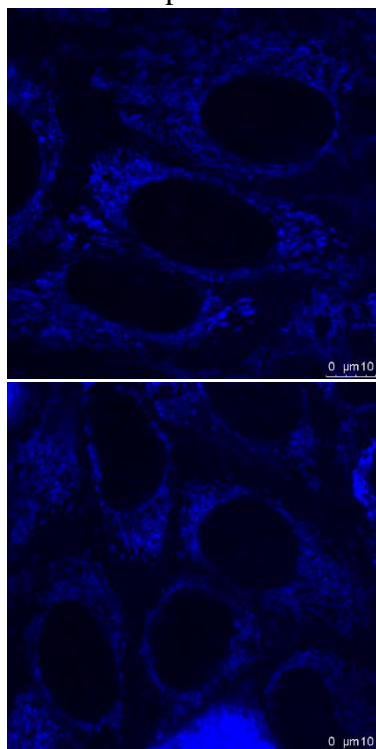
ER-Tracker™ Red



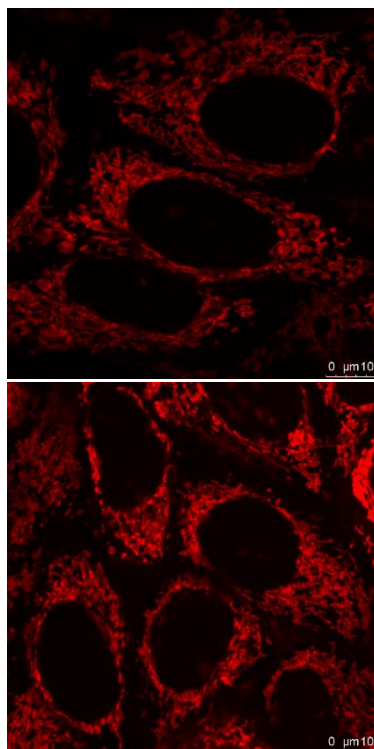
Merged



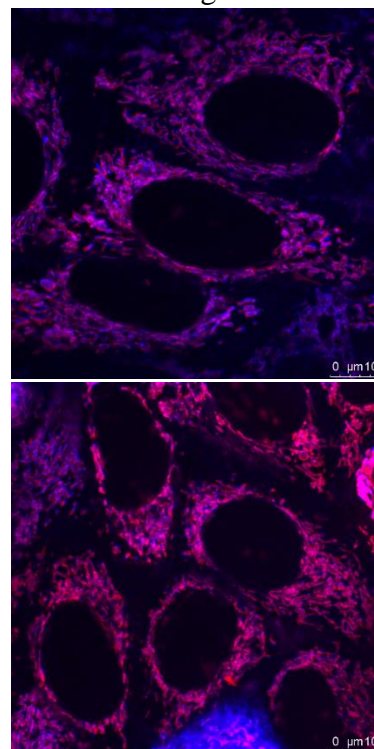
Compound 5c



MitoTracker® Red



Merged



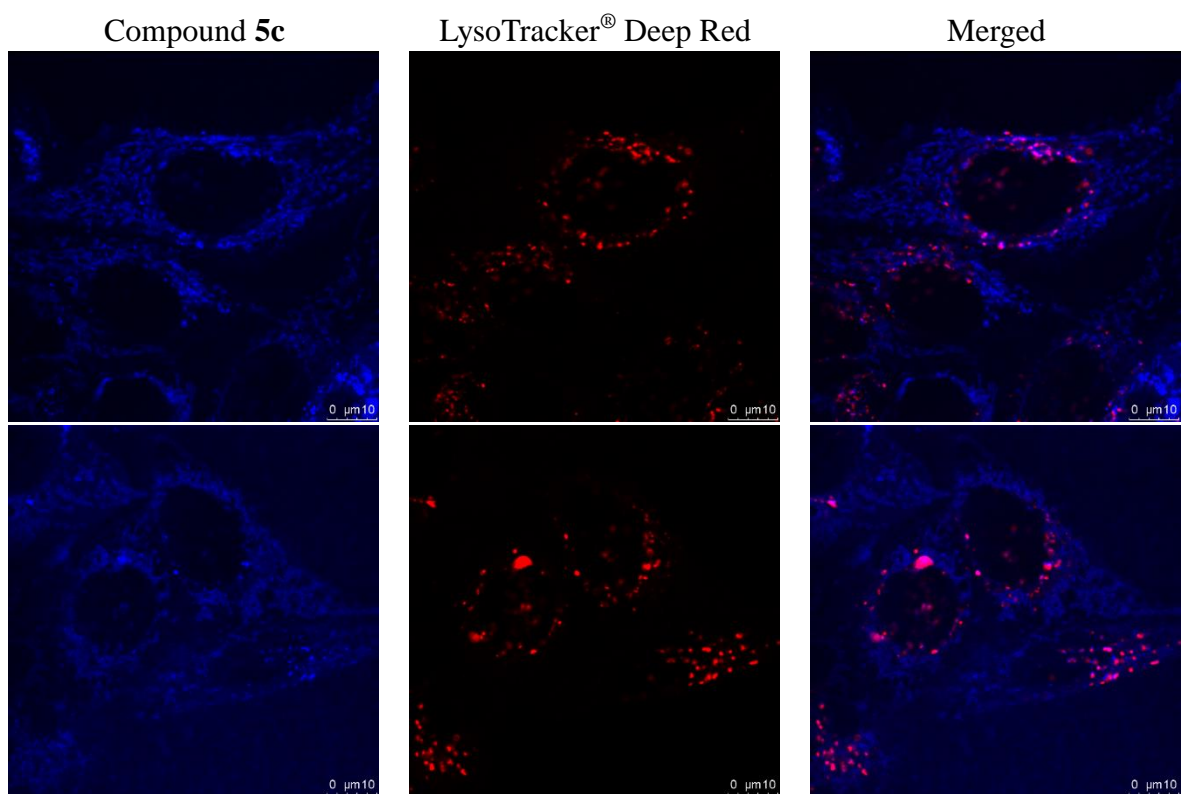
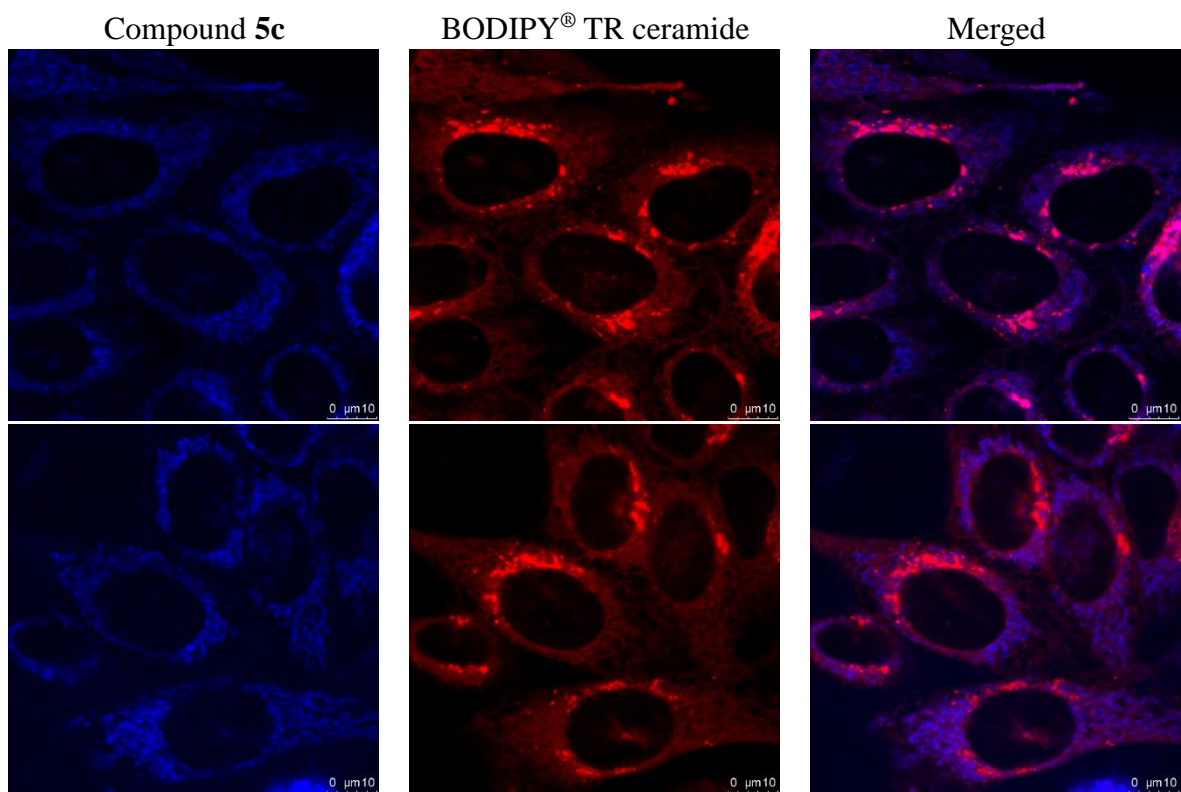
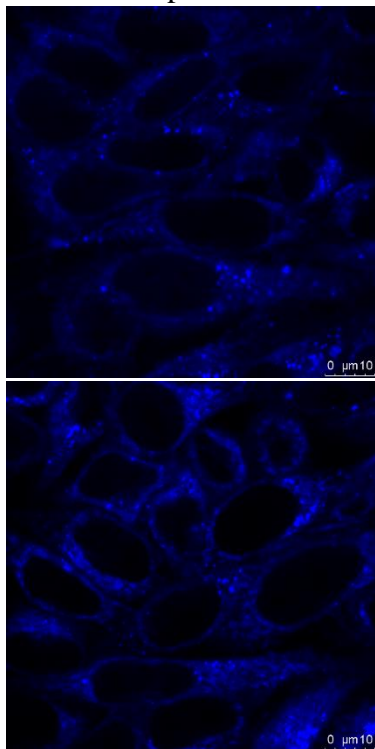
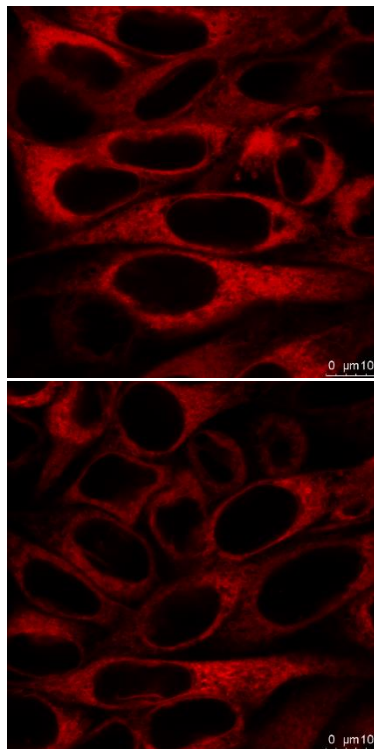


Figure S19 Confocal fluorescence microscopic images of HeLa cells with quinolizinium compounds **5c** colocalized with ER-Tracker[™] Red, MitoTracker[®] Red, BODIPY[®] TR ceramide and LysoTracker[®] Deep Red, respectively.

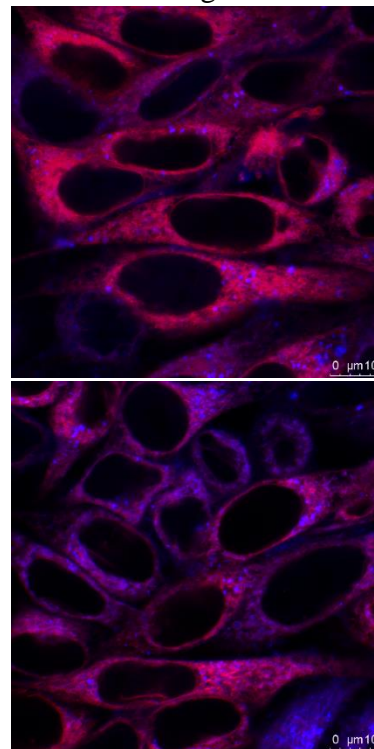
Compound 41



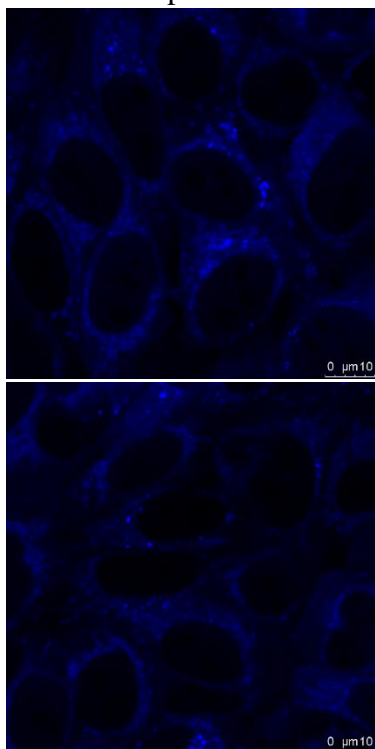
ER-Tracker™ Red



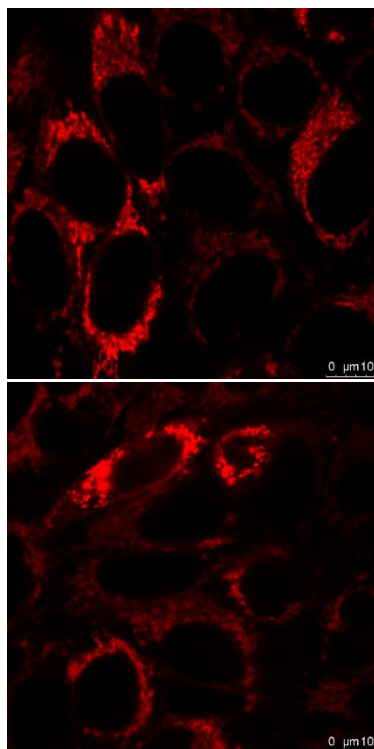
Merged



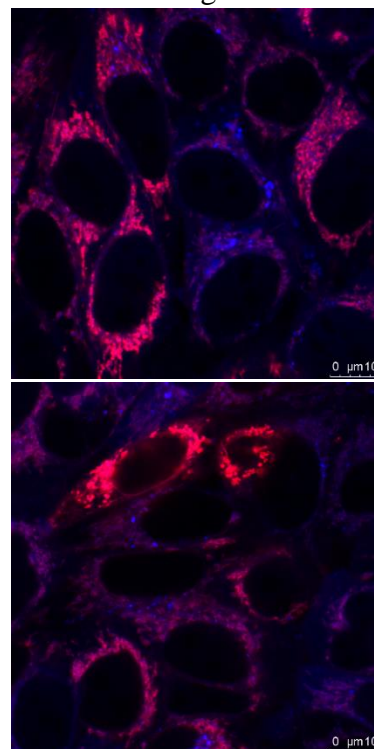
Compound 41



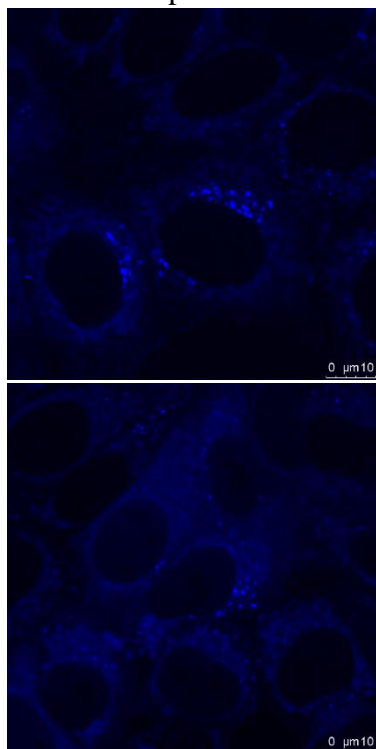
MitoTracker® Red



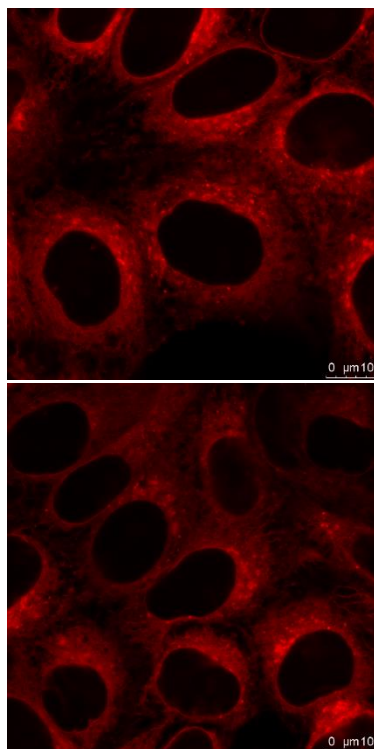
Merged



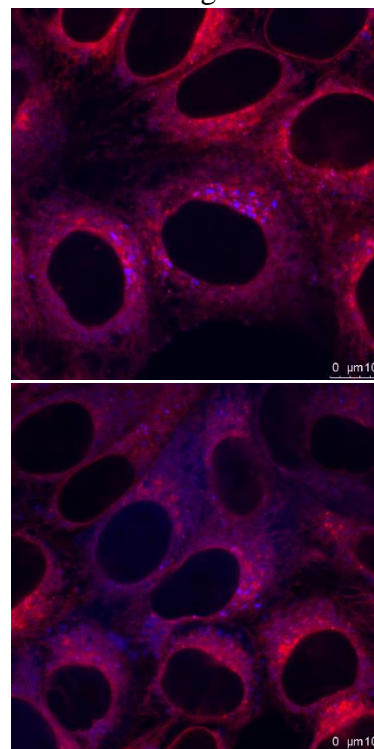
Compound 41



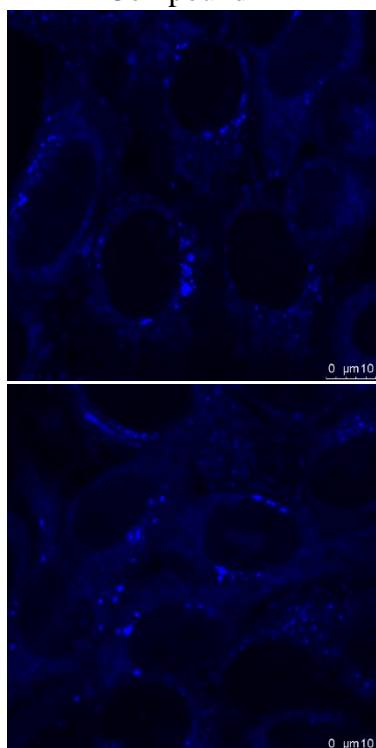
BODIPY[®] TR ceramide



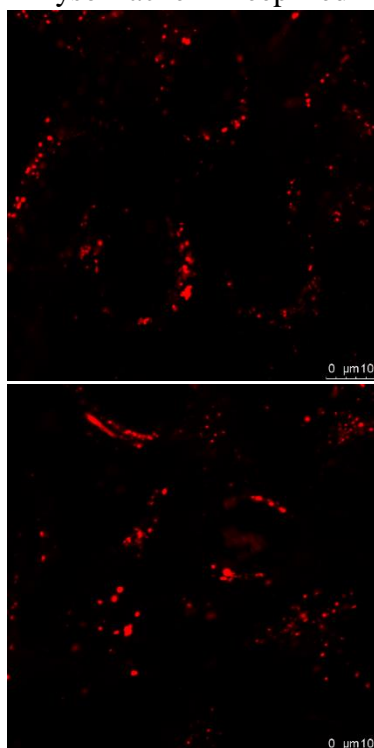
Merged



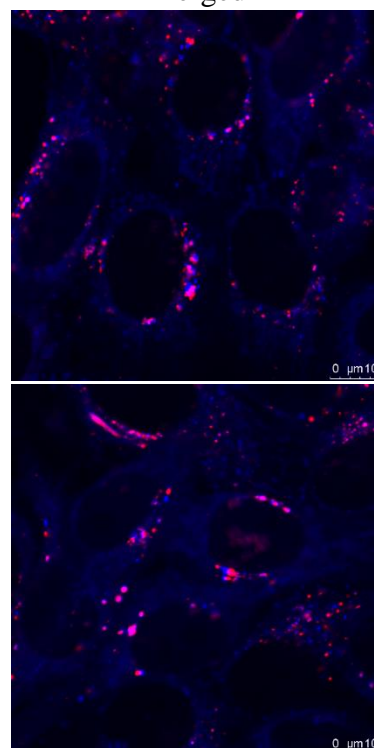
Compound 41



LysoTracker[®] Deep Red



Merged



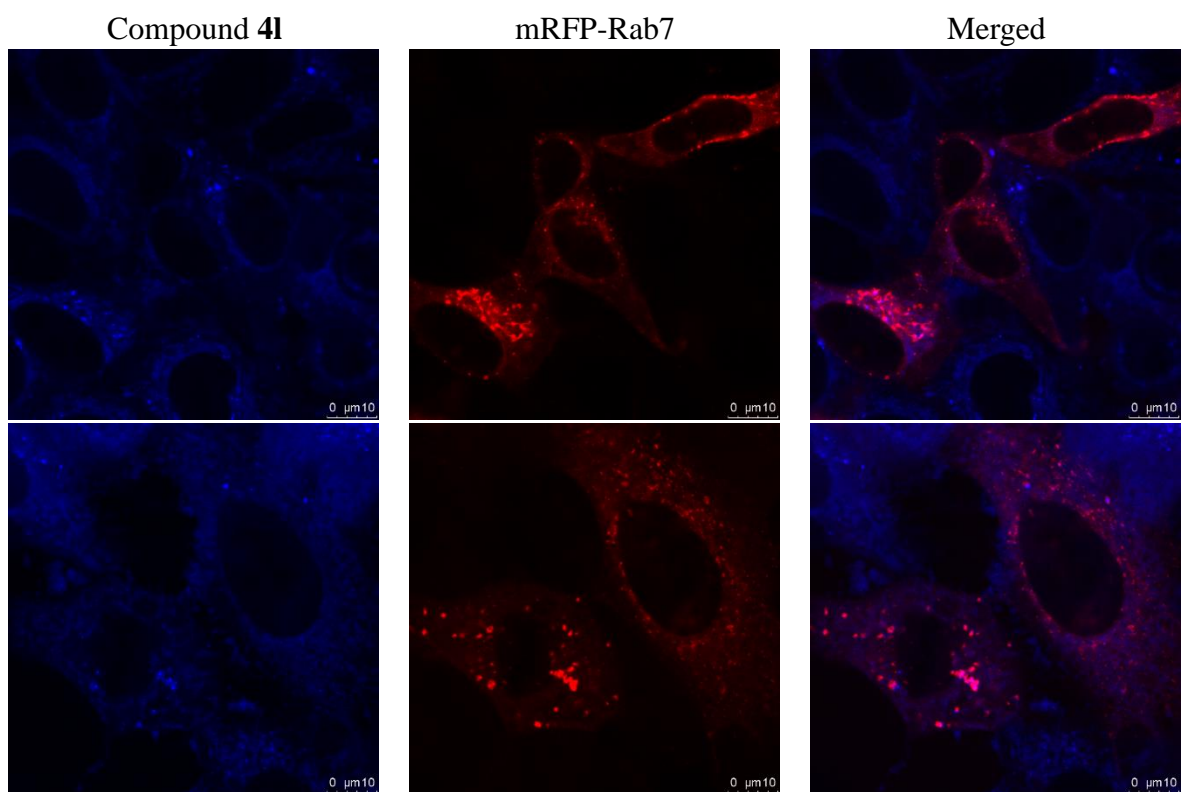
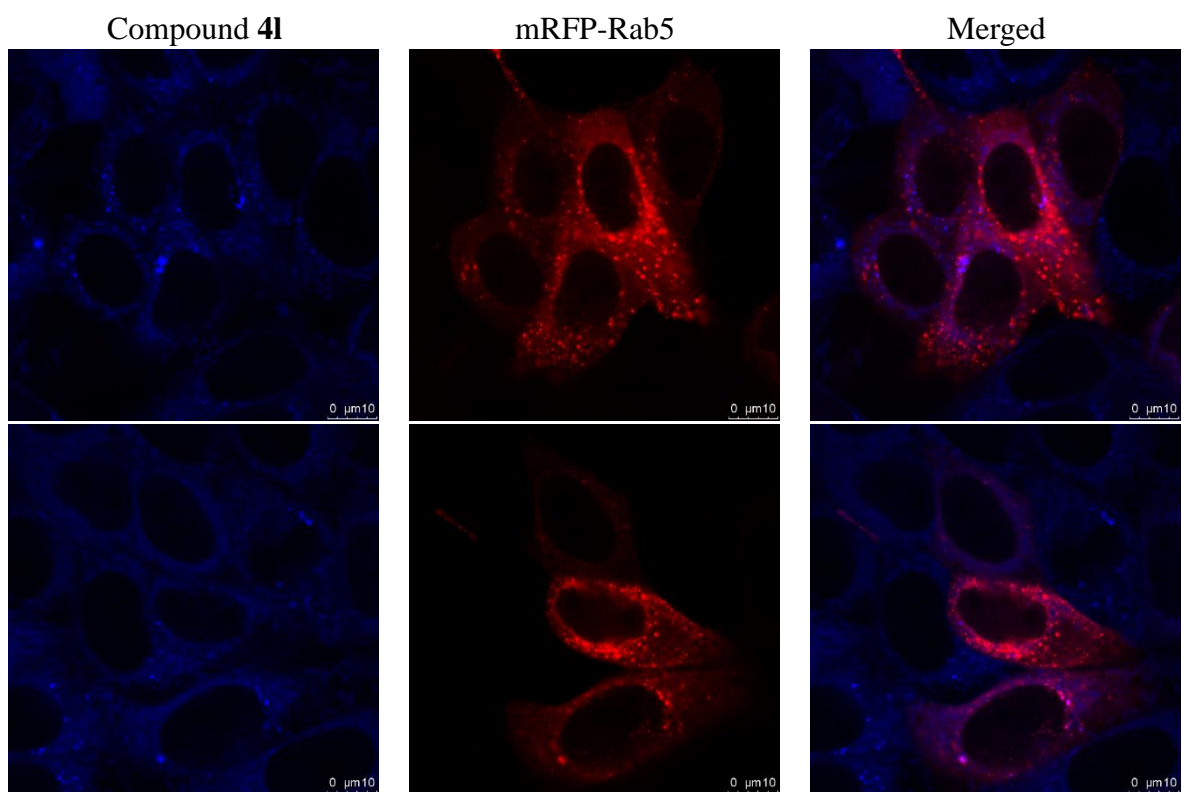


Figure S20 Confocal fluorescence microscopic images of HeLa cells with quinolizinium compounds **5c** colocalized with ER-Tracker™ Red, MitoTracker® Red, BODIPY® TR ceramide and LysoTracker® Deep Red, respectively or transfected with cDNA *via* ViaFect™ Transfection Reagent.

Crystal structure analysis of compound **4b**

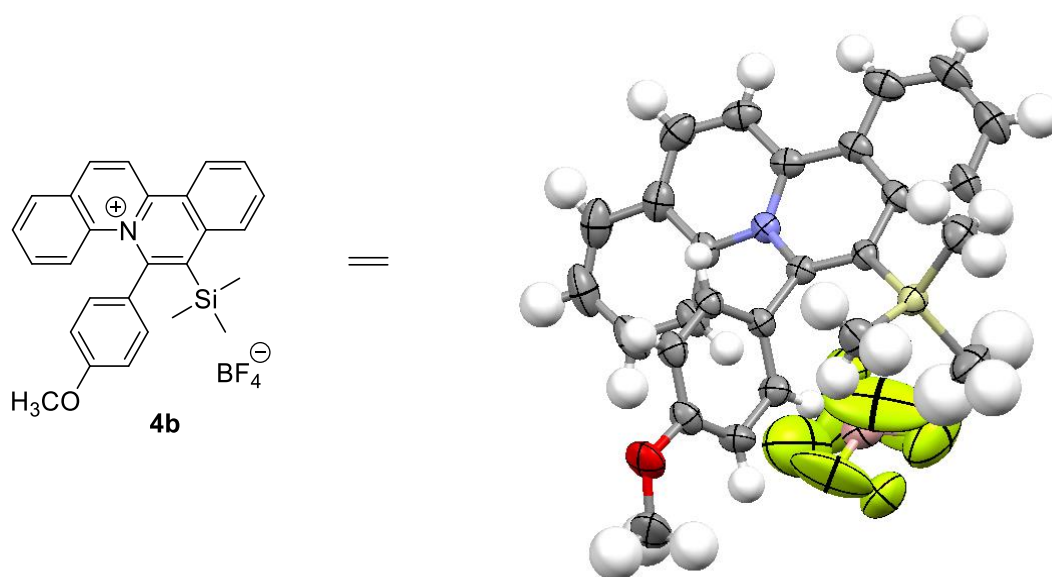


Figure S21 X-ray crystal structure of compound **4b**.

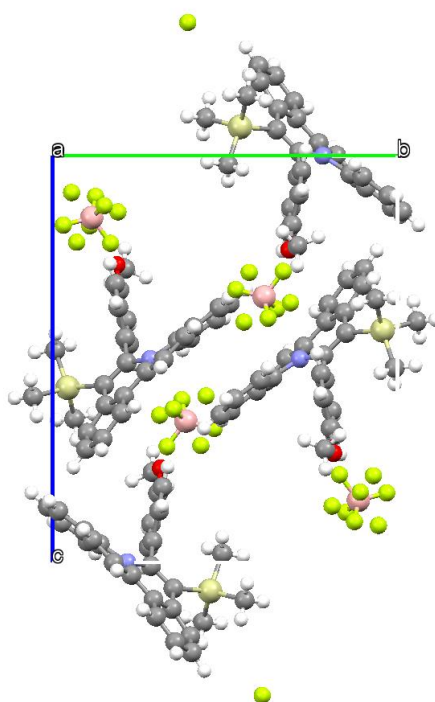


Figure S22 A representation (view along a axis) of packing in a single crystal of **4b**.

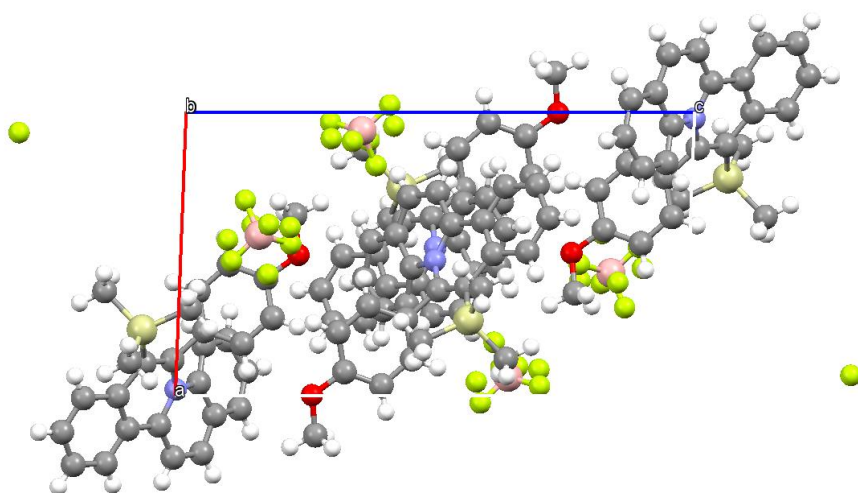


Figure S23 A representation (view along b axis) of packing in a single crystal of **4b**.

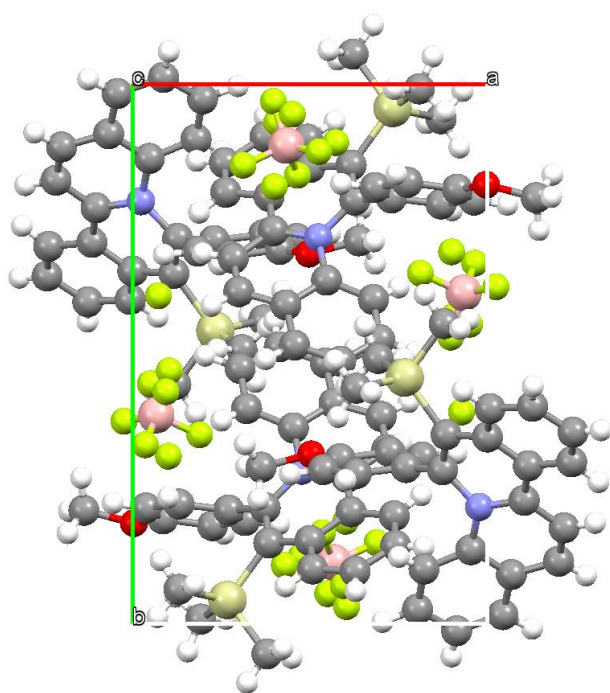


Figure S24 A representation (view along c axis) of packing in a single crystal of **4b**.

Table S7 Crystal data and structure refinement for quinolizinium compound **4b**.

Empirical formula	Si(CH ₃) ₃ (C ₂₄ H ₁₄ NO) .(BF ₄)	
Formula weight	495.39	
Temperature	298(2) K	
Wavelength	0.71073 Å	
Crystal system	Monoclinic	
Space group	P2(1)/n	
Unit cell dimensions	a = 9.6894(7) Å	α = 90 °
	b = 14.7175(11) Å	β = 92.186(2) °
	c = 17.3626(13) Å	γ = 90 °
Volume	2474.2(3) Å ³	
Z	4	
Density (calculated)	1.330 Mg/m ³	
Absorption coefficient	0.146 mm ⁻¹	
F(000)	1032	
Crystal size	0.18 x 0.12 x 0.08 mm ³	
Theta range for data collection	2.37 to 27.41 °	
Index ranges	-12<=h<=12, -18<=k<=18, -22<=l<=22	
Reflections collected	118973	
Independent reflections	5151 [R(int) = 0.0837]	
Completeness to theta = 27.41 °	91.3 %	
Absorption correction	Semi-empirical from equivalent	
Max. and min. transmission	0.7456 and 0.7110	
Refinement method	Full-matrix least-squares on F ²	
Data / restraints / parameters	5151 / 42 / 385	
Goodness-of-fit on F ²	1.002	
Final R indices [I>2sigma(I)]	R1 = 0.0745, wR2 = 0.1647	
R indices (all data)	R1 = 0.1167, wR2 = 0.1865	
Largest diff. peak and hole	0.405 and -0.613 e.Å ⁻³	

Table S8 Atomic coordinates ($\times 10^4$) and equivalent isotropic displacement parameters ($\text{\AA}^2 \times 10^3$) for **4b**. U(eq) is defined as one third of the trace of the orthogonalized U^{ij} tensor.

	x	y	z	U(eq)
Si(1)	7329(1)	436(1)	5706(1)	42(1)
O(1)	9966(2)	1861(1)	2685(1)	65(1)
N(1)	5231(2)	2836(1)	5000(1)	35(1)
C(1)	6161(2)	1496(1)	5641(1)	36(1)
C(2)	6265(2)	2147(1)	5089(1)	34(1)
C(3)	5468(2)	3630(1)	4554(1)	39(1)
C(4)	6786(2)	3988(1)	4483(1)	46(1)
C(5)	6969(3)	4734(1)	4019(1)	59(1)
C(6)	5866(3)	5133(2)	3630(1)	72(1)
C(7)	4563(3)	4834(2)	3737(1)	67(1)
C(8)	4322(2)	4089(1)	4221(1)	50(1)
C(9)	2992(2)	3843(2)	4446(1)	58(1)
C(10)	2836(2)	3224(1)	5008(1)	51(1)
C(11)	3964(2)	2713(1)	5307(1)	39(1)
C(12)	3847(2)	2073(1)	5920(1)	41(1)
C(13)	2626(2)	1999(2)	6333(1)	54(1)
C(14)	2585(2)	1449(2)	6960(1)	64(1)
C(15)	3729(3)	969(2)	7210(1)	65(1)
C(16)	4926(2)	1013(2)	6815(1)	53(1)
C(17)	4999(2)	1540(1)	6141(1)	40(1)
C(18)	7295(2)	2106(1)	4480(1)	35(1)
C(19)	6835(2)	1910(1)	3726(1)	39(1)
C(20)	7751(2)	1815(1)	3151(1)	46(1)
C(21)	9150(2)	1942(1)	3305(1)	46(1)
C(22)	9627(2)	2145(1)	4045(1)	48(1)
C(23)	8694(2)	2217(1)	4630(1)	43(1)
C(24)	11378(2)	2100(2)	2782(2)	84(1)
C(25)	6216(2)	-563(1)	5926(1)	57(1)
C(26)	8081(2)	82(2)	4783(1)	60(1)
C(27)	8697(3)	634(2)	6470(2)	73(1)
B(1)	9336(3)	3866(2)	6527(2)	74(1)
F(1)	10246(3)	3753(3)	6002(2)	167(1)
F(2)	8112(2)	3502(2)	6230(1)	97(1)

F(3)	8969(4)	4687(2)	6708(2)	171(1)
F(4)	9646(4)	3316(3)	7155(2)	172(2)
F(1')	9063(8)	4300(5)	7129(3)	219(3)
F(2')	8993(8)	3104(5)	6383(5)	253(3)
F(3')	9502(9)	4448(5)	5907(5)	190(4)
F(4')	10726(5)	3921(4)	6726(3)	106(2)

Table S9 Bond lengths [\AA] and angles [$^\circ$] for **4b**.

Si(1)-C(26)	1.860(2)
Si(1)-C(27)	1.862(3)
Si(1)-C(25)	1.871(2)
Si(1)-C(1)	1.9281(19)
O(1)-C(21)	1.365(2)
O(1)-C(24)	1.416(3)
N(1)-C(11)	1.370(2)
N(1)-C(3)	1.425(2)
N(1)-C(2)	1.430(2)
C(1)-C(2)	1.361(2)
C(1)-C(17)	1.449(3)
C(2)-C(18)	1.484(2)
C(3)-C(4)	1.391(3)
C(3)-C(8)	1.404(3)
C(4)-C(5)	1.377(3)
C(4)-H(4A)	0.91(2)
C(5)-C(6)	1.375(4)
C(5)-H(5A)	1.02(2)
C(6)-C(7)	1.357(4)
C(6)-H(6A)	0.9300
C(7)-C(8)	1.407(3)
C(7)-H(7A)	0.96(2)
C(8)-C(9)	1.408(3)
C(9)-C(10)	1.347(3)
C(9)-H(9A)	0.9300
C(10)-C(11)	1.409(3)
C(10)-H(10A)	0.9300
C(11)-C(12)	1.429(3)

C(12)-C(17)	1.406(3)
C(12)-C(13)	1.411(3)
C(13)-C(14)	1.358(3)
C(13)-H(13A)	0.96(2)
C(14)-C(15)	1.371(3)
C(14)-H(14A)	0.92(2)
C(15)-C(16)	1.371(3)
C(15)-H(15A)	0.96(3)
C(16)-C(17)	1.408(3)
C(16)-H(16A)	0.9300
C(18)-C(23)	1.380(3)
C(18)-C(19)	1.396(3)
C(19)-C(20)	1.369(3)
C(19)-H(19A)	0.948(17)
C(20)-C(21)	1.384(3)
C(20)-H(20A)	0.9300
C(21)-C(22)	1.380(3)
C(22)-C(23)	1.389(3)
C(22)-H(22A)	0.9300
C(23)-H(23A)	0.929(17)
C(24)-H(24A)	0.9600
C(24)-H(24B)	0.9600
C(24)-H(24C)	0.9600
C(25)-H(25A)	0.9600
C(25)-H(25B)	0.9600
C(25)-H(25C)	0.9600
C(26)-H(26A)	0.9600
C(26)-H(26B)	0.9600
C(26)-H(26C)	0.9600
C(27)-H(27A)	0.9600
C(27)-H(27B)	0.9600
C(27)-H(27C)	0.9600
B(1)-F(2')	1.194(7)
B(1)-F(1')	1.262(6)
B(1)-F(1)	1.302(4)
B(1)-F(3)	1.302(4)
B(1)-F(4')	1.380(5)
B(1)-F(4)	1.383(5)

B(1)-F(2)	1.383(4)
B(1)-F(3')	1.389(8)
C(26)-Si(1)-C(27)	111.49(12)
C(26)-Si(1)-C(25)	101.78(10)
C(27)-Si(1)-C(25)	112.18(11)
C(26)-Si(1)-C(1)	115.11(9)
C(27)-Si(1)-C(1)	108.35(10)
C(25)-Si(1)-C(1)	107.82(9)
C(21)-O(1)-C(24)	118.10(18)
C(11)-N(1)-C(3)	119.04(15)
C(11)-N(1)-C(2)	119.87(14)
C(3)-N(1)-C(2)	120.99(15)
C(2)-C(1)-C(17)	118.04(16)
C(2)-C(1)-Si(1)	123.48(14)
C(17)-C(1)-Si(1)	117.96(13)
C(1)-C(2)-N(1)	120.41(16)
C(1)-C(2)-C(18)	122.88(16)
N(1)-C(2)-C(18)	116.02(14)
C(4)-C(3)-C(8)	119.72(17)
C(4)-C(3)-N(1)	121.70(17)
C(8)-C(3)-N(1)	118.46(17)
C(5)-C(4)-C(3)	119.5(2)
C(5)-C(4)-H(4A)	120.4(13)
C(3)-C(4)-H(4A)	119.8(13)
C(6)-C(5)-C(4)	120.9(2)
C(6)-C(5)-H(5A)	123.6(14)
C(4)-C(5)-H(5A)	115.5(14)
C(7)-C(6)-C(5)	120.3(2)
C(7)-C(6)-H(6A)	119.9
C(5)-C(6)-H(6A)	119.9
C(6)-C(7)-C(8)	120.8(2)
C(6)-C(7)-H(7A)	124.5(15)
C(8)-C(7)-H(7A)	114.7(15)
C(3)-C(8)-C(7)	118.3(2)
C(3)-C(8)-C(9)	118.69(19)
C(7)-C(8)-C(9)	122.7(2)
C(10)-C(9)-C(8)	120.2(2)
C(10)-C(9)-H(9A)	119.9

C(8)-C(9)-H(9A)	119.9
C(9)-C(10)-C(11)	121.4(2)
C(9)-C(10)-H(10A)	119.3
C(11)-C(10)-H(10A)	119.3
N(1)-C(11)-C(10)	118.66(17)
N(1)-C(11)-C(12)	118.39(16)
C(10)-C(11)-C(12)	122.94(18)
C(17)-C(12)-C(13)	119.37(18)
C(17)-C(12)-C(11)	119.10(17)
C(13)-C(12)-C(11)	121.45(18)
C(14)-C(13)-C(12)	120.3(2)
C(14)-C(13)-H(13A)	122.6(13)
C(12)-C(13)-H(13A)	117.0(13)
C(13)-C(14)-C(15)	120.9(2)
C(13)-C(14)-H(14A)	120.0(14)
C(15)-C(14)-H(14A)	119.1(13)
C(14)-C(15)-C(16)	120.4(2)
C(14)-C(15)-H(15A)	121.5(15)
C(16)-C(15)-H(15A)	118.1(15)
C(15)-C(16)-C(17)	120.8(2)
C(15)-C(16)-H(16A)	119.6
C(17)-C(16)-H(16A)	119.6
C(12)-C(17)-C(16)	118.01(18)
C(12)-C(17)-C(1)	119.23(16)
C(16)-C(17)-C(1)	122.57(18)
C(23)-C(18)-C(19)	118.48(17)
C(23)-C(18)-C(2)	122.93(16)
C(19)-C(18)-C(2)	118.54(16)
C(20)-C(19)-C(18)	120.86(17)
C(20)-C(19)-H(19A)	119.8(10)
C(18)-C(19)-H(19A)	119.3(10)
C(19)-C(20)-C(21)	120.12(18)
C(19)-C(20)-H(20A)	119.9
C(21)-C(20)-H(20A)	119.9
O(1)-C(21)-C(22)	124.66(18)
O(1)-C(21)-C(20)	115.33(18)
C(22)-C(21)-C(20)	120.01(18)
C(21)-C(22)-C(23)	119.51(18)

C(21)-C(22)-H(22A)	120.2
C(23)-C(22)-H(22A)	120.2
C(18)-C(23)-C(22)	120.98(18)
C(18)-C(23)-H(23A)	118.5(11)
C(22)-C(23)-H(23A)	120.5(11)
O(1)-C(24)-H(24A)	109.5
O(1)-C(24)-H(24B)	109.5
H(24A)-C(24)-H(24B)	109.5
O(1)-C(24)-H(24C)	109.5
H(24A)-C(24)-H(24C)	109.5
H(24B)-C(24)-H(24C)	109.5
Si(1)-C(25)-H(25A)	109.5
Si(1)-C(25)-H(25B)	109.5
H(25A)-C(25)-H(25B)	109.5
Si(1)-C(25)-H(25C)	109.5
H(25A)-C(25)-H(25C)	109.5
H(25B)-C(25)-H(25C)	109.5
Si(1)-C(26)-H(26A)	109.5
Si(1)-C(26)-H(26B)	109.5
H(26A)-C(26)-H(26B)	109.5
Si(1)-C(26)-H(26C)	109.5
H(26A)-C(26)-H(26C)	109.5
H(26B)-C(26)-H(26C)	109.5
Si(1)-C(27)-H(27A)	109.5
Si(1)-C(27)-H(27B)	109.5
H(27A)-C(27)-H(27B)	109.5
Si(1)-C(27)-H(27C)	109.5
H(27A)-C(27)-H(27C)	109.5
H(27B)-C(27)-H(27C)	109.5
F(2')-B(1)-F(1')	125.7(6)
F(2')-B(1)-F(1)	85.6(5)
F(1')-B(1)-F(1)	144.4(5)
F(2')-B(1)-F(3)	147.8(5)
F(1')-B(1)-F(3)	42.4(4)
F(1)-B(1)-F(3)	119.2(3)
F(2')-B(1)-F(4')	111.6(5)
F(1')-B(1)-F(4')	89.8(5)
F(1)-B(1)-F(4')	60.2(3)

F(3)-B(1)-F(4')	99.1(3)
F(2')-B(1)-F(4)	70.4(5)
F(1')-B(1)-F(4)	71.8(4)
F(1)-B(1)-F(4)	110.1(3)
F(3)-B(1)-F(4)	113.9(3)
F(4')-B(1)-F(4)	69.9(3)
F(2')-B(1)-F(2)	48.0(4)
F(1')-B(1)-F(2)	107.5(4)
F(1)-B(1)-F(2)	106.5(3)
F(3)-B(1)-F(2)	102.2(3)
F(4')-B(1)-F(2)	158.6(4)
F(4)-B(1)-F(2)	103.0(3)
F(2')-B(1)-F(3')	117.2(6)
F(1')-B(1)-F(3')	111.3(5)
F(1)-B(1)-F(3')	55.7(4)
F(3)-B(1)-F(3')	69.9(4)
F(4')-B(1)-F(3')	91.0(5)
F(4)-B(1)-F(3')	160.8(5)
F(2)-B(1)-F(3')	94.2(4)

Table S10 Torsion angles [°] for **4b**.

C(26)-Si(1)-C(1)-C(2)	-24.83(19)
C(27)-Si(1)-C(1)-C(2)	100.74(17)
C(25)-Si(1)-C(1)-C(2)	-137.63(16)
C(26)-Si(1)-C(1)-C(17)	146.73(14)
C(27)-Si(1)-C(1)-C(17)	-87.70(16)
C(25)-Si(1)-C(1)-C(17)	33.93(17)
C(17)-C(1)-C(2)-N(1)	-1.6(2)
Si(1)-C(1)-C(2)-N(1)	170.00(12)
C(17)-C(1)-C(2)-C(18)	-171.64(16)
Si(1)-C(1)-C(2)-C(18)	-0.1(2)
C(11)-N(1)-C(2)-C(1)	-18.1(2)
C(3)-N(1)-C(2)-C(1)	165.74(16)
C(11)-N(1)-C(2)-C(18)	152.64(16)
C(3)-N(1)-C(2)-C(18)	-23.5(2)
C(11)-N(1)-C(3)-C(4)	154.11(17)

C(2)-N(1)-C(3)-C(4)	-29.7(2)
C(11)-N(1)-C(3)-C(8)	-21.8(2)
C(2)-N(1)-C(3)-C(8)	154.41(16)
C(8)-C(3)-C(4)-C(5)	-6.9(3)
N(1)-C(3)-C(4)-C(5)	177.25(17)
C(3)-C(4)-C(5)-C(6)	0.5(3)
C(4)-C(5)-C(6)-C(7)	4.3(3)
C(5)-C(6)-C(7)-C(8)	-2.7(4)
C(4)-C(3)-C(8)-C(7)	8.4(3)
N(1)-C(3)-C(8)-C(7)	-175.60(17)
C(4)-C(3)-C(8)-C(9)	-165.29(19)
N(1)-C(3)-C(8)-C(9)	10.7(3)
C(6)-C(7)-C(8)-C(3)	-3.7(3)
C(6)-C(7)-C(8)-C(9)	169.8(2)
C(3)-C(8)-C(9)-C(10)	4.6(3)
C(7)-C(8)-C(9)-C(10)	-168.9(2)
C(8)-C(9)-C(10)-C(11)	-9.3(3)
C(3)-N(1)-C(11)-C(10)	17.4(2)
C(2)-N(1)-C(11)-C(10)	-158.87(17)
C(3)-N(1)-C(11)-C(12)	-162.47(16)
C(2)-N(1)-C(11)-C(12)	21.3(2)
C(9)-C(10)-C(11)-N(1)	-1.9(3)
C(9)-C(10)-C(11)-C(12)	177.9(2)
N(1)-C(11)-C(12)-C(17)	-5.3(3)
C(10)-C(11)-C(12)-C(17)	174.91(18)
N(1)-C(11)-C(12)-C(13)	171.34(17)
C(10)-C(11)-C(12)-C(13)	-8.5(3)
C(17)-C(12)-C(13)-C(14)	3.0(3)
C(11)-C(12)-C(13)-C(14)	-173.6(2)
C(12)-C(13)-C(14)-C(15)	1.1(3)
C(13)-C(14)-C(15)-C(16)	-2.2(4)
C(14)-C(15)-C(16)-C(17)	-0.8(3)
C(13)-C(12)-C(17)-C(16)	-5.8(3)
C(11)-C(12)-C(17)-C(16)	170.87(17)
C(13)-C(12)-C(17)-C(1)	169.30(17)
C(11)-C(12)-C(17)-C(1)	-14.0(3)
C(15)-C(16)-C(17)-C(12)	4.8(3)
C(15)-C(16)-C(17)-C(1)	-170.1(2)

C(2)-C(1)-C(17)-C(12)	17.3(3)
Si(1)-C(1)-C(17)-C(12)	-154.70(14)
C(2)-C(1)-C(17)-C(16)	-167.79(18)
Si(1)-C(1)-C(17)-C(16)	20.2(2)
C(1)-C(2)-C(18)-C(23)	-69.6(2)
N(1)-C(2)-C(18)-C(23)	119.93(19)
C(1)-C(2)-C(18)-C(19)	107.8(2)
N(1)-C(2)-C(18)-C(19)	-62.6(2)
C(23)-C(18)-C(19)-C(20)	1.2(3)
C(2)-C(18)-C(19)-C(20)	-176.35(17)
C(18)-C(19)-C(20)-C(21)	-2.2(3)
C(24)-O(1)-C(21)-C(22)	-7.5(3)
C(24)-O(1)-C(21)-C(20)	171.7(2)
C(19)-C(20)-C(21)-O(1)	-177.85(18)
C(19)-C(20)-C(21)-C(22)	1.5(3)
O(1)-C(21)-C(22)-C(23)	179.52(19)
C(20)-C(21)-C(22)-C(23)	0.3(3)
C(19)-C(18)-C(23)-C(22)	0.6(3)
C(2)-C(18)-C(23)-C(22)	177.99(18)
C(21)-C(22)-C(23)-C(18)	-1.3(3)

Reference

1. R. Bortolozzi, H. Ihmels, L. Thomas, M. Tian and G. Viola, *Chem. - Eur. J.*, 2013, **19**, 8736.
2. G. Zhang, L. Yang, Y. Wang, Y. Xie and H. Huang, *J. Am. Chem. Soc.*, 2013, **135**, 8850.
3. Brannon, J. H.; Magde D. *J. Phys. Chem.* **1978**, *82*, 705.
4. (a) J. R. Lakowicz, *Principles of Fluorescence Spectroscopy*, third ed.; Springer: New York, **2006**; (b) Y. Cheng, G. Li, Y. Liu, Y. Shi, G. Gao, D. Wu, J. Lan and J. You, *J. Am. Chem. Soc.*, 2016, **138**, 4730.
5. (a) Ł. Woźniak, J. J. Murphy and P. Melchiorre *J. Am. Chem. Soc.*, 2015, **137**, 5678; (b) A. Tlahuext-Aca, M. N. Hopkinson, B. Sahoo and F. Glorius, *Chem. Sci.*, 2016, **7**, 89.
6. F. Neese, *WIREs Comput. Mol. Sci.*, 2012, **2**, 73.
7. A. D. Becke, *J. Chem. Phys.*, 1993, **98**, 5648.
8. C. Lee, W. Yang and R. G. Parr, *Phys. Rev. B: Condens. Matter*, 1988, **37**, 785.
9. F. Weigend and R. Ahlrichs, *Phys. Chem. Chem. Phys.* **2005**, *7*, 3297.
10. (a) K. Eichkron, O. Treutler, H. Öhm, M. Häser and R. Ahlrichs, *Chem. Phys. Lett.*, 1995, **242**, 652; (b) K. Eichkorn, F. Weigend, O. Treutler and R. Ahlrichs, *Theor. Chem. Acc.*, 1997, **97**, 119.
11. (a) F. J. Neese, *Comput. Chem.*, 2003, **24**, 1740; (b) F. Neese, F. Wenmohs, A. Hansen and U. Becker, *Chem. Phys.*, 2009, **356**, 98; (c) S. Kossmann and F. Neese, *Chem. Phys. Lett.*, 2009, **481**, 240.
12. A. Klamt and G. Schürmann, *J. Chem. Soc., Perkin Trans.*, 1993, **2**, 799.

UV/visible absorption spectrum of quinolizinium compounds

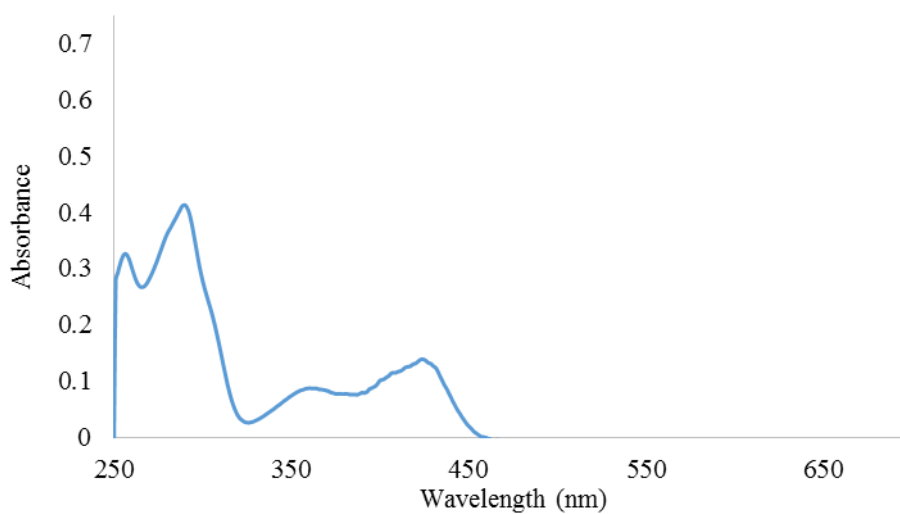


Figure S25 Absorption spectrum of compound **4a**.

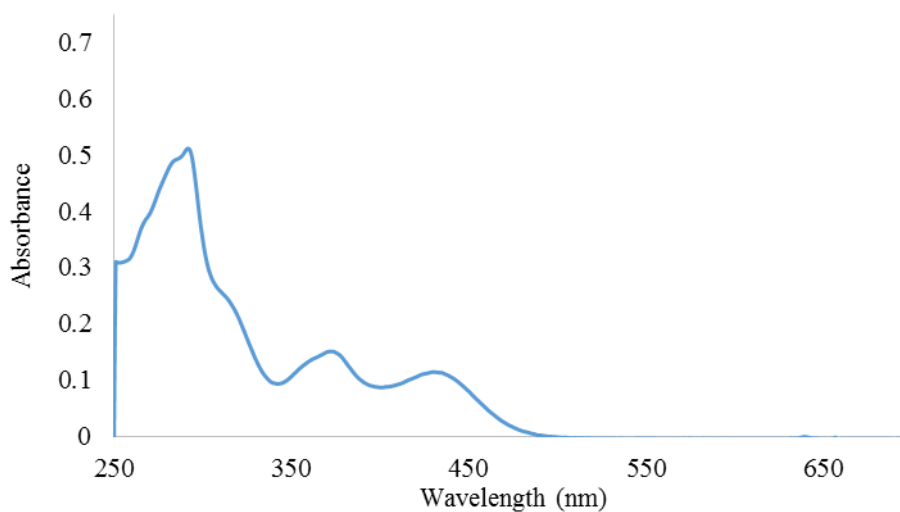


Figure S26 Absorption spectrum of compound **4b**.

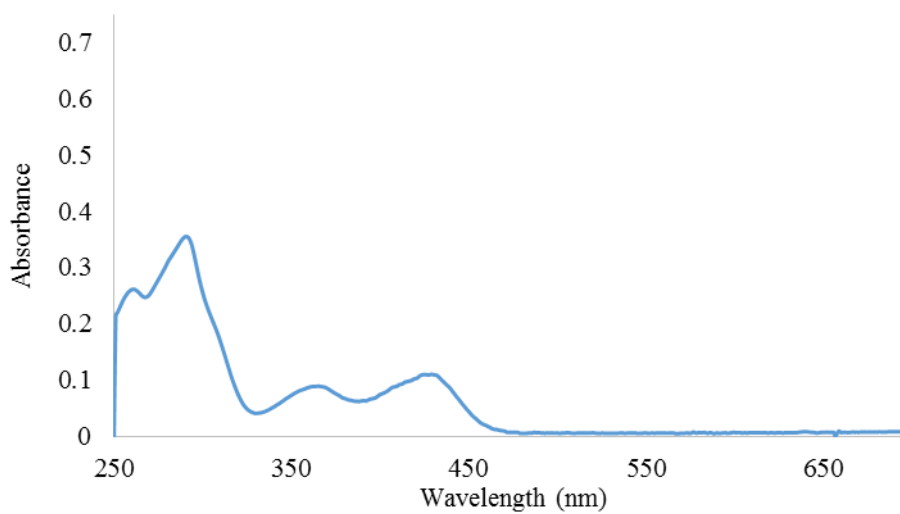


Figure S27 Absorption spectrum of compound **4c**.

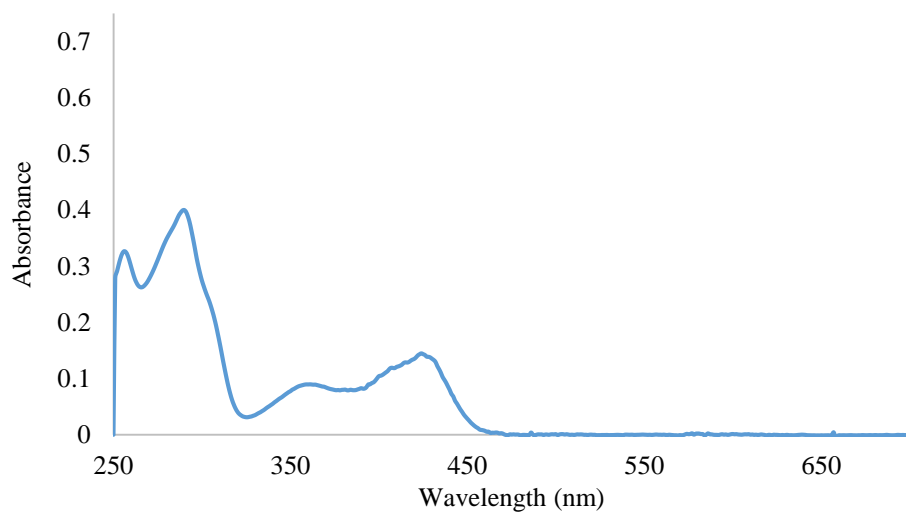


Figure S28 Absorption spectrum of compound **4d**.

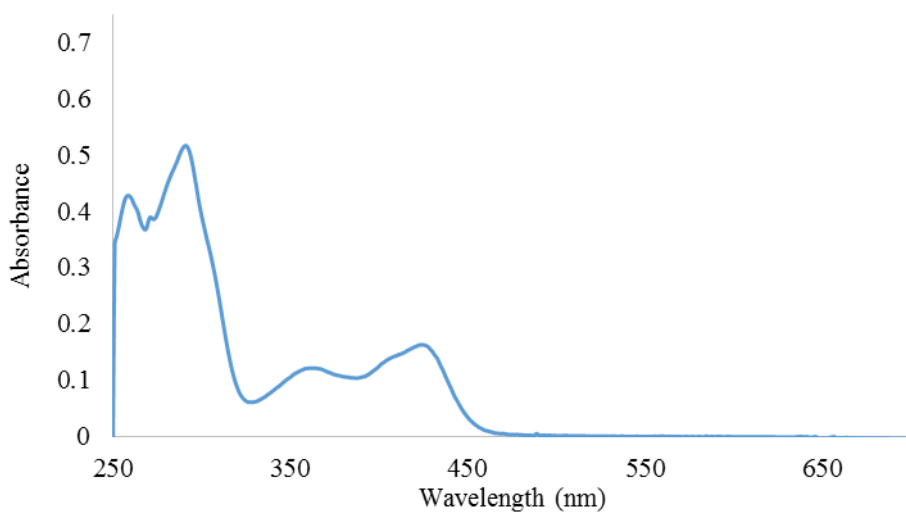


Figure S29 Absorption spectrum of compound **4e**.

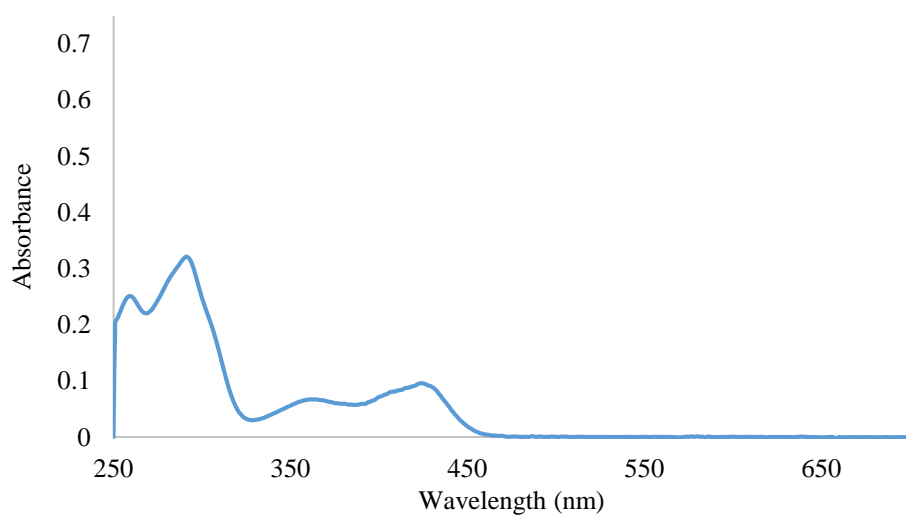


Figure S30 Absorption spectrum of compound **4f**.

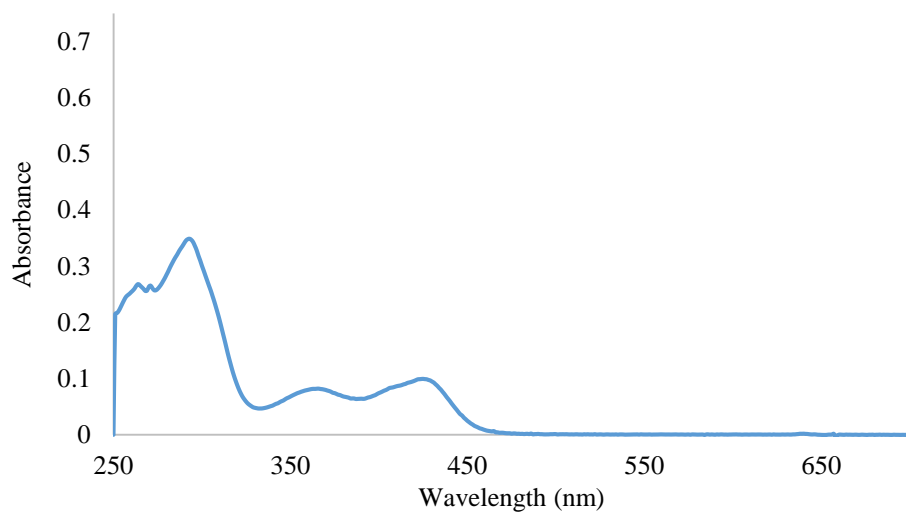


Figure S31 Absorption spectrum of compound **4g**.

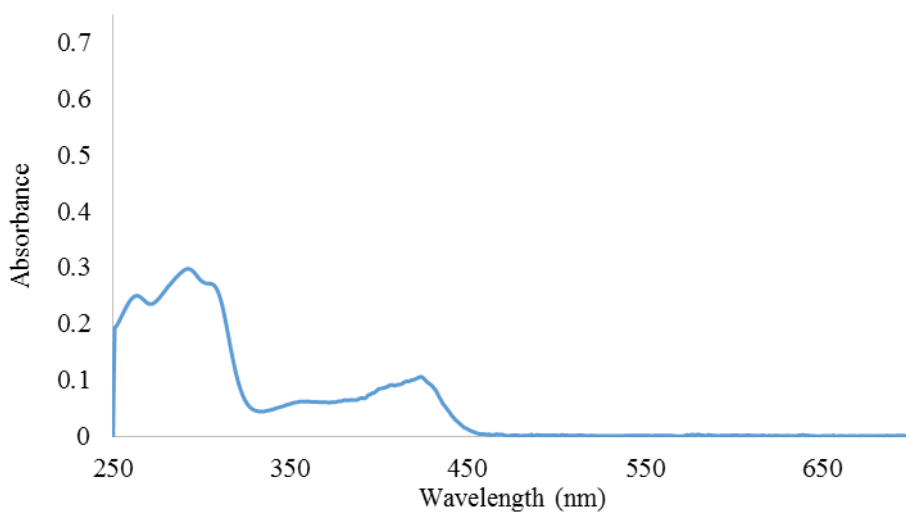


Figure S32 Absorption spectrum of compound **4h**.

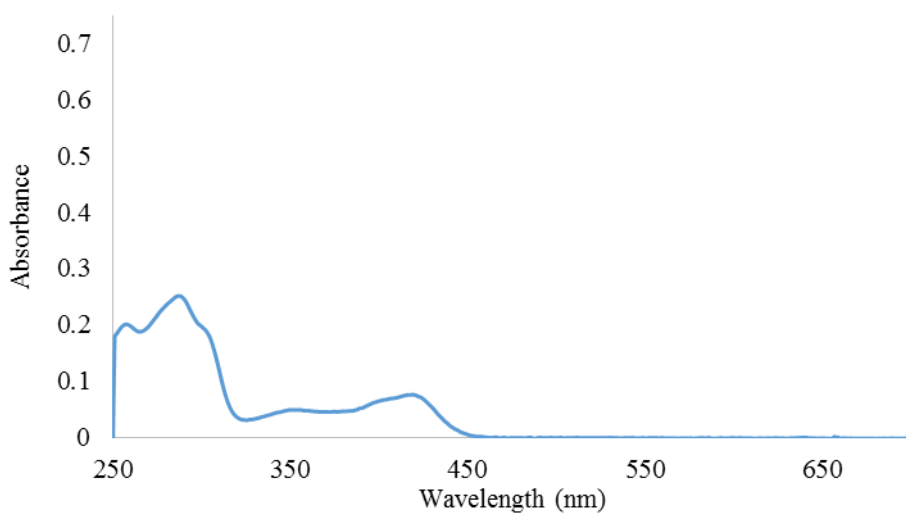


Figure S33 Absorption spectrum of compound **4i**.

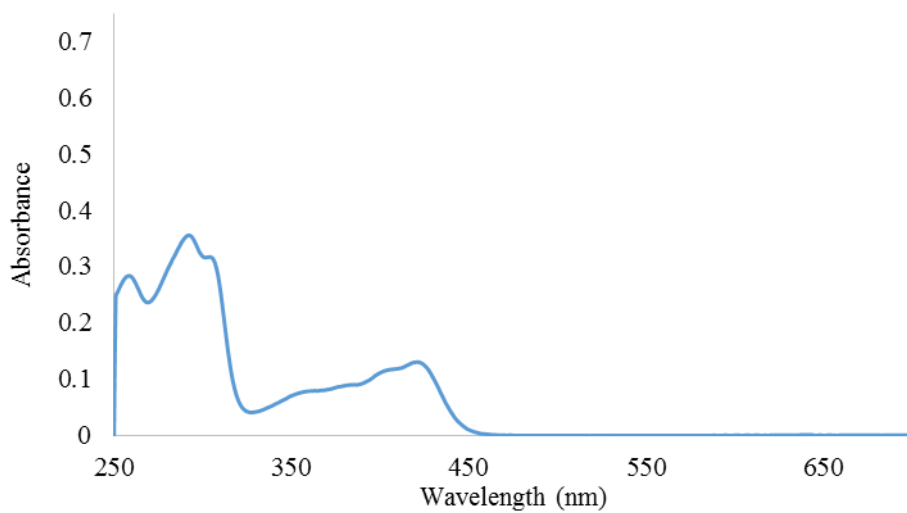


Figure S34 Absorption spectrum of compound **4j**.

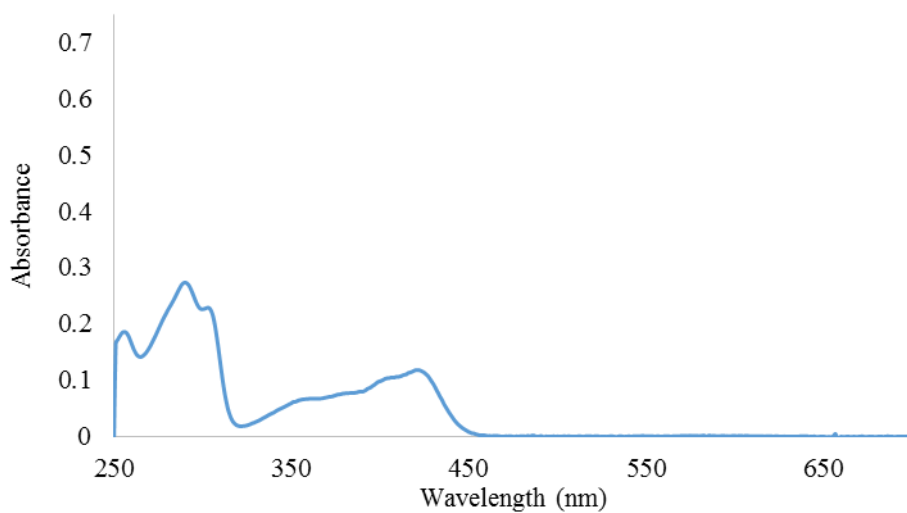


Figure S35 Absorption spectrum of compound **4k**.

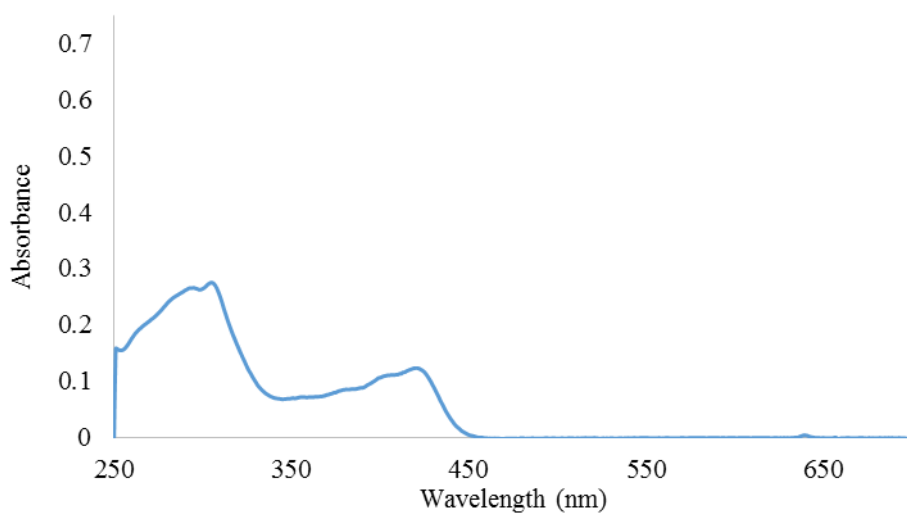


Figure S36 Absorption spectrum of compound **4l**.

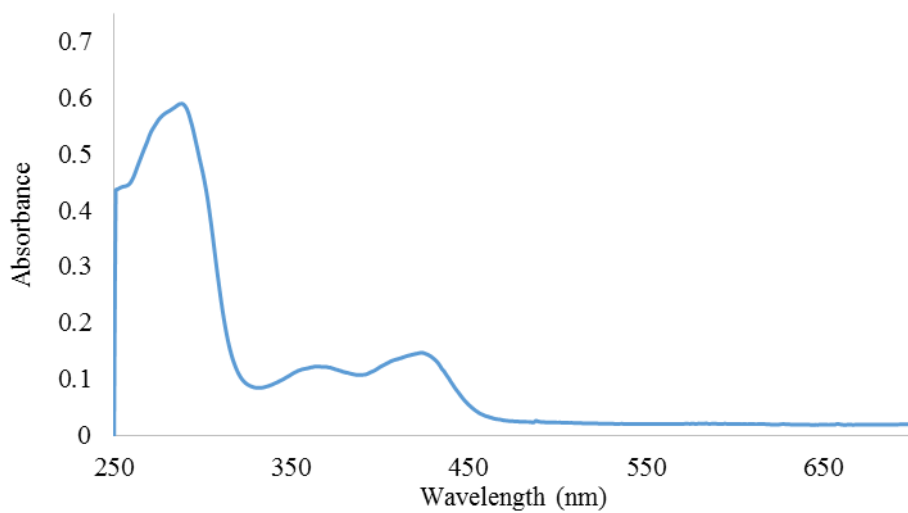


Figure S37 Absorption spectrum of compound **4m**.

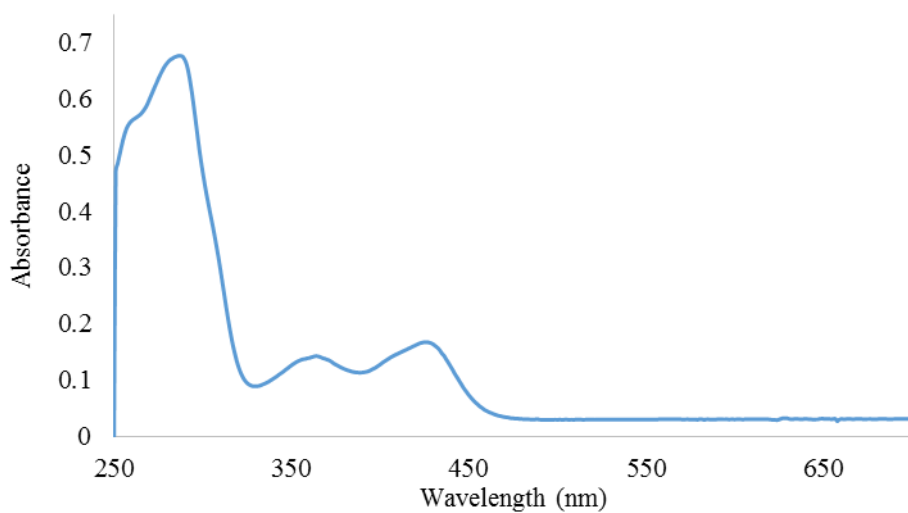


Figure S38 Absorption spectrum of compound **4n**.

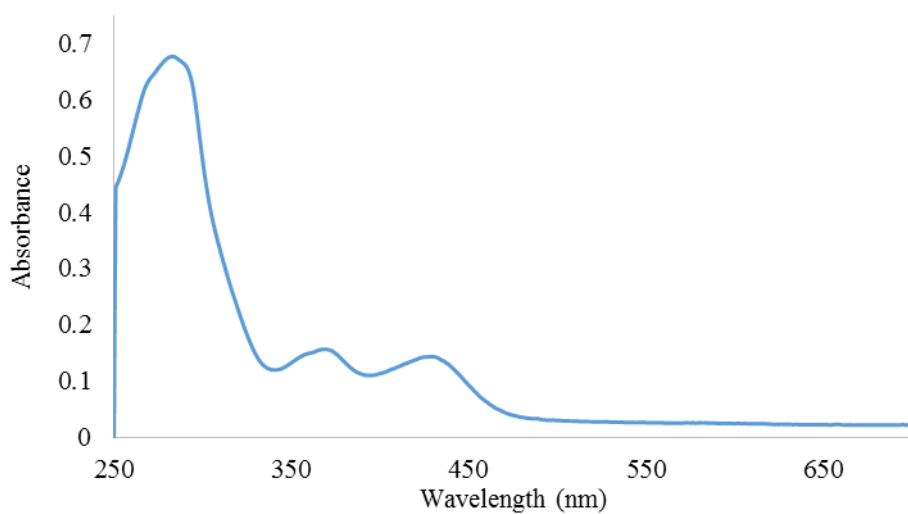


Figure S39 Absorption spectrum of compound **4o**.

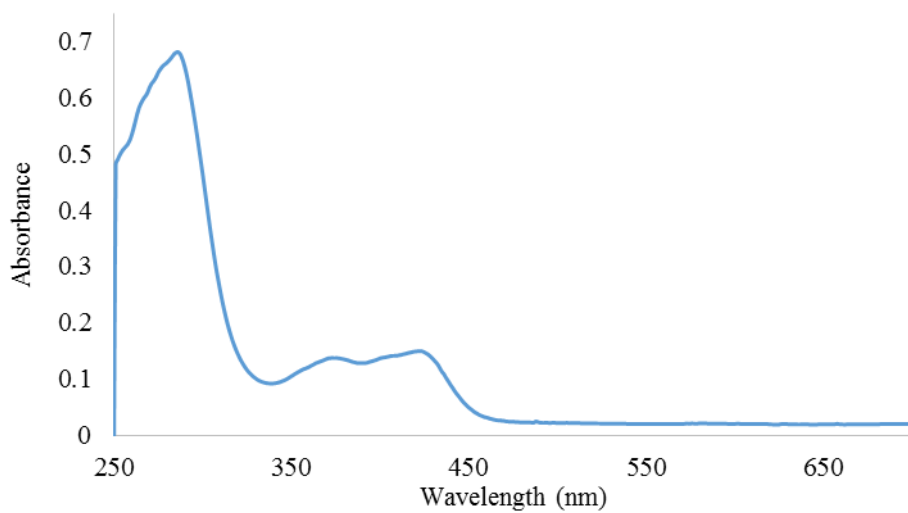


Figure S40 Absorption spectrum of compound **4p**.

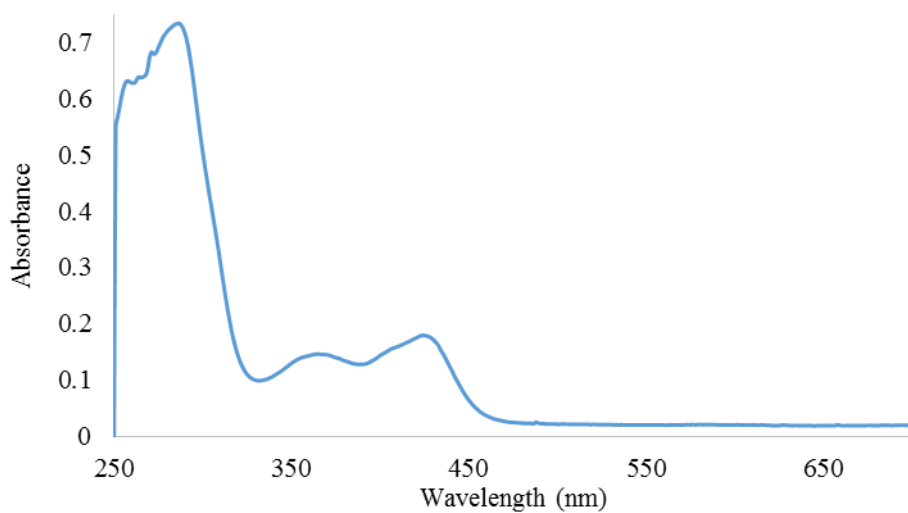


Figure S41 Absorption spectrum of compound **4q**.

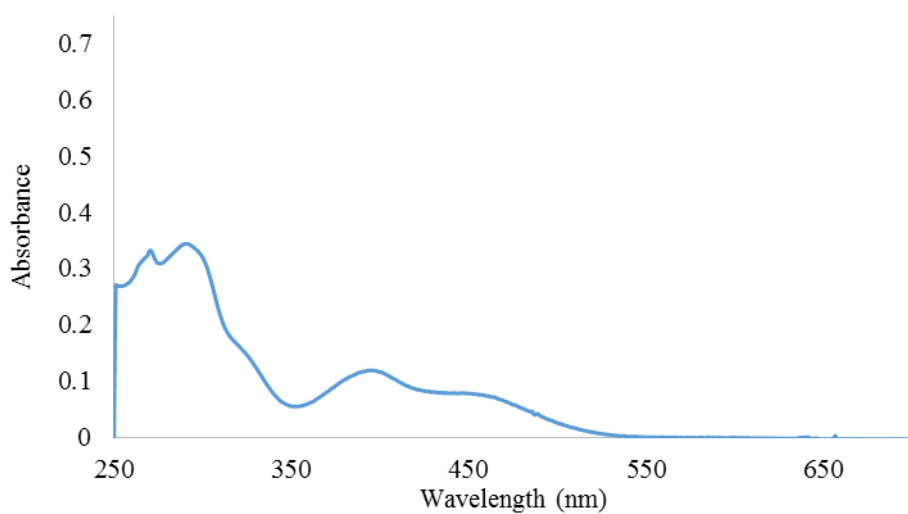


Figure S42 Absorption spectrum of compound **4s**.

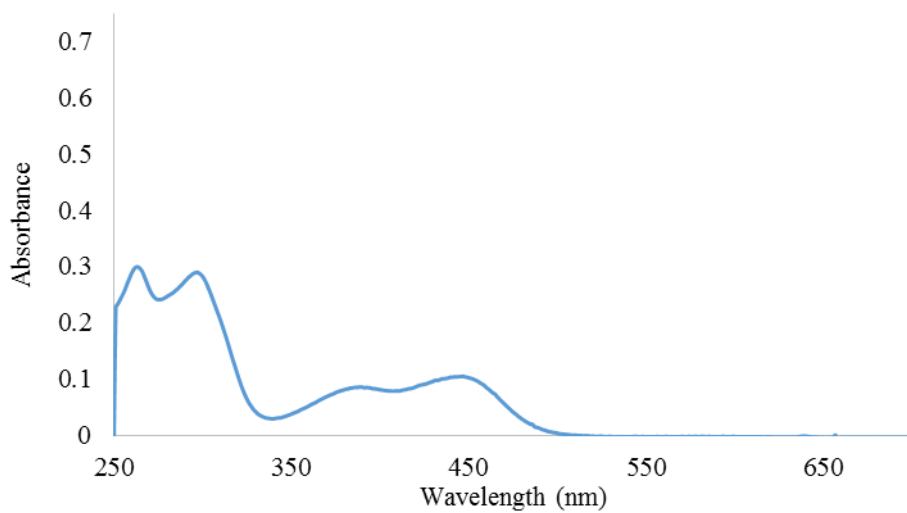


Figure S43 Absorption spectrum of compound **4t**.

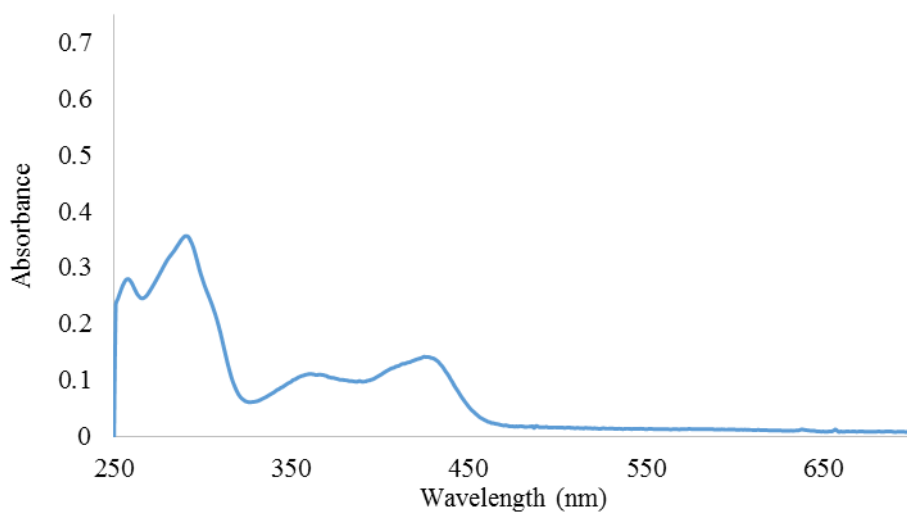


Figure S44 Absorption spectrum of compound **4u**.

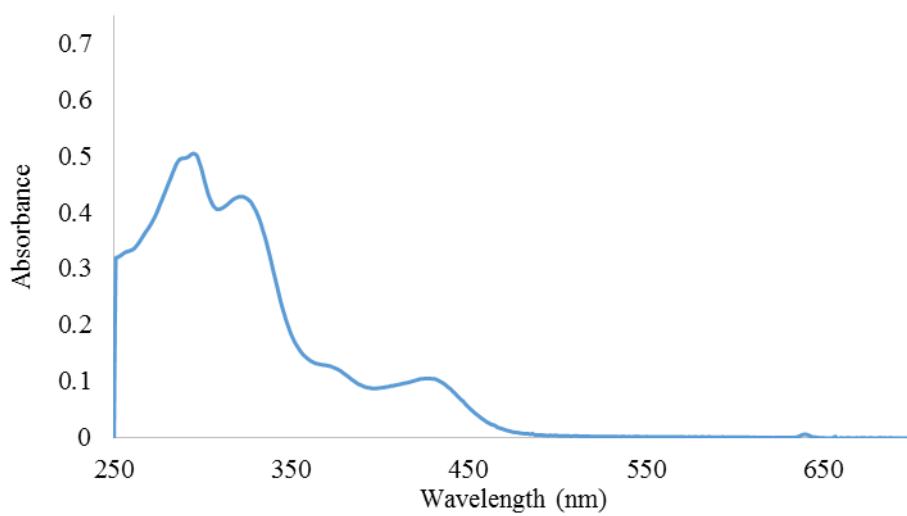


Figure S45 Absorption spectrum of compound **4w**.

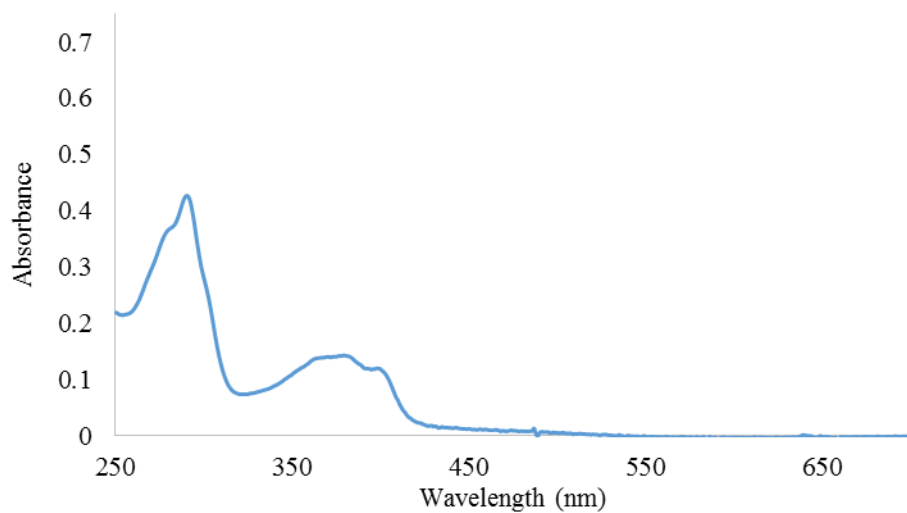


Figure S46 Absorption spectrum of compound **5a**.

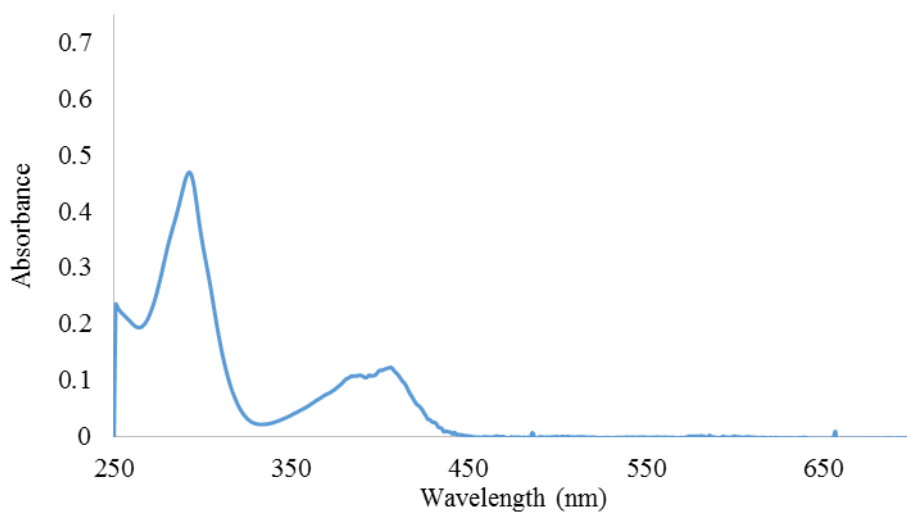


Figure S47 Absorption spectrum of compound **5b**.

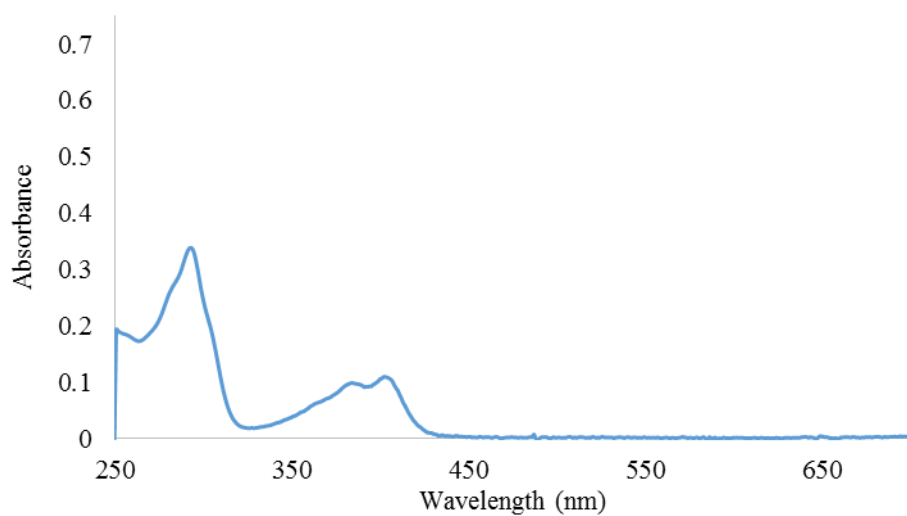


Figure S48 Absorption spectrum of compound **5c**.

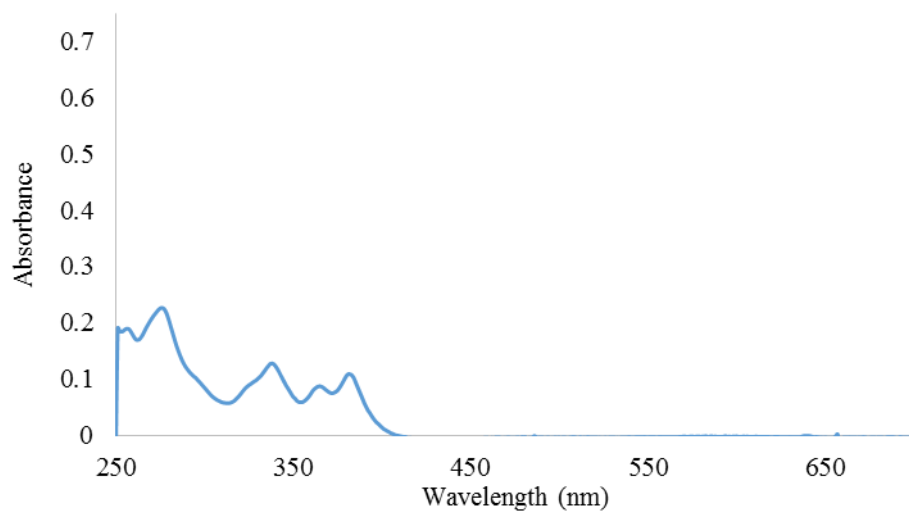


Figure S49 Absorption spectrum of compound **6a**.

Emission spectrum of quinolizinium compounds

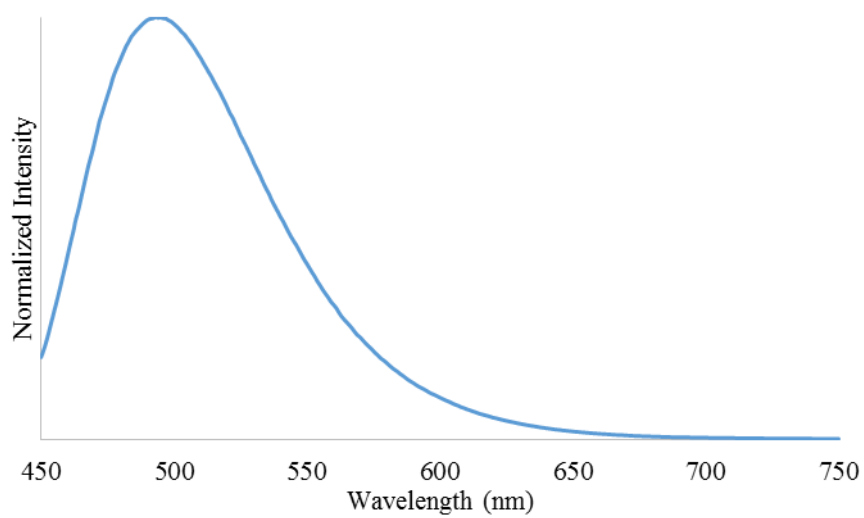


Figure S50 Emission spectrum of compound **4a**.

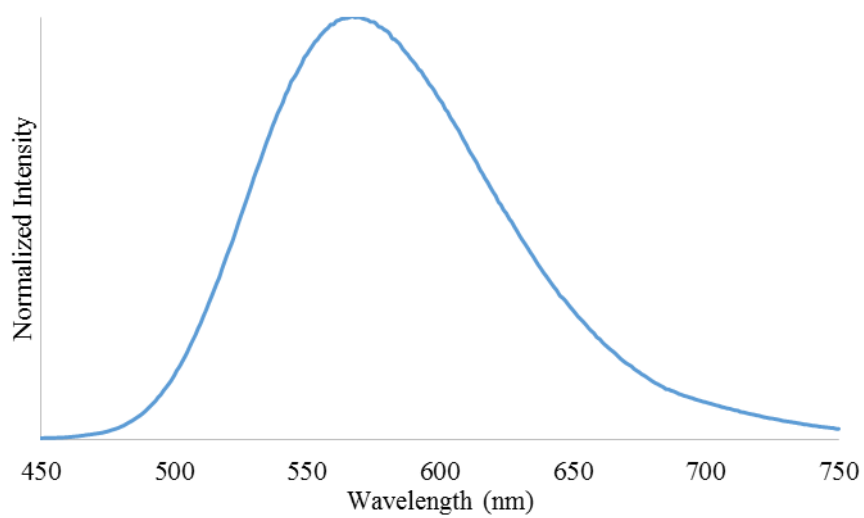


Figure S51 Emission spectrum of compound **4b**.

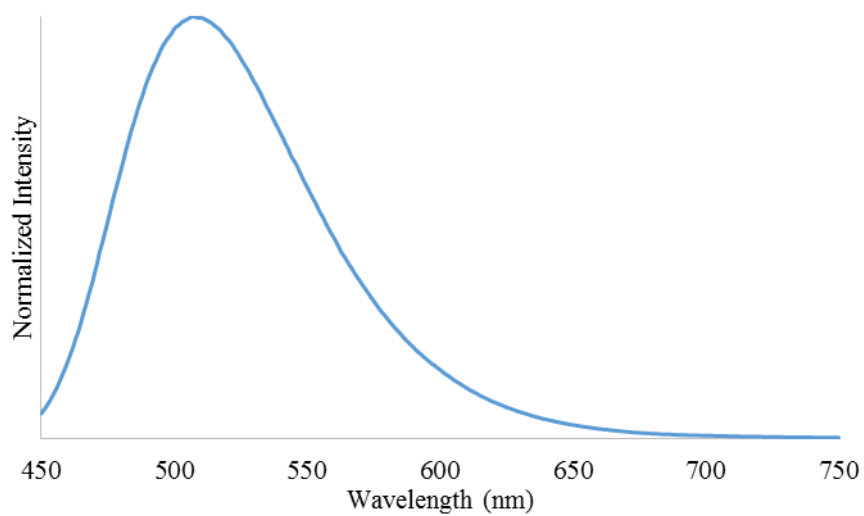


Figure S52 Emission spectrum of compound **4c**.

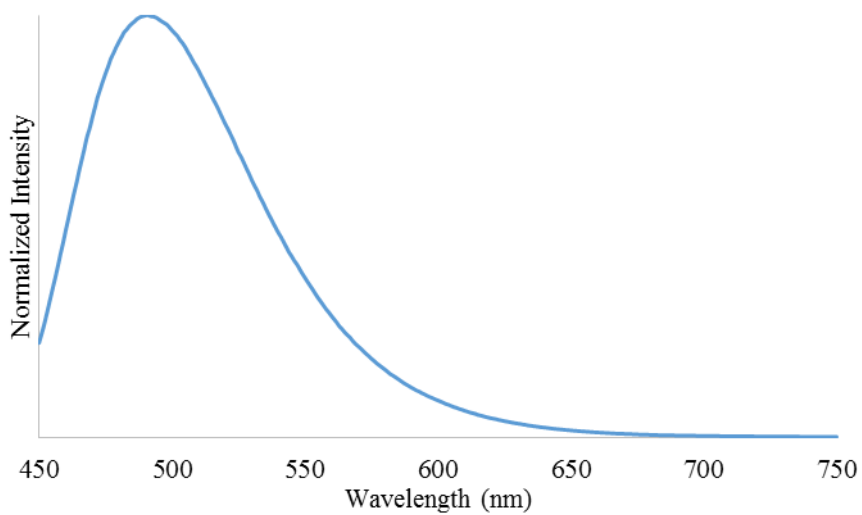


Figure S53 Emission spectrum of compound **4d**.

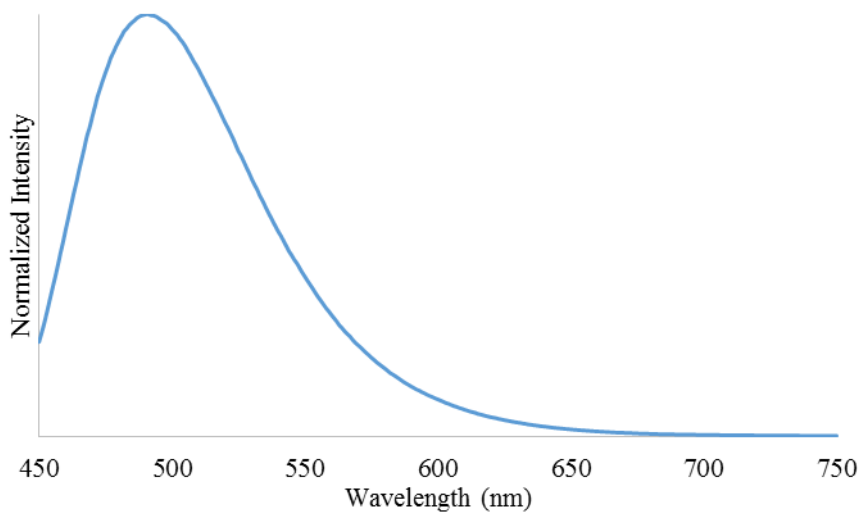


Figure S54 Emission spectrum of compound **4e**.

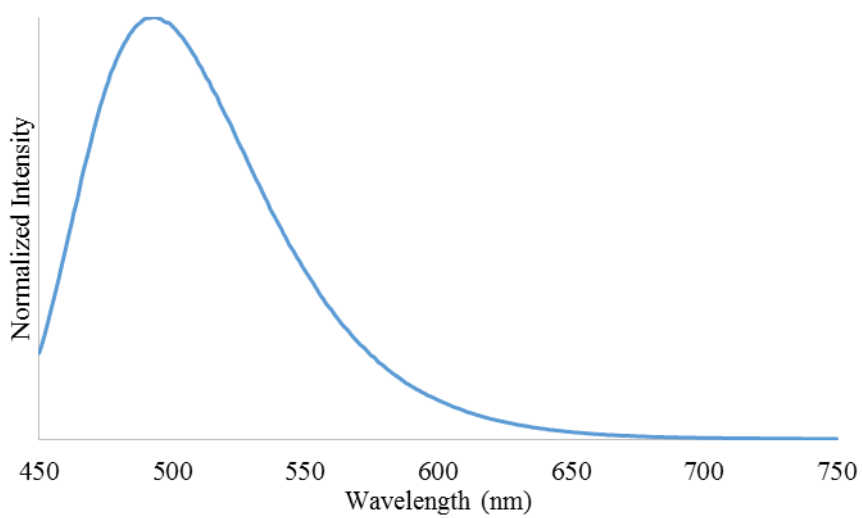


Figure S55 Emission spectrum of compound **4f**.

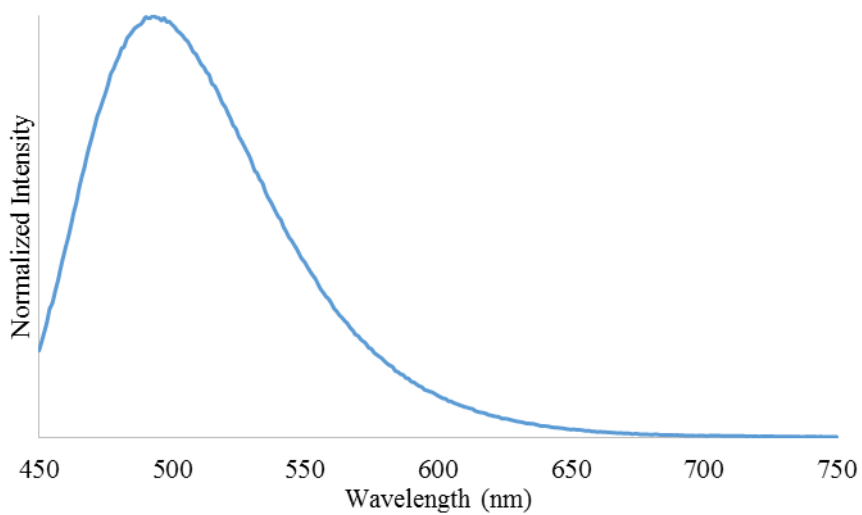


Figure S56 Emission spectrum of compound **4g**.

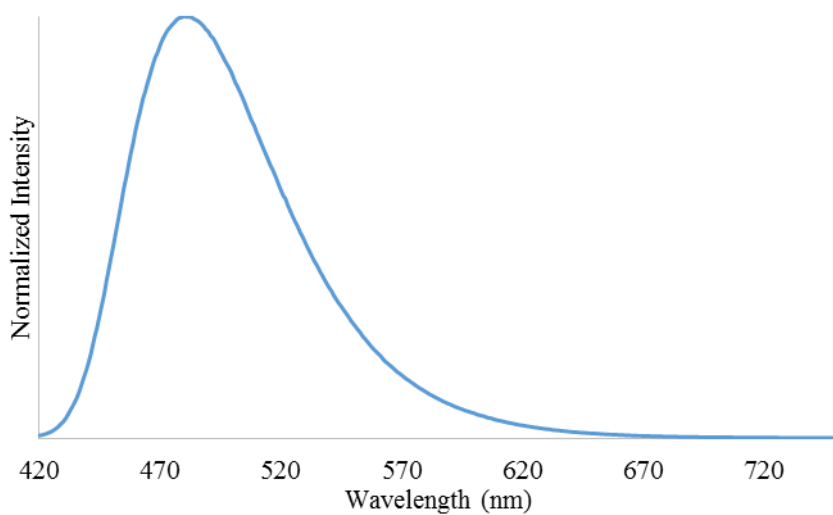


Figure S57 Emission spectrum of compound **4h**.

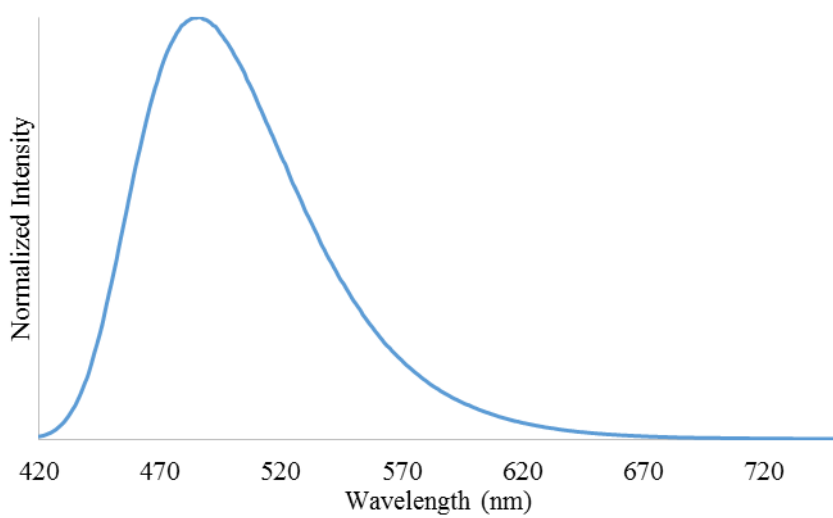


Figure S58 Emission spectrum of compound **4i**.

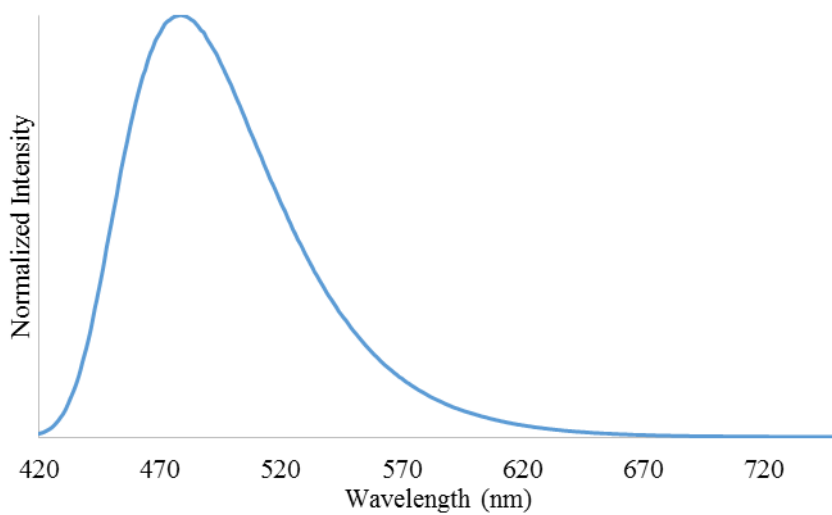


Figure S59 Emission spectrum of compound **4j**.

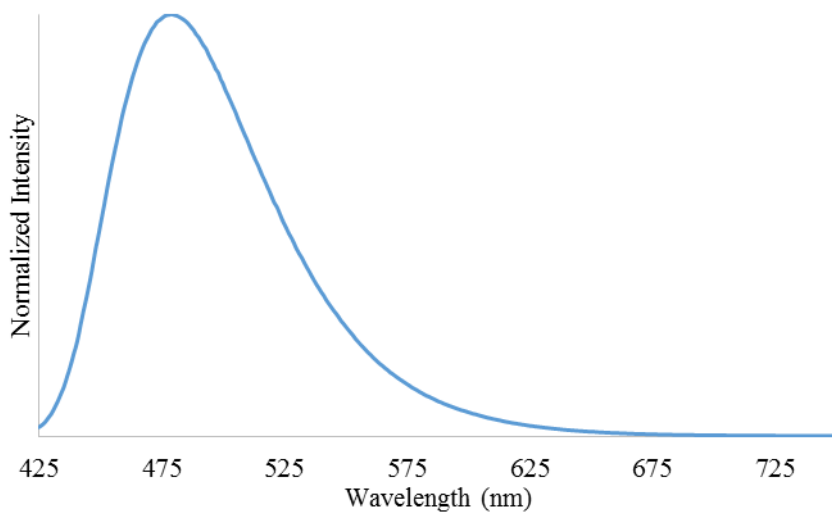


Figure S60 Emission spectrum of compound **4k**.

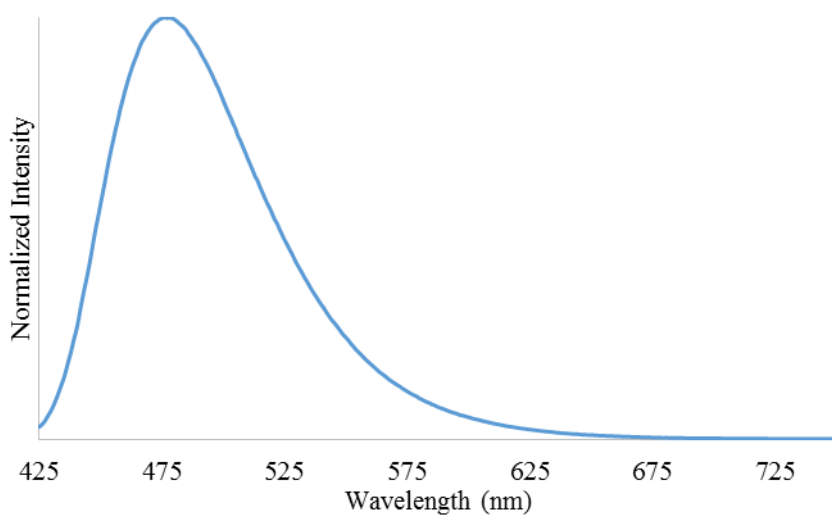


Figure S61 Emission spectrum of compound **4l**.

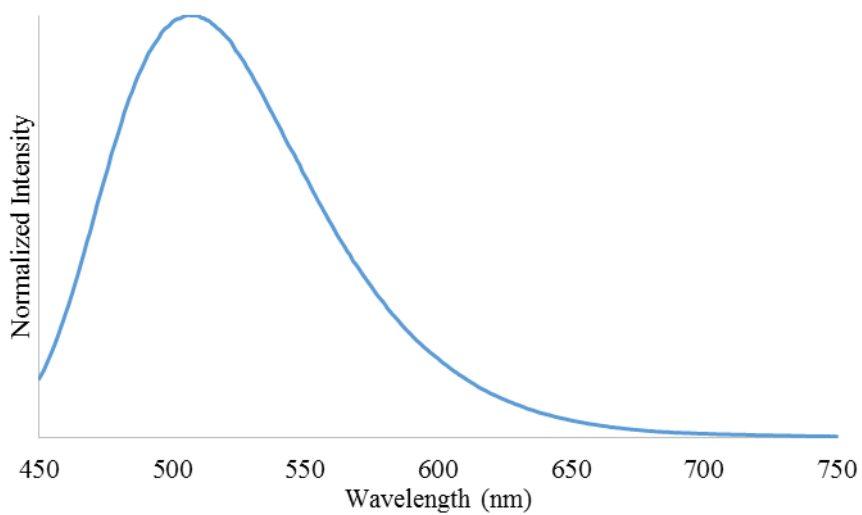


Figure S62 Emission spectrum of compound **4m**.

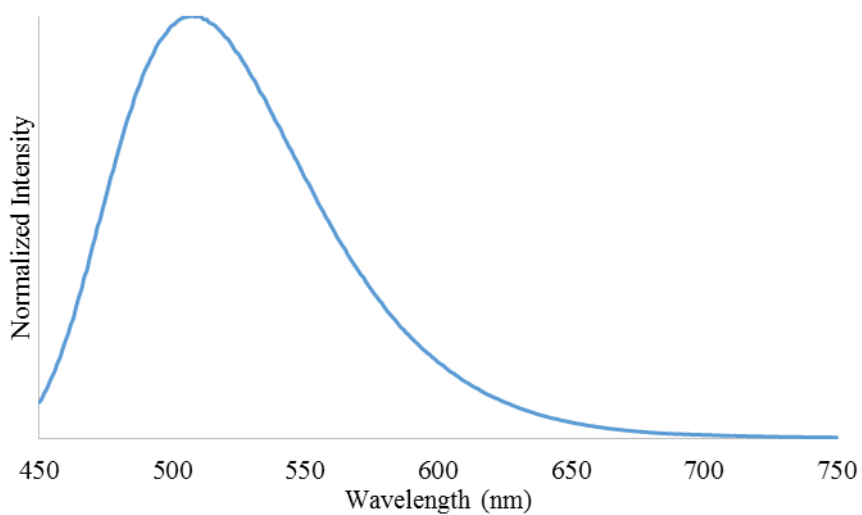


Figure S63 Emission spectrum of compound **4n**.

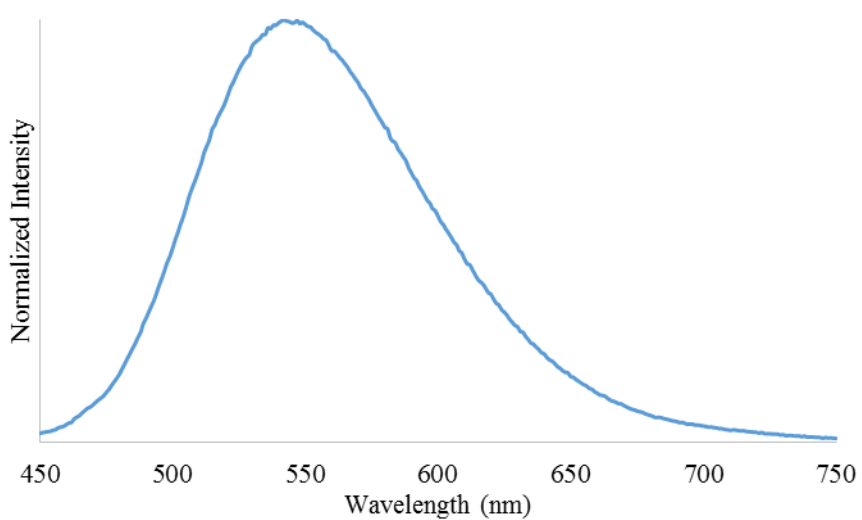


Figure S64 Emission spectrum of compound **4o**.

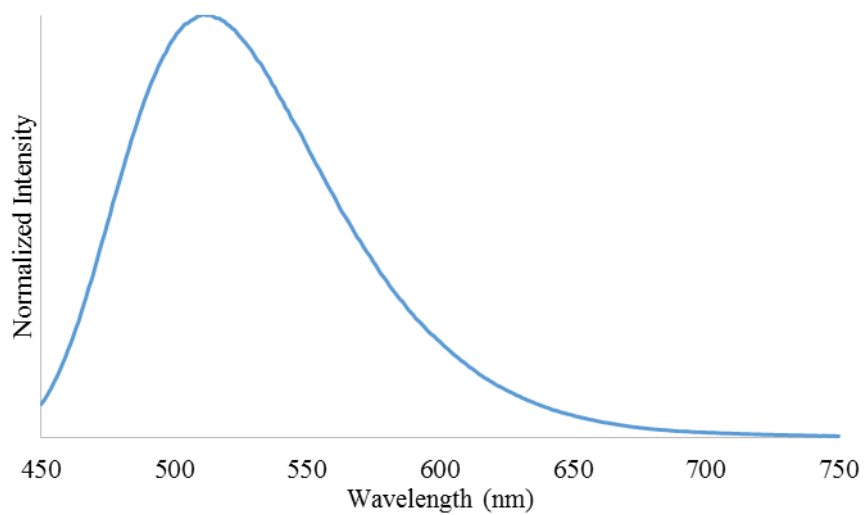


Figure S65 Emission spectrum of compound **4p**.

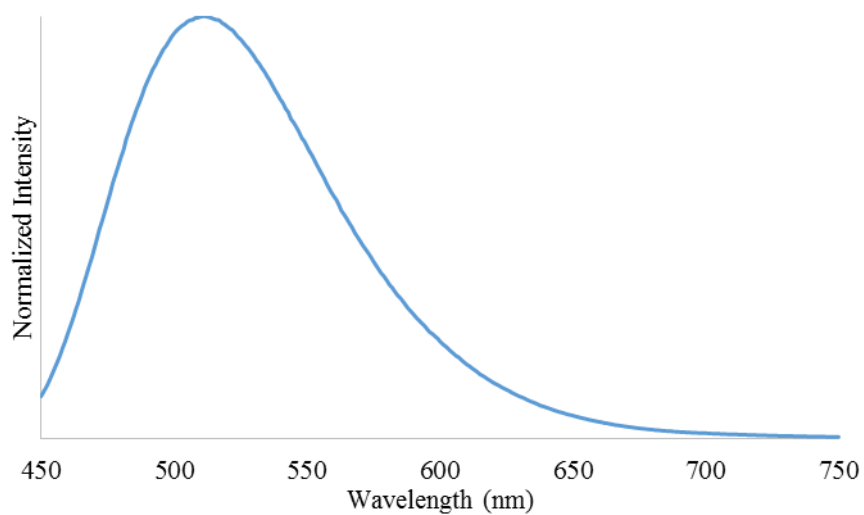


Figure S66 Emission spectrum of compound **4q**.

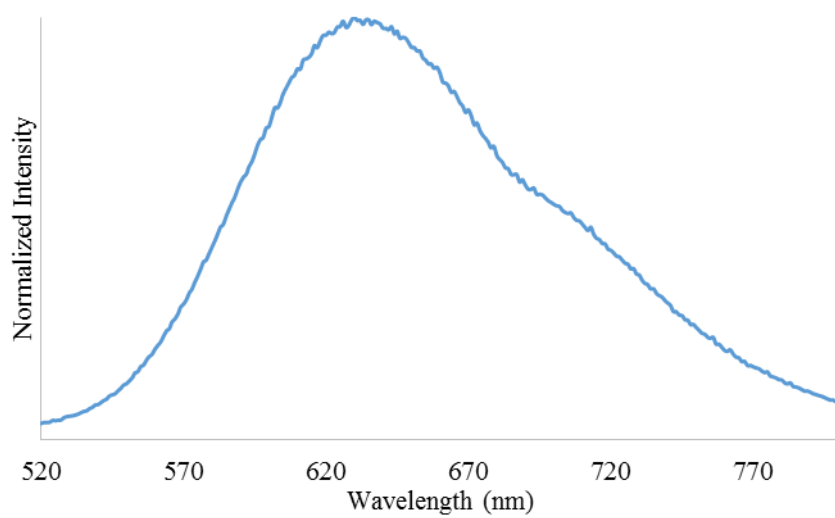


Figure S67 Emission spectrum of compound **4s**.

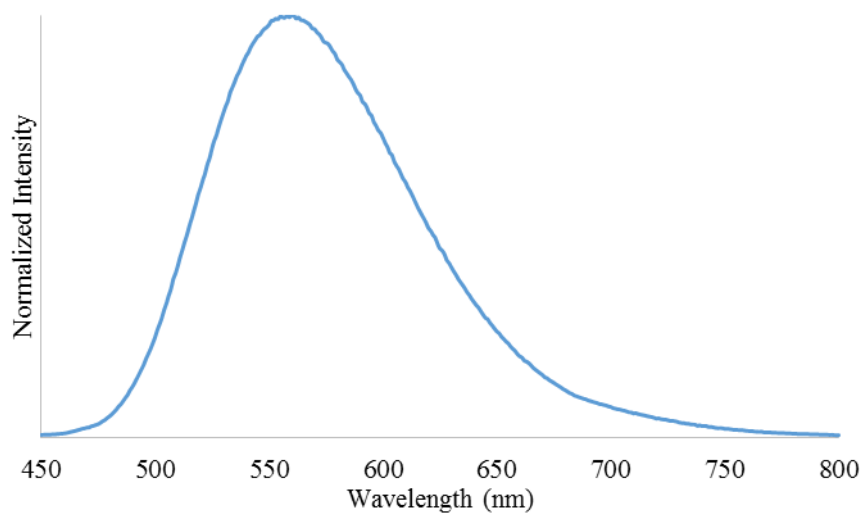


Figure S68 Emission spectrum of compound **4t**.

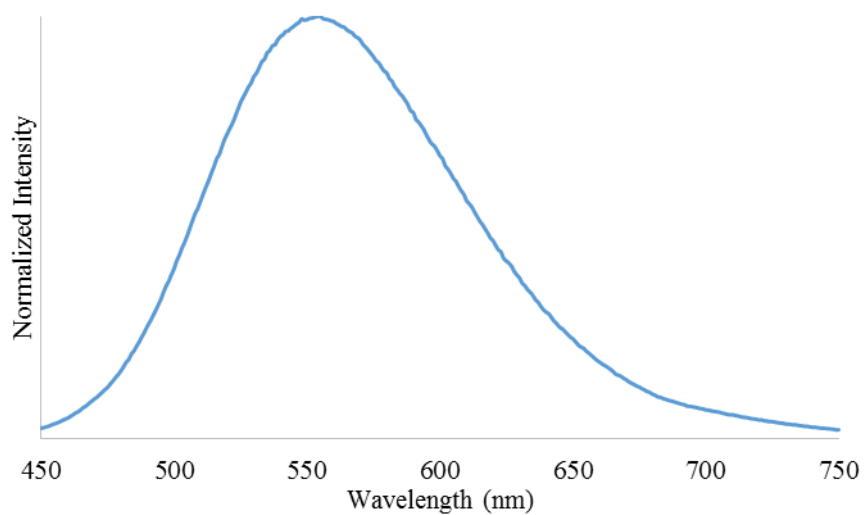


Figure S69 Emission spectrum of compound **4u**.

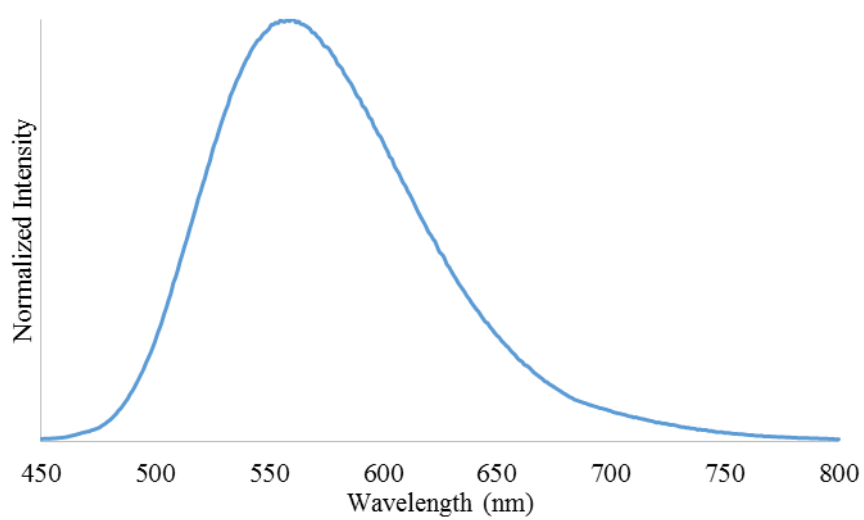


Figure S70 Emission spectrum of compound **4w**.

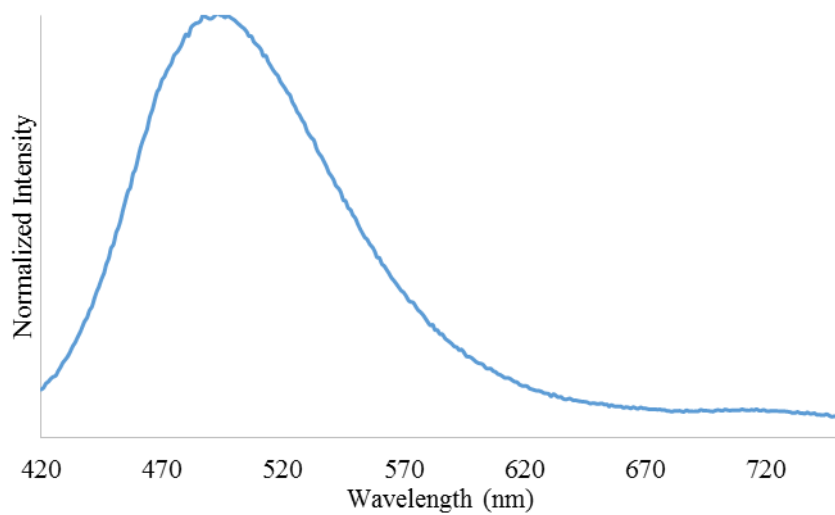


Figure S71 Emission spectrum of compound **5a**.

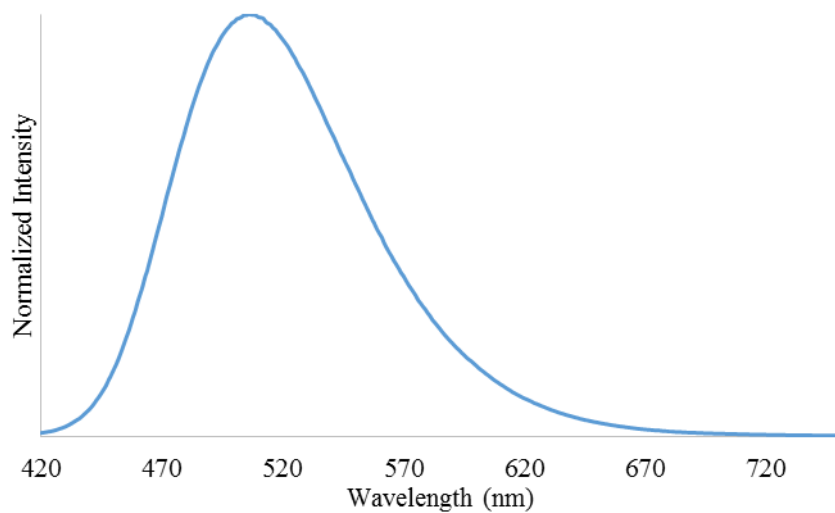


Figure S72 Emission spectrum of compound **5b**.

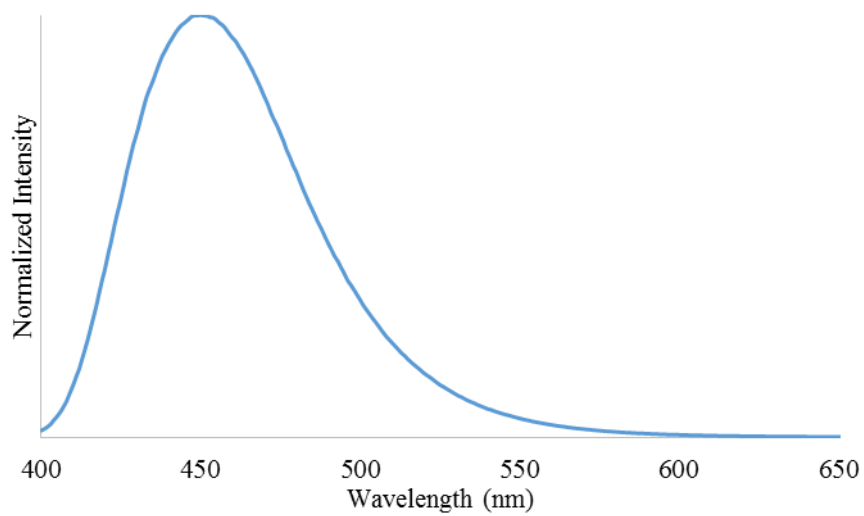


Figure S73 Emission spectrum of compound **5c**.

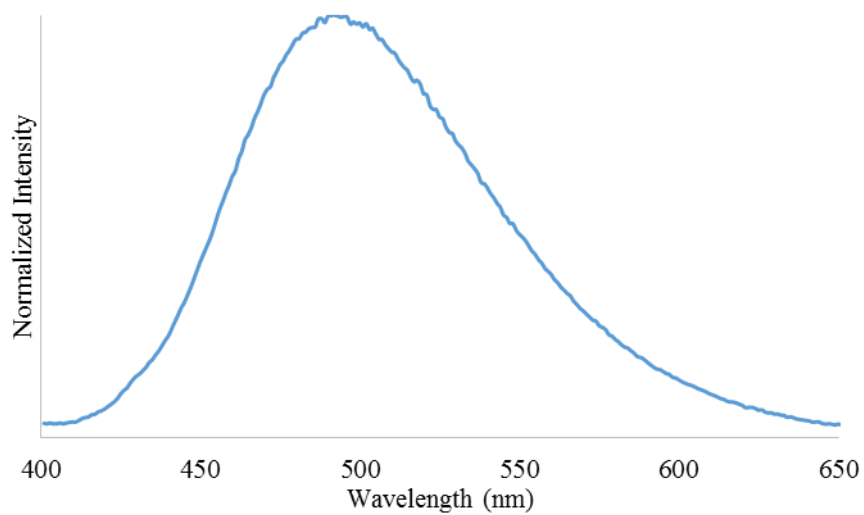


Figure S74 Emission spectrum of compound **6a**.

Cyclic voltammograms of selected quinolizinium compounds

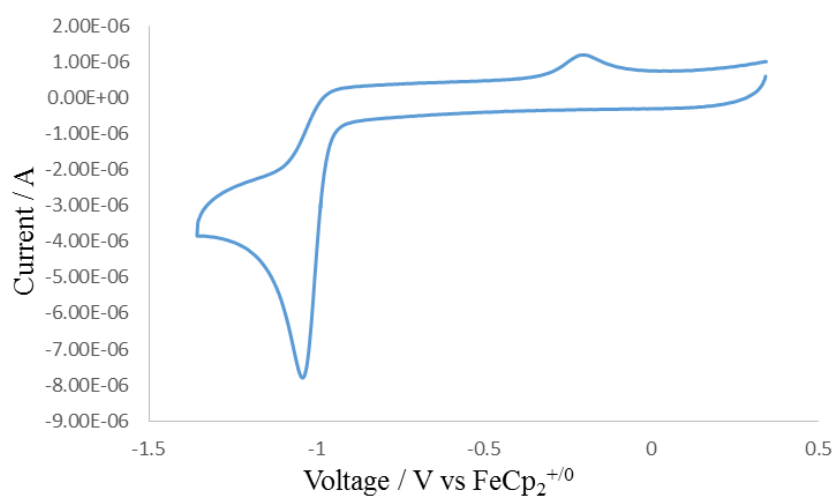
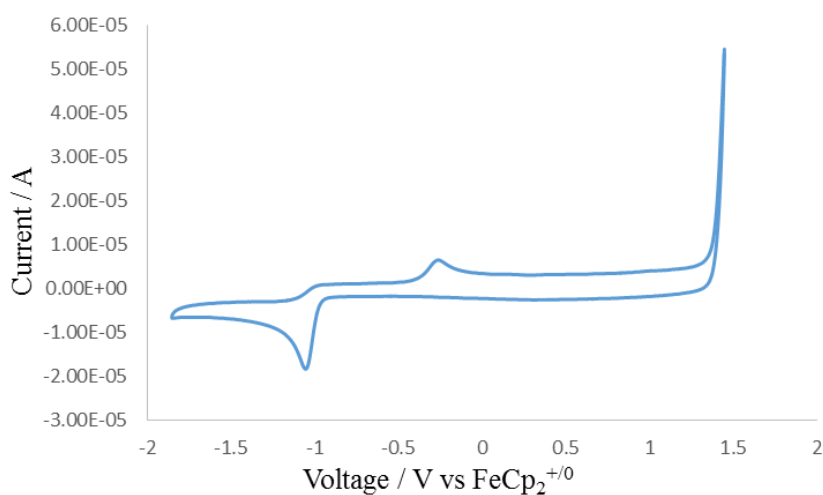


Figure S75 Cyclic voltammogram of compound **4a**.



voltammogram **Figure S76** Cyclic of compound **4b**.

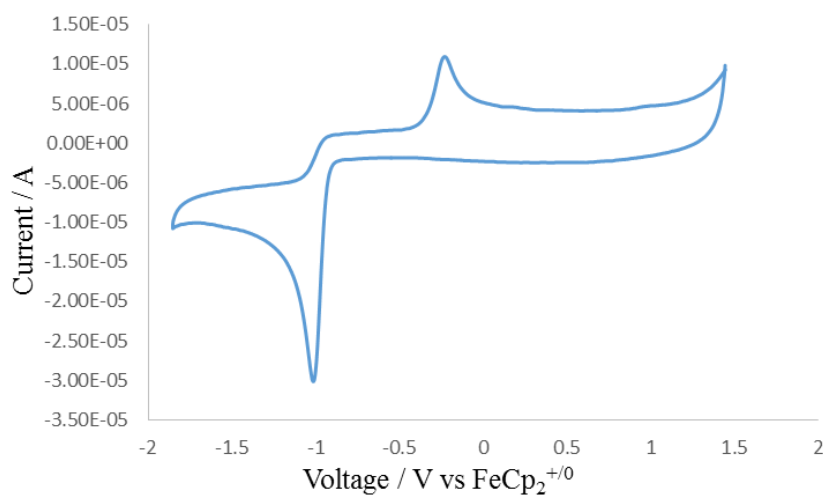


Figure S77 Cyclic voltammogram of compound **4e**.

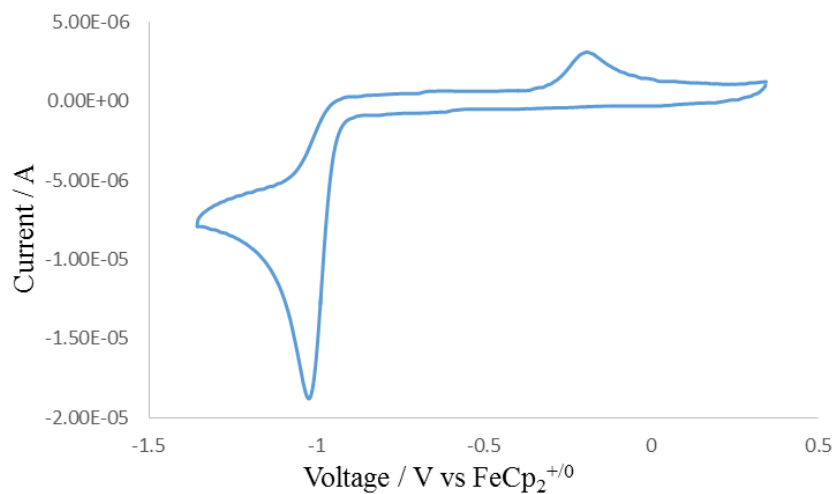


Figure S78 Cyclic voltammogram of compound **4f**.

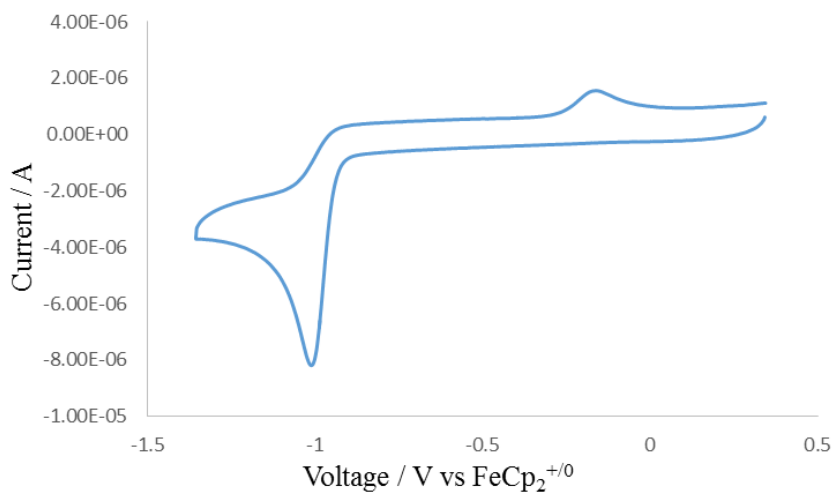


Figure S79 Cyclic voltammogram of compound **4j**.

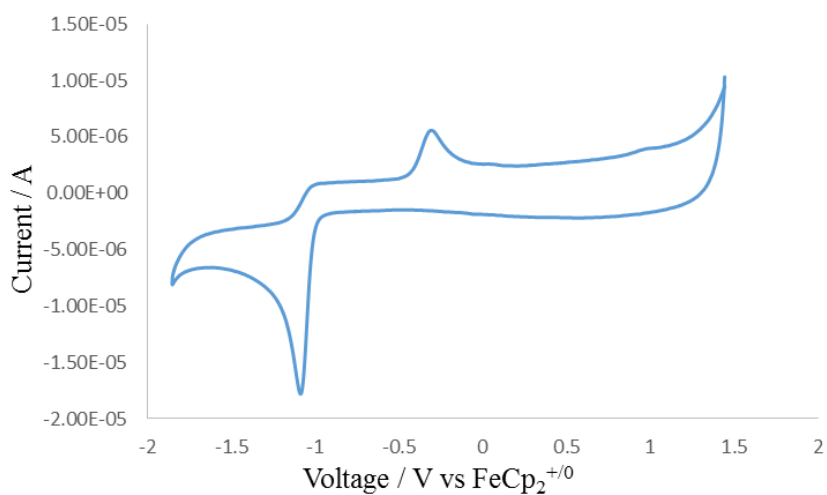


Figure S80 Cyclic voltammogram of compound **4p**.

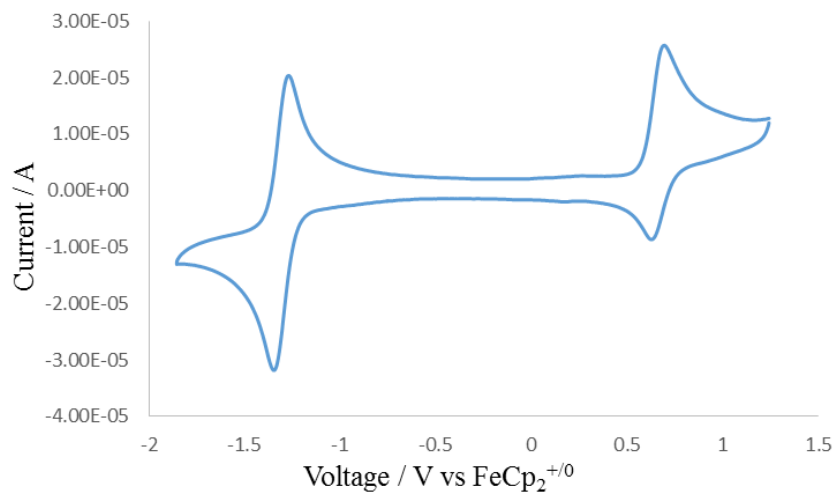


Figure S81 Cyclic voltammogram of compound **5a**.

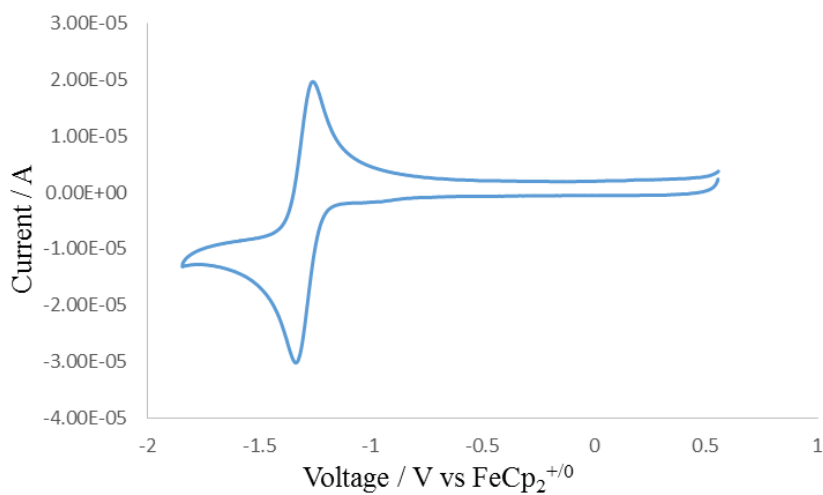


Figure S82 Cyclic voltammogram of compound **5c**.

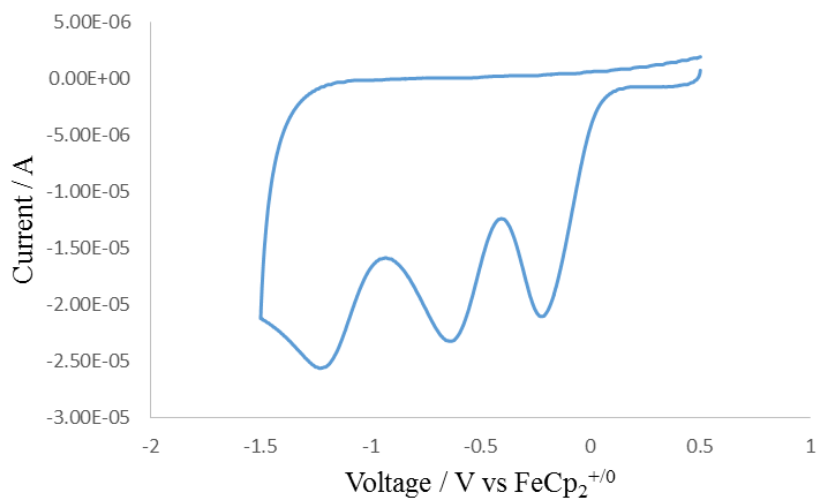
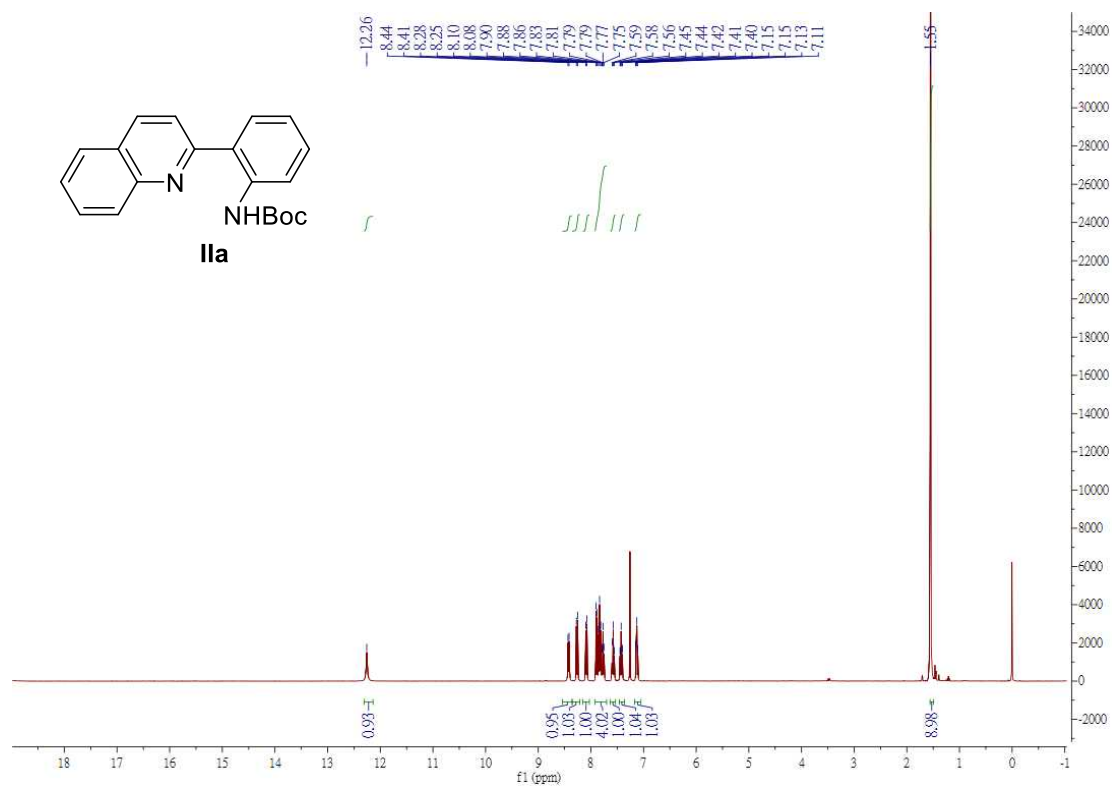
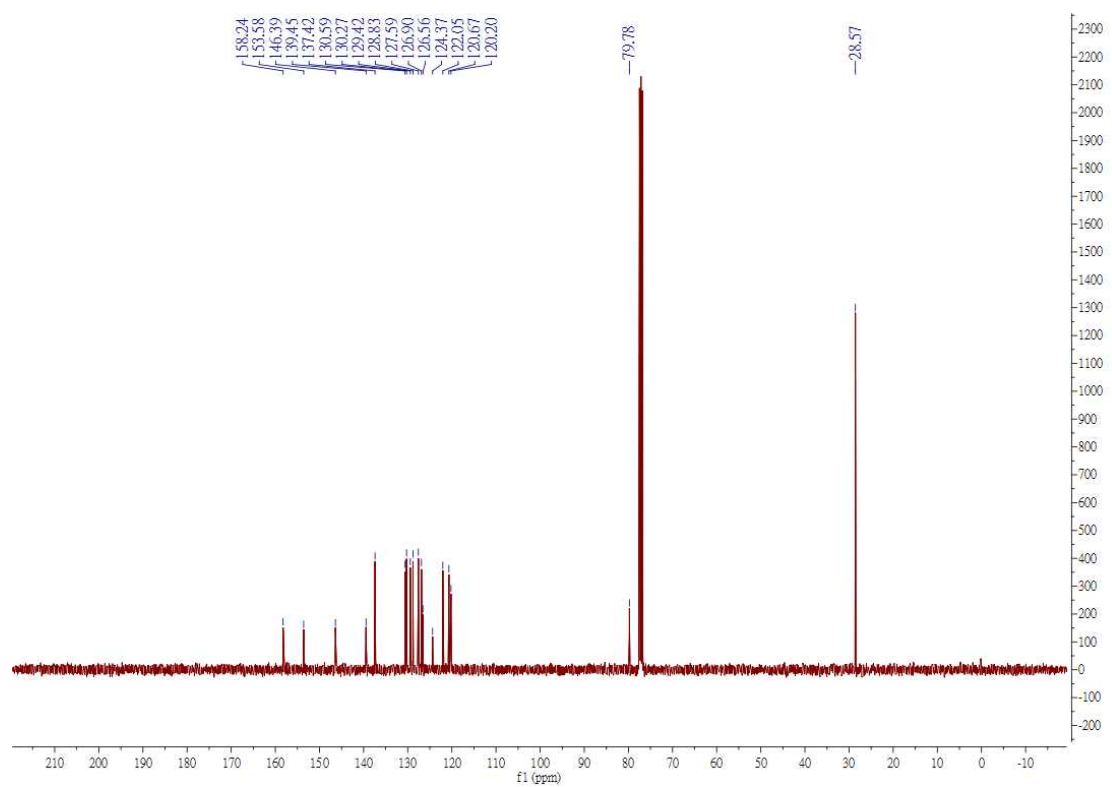


Figure S83 Cyclic voltammogram of compound **1a**.

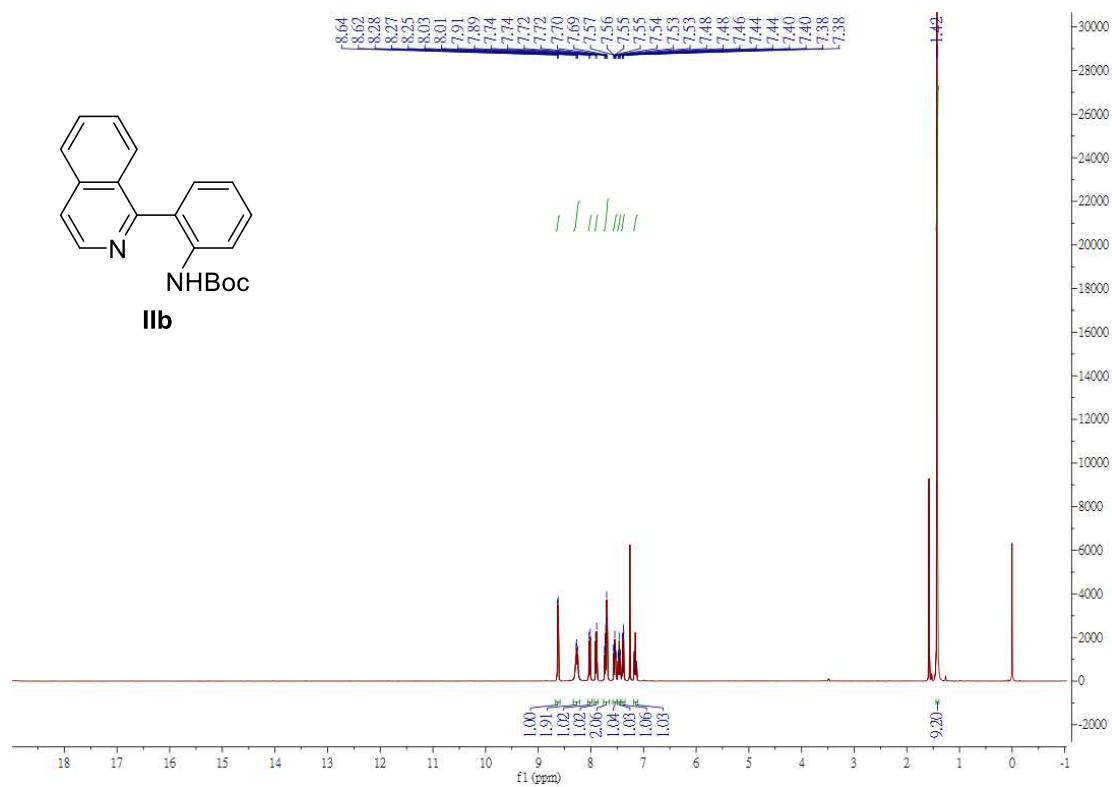
¹H NMR



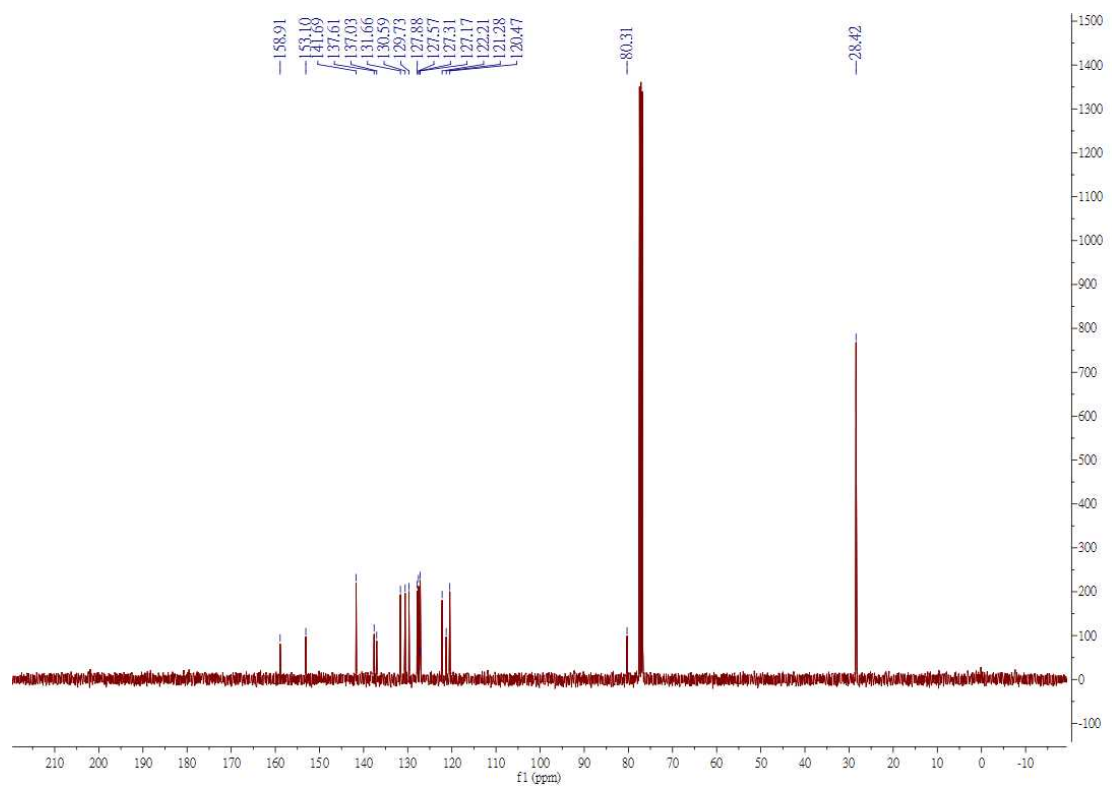
¹³C NMR



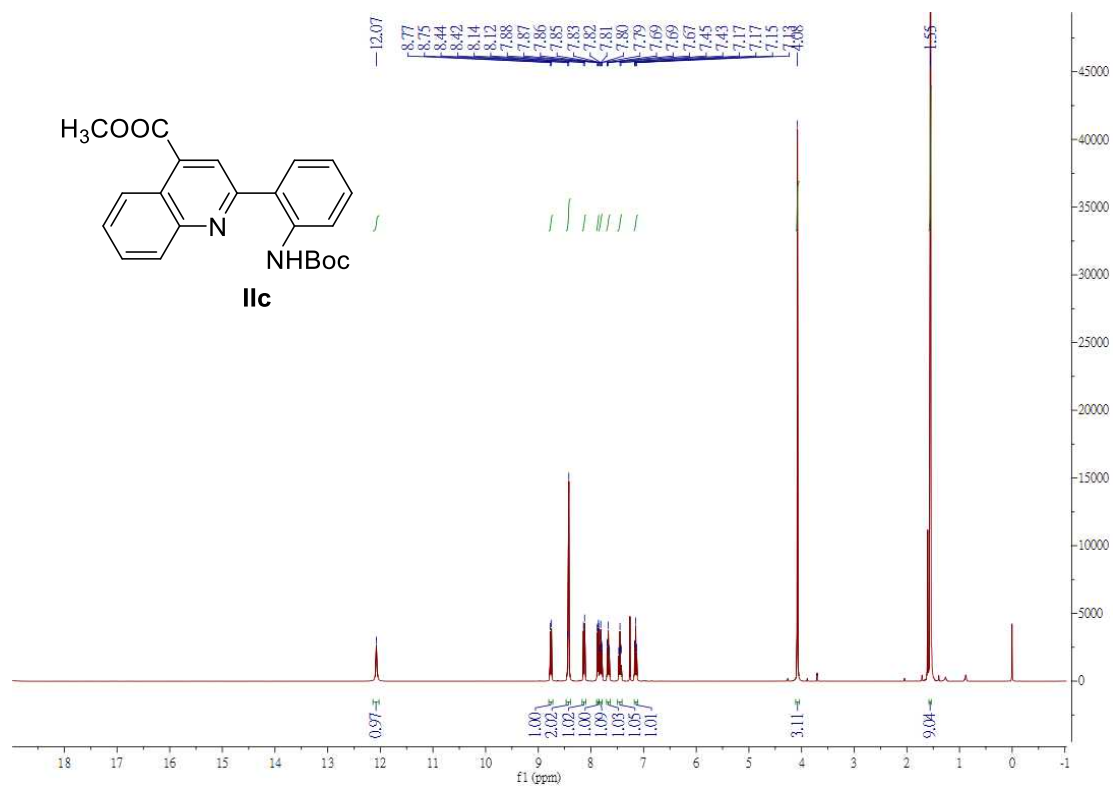
¹H NMR



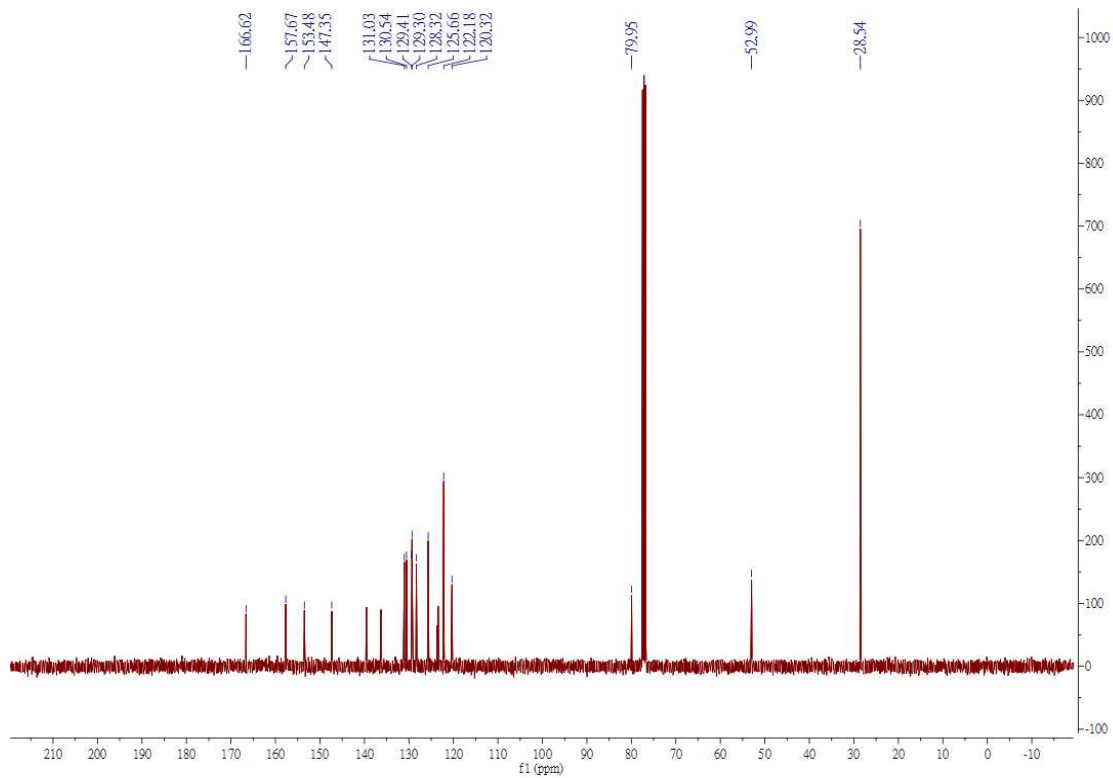
¹³C NMR



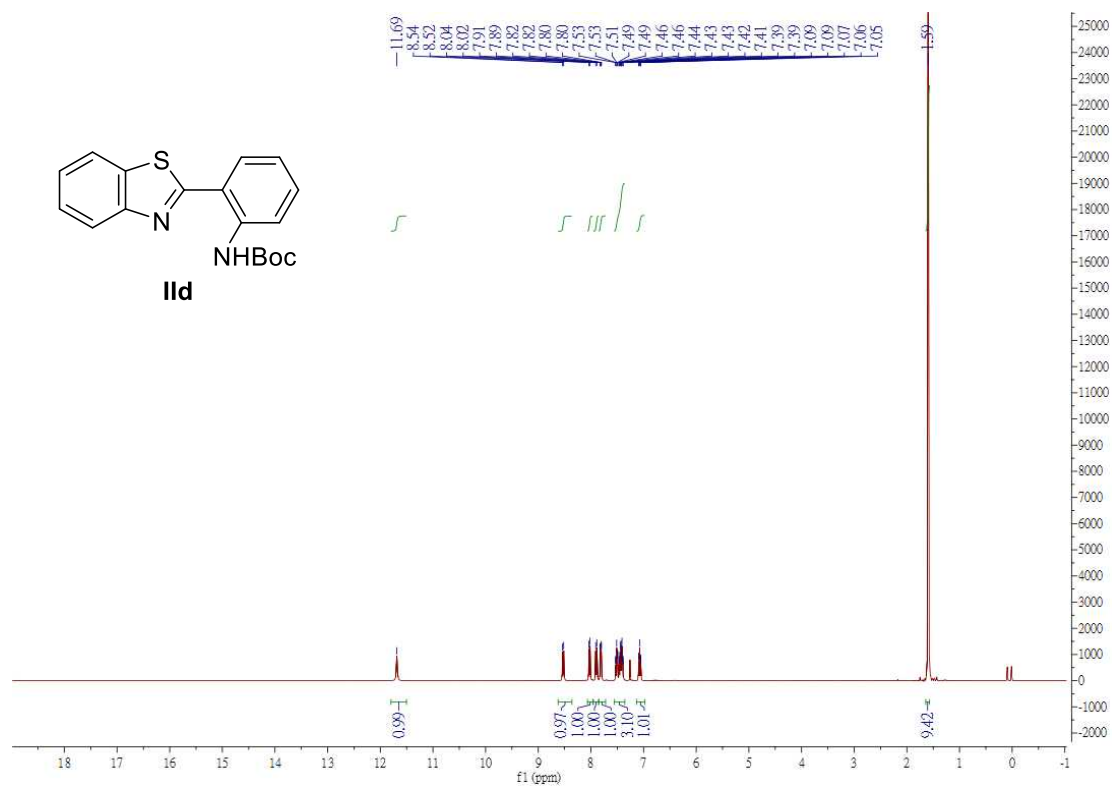
¹H NMR



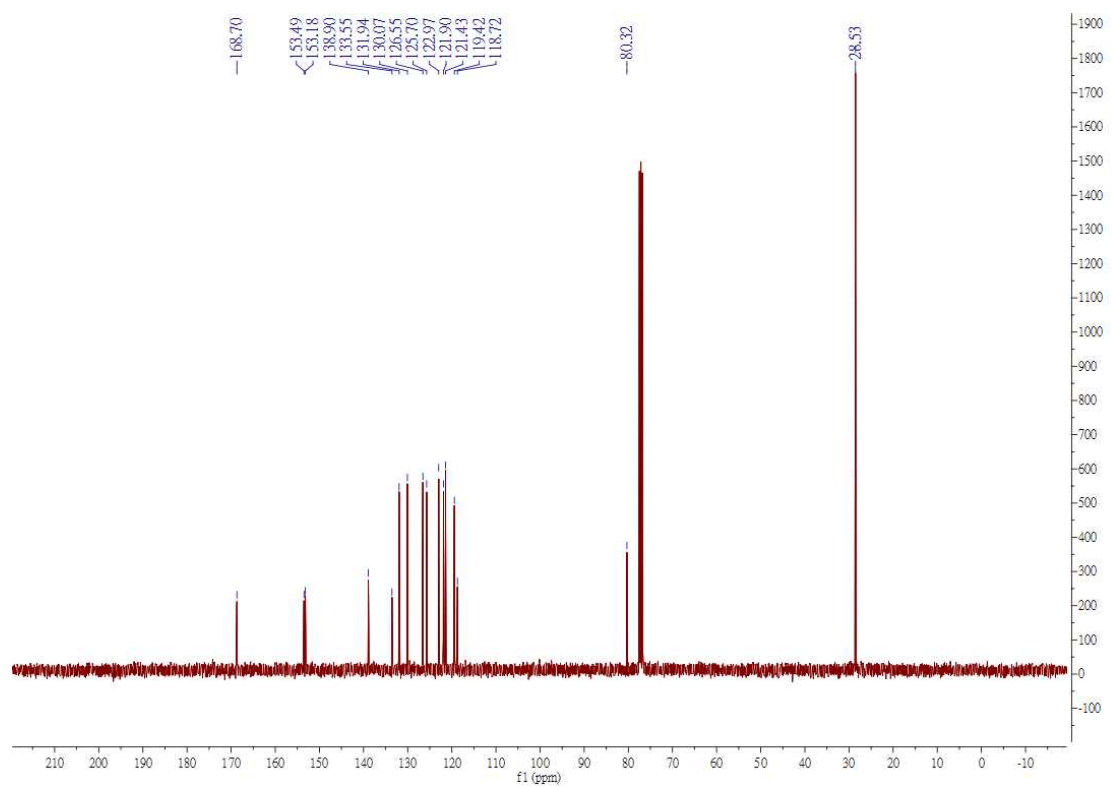
¹³C NMR



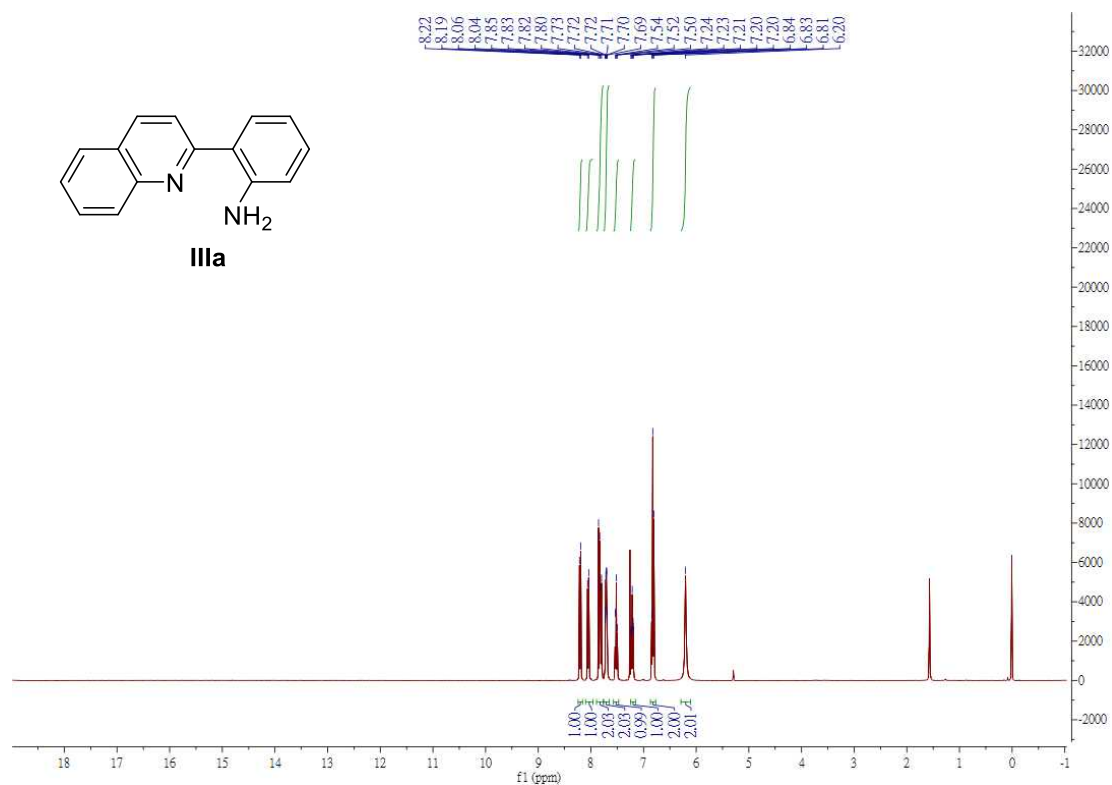
¹H NMR



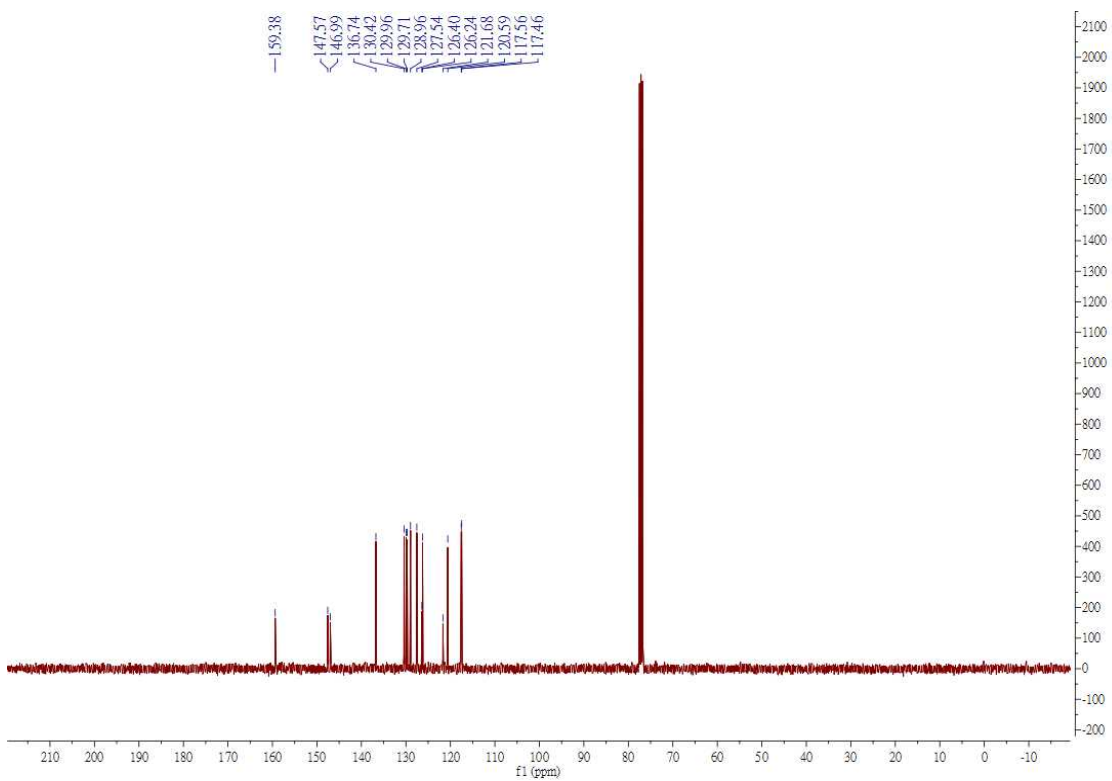
¹³C NMR



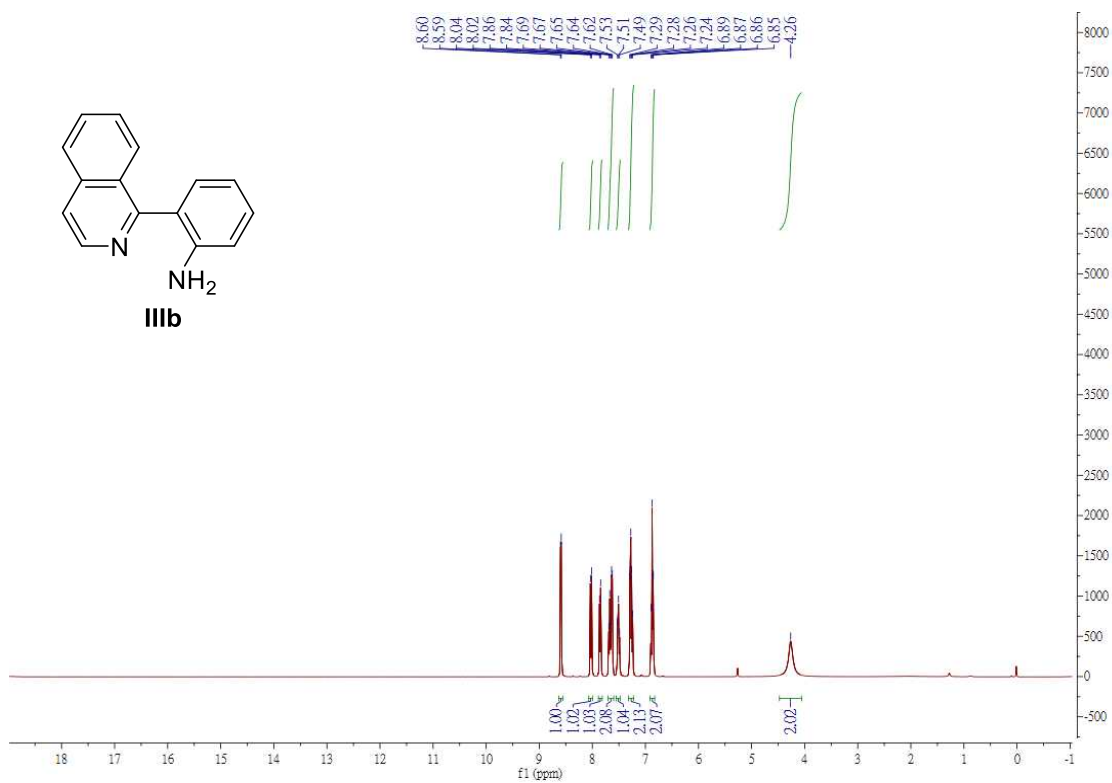
¹H NMR



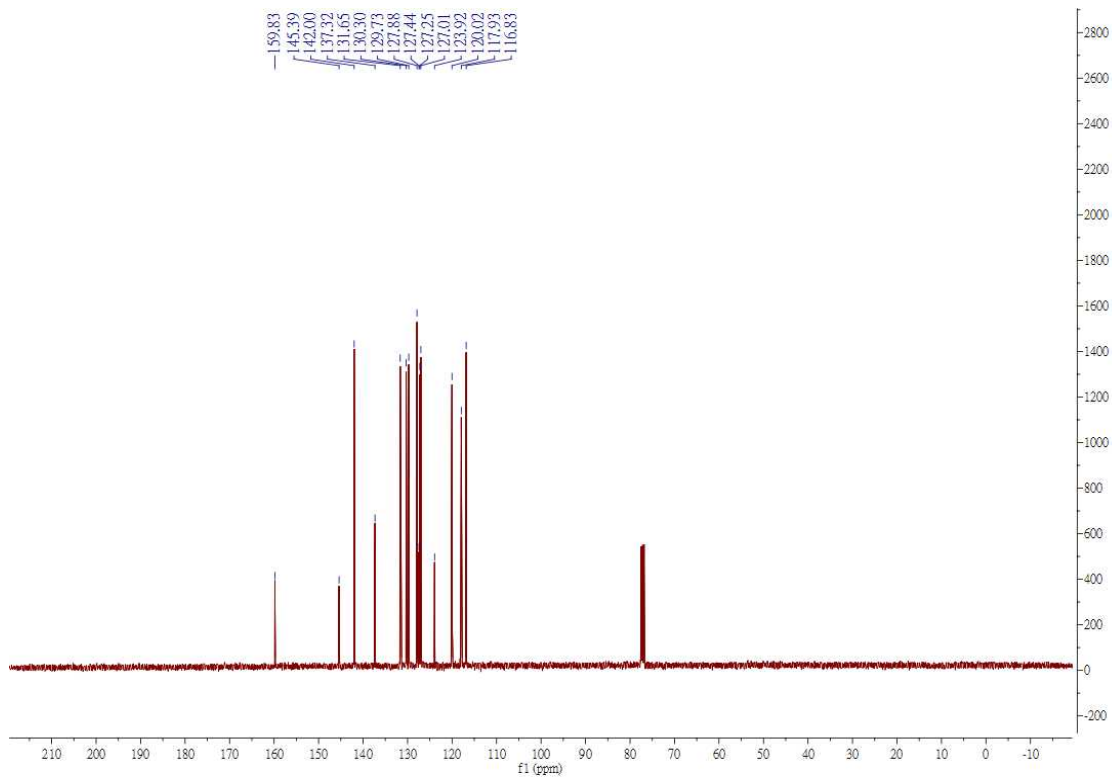
¹³C NMR



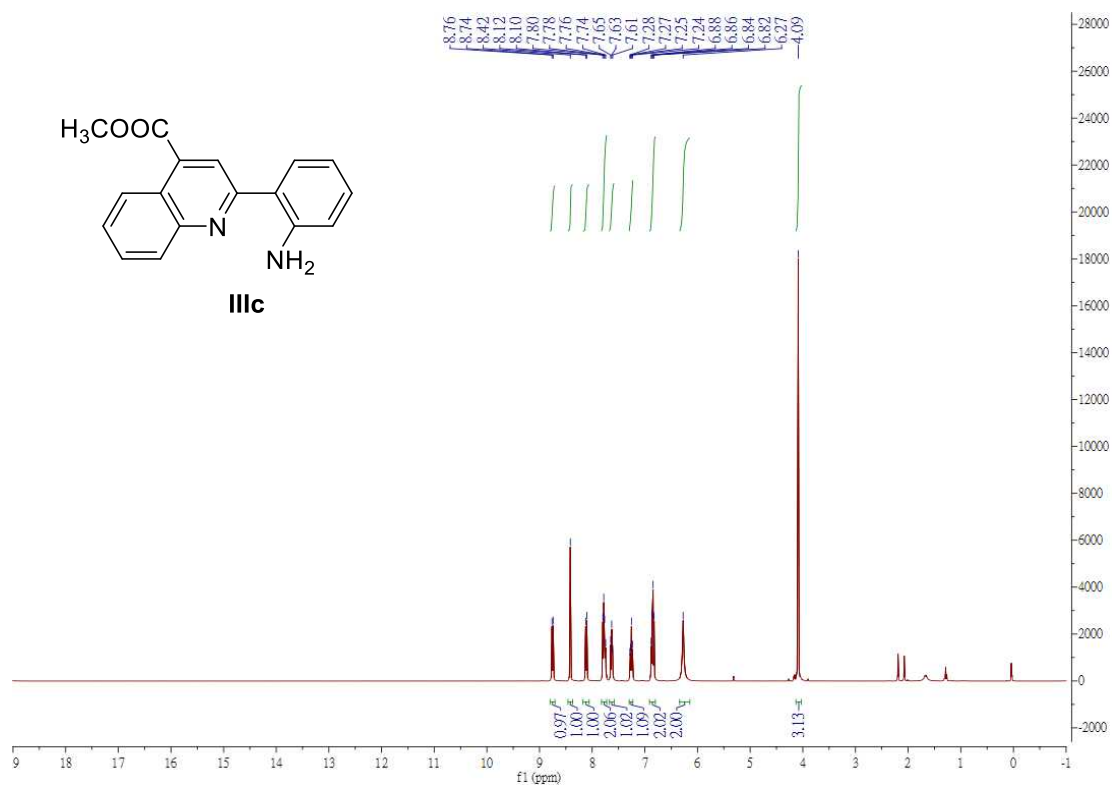
¹H NMR



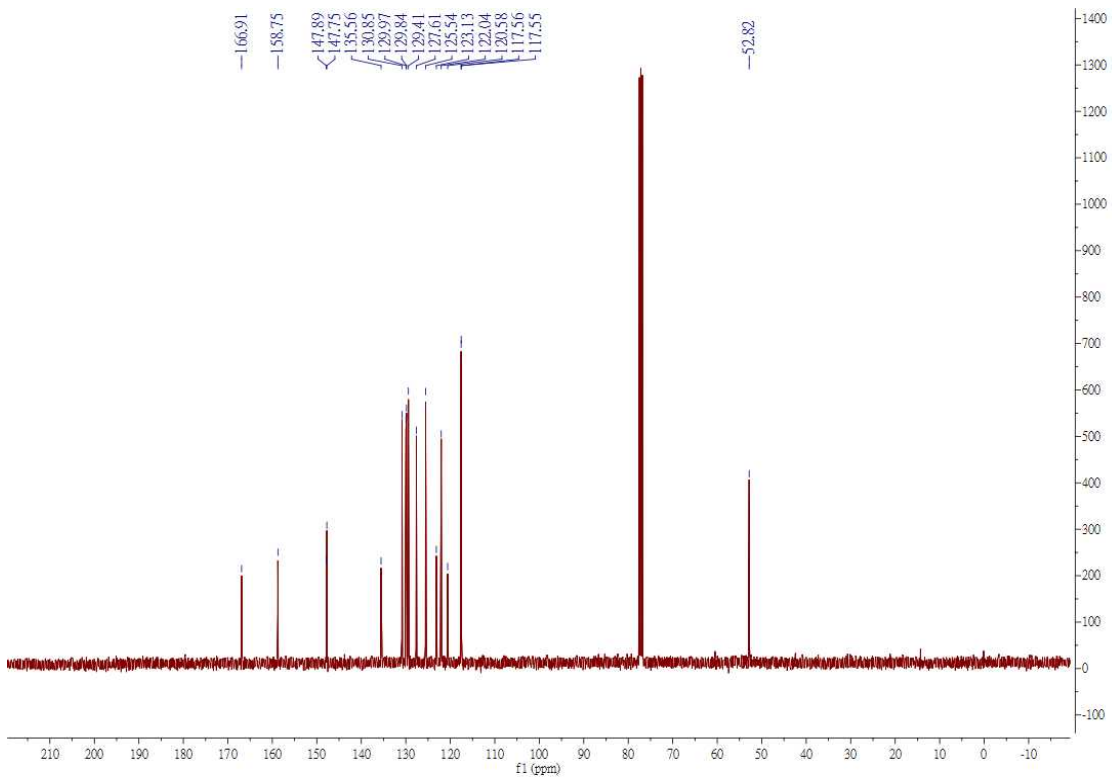
¹³C NMR



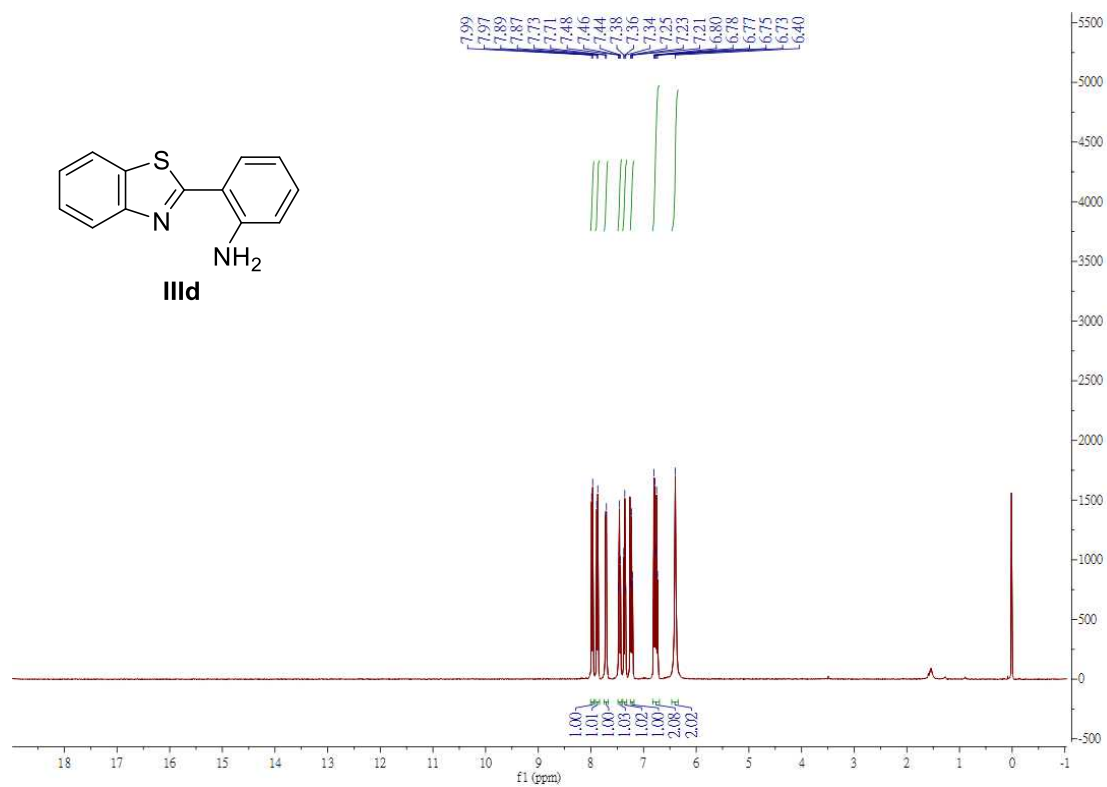
¹H NMR



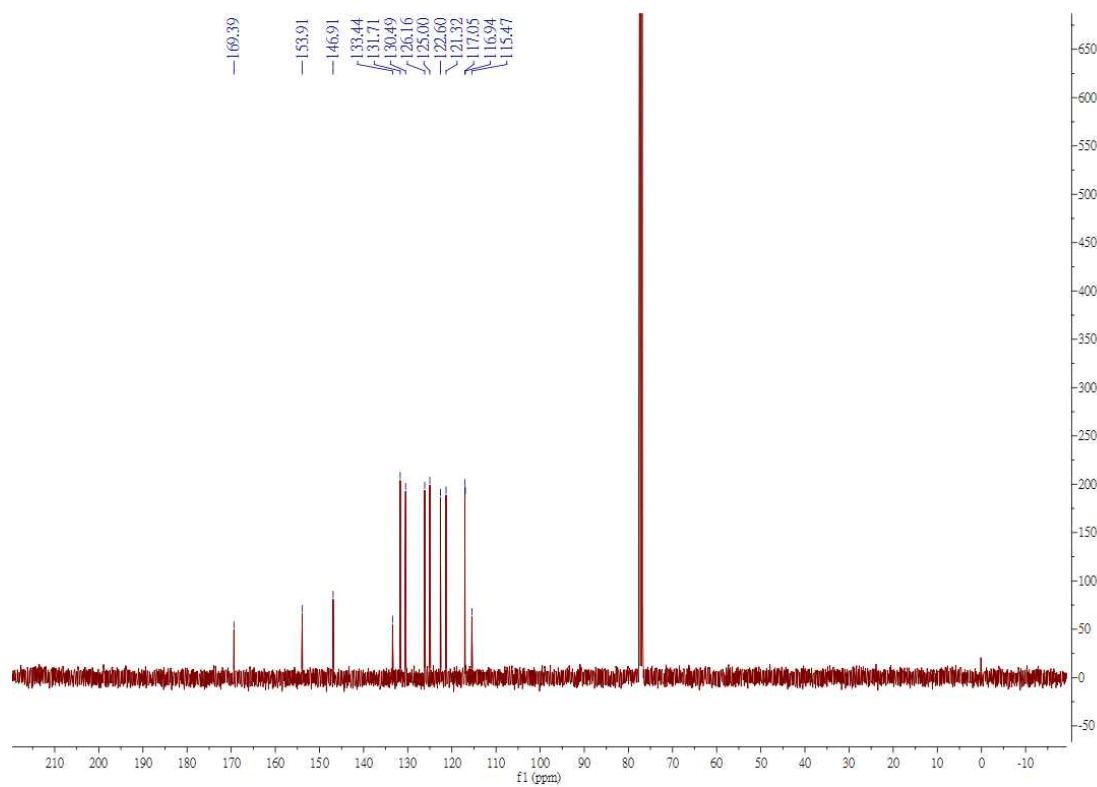
¹³C NMR



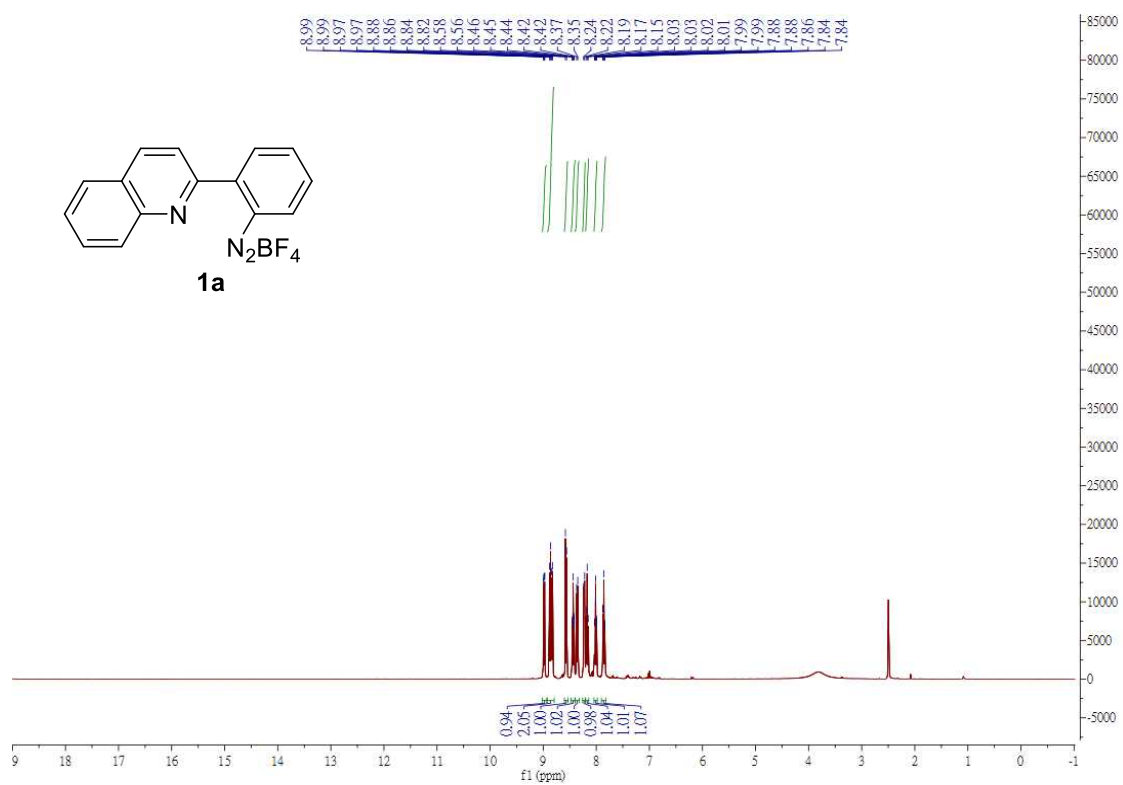
¹H NMR



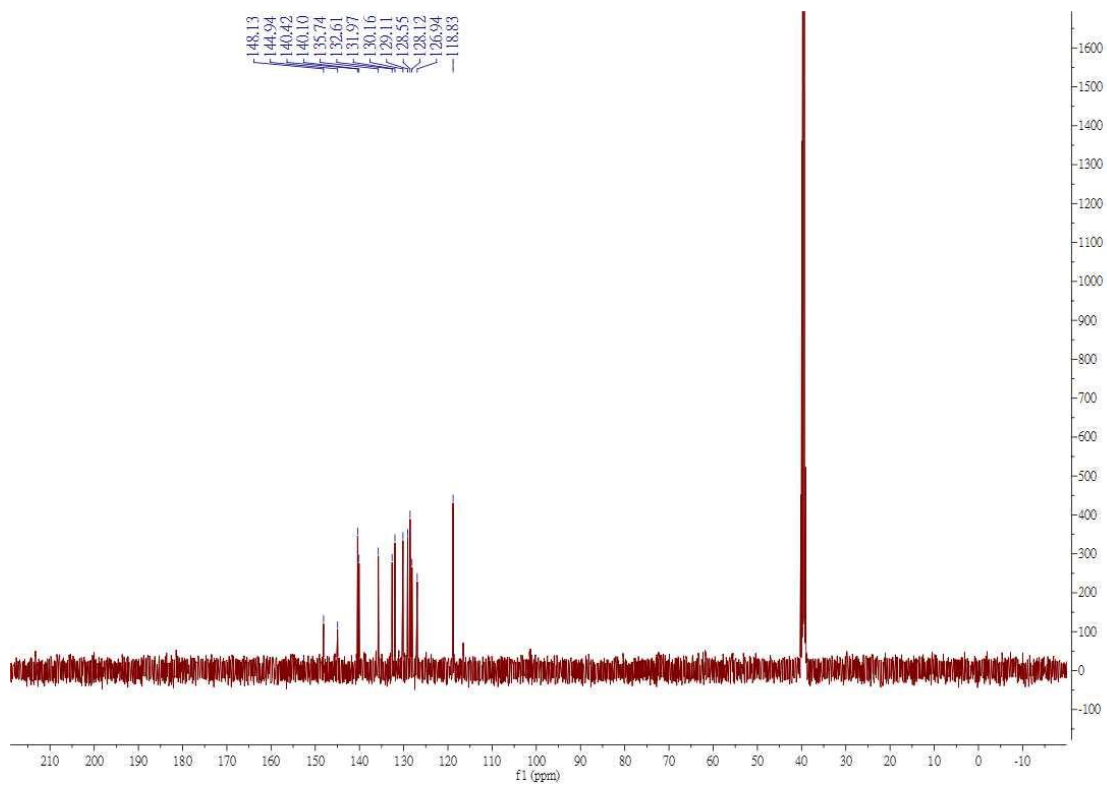
¹³C NMR



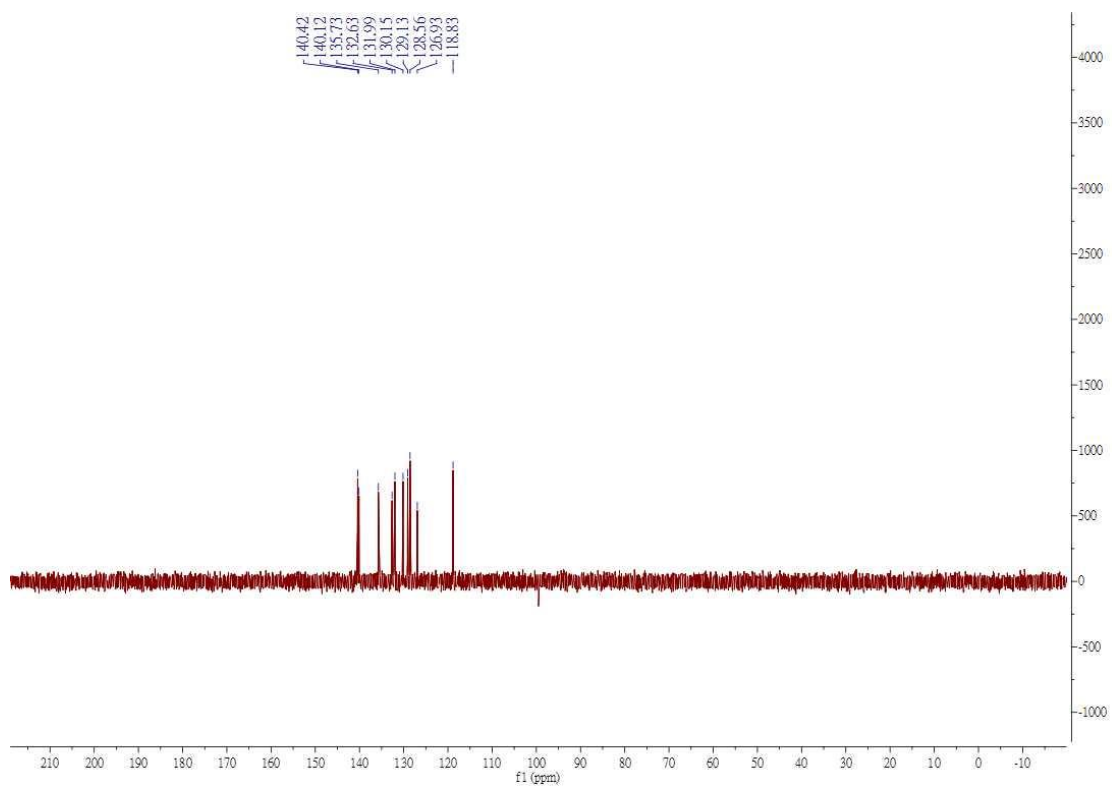
¹H NMR



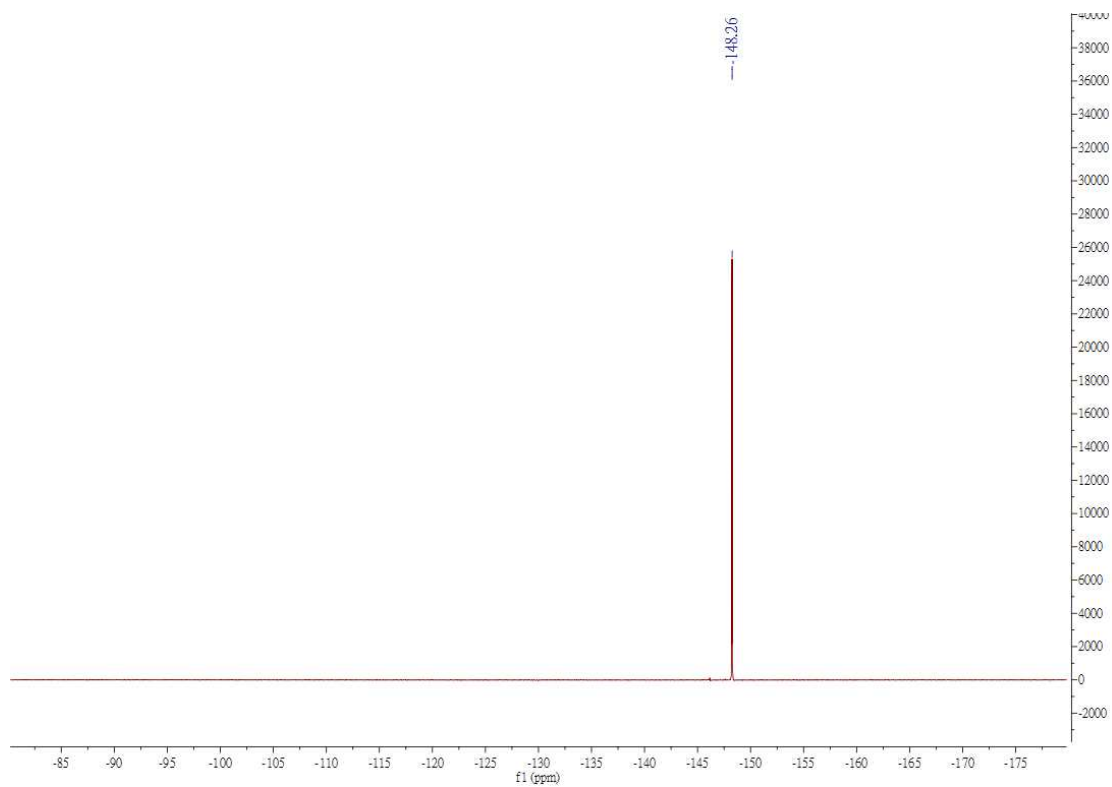
¹³C NMR



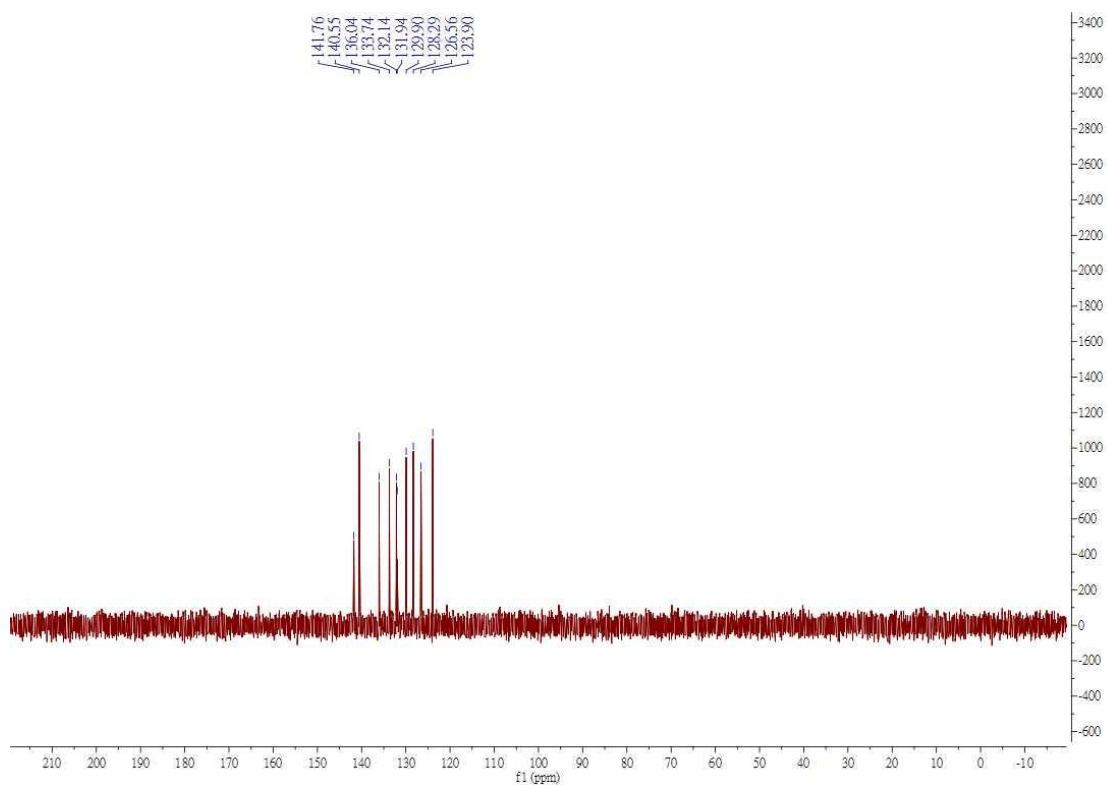
DEPT 135



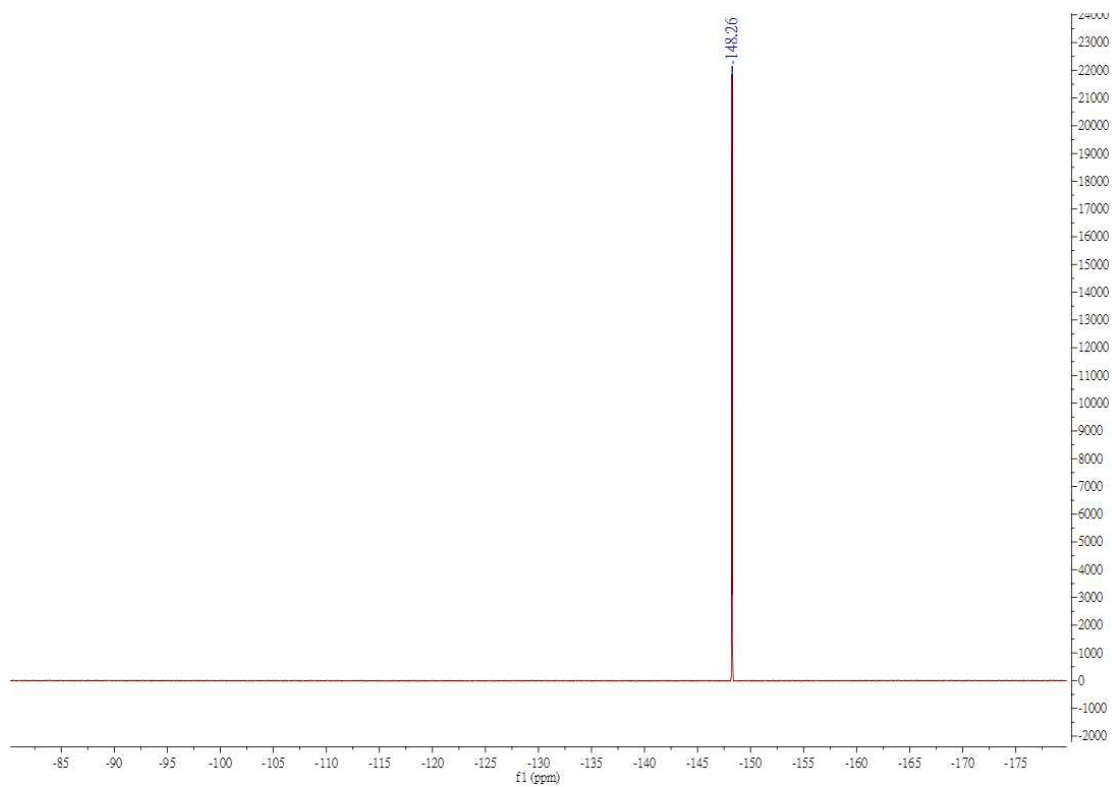
¹⁹F NMR



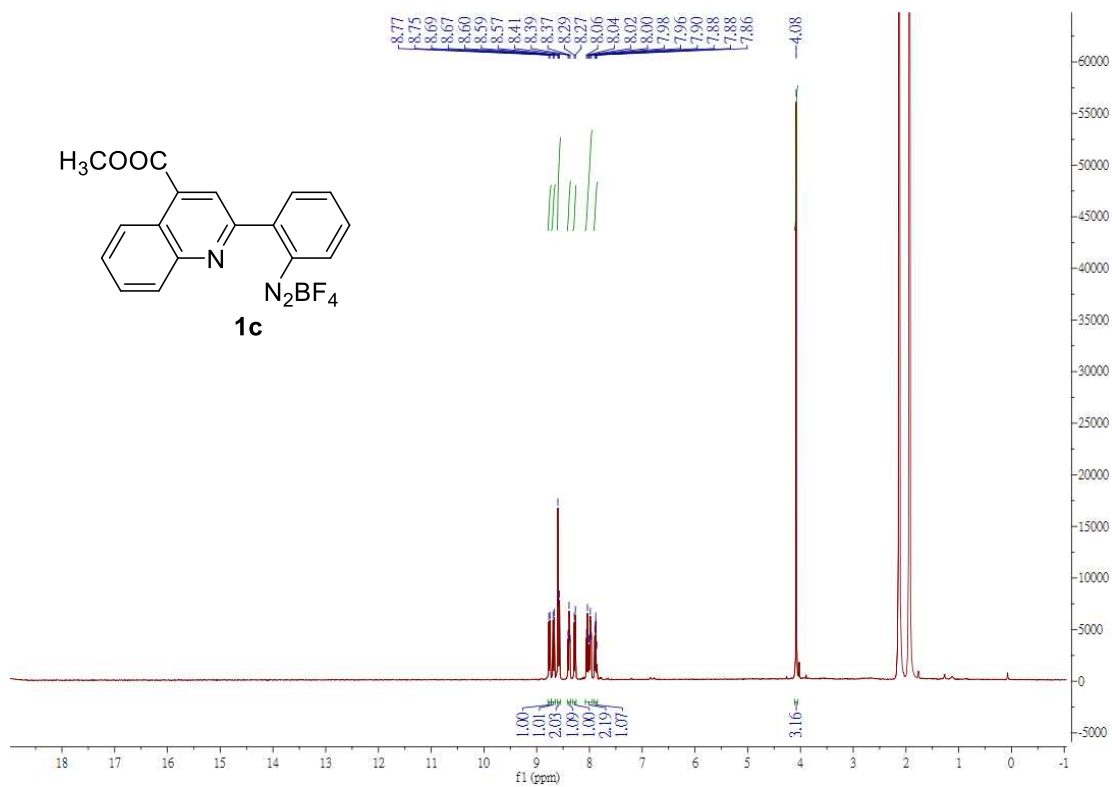
DEPT 135



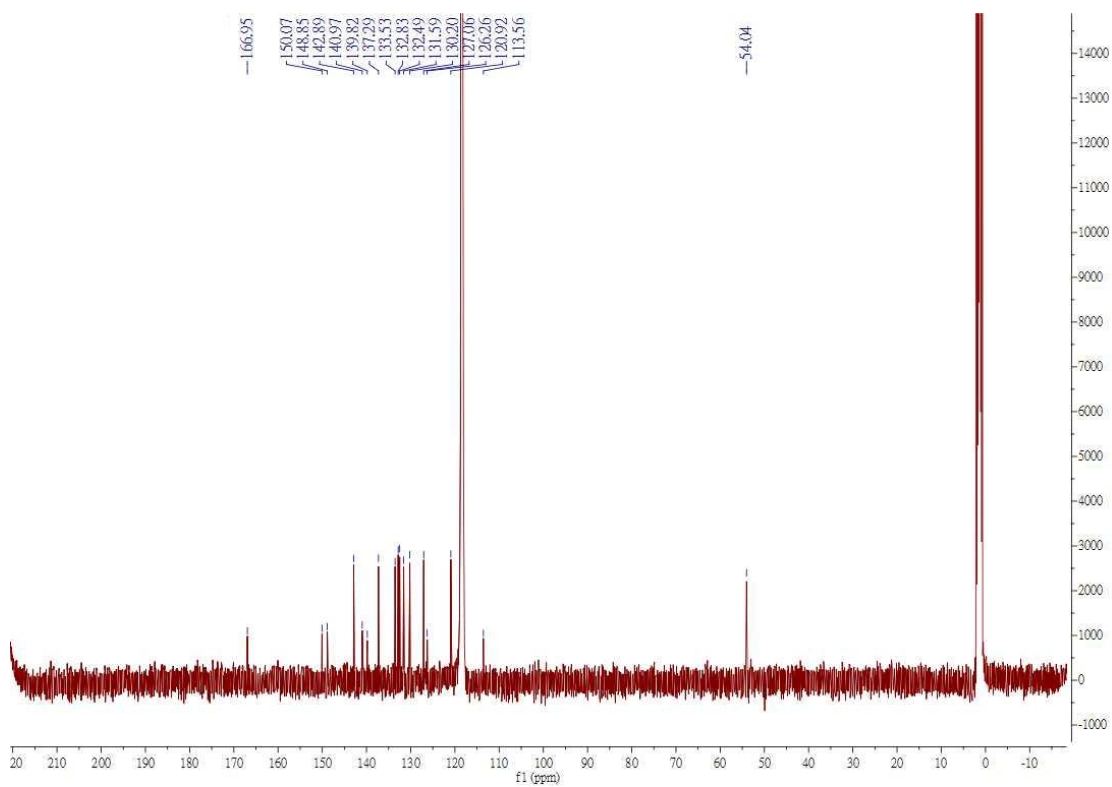
¹⁹F NMR



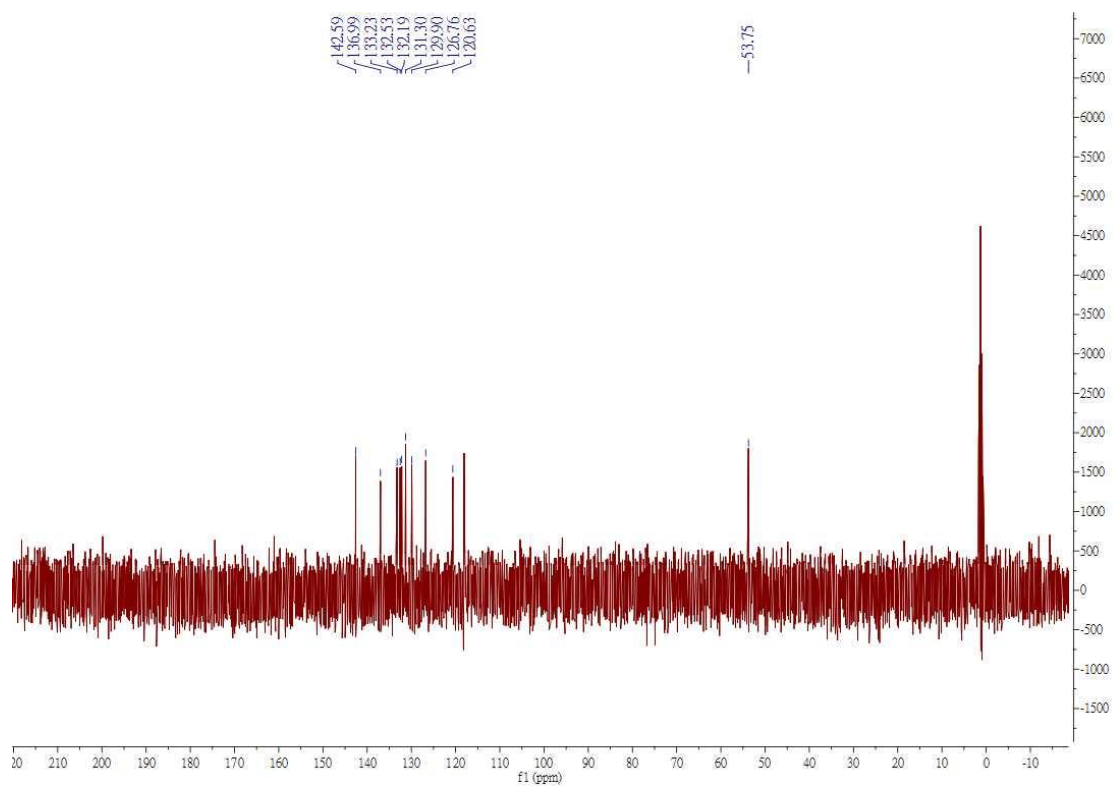
¹H NMR



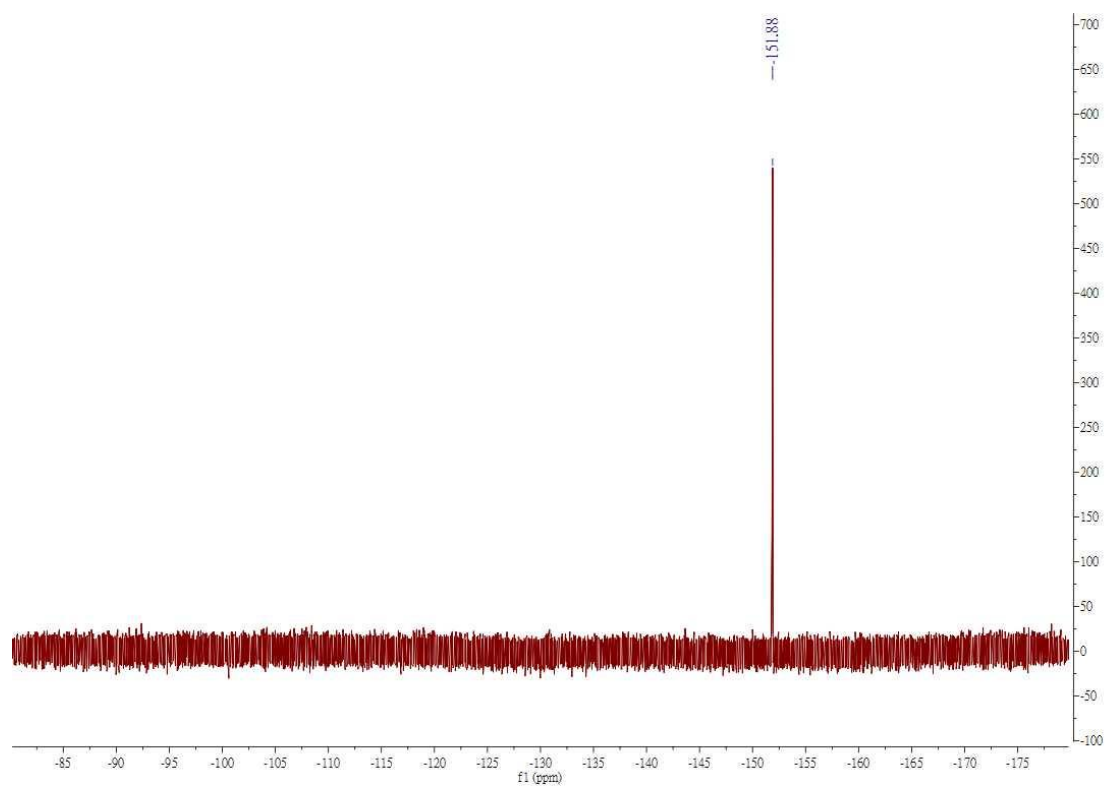
¹³C NMR



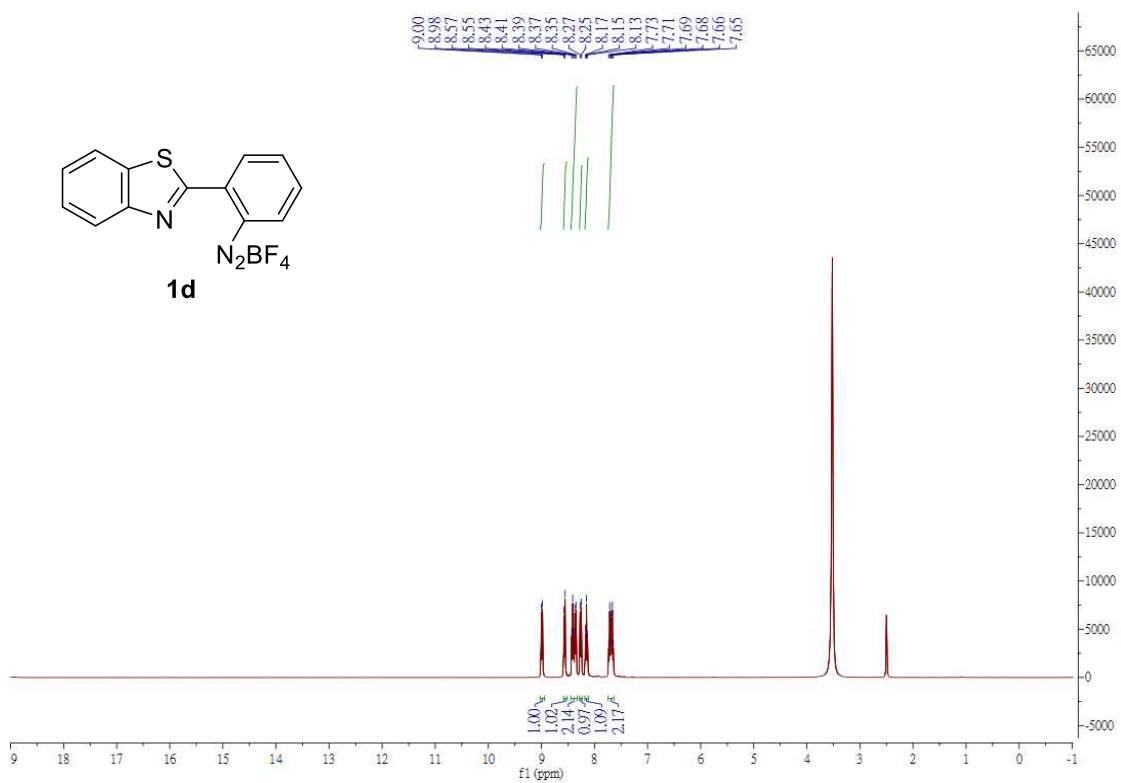
DEPT 135



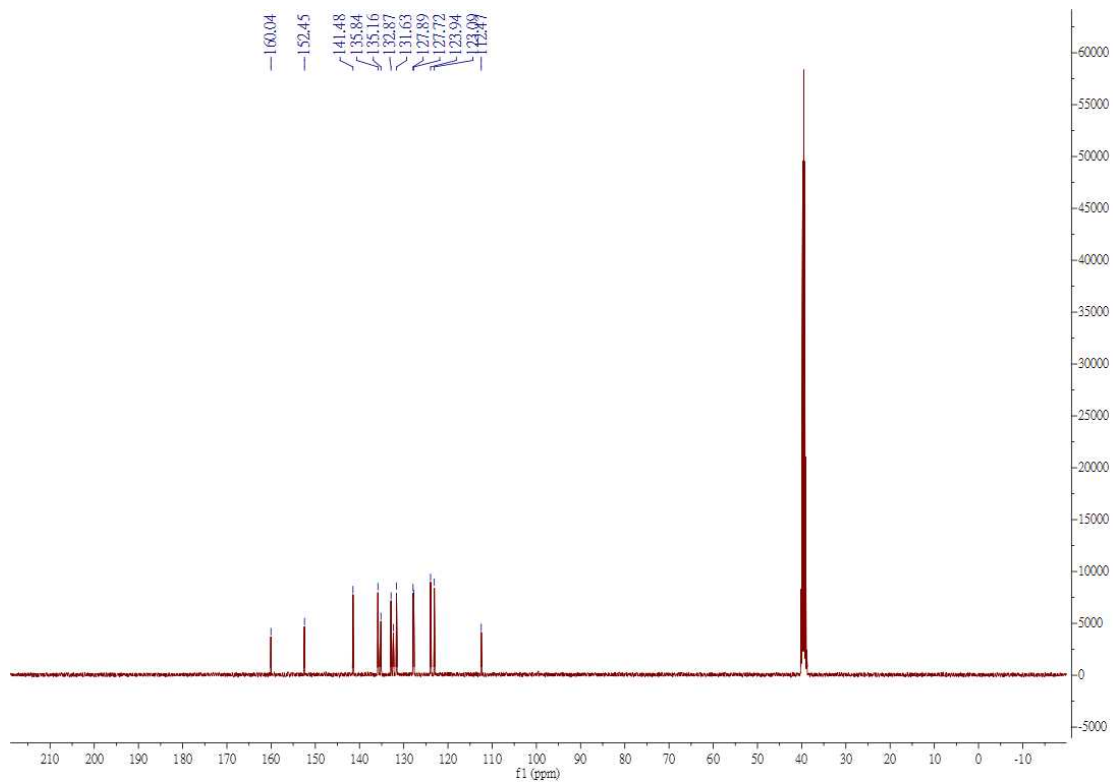
¹⁹F NMR



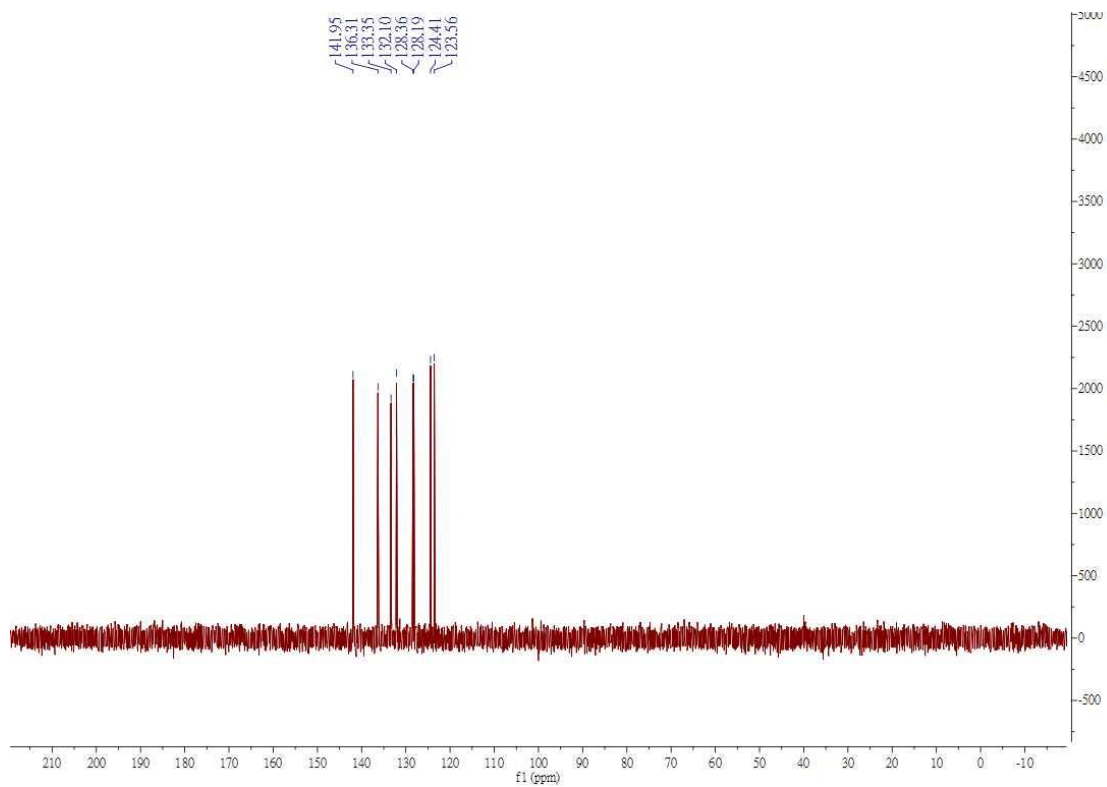
¹H NMR



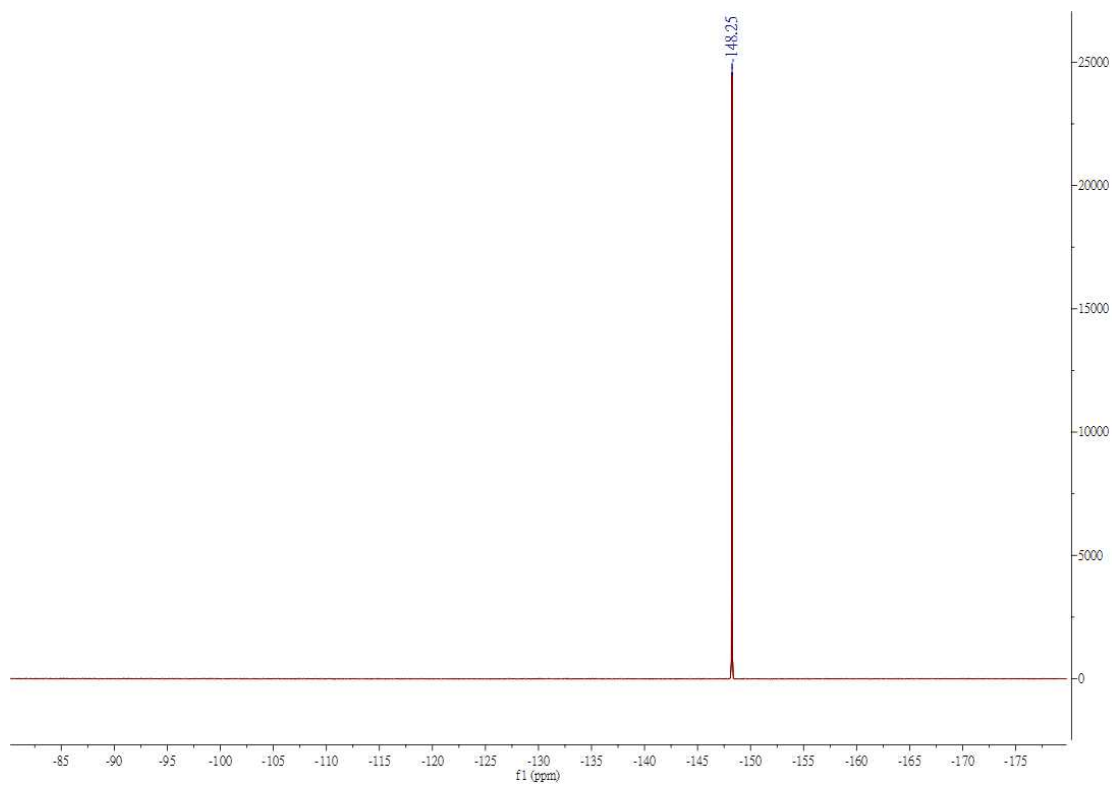
¹³C NMR



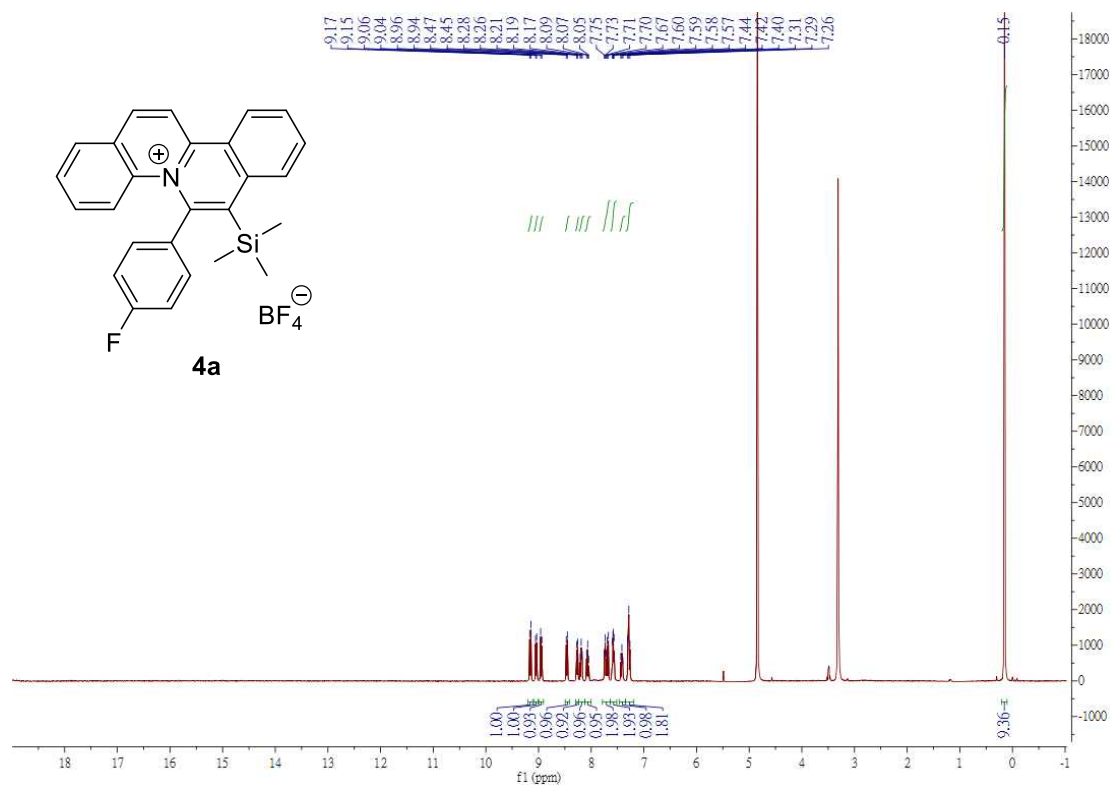
DEPT 135



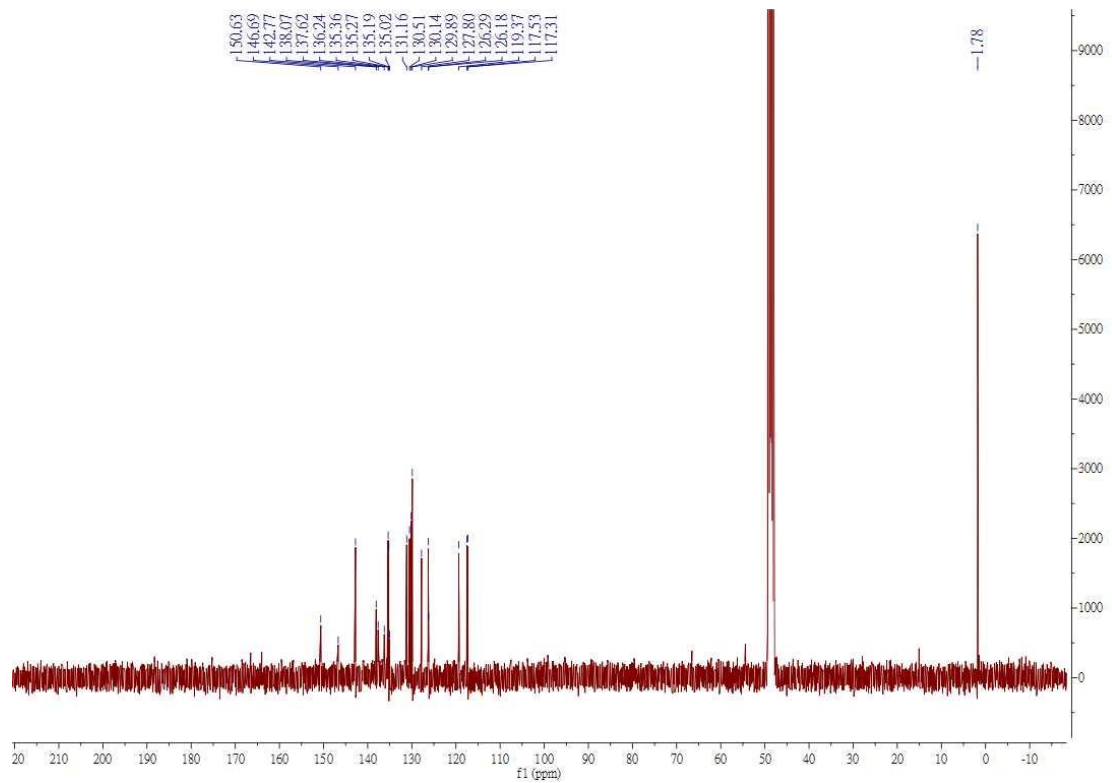
¹⁹F NMR



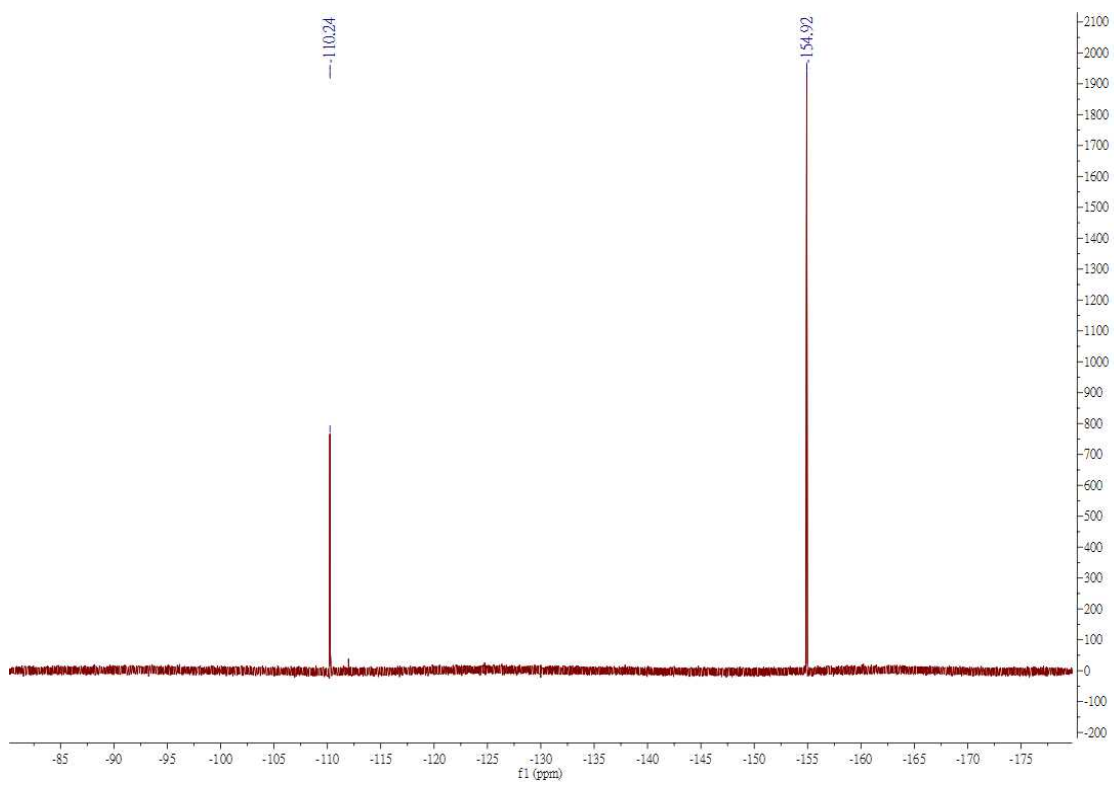
¹H NMR



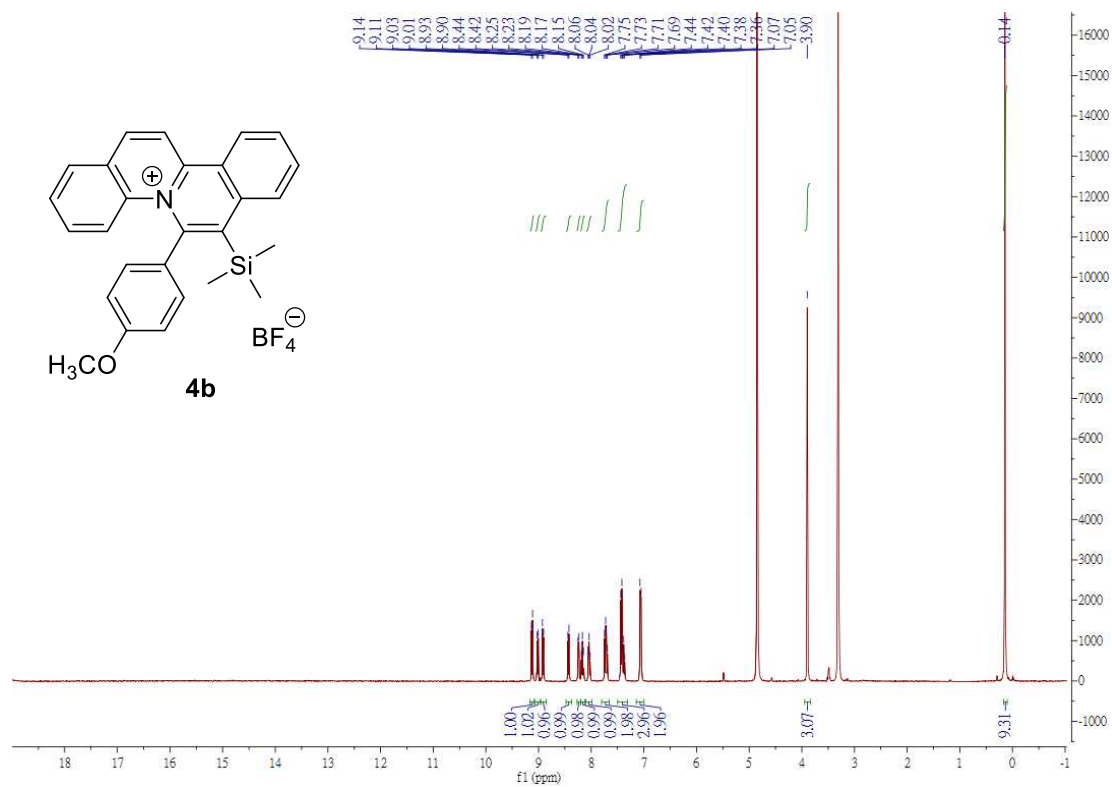
¹³C NMR



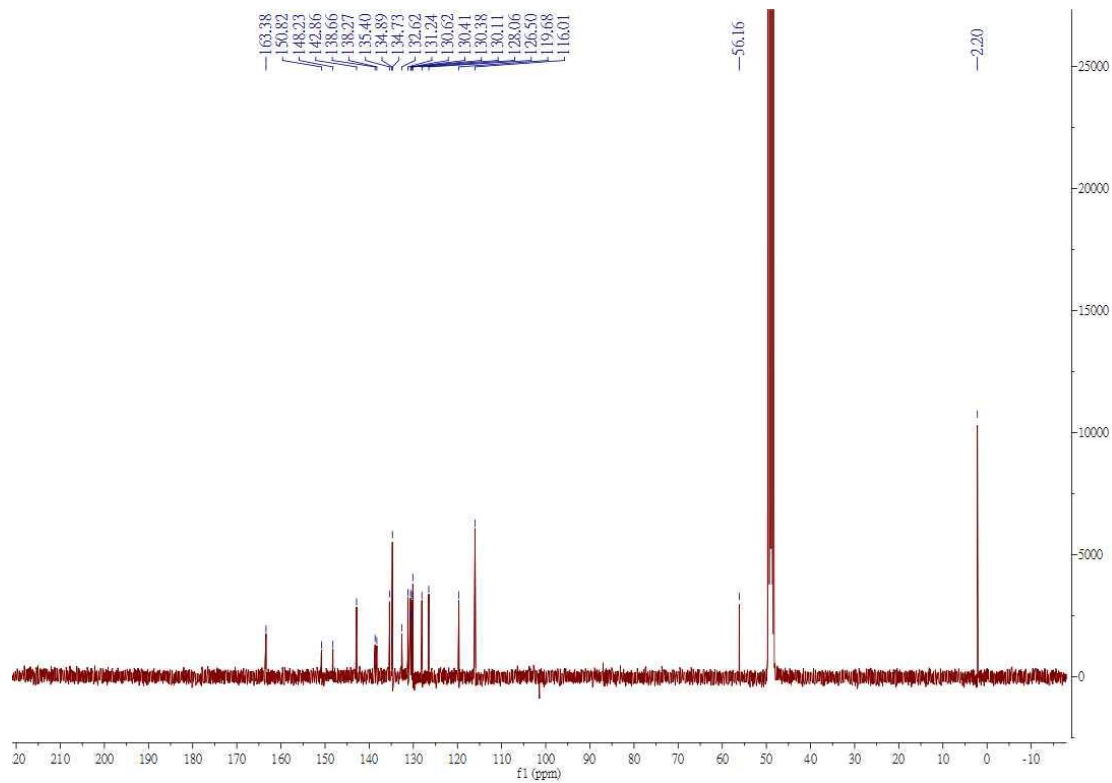
^{19}F NMR



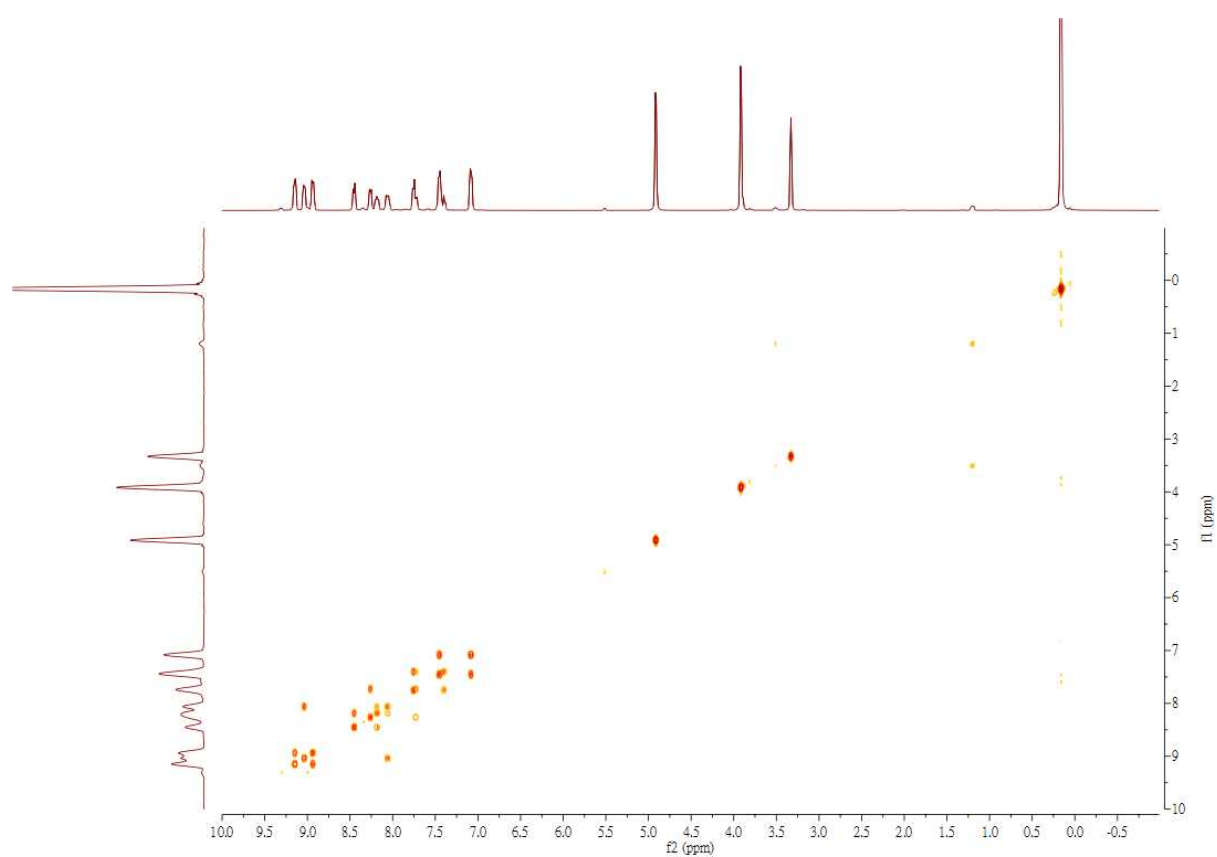
¹H NMR



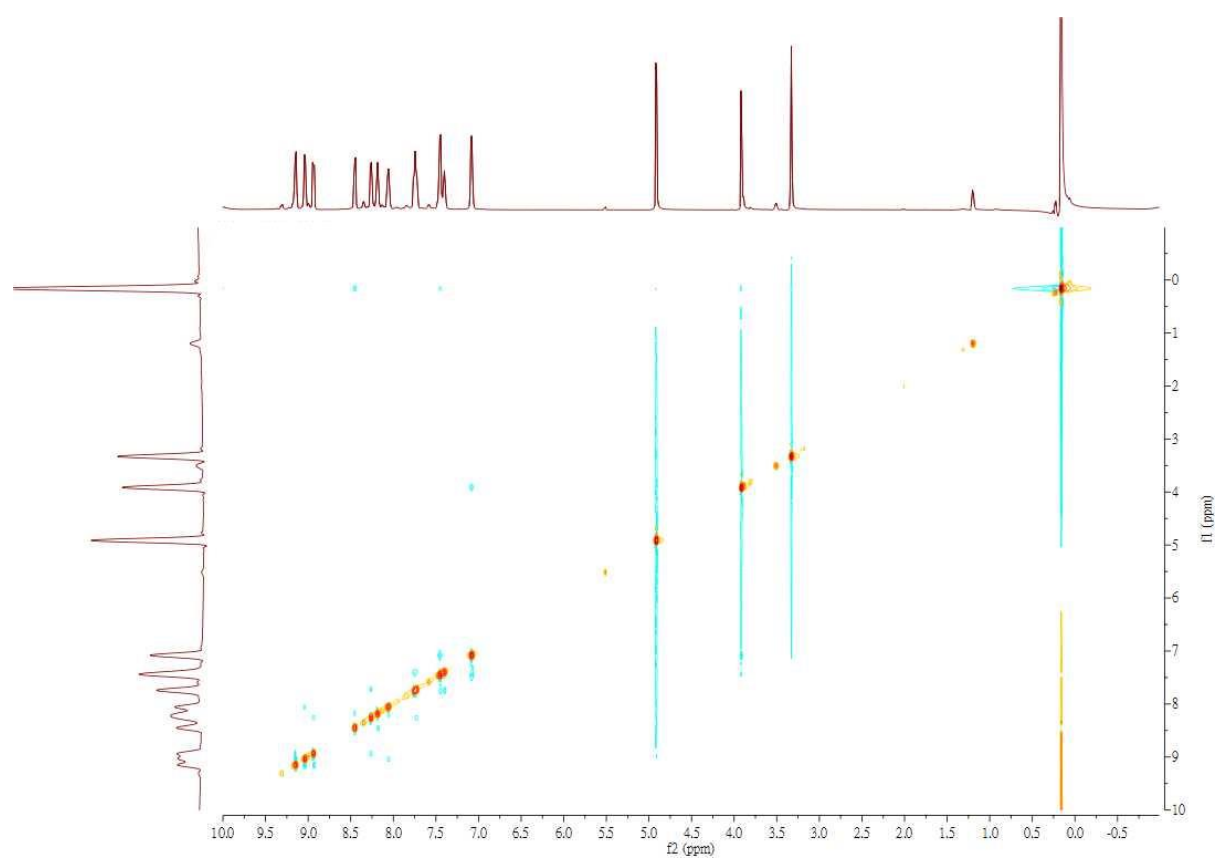
¹³C NMR



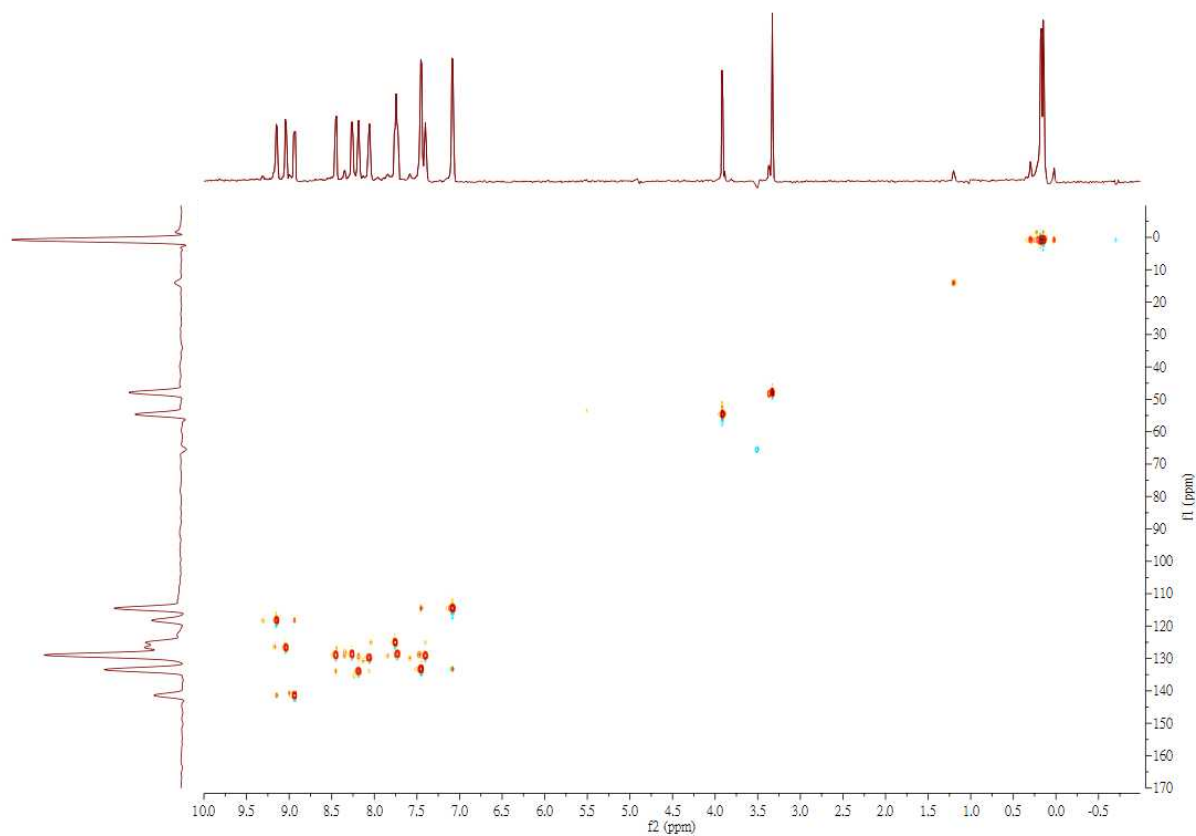
COSY



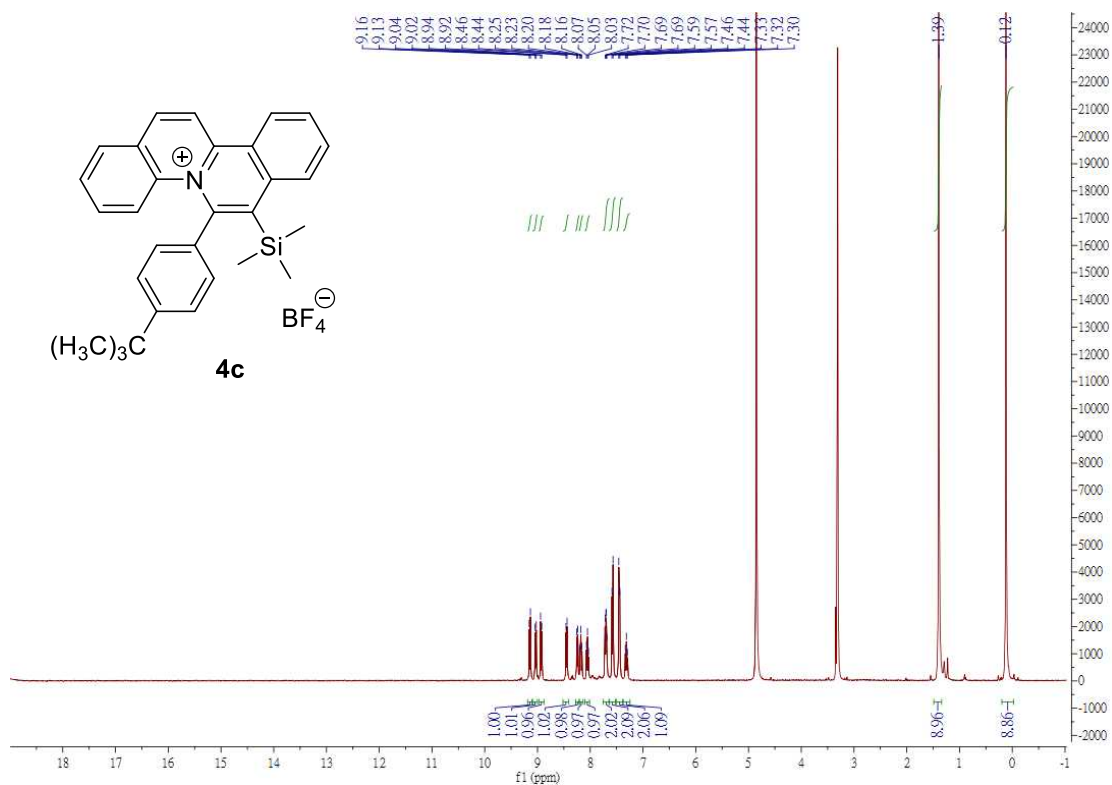
NOESY



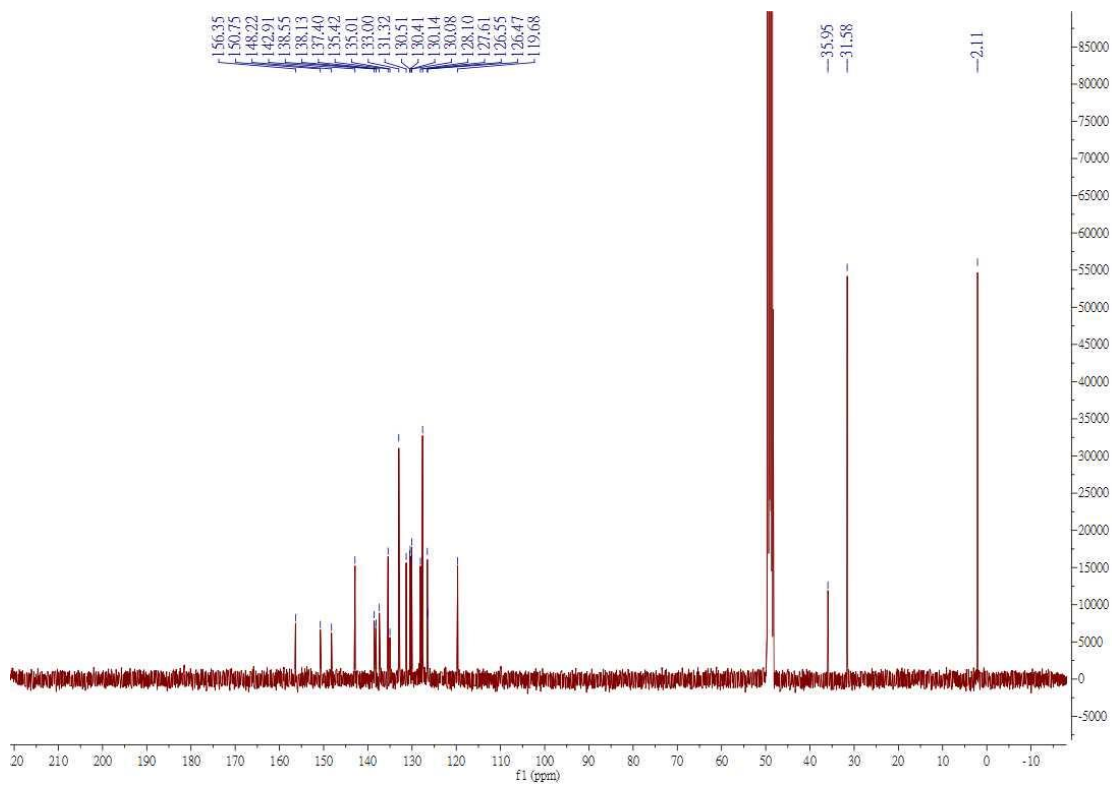
HSQC



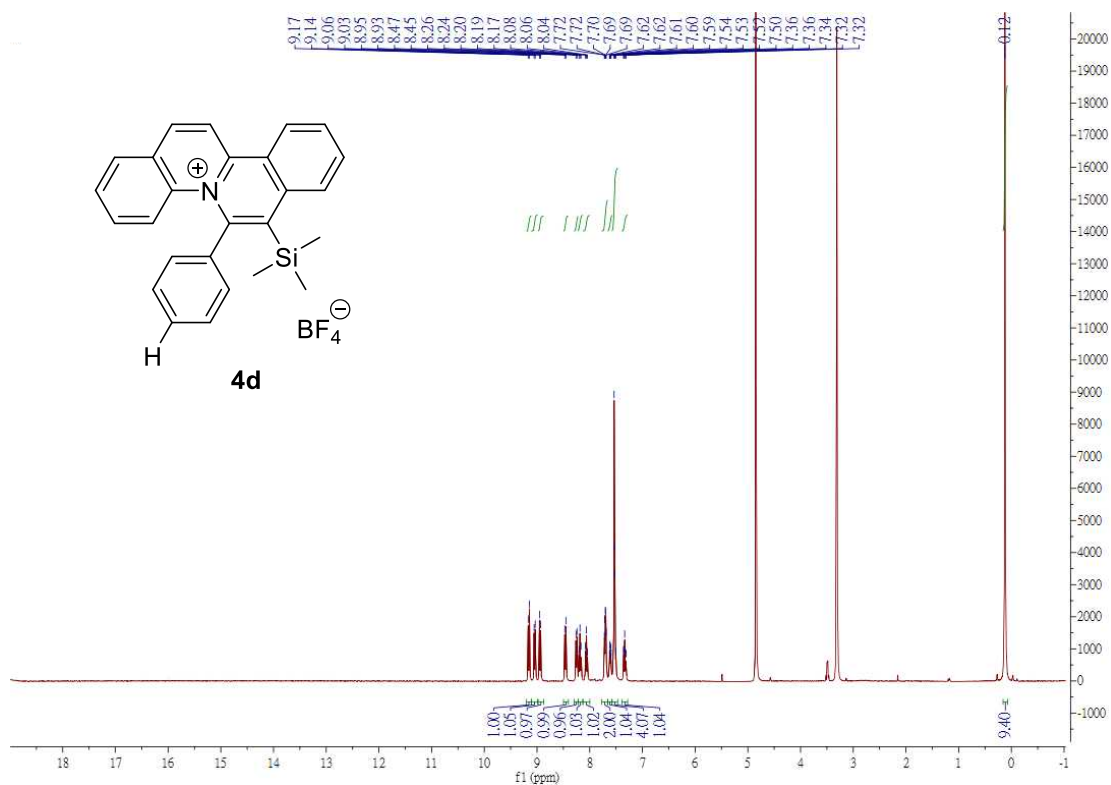
¹H NMR



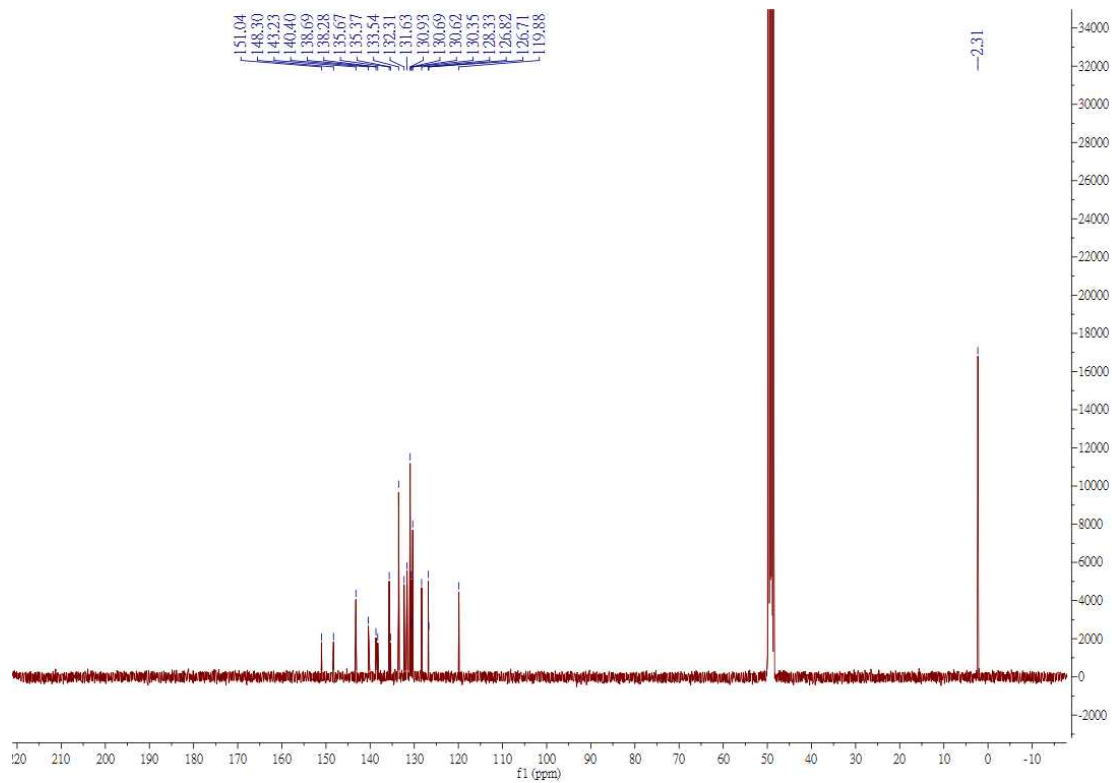
¹³C NMR



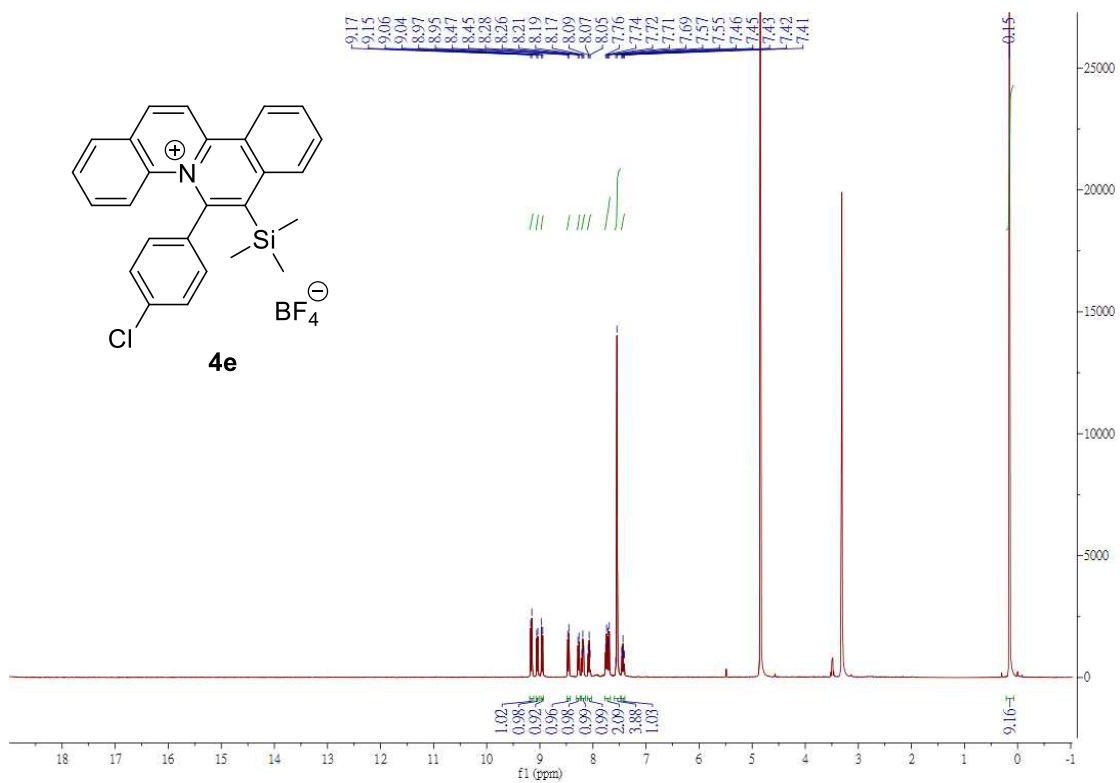
¹H NMR



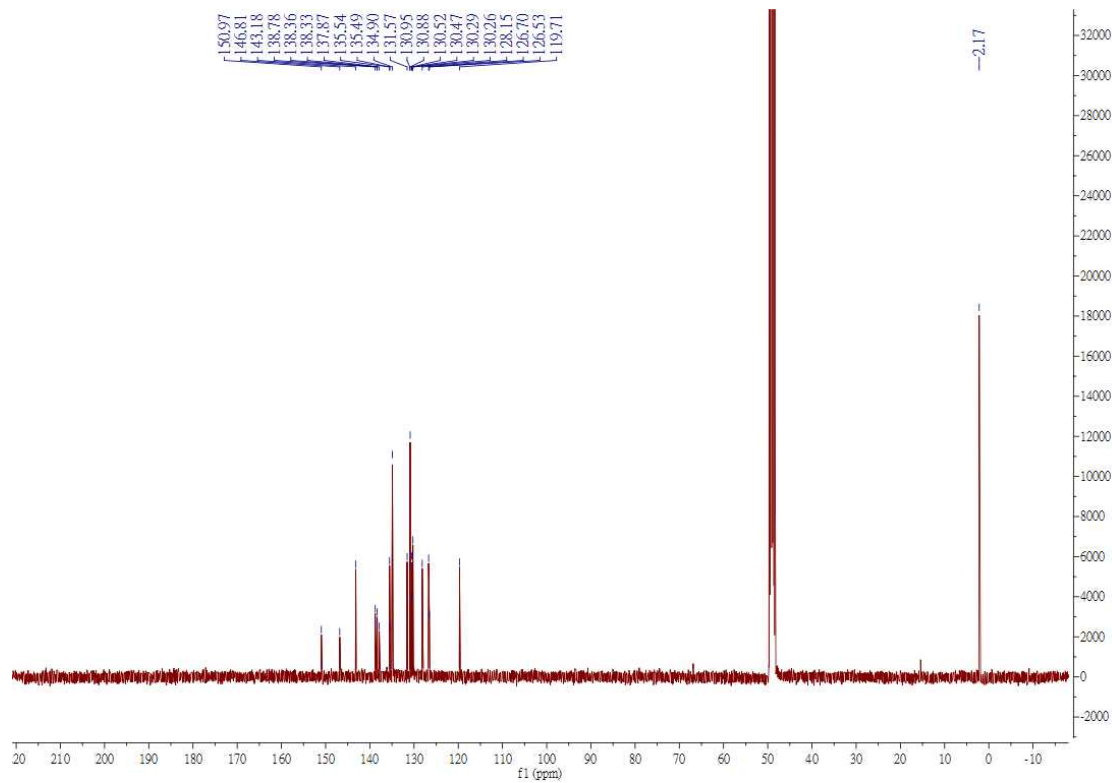
¹³C NMR



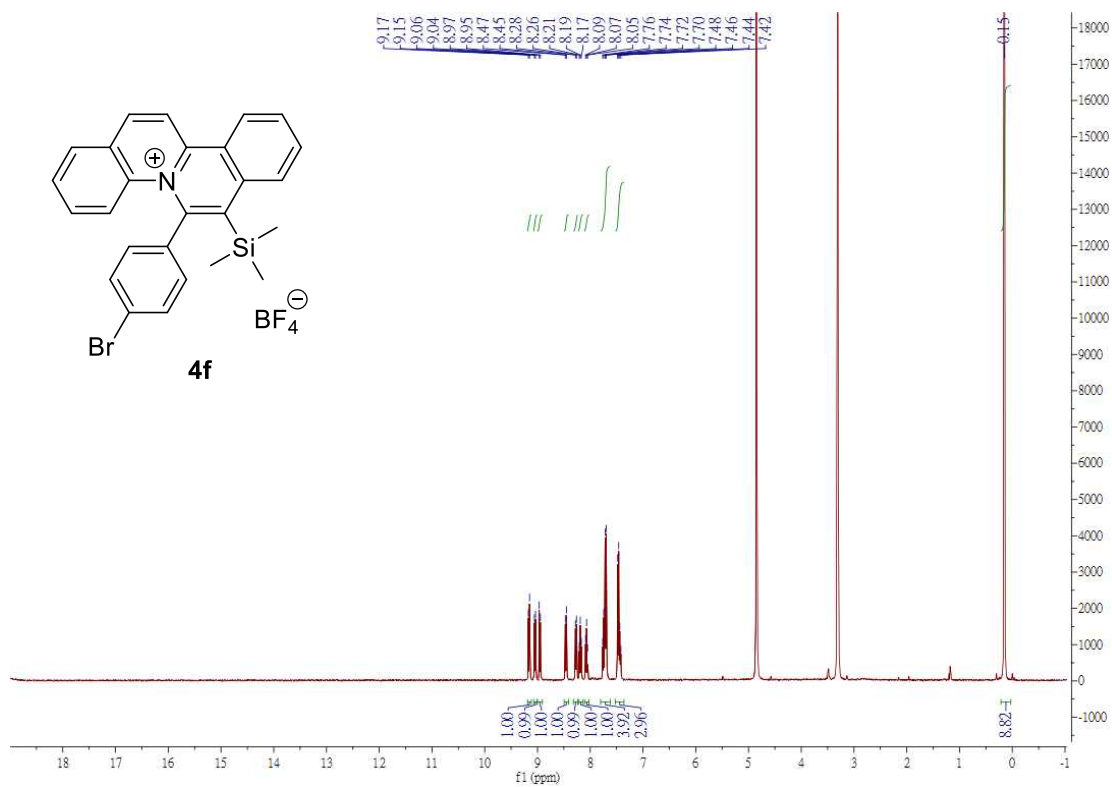
¹H NMR



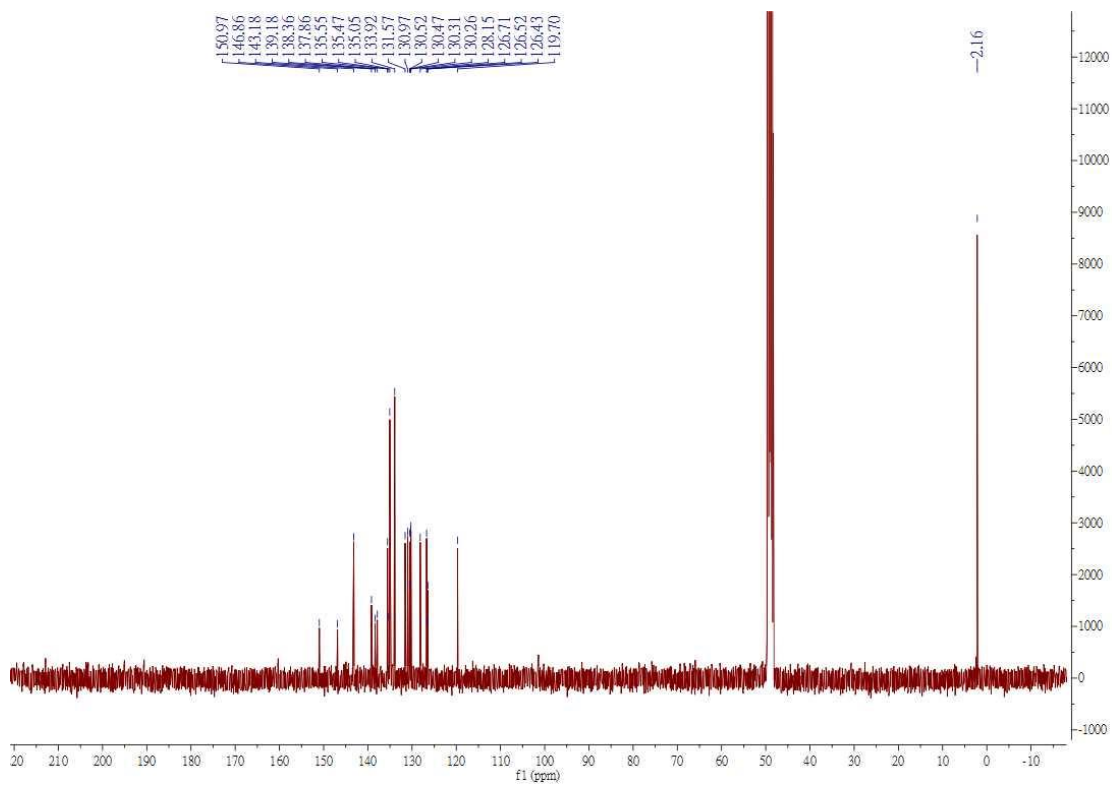
¹³C NMR



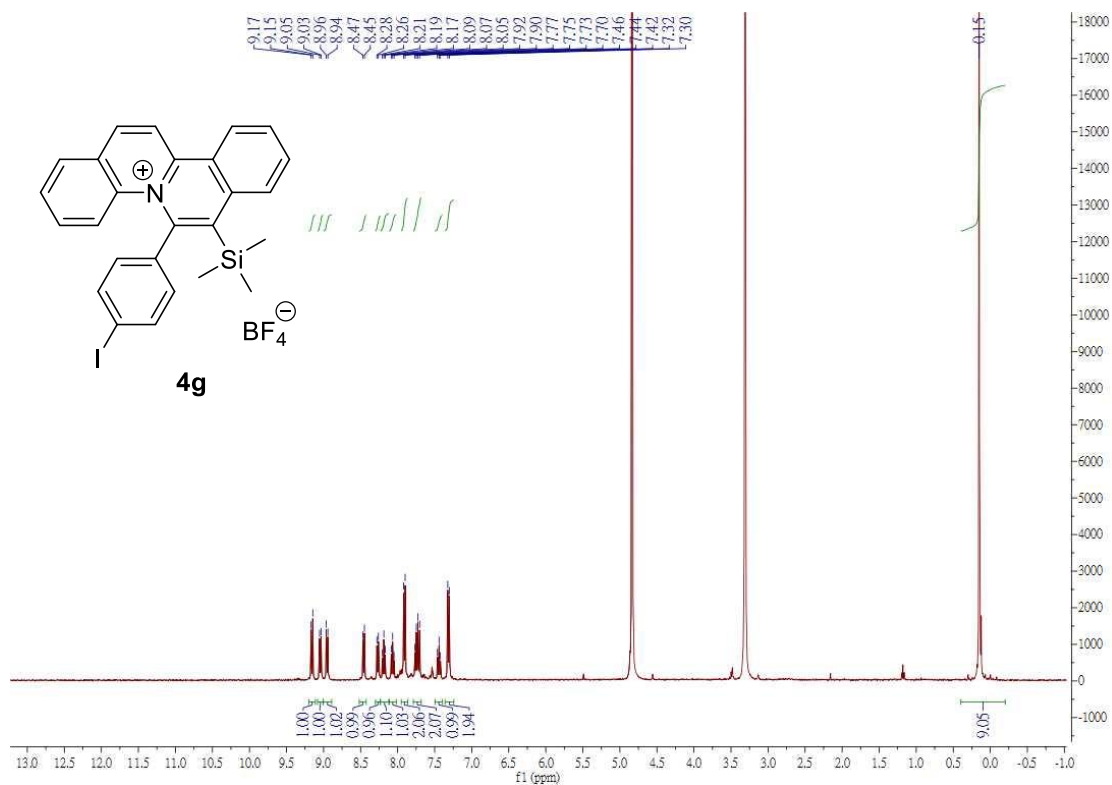
¹H NMR



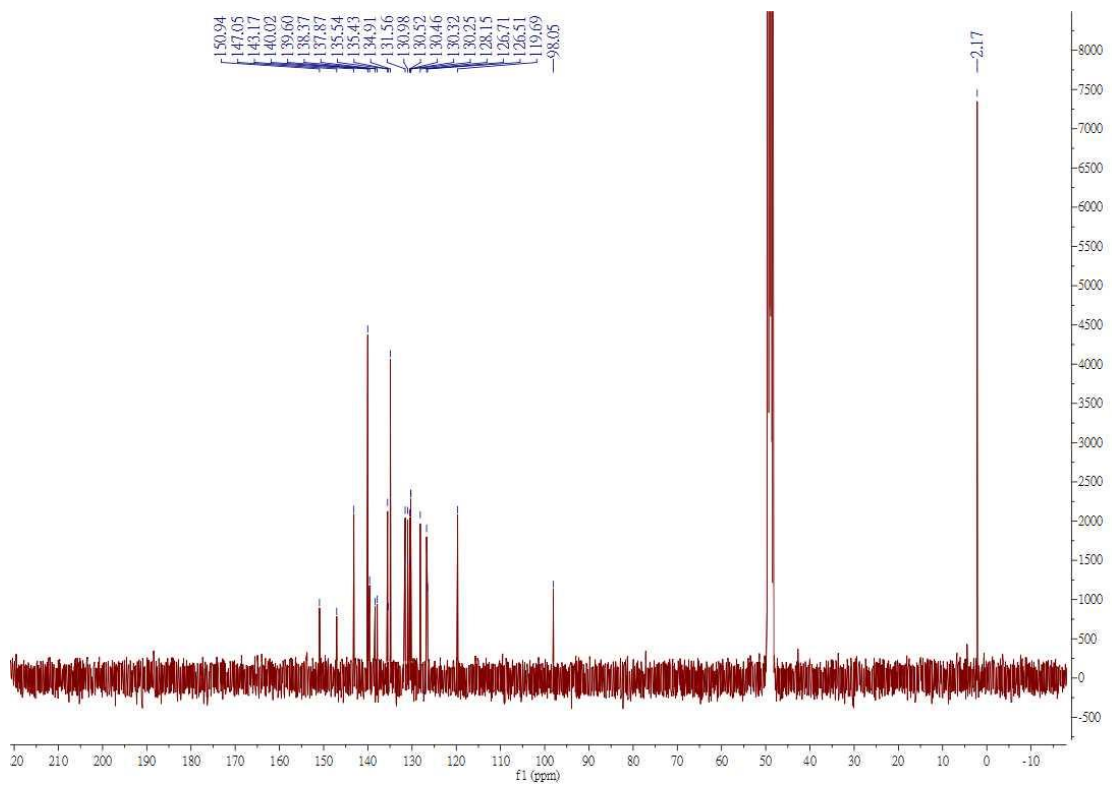
¹³C NMR



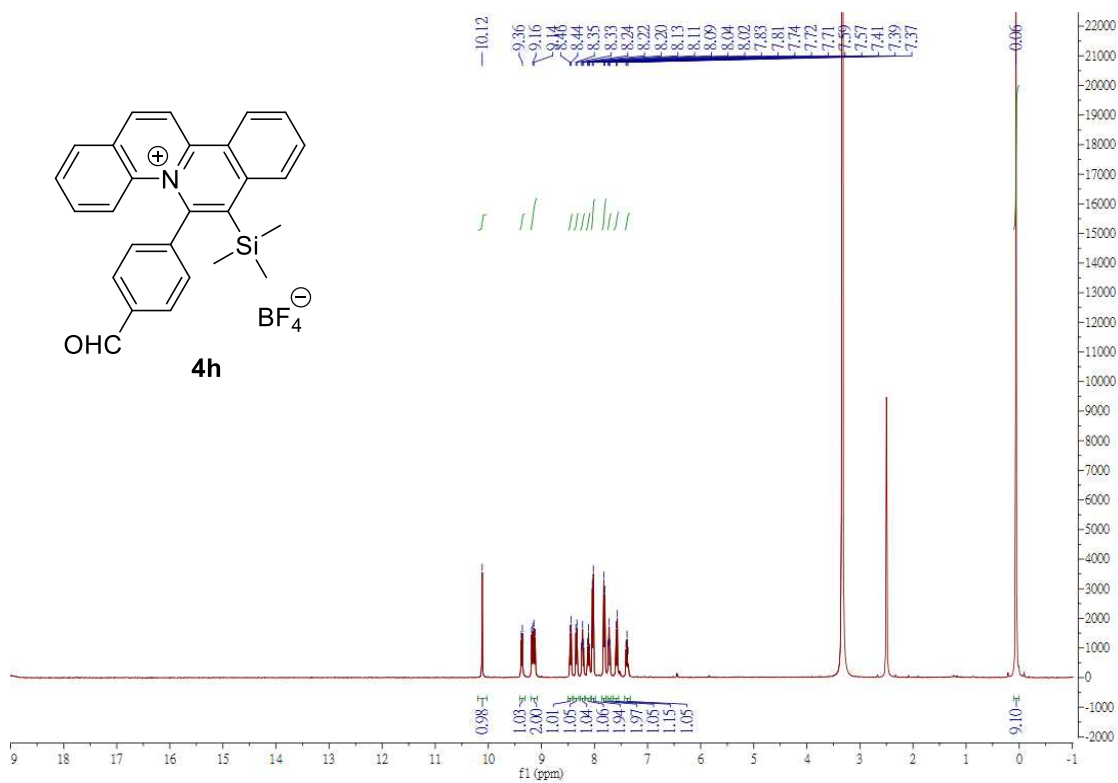
¹H NMR



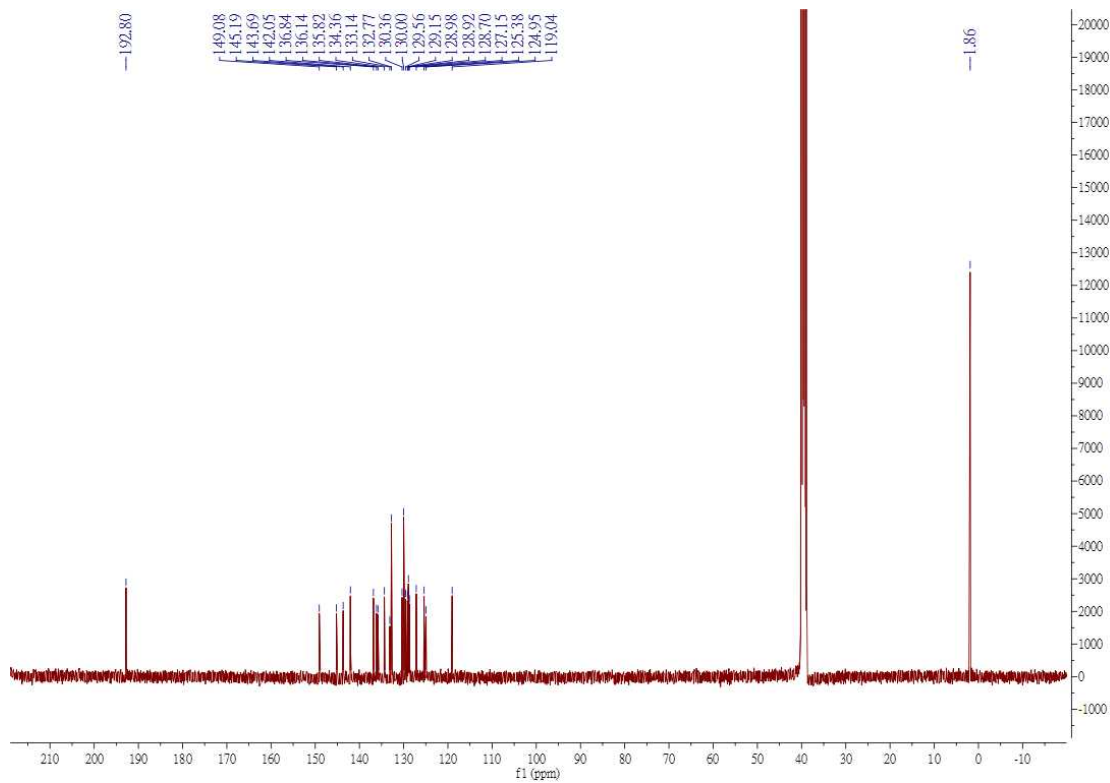
¹³C NMR



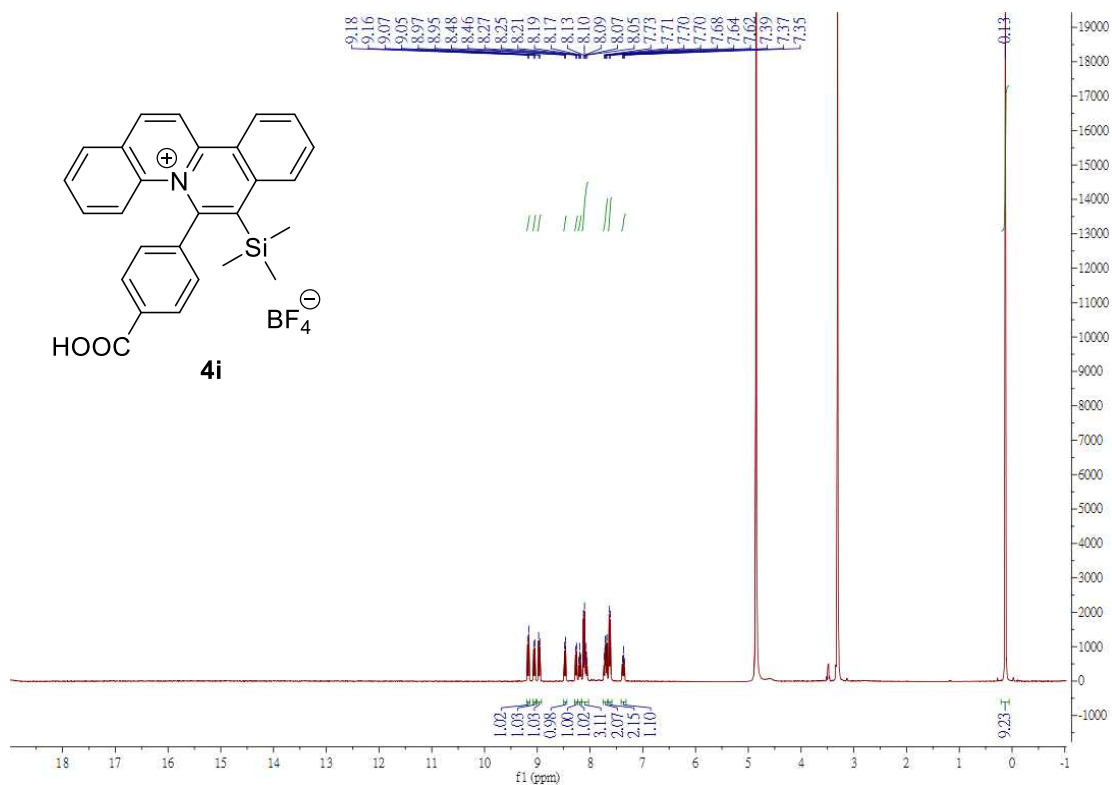
¹H NMR



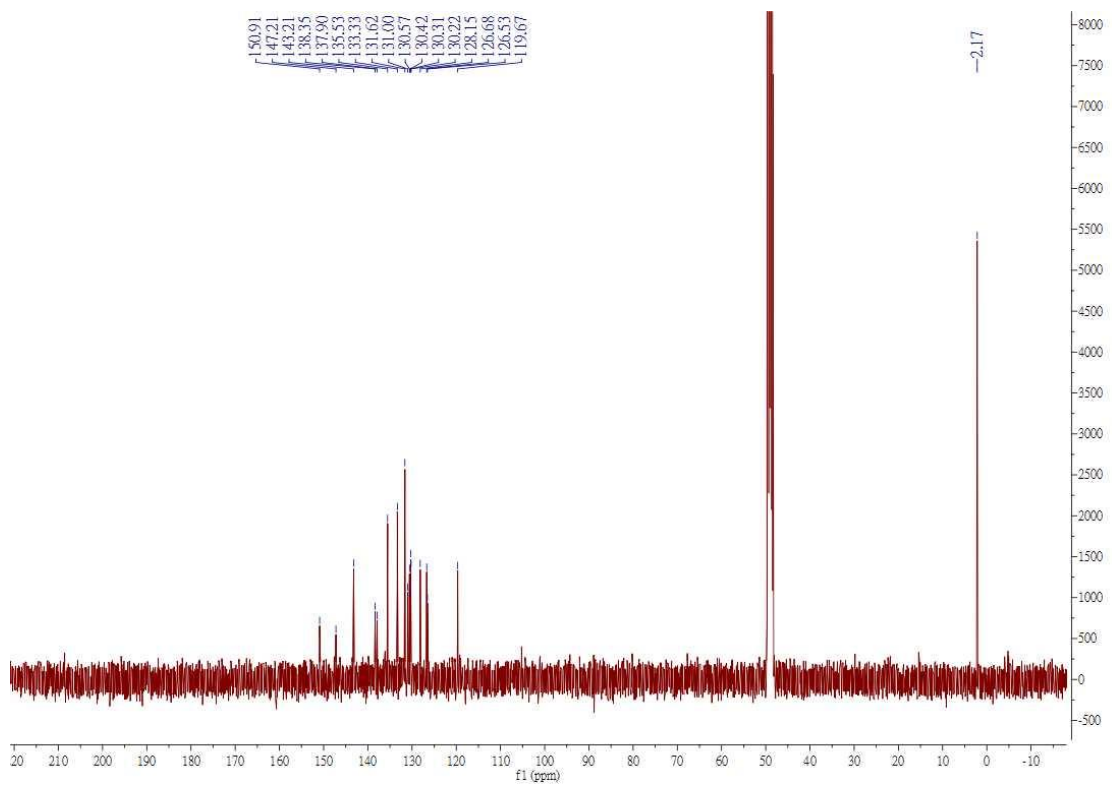
¹³C NMR



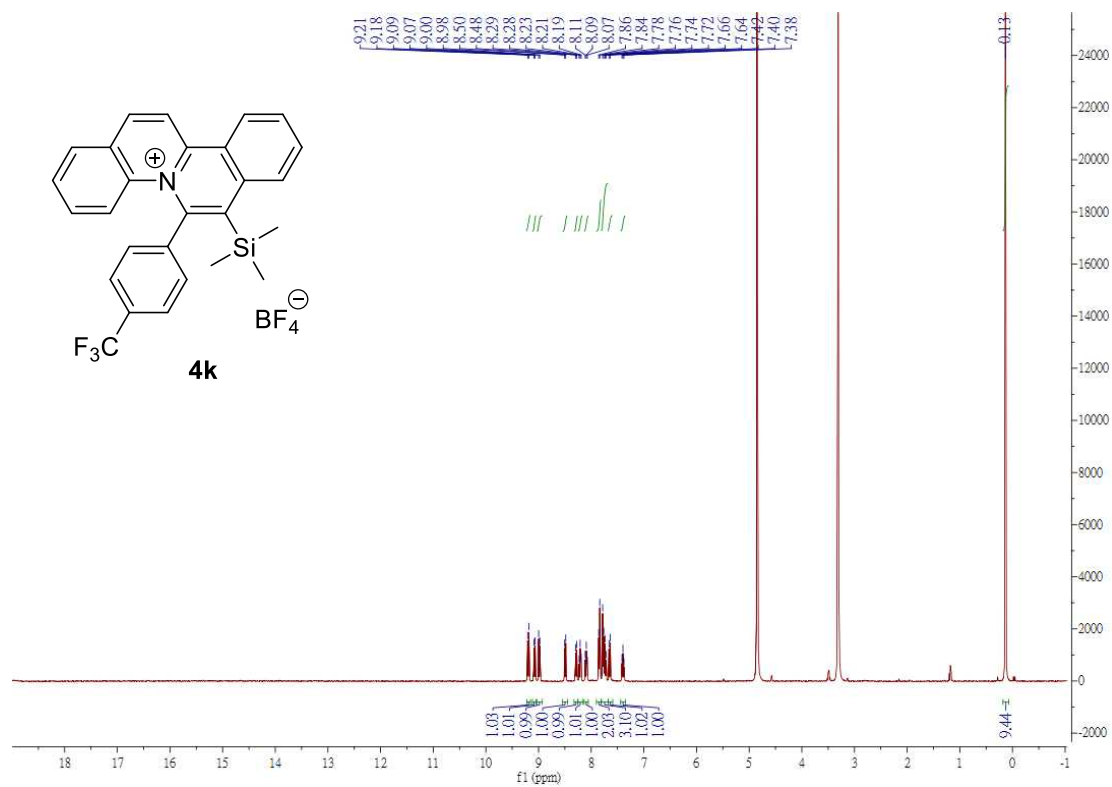
¹H NMR



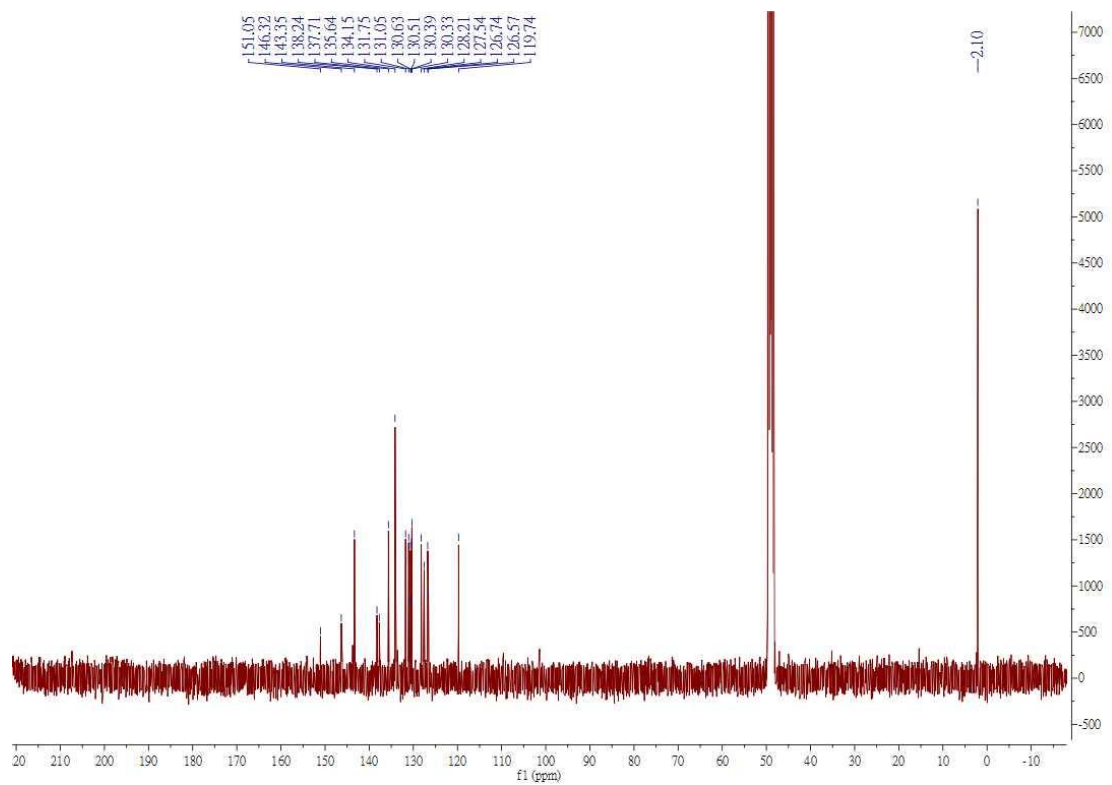
¹³C NMR



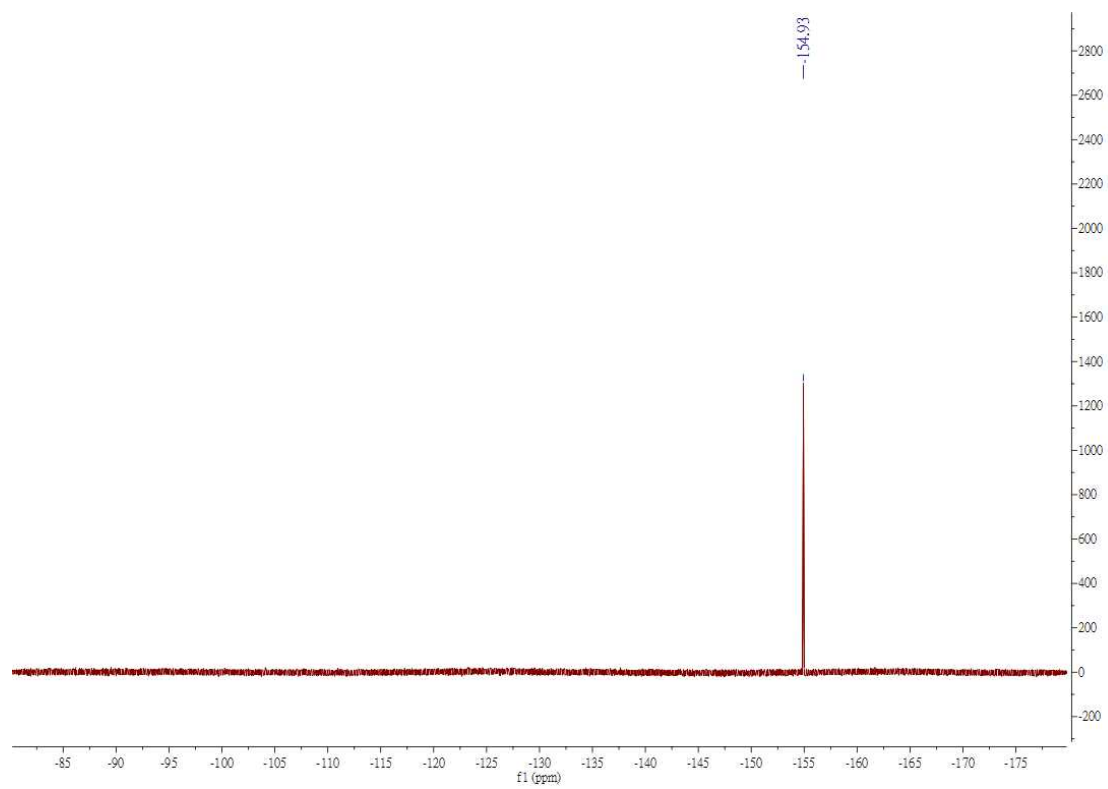
¹H NMR



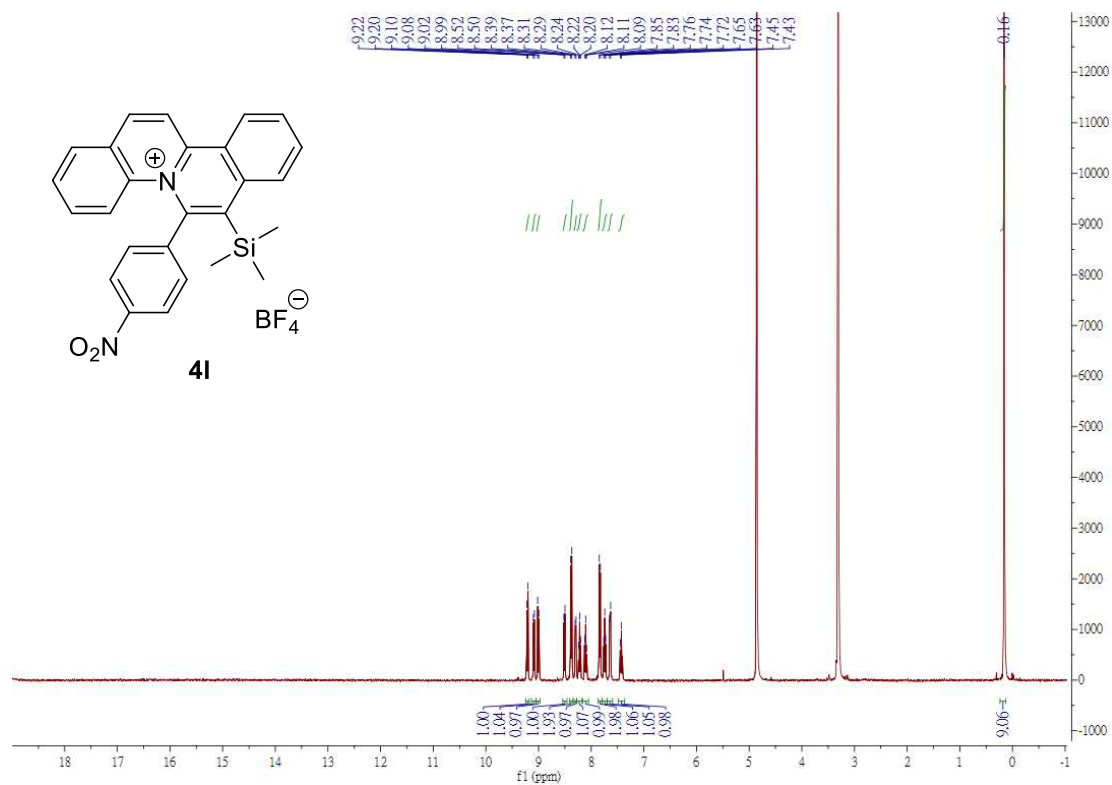
¹³C NMR



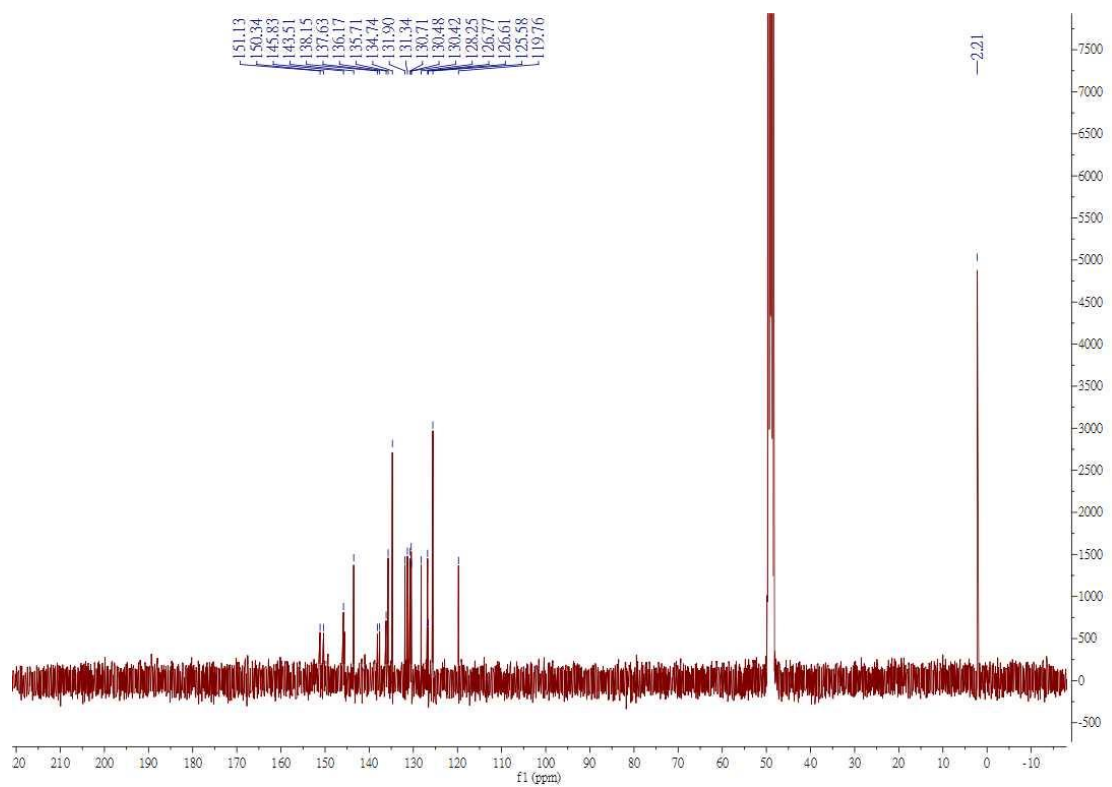
^{19}F NMR



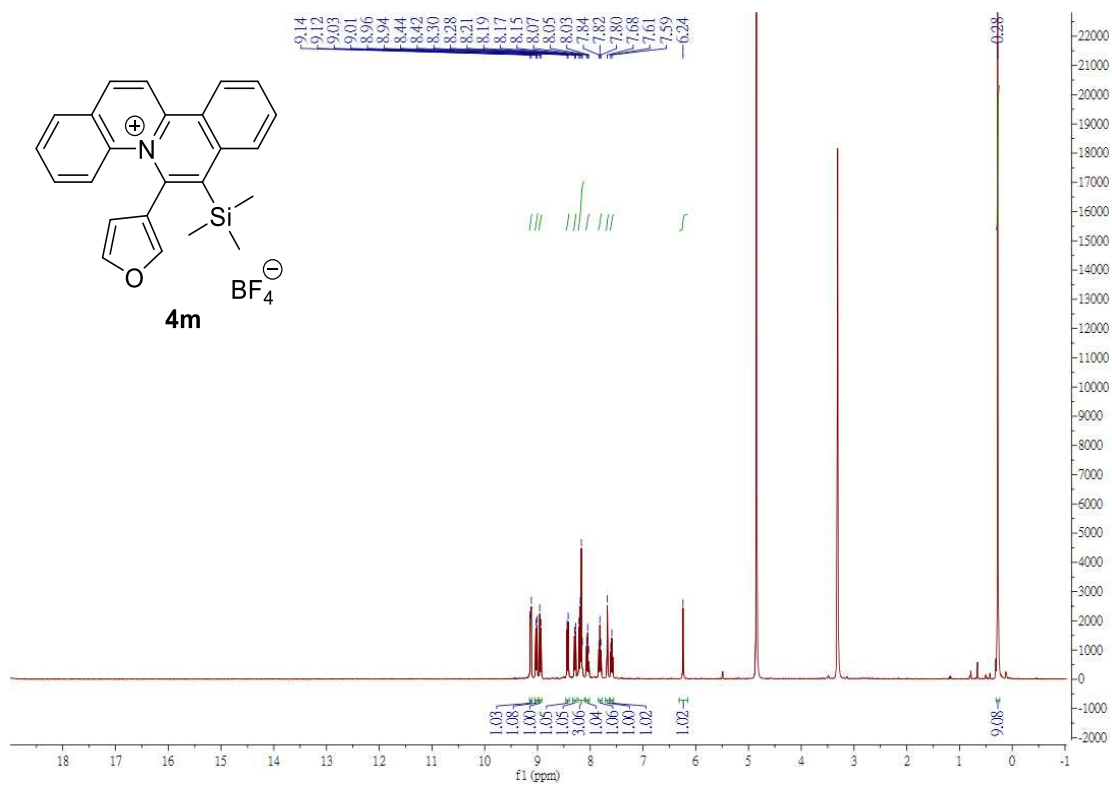
¹H NMR



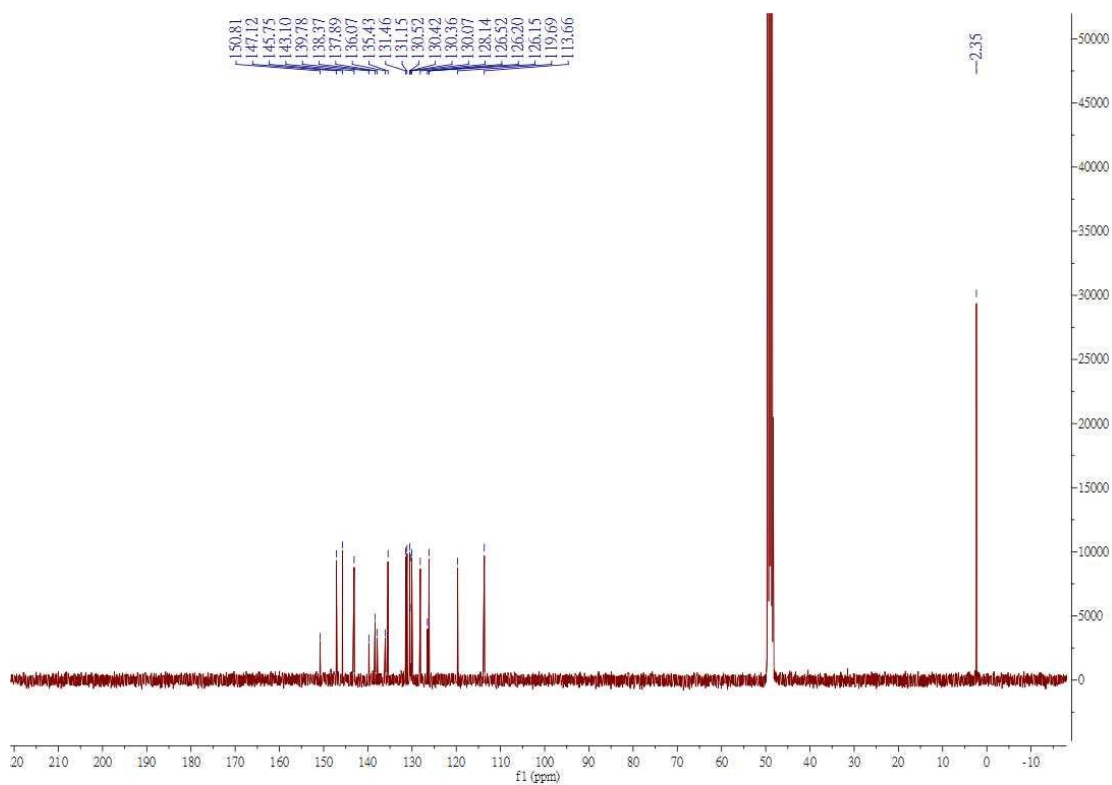
¹³C NMR



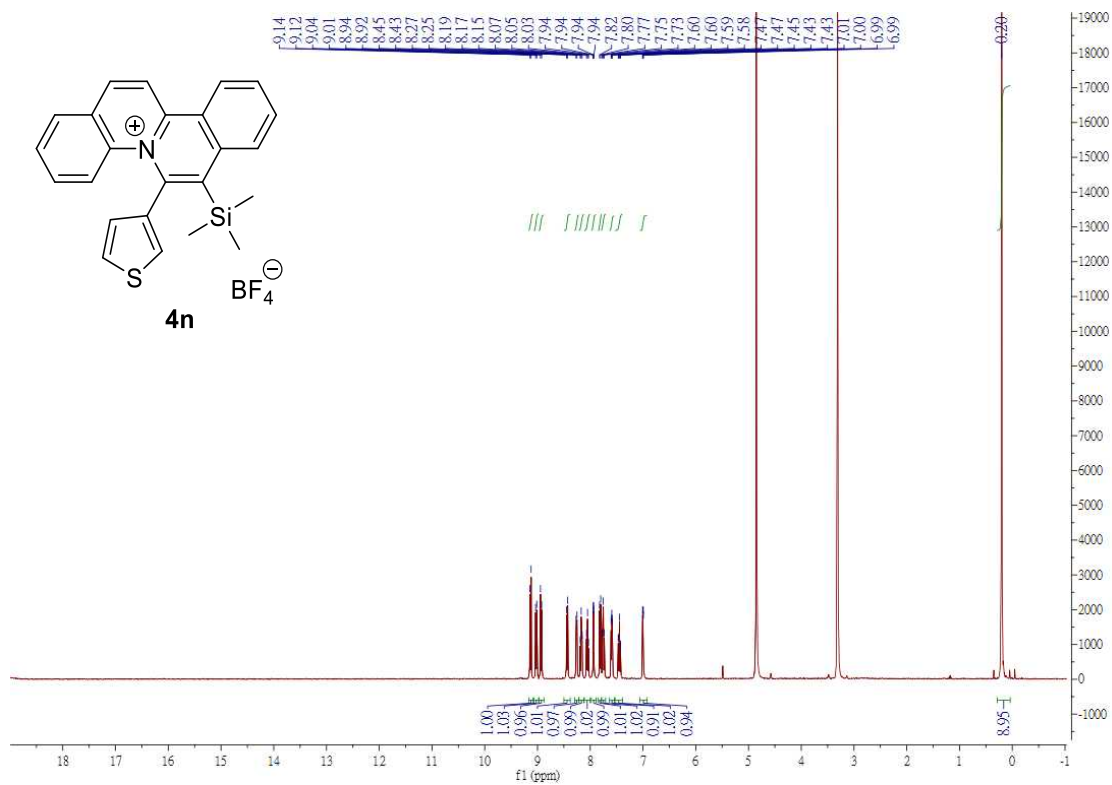
¹H NMR



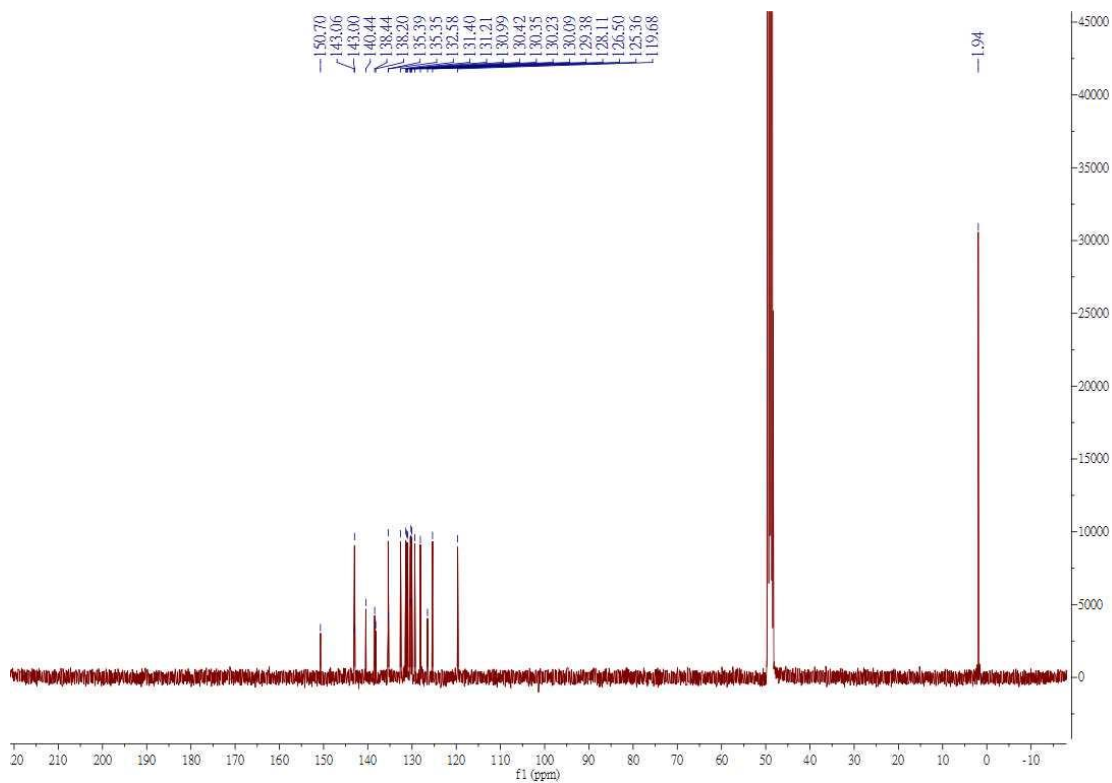
¹³C NMR



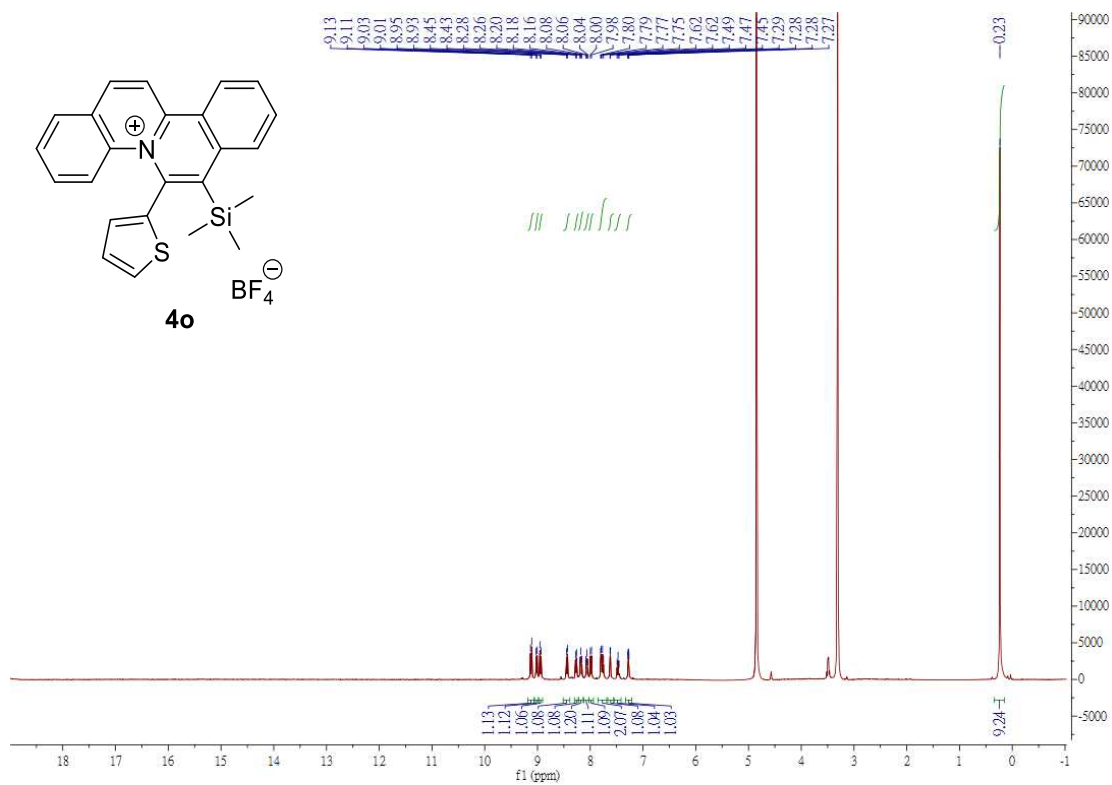
¹H NMR



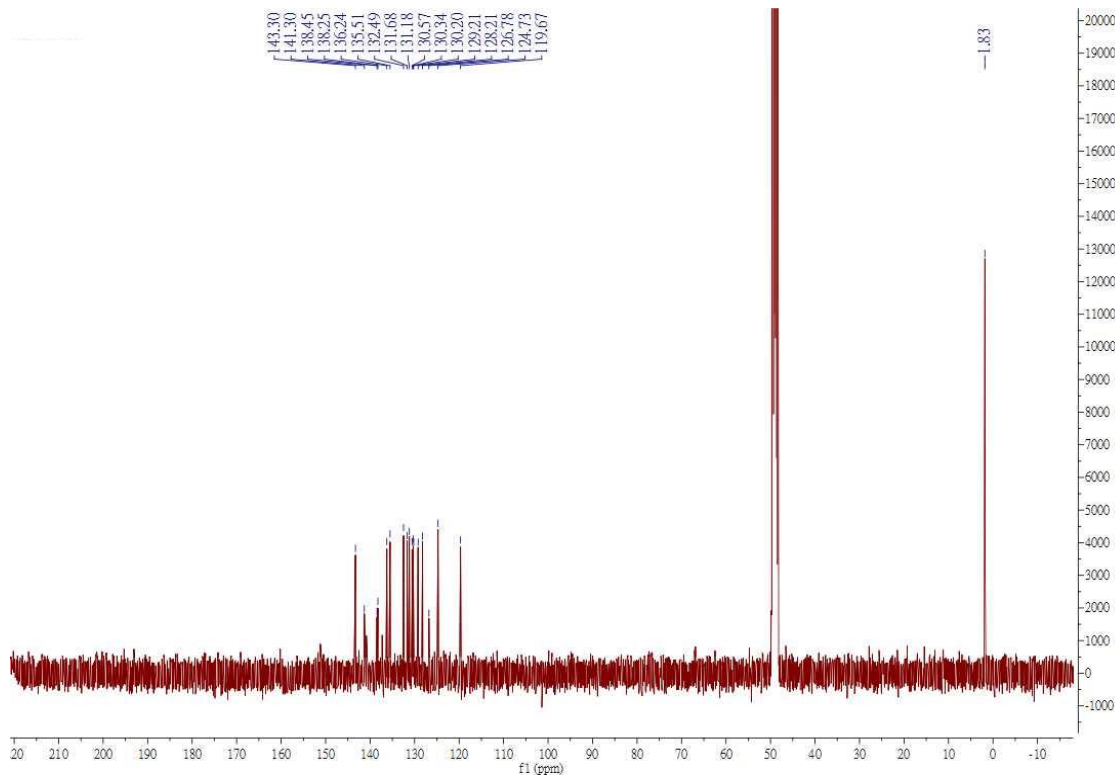
¹³C NMR



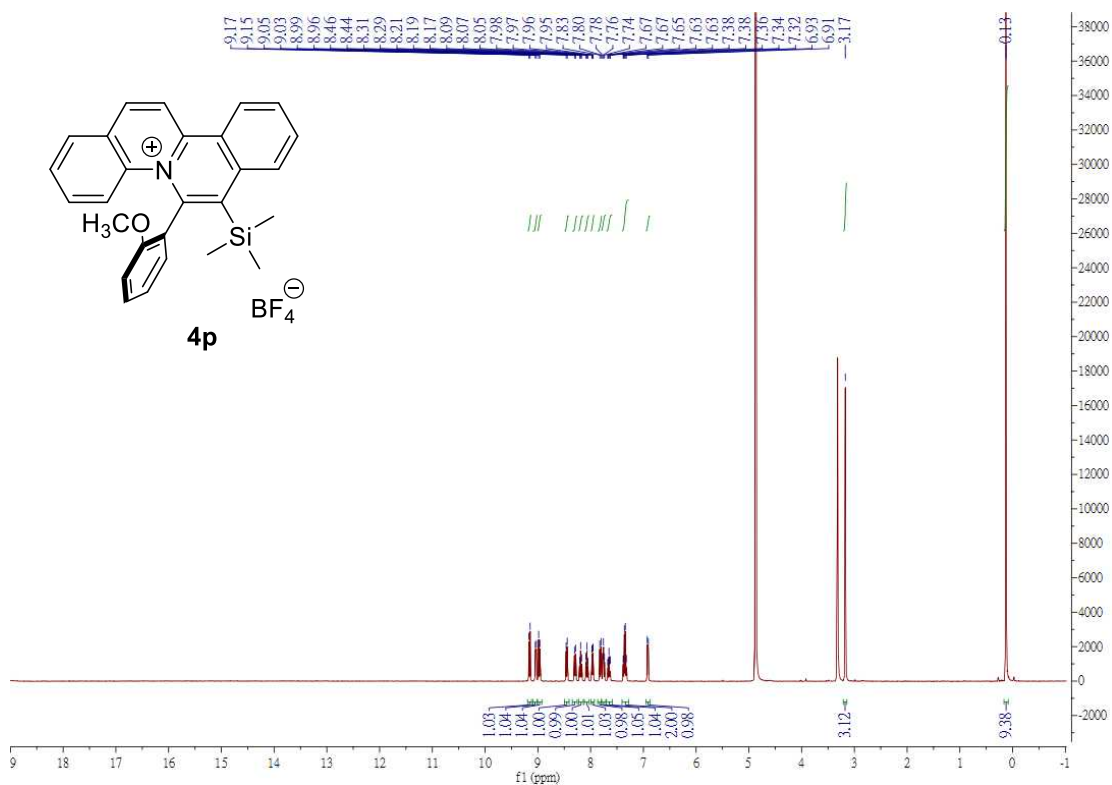
¹H NMR



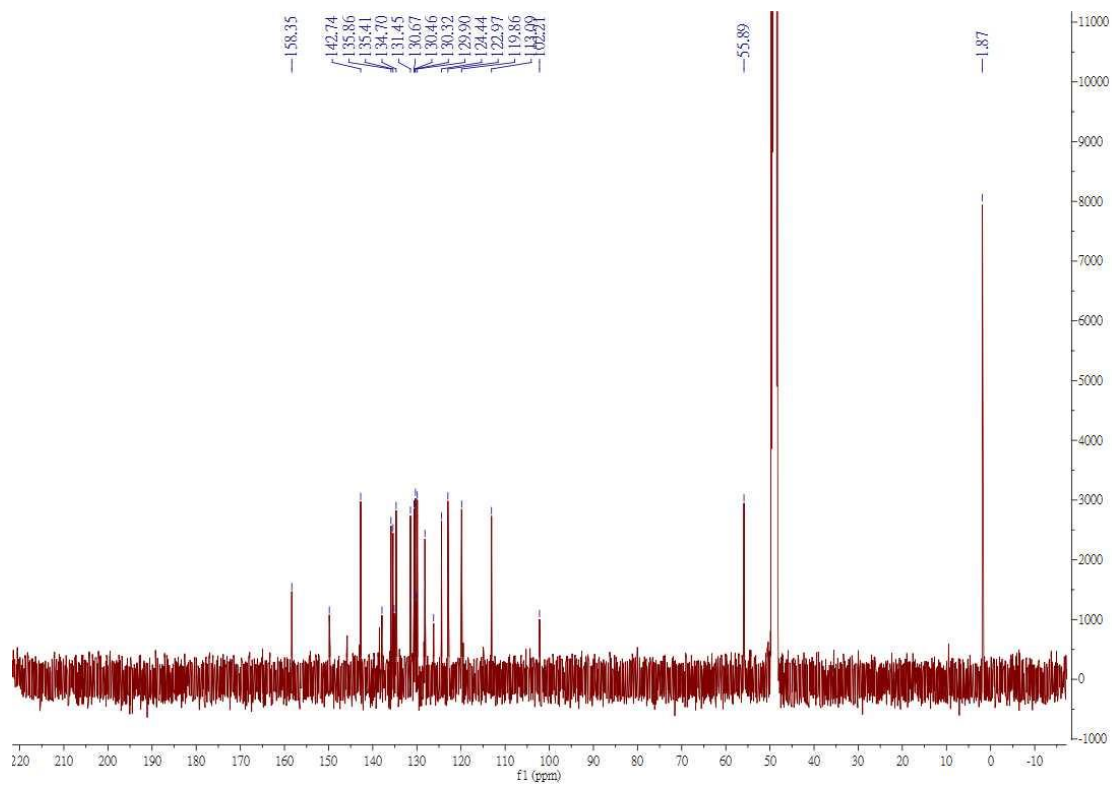
¹³C NMR



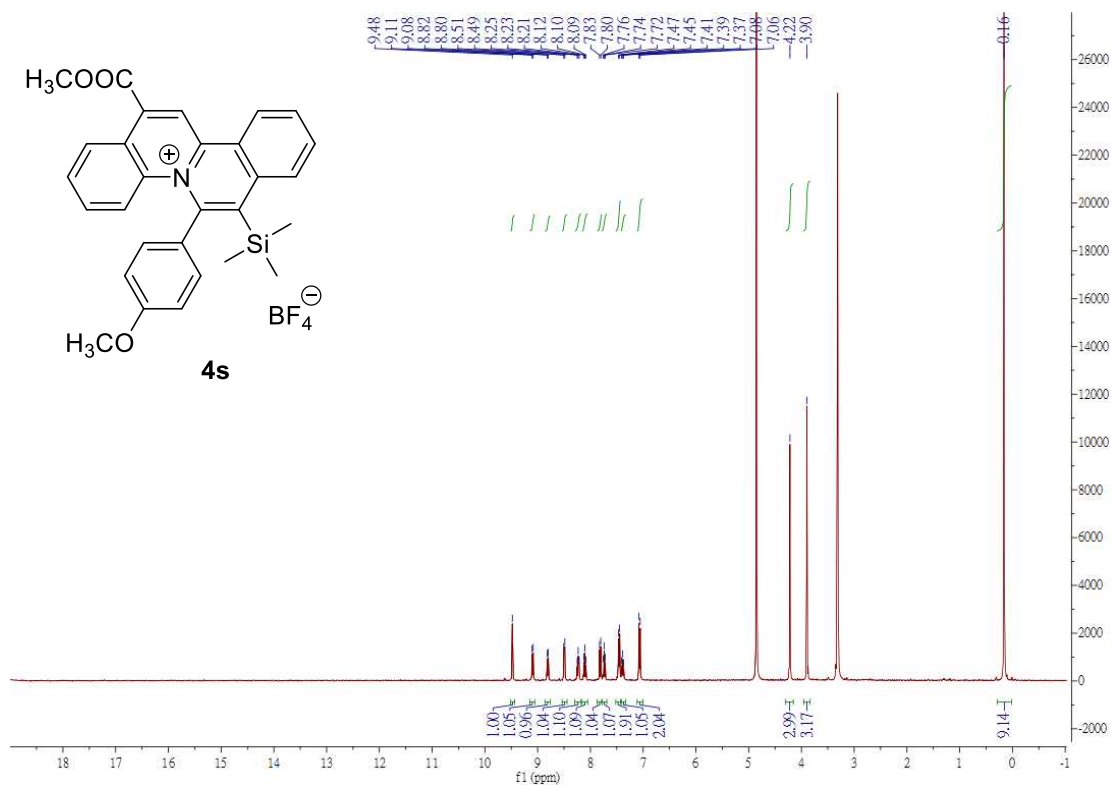
¹H NMR



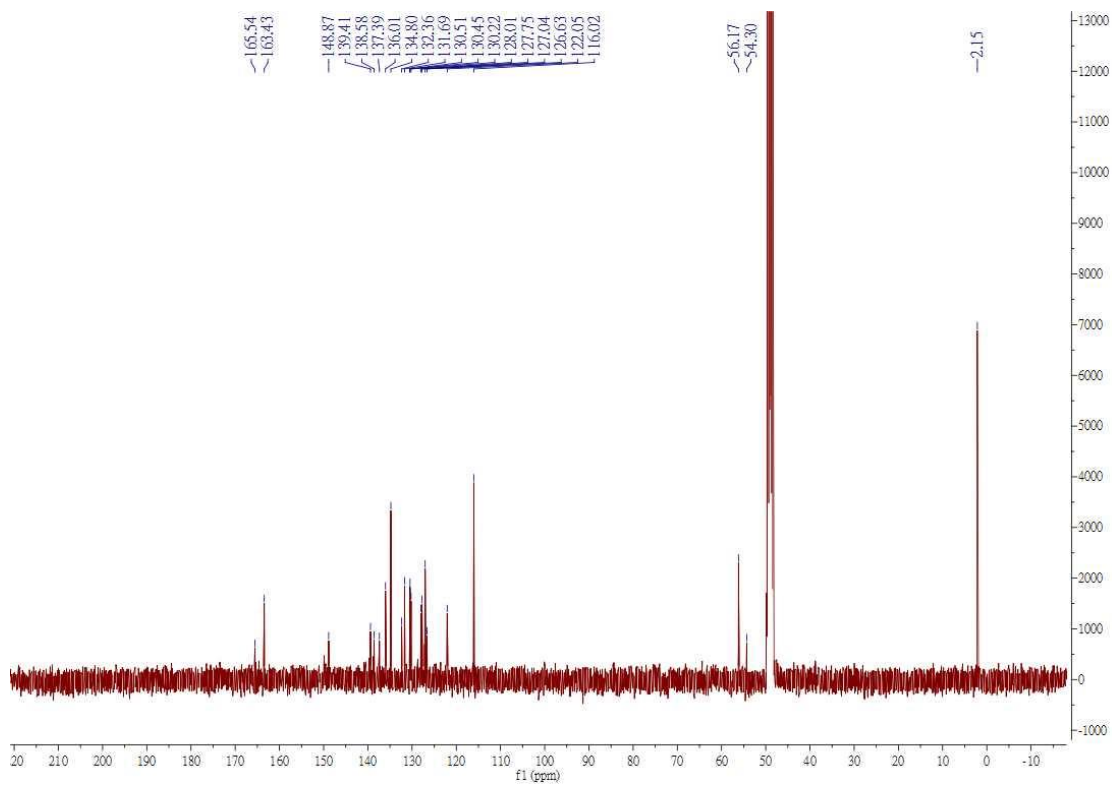
¹³C NMR



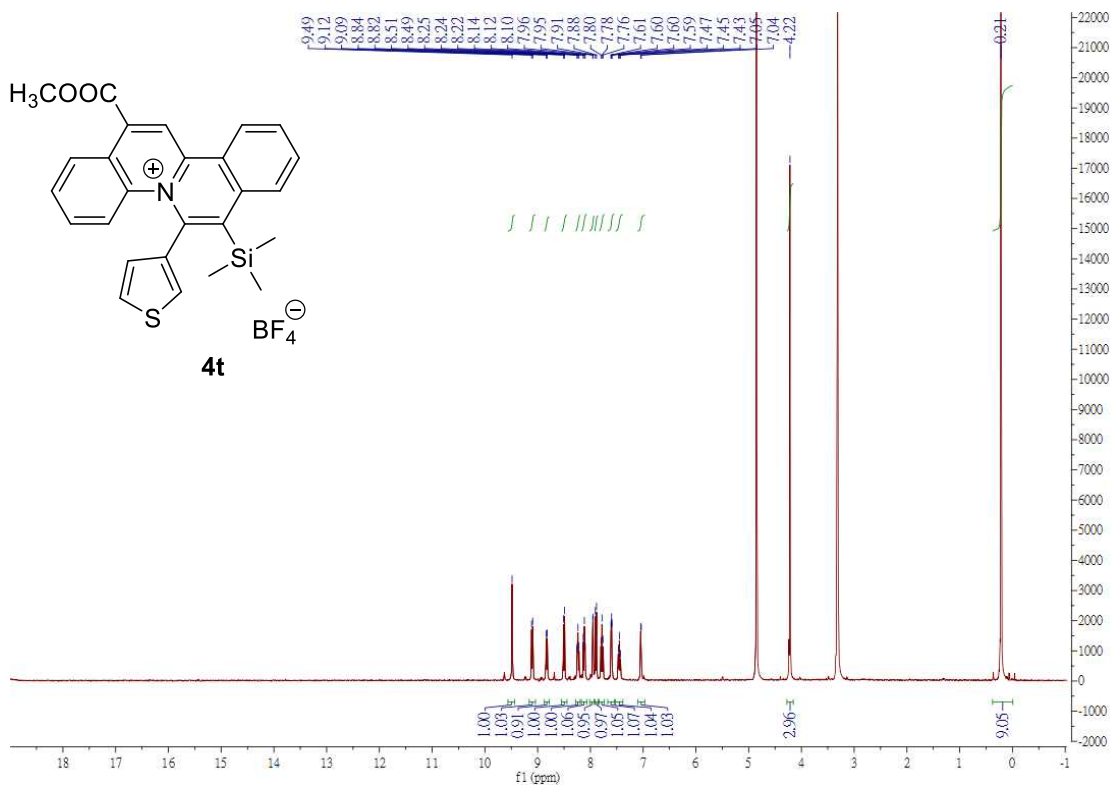
¹H NMR



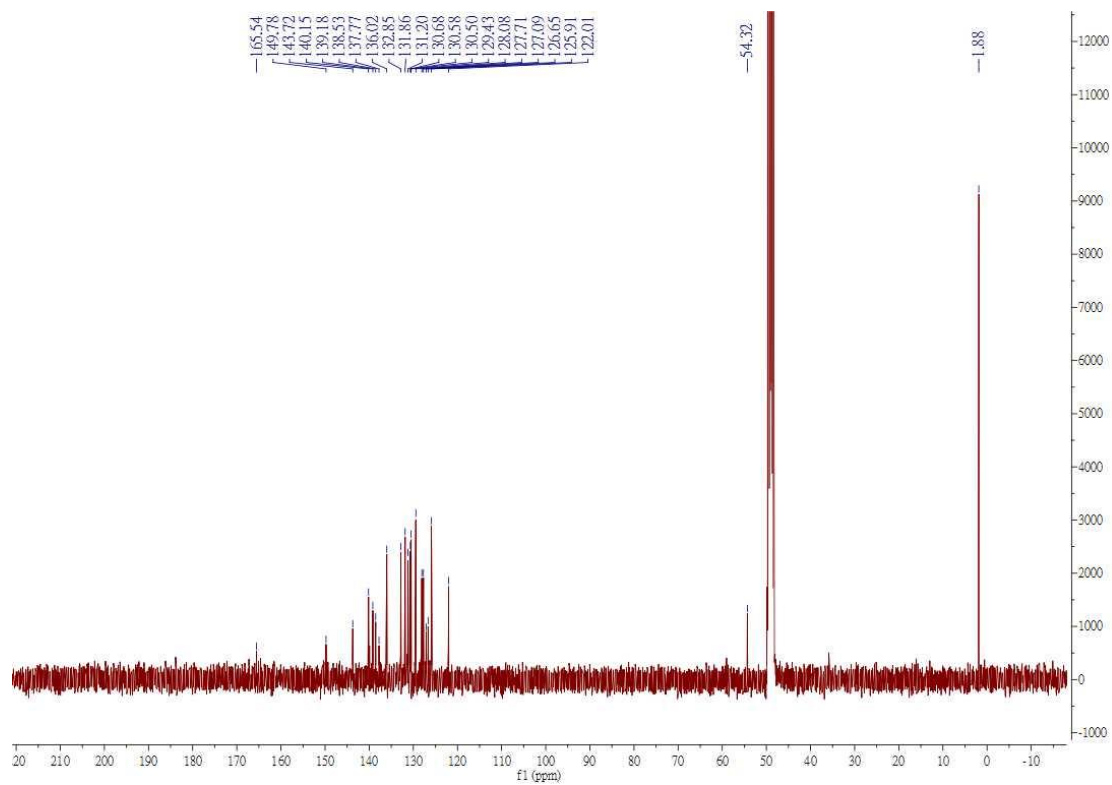
¹³C NMR



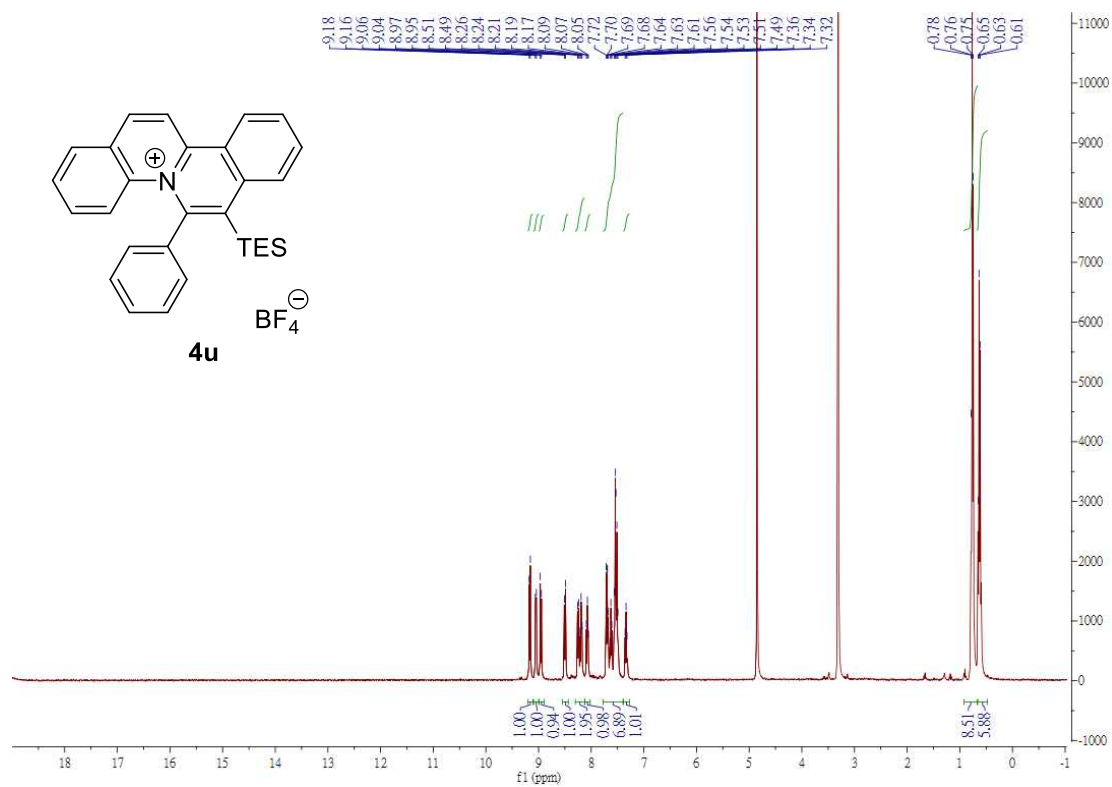
¹H NMR



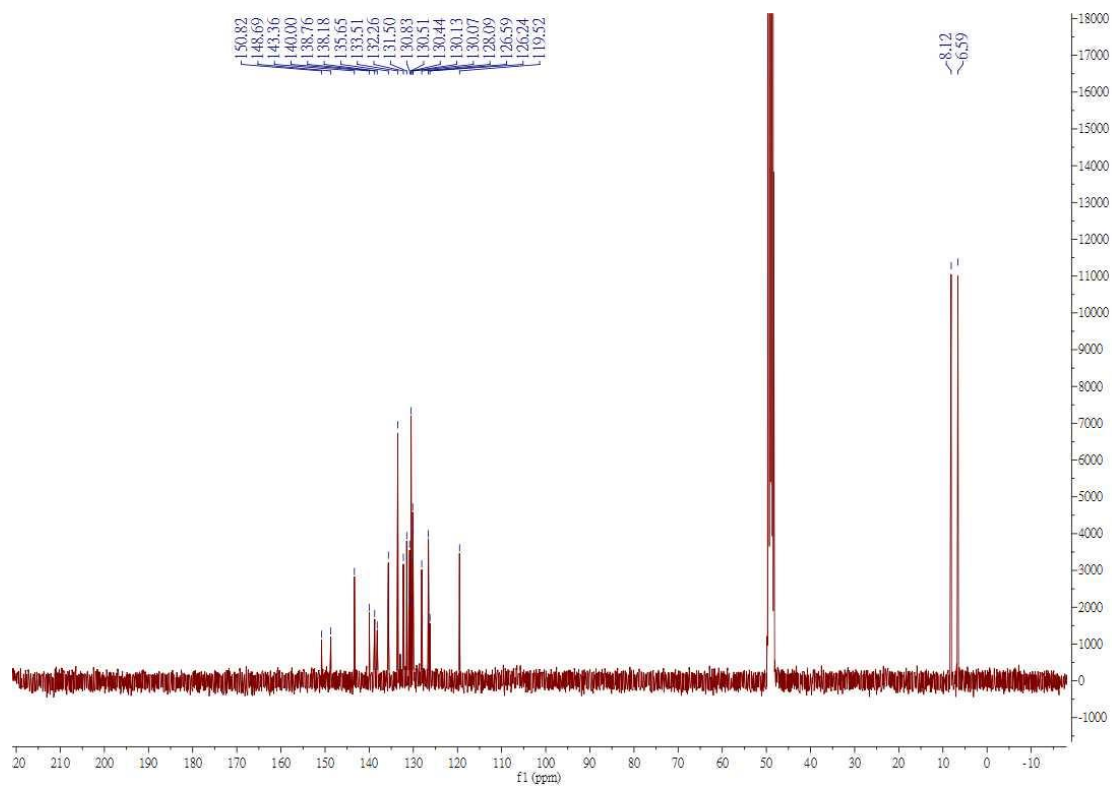
¹³C NMR



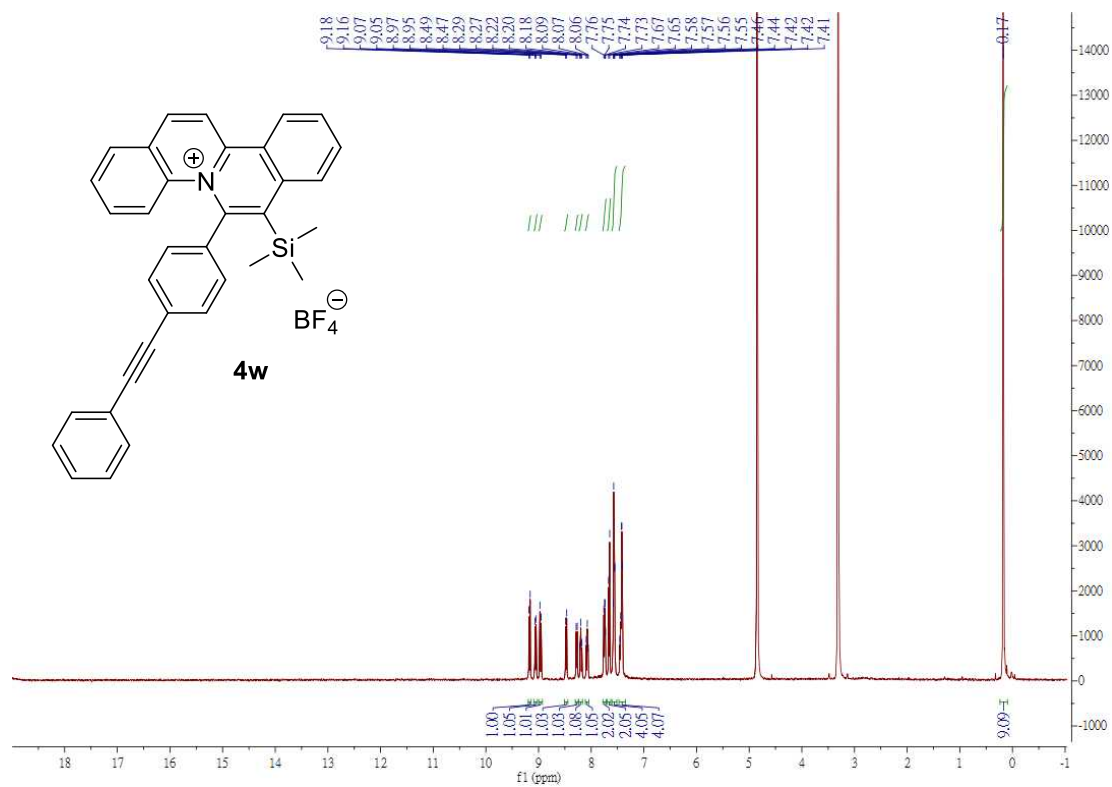
¹H NMR



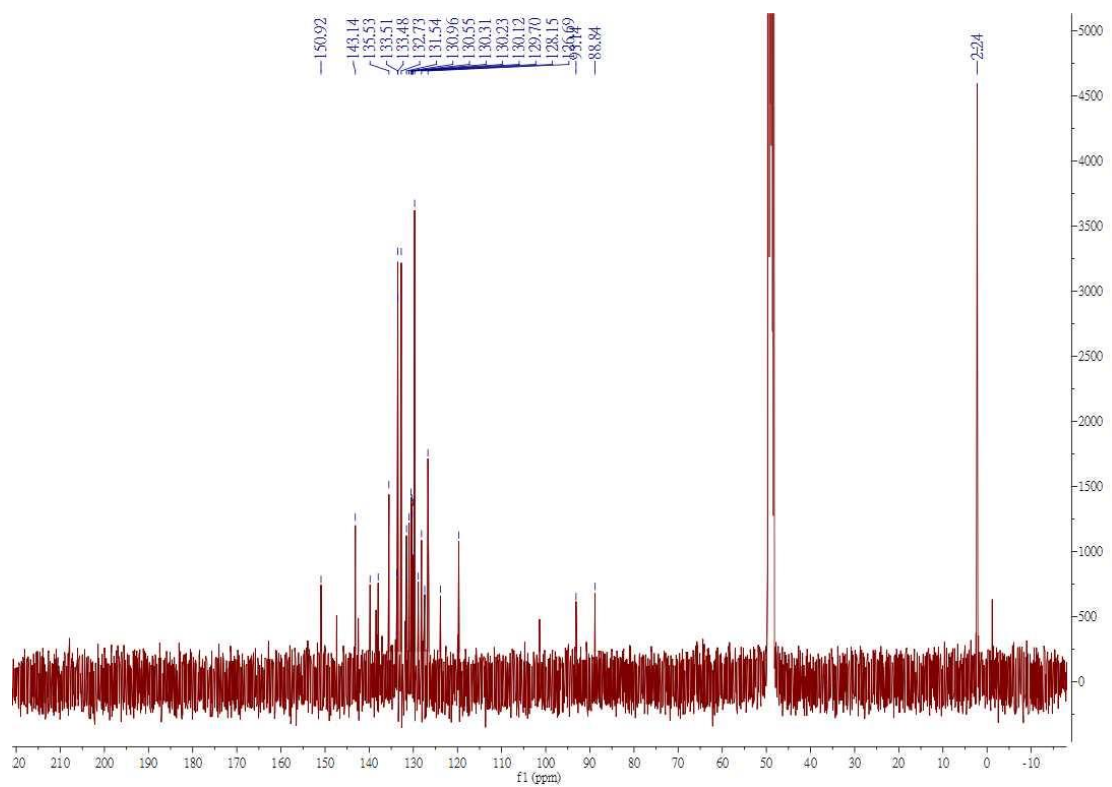
¹³C NMR



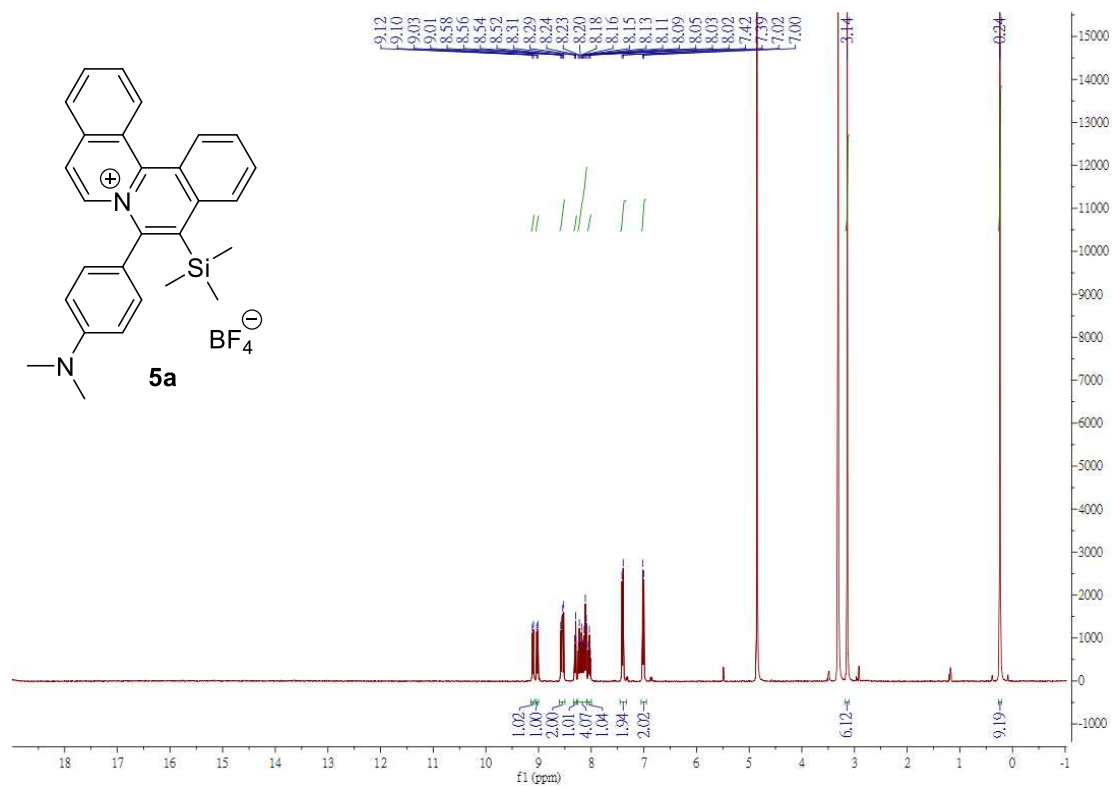
¹H NMR



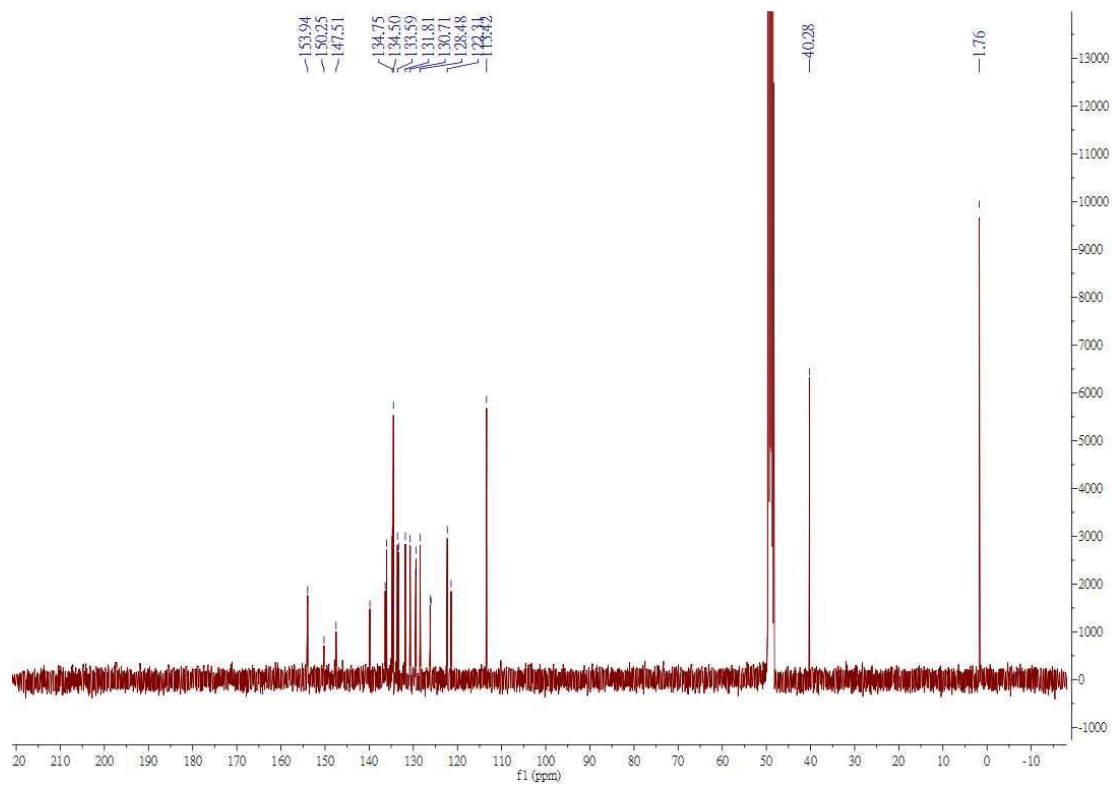
¹³C NMR



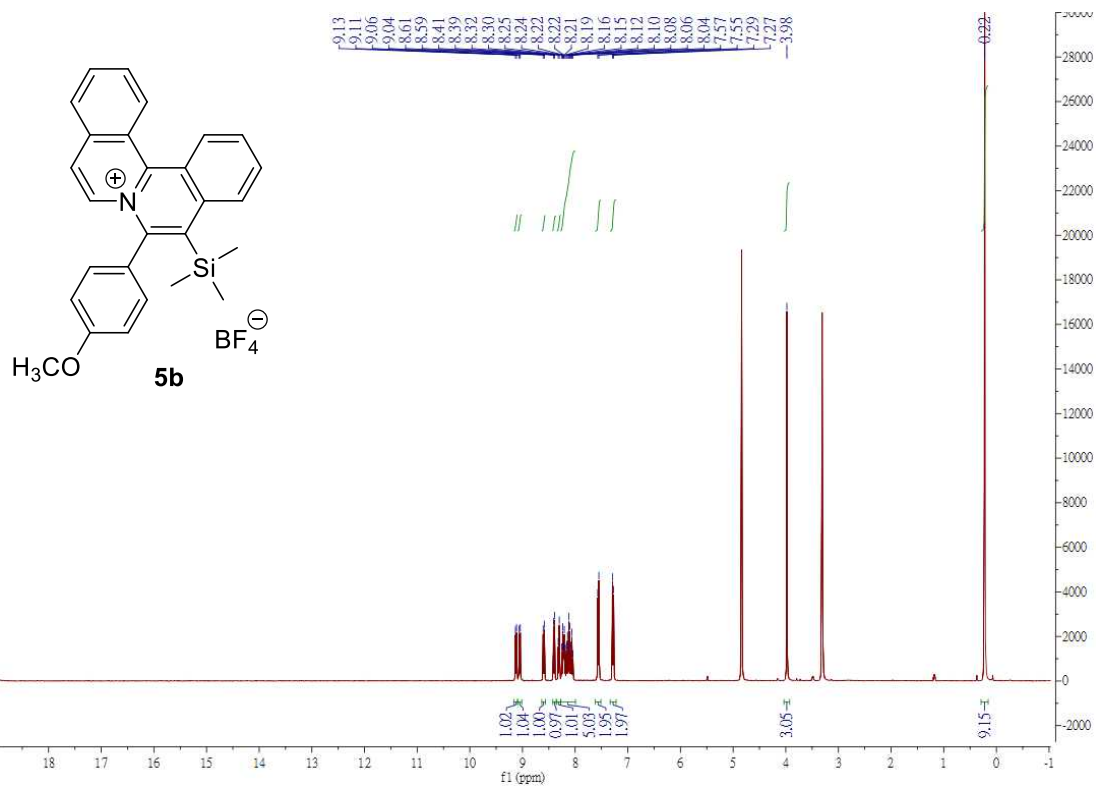
¹H NMR



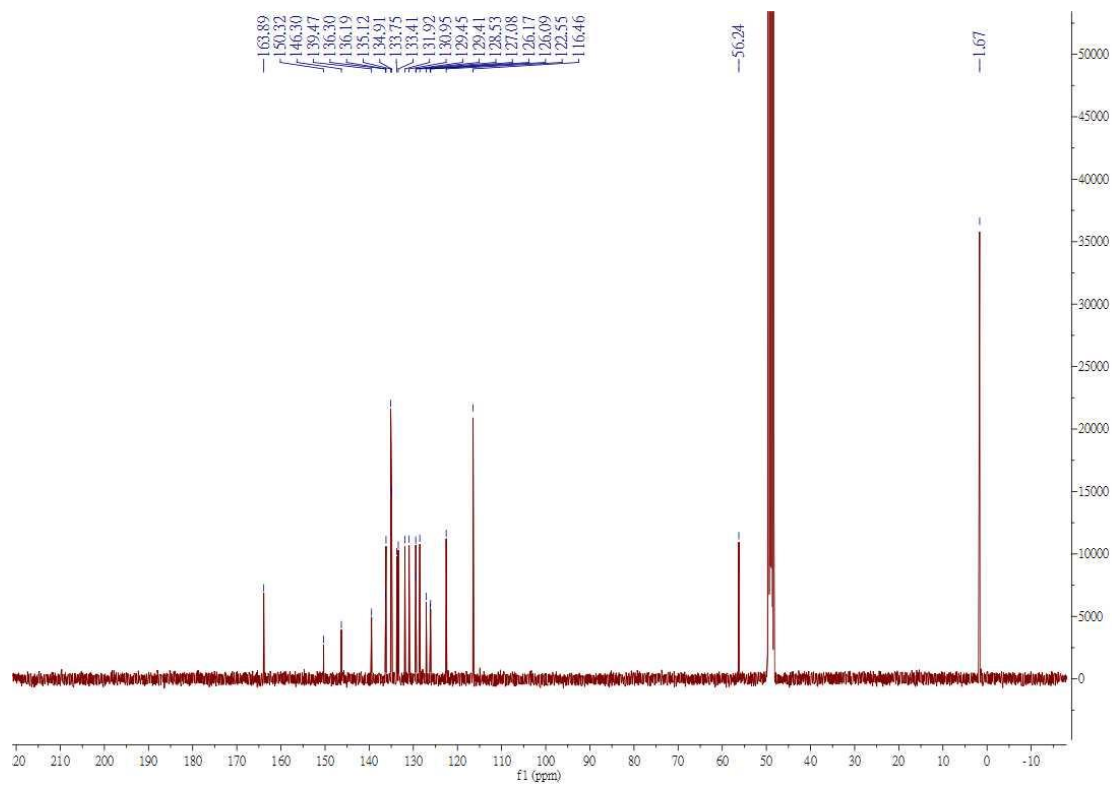
¹³C NMR



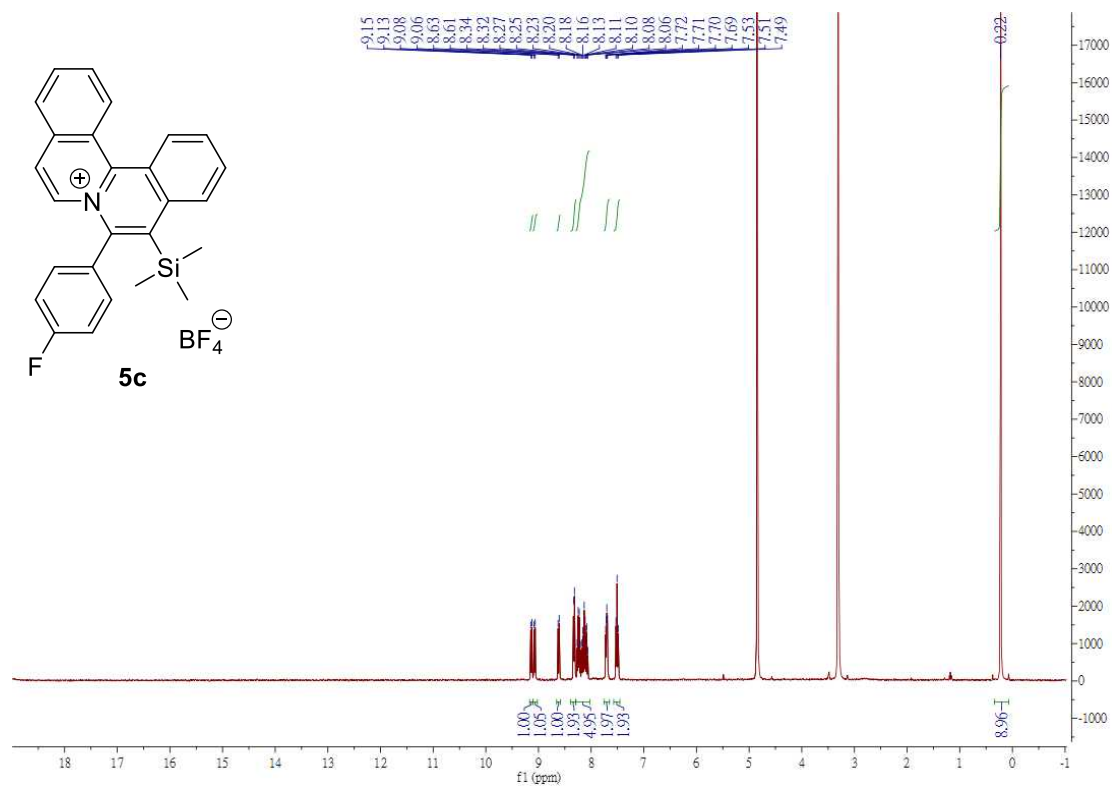
¹H NMR



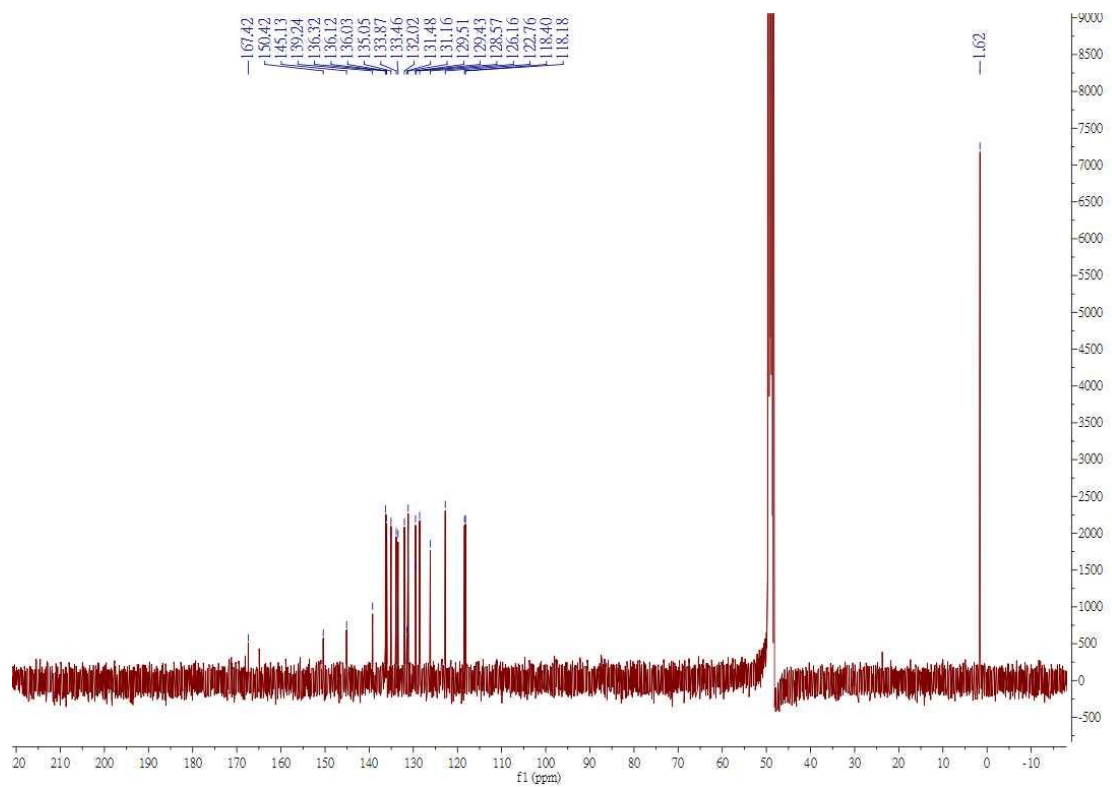
¹³C NMR



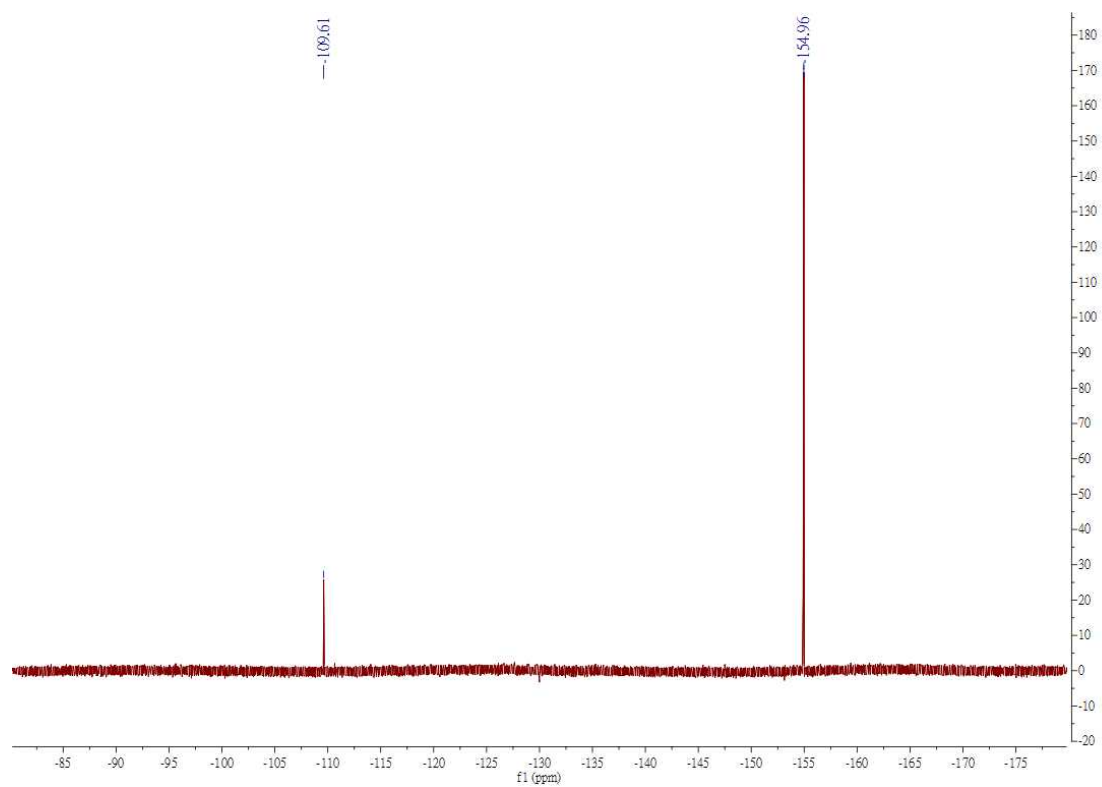
¹H NMR



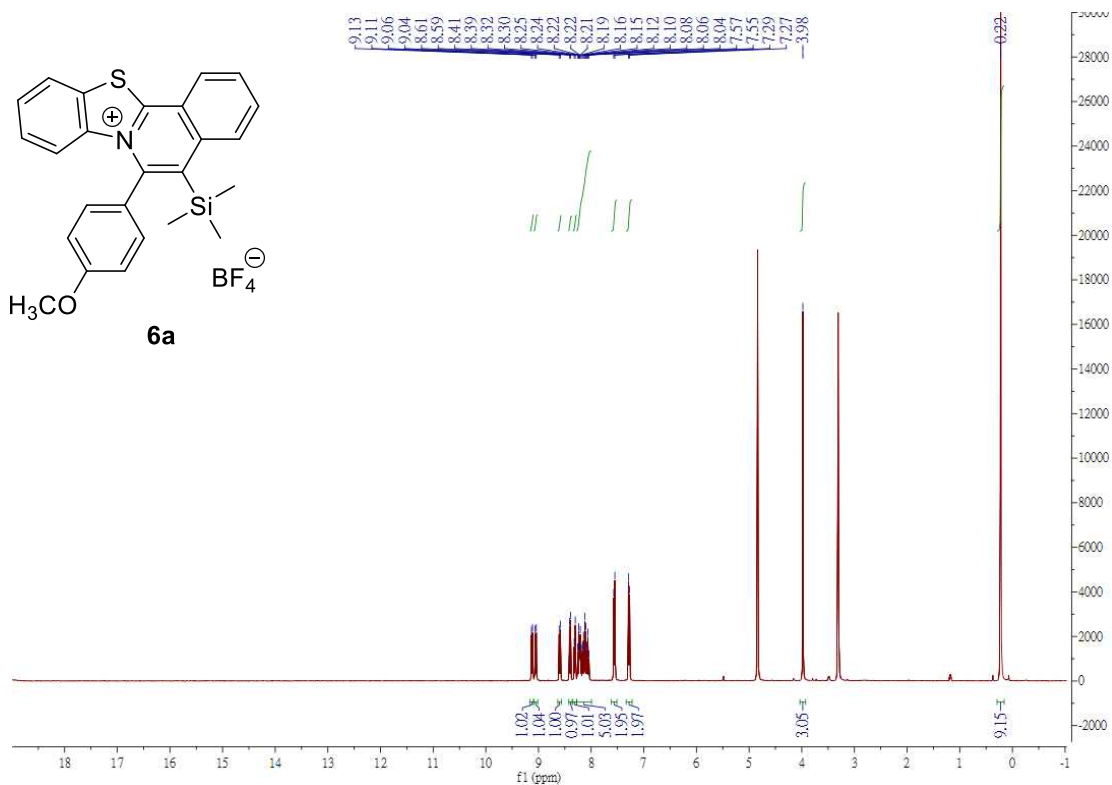
¹³C NMR



^{19}F NMR



¹H NMR



¹³C NMR

